NASA-CR-167,855

LANGLEY RESEARCH CENTER
3 1176 00504 3261

NASA CR-167855
SSS-R-82-5249

NASA-CR-167855
19820017934

ADDITIONAL EXTENSIONS TO THE NASCAP COMPUTER CODE, Volume I

M.J. Mandell
I. Katz
P.R. Stannard

S-CUBED

Prepared for
National Aeronautics and Space Administration
Lewis Research Center

Contract NAS3-22536

NF02683

1 Report No NASA CR-167855	2 Government Accession No	3 Recipient's Catalog No
4 Title and Subtitle ADDITIONAL EXTENSIONS TO THE NASCAP COMPUTER CODE, VOLUME I		5 Report Date October 1981 6 Performing Organization Code
7 Author(s) M. J. Mandell, I. Katz, P. R Stannard		8 Performing Organization Report No SSS-R-82-5249 10 Work Unit No
9 Performing Organization Name and Address S-CUBED P. O. Box 1620 La Jolla, CA 92038		11 Contract or Grant No NAS3-22536
12 Sponsoring Agency Name and Address National Aeronautics and Space Administration Lewis Research Center 21000 Brookpark Road, Cleveland, OH 44135		13 Type of Report and Period Covered Contractor Report 9/9/1980 - 12/22/1981 14 Sponsoring Agency Code 5532

15 Supplementary Notes

Project Manager, James C. Roche, NASA-Lewis Research Center, Cleveland, OH

16 Abstract

NASCAP is a computer code that comprehensively analyzes problems of spacecraft charging. Using a fully three-dimensional approach, it can accurately predict spacecraft potentials under a variety of conditions. Under Contract No. NAS3-22536 several revisions and a few extensions were implemented with a view toward making NASCAP more powerful and easier to use. Among the extensions are a multiple electron/ion gun test tank capability, and the ability to model anisotropic and time-dependent space environments. These extensions and revisions are documented in this volume.

Also documented here are a greatly extended MATCHG program and the preliminary version of NASCAP/LEO. The interactive MATCHG code has been developed into an extremely powerful tool for the study of material-environment interactions. NASCAP/LEO, a three-dimensional code to study current collection under conditions of high voltages and short Debye lengths, has been distributed for preliminary testing.

There are two companion volumes to this report. Volume II, NASA CR-167856, contains chapters entitled "Validation of the NASCAP Model Using Satellite Data", "NASCAP Applications Guide", "Differential Charging of High-Voltage Spacecraft· The Equilibrium Potential of Insulated Surfaces", and "Large Space Structure Modeling". Volume III, NASA CR-167857, documents a computer code for the modeling of plasmas external to ion thrusters

17 Key Words (Suggested by Author(s))	18 Distribution Statement
NASCAP Spacecraft Charging Plasma Collection Computer Simulation	Publicly available (no restrictions on provision to domestic or foreign requesters)

19 Security Classif (of this report)	20 Security Classif (of this page)	21 No of Pages	22 Price*
UNCLASSIFIED	UNCLASSIFIED	250	

* For sale by the National Technical Information Service, Springfield Virginia 22161

NASA-C-168 (Rev 10-75)

N82-25810#

TABLE OF CONTENTS

Chapter		Page
	SUMMARY	1
1.	INTRODUCTION	3
2.	NASCAP/GEO REVISIONS	5
	2.1 CONVERSION TO ASCII FORTRAN	5
	2.2 NASCAP POCKET GUIDE	8
	2.2.1 NASCAP Pocket Guide	8
	2.2.2 Errata and Updates	15
	2.3 OPTION REVISIONS	17
	2.3.1 Justifications for New Options	17
	2.3.1.1 Flux Definition	19
	2.3.1.2 Options Not Documented	19
	2.3.2 Description of New Options	19
	2.4 OUTPUT REVISIONS	26
	2.5 SECONDARY ELECTRON REVIEW	28
	2.5.1 A Reformulation of Secondary Electron Emission	28
	2.5.2 Fitting of Four Parameter Form to Stopping Power Data	32
	2.5.3 Ion-Induced Secondary Electron Emission	42
3.	NASCAP/GEO EXTENSIONS	44
	3.1 OBJDEF EXTENSION	44
	3.2 NEW DISCHARGE CAPABILITY	44
	3.2.1 General Principles Governing Discharges	44
	3.2.2 Charge Redistribution - Specific Cases	48

TABLE OF CONTENTS (Continued)

Chapter			Page
	3.3	MULTIPLE TEST TANK ENVIRONMENT	51
		3.3.1 Theory	51
		3.3.2 Implementation	58
		3.3.2.1 General Considerations . .	58
		3.3.2.2 Usage	59
		3.3.2.3 Gun Definition Input Specification	60
		3.3.2.4 Examples	62
		3.3.3 Cylindrical Tank	66
	3.4	SPACE ENVIRONMENT	69
		3.4.1 Anisotropic Flux	69
		3.4.1.1 The Coordinate System . .	70
		3.4.1.2 Angular Distribution Function	72
		3.4.1.3 Current Collection	73
		3.4.1.4 Fitting Data	77
		3.4.2 DIRECT and UPDATE	83
		3.4.2.1 DIRECT	83
		3.4.2.2 Anisotropic	86
		3.4.2.3 UPDATE	87
		3.4.2.4 Summary	89
		3.4.3 Format for Tabulated Spectral Data	90
4.		PLOTTING EXTENSIONS - NASCAP*PLOTREAD	94
5.		NASCAP*MATCHG	100
	5.1	PROGRAM STRUCTURE	104
	5.2	MATCHG HELP	108
	5.3	INPUT	115
	5.4	OUTPUT	124
	5.5	INSTRUCTIONS FOR USE	124
	5.6	MATCHG TEST RUN	125
6.		NASCAP*TERMTALK	187

TABLE OF CONTENTS (Concluded)

Chapter		Page
7.	NASCAP/LEO	189
	7.1 GENERAL	189
	7.2 MAIN CODE MODULES	189
	7.3 RDOPT MODULE	190
	7.4 OBJDEF MODULE	192
	7.5 POTENT MODULE	193
	7.6 CURRENt MODULE	195
	7.7 MOVEP MODULE	196
	7.8 APRT MODULE	196
	7.9 INTERFACING THE BIGLEO AND BIGFINE CODES	196
	7.10 TREATMENT OF RAM EFFECTS IN BIGLEO CODE	197
	7.11 SAMPLE RUN OF BIGLEO AND BIGFINE CODES	200
	APPENDIX A - NASCAP BIBLIOGRAPHY	213
	APPENDIX B - NASCAP SIMULATION OF LABORATORY SPACECRAFT CHARGING TESTS USING MULTIPLE ELECTRON GUNS	217
	APPENDIX C - "BOOTSTRAP" CHARGING OF SURFACES COMPOSED OF MULTIPLE MATERIALS	223
	APPENDIX D - FLUID MODEL OF PLASMA OUTSIDE A HOLLOW CATHODE NEUTRALIZER	231
	REFERENCES	239

LIST OF FIGURES

Figure No.		Page
2.1	New format for NASCAP option summary, indicating default options	27
2.2a	Energy deposition profiles of primary electrons for incident energies E^0	30
2.2b	Generalized yield curve	30
2.3	Comparison of new and old MATCHG yields for kapton	40
2.4	Comparison of new and old MATCHG yields for aluminum	41
3.1	Three nested octagons	45
3.2	Two octagons meeting at a slanted side . .	46
3.3	Geometry for electron gun aimed at a sphere	52
3.4	Geometrical quantities used to calculate current density	55
3.5	Potential contours - cylindrical tank of radius 10 grid units about Z-axis	67
3.6	Potential contours - cylindrical tank of radius 10 grid units about Z-axis	68
3.7	The projection of an incident vector $\vec{r}$ upon the surface normal, in the "fan-like" co-ordinated system	71
3.8	Anisotropic flux distribution with R = -0.35	78
3.9	Anisotropic flux distribution with R = -0.10	79
3.10	Isotropic flux distribution	80
3.11	Anisotropic flux distribution with R = 0.10	81
3.12	Anisotropic flux distribution with R = 0.50	82

LIST OF FIGURES (Concluded)

Figure No.		Page
3.13	File examples for DETECT and ANISOTROPIC fluxes	85
5.1	Block diagram of MATCHG	105

LIST OF TABLES

Table No.		Page
2.1	New, Revised, and Obsolete Option Words . .	18
2.2	Four Parameter Stopping Power Fits	34
2.3	Three Parameter Stopping Power Fits	34
2.4	Comparison of Three and Four Parameter Fits With ATAR	35
2.5	Comparison of Old and New Version Yields .	38
2.6	Secondary Yield for 1 keV Ions on Mo . . .	43
3.1	Syntax	84
3.2	Example of a DIRECT Data File	93
4.1	NASCAP-Pseudo Graphics Subroutines	95
4.2	IGS and DISSPLA Routines Called by NASCAP and PLOTREAD	98
5.1	MATCHG Commands	101
5.2	Command Formats	102
5.3	Initial Default Values	104
5.4	User/Code Interfacing Routines	106
5.5	Material Properties	116

SUMMARY

NASCAP is a computer code that comprehensively analyzes problems of spacecraft charging. Using a fully three-dimensional approach, it can accurately predict spacecraft potentials under a variety of conditions. Under Contract No. NAS3-22536 several revisions and a few extensions were implemented with a view toward making NASCAP more powerful and easier to use. Among the extensions are a multiple electron/ion gun test tank capability, and the ability to model anisotropic and time-dependent space environments. These extensions and revisions are documented in this volume.

Also documented here are a greatly extended MATCHG program and the preliminary version of NASCAP/LEO. The interactive MATCHG code has been developed into an extremely powerful tool for the study of material-environment interactions. NASCAP/LEO, a three-dimensional code to study current collection under conditions of high voltages and short Debye lengths, has been distributed for preliminary testing.

There are two companion volumes to this report. Volume II, NASA CR-167856, contains chapters entitled "Validation of the NASCAP Model Using Satellite Data", "NASCAP Applications Guide", "Differential Charging of High-Voltage Spacecraft: The Equilibrium Potential of Insulted Surfaces", and "Large Space Structure Modeling". Volume III, NASA CR-167857, documents a computer code for the modeling of plasmas external to ion thrusters.

1. INTRODUCTION

This is the final report on the NASCAP code development tasks (Tasks 1 and 2) of Contract No. NAS3-22536, "Additional Extensions to the NASCAP Computer Code". The work was performed by Systems, Science and Software between 29 September 1980 and 30 September 1981.

This report includes information from monthly reports published throughout the contract period, as well as some new items. There are two other volumes of the final report. Volume II, "Ion Thruster Code Manual", documents the preliminary version of a two-dimensional (R-Z) model for calculating plasma densities, current densities, potentials, and temperatures in the plasmas external to an ion thruster (Task 7). Volume III, "Validation of the NASCAP SCATHA Model", describes research directly related to the SCATHA spacecraft (Task 3).

NASCAP/GEO (NASA Charging Analyzer Program/Geosynchronous Earth Orbit, henceforth referred to as NASCAP) is a powerful computer program for studying spacecraft charging. It is intended as a tool for spacecraft designers to help them avoid the problems of electrical charging in space, and for scientific experimenters to aid in the design and interpretation of flight experiments. As there is now a group of researchers using NASCAP on a day-to-day basis, the emphasis of this year's work was on consolidation and validation rather than on extension.

The work directly related to the NASCAP/GEO code has been divided somewhat arbitrarily into revisions (described in Chapter 2) and extensions (described in Chapter 3). The revisions (Chapter 2) are those changes intended to promote ease of installation, use, and interpretation. The largest task in this category was conversion from FORTRAN V to ASCII FORTRAN. Other revisions included production of a NASCAP Pocket Guide, revision of the RDOPT input, substantial review and revision of the code output, and a review of NASCAP's treatment of

secondary electron production. Extensions to NASCAP (Chapter 3) include revision of the treatment of right triangles in OBJDEF to allow definition of previously illegal objects; replacement of the previous, unsatisfactory, discharge simulation; incorporation of a fast-running multigun test tank environment; and extension of the space environment to allow anisotropic and time-dependent fluxes.

Chapters 4, 5 and 6 deal with codes auxiliary to NASCAP. NASCAP*PLOTREAD (Chapter 4) is a graphics interface routine which has enhanced the transferability of NASCAP to other installations. NASCAP*MATCHG (Chapter 5) has been enhanced to make it a very powerful, fast-running, interactive tool for the study of material-environment interactions. NASCAP*TERMTALK (Chapter 6) has been extended to give flux breakdown printouts.

Chapter 7 describes the NASCAP/LEO (NASCAP/Low Earth Orbit) code. A preliminary version of this code has been installed at NASA/LeRC.

The appendices include a list of NASCAP-related reports and publications, as well as several publications written under this contract.

2. NASCAP/GEO REVISIONS

2.1 CONVERSION TO ASCII FORTRAN

The first major undertaking of this year's contract was conversion of the NASCAP code from UNIVAC FORTRAN V to ASCII FORTRAN. Among the reasons for this conversion were:

1. Demands by NASA/LeRC systems personnel.
2. Impending unavailability of a FORTRAN V plot library at S-Cubed.
3. Hopes for shortened execution time and improved diagnostics.
4. Closer approach to IBM compatibility.

It was elected to eschew the new, allegedly advantageous, features of ASCII FORTRAN (e.g., character variables, if-then-else logic, offset array subscripts) as these are imperfectly implemented and not CDC compatible. Rather, the needed changes were, as much as possible, made line by line. Nonetheless, the discovery of residual conversion errors continued for several months after the ASCII version was declared the official version of NASCAP. This shows that the compiler dependence of coding can often be rather subtle.

The FORTRAN V-ASCII FORTRAN difference affecting by far the greatest number of lines of code is the representation of literals. FORTRAN V represents literals in words of six FIELDATA characters, while ASCII FORTRAN uses words of four nine-bit ASCII characters. We elected to make NASCAP literals four-character significant. A few exceptions (TANKCUR, TANKTRAJ, PATCHW, PATCHR) were made eight-character significant.

We were then left with a language quirk to deal with. While the statement

```
A = 'B'
```

is legal, the statement

```
IF (A.EQ.'B') . . .
```

is arbitrarily declared illegal in ASCII FORTRAN. The initial idea to circumvent this was to use

```
IF (XOR(A,'B').EQ.0) . . .
```

The problem which quickly arose was that A might inadvertently contain lower case letters. Therefore a new subroutine, XORR, was written which converted both arguments to upper case before comparing. The code conversion was accomplished using XORR for literal compares. However, this syntax proved rather awkward. Accordingly, logical function routines EQUAL and NOTEQL were written, and all new coding uses those routines (which call XORR) for literal compares.

The different representation of literals also affected FORMAT statements and array lengths. Numerous A6's had to be changed to A4's, and arrays had to be lengthened to accommodate fewer letters per word. (The latter constituted a large portion of the residual conversion problems.) Many FORMAT statements were also affected by different printing of numbers under 'E' conversion.

A few assembly language subroutines (S3MCOR, TIMLFT, FASTIO) were originally written with the FORTRAN V protocol. These routines were left unchanged, necessitating the use of EXTERNAL* entrypoint statements in the calling routines.

NASCAP's dynamic storage allocation (S3MCOR) was found to conflict with ASCII FORTRAN's dynamic allocation of I/O buffers. This necessitated writing an assembler routine F2FCA to provide buffers in the main segment. Since the resulting buffer space was limited, care had to be taken to avoid gratuitously opening files, and to close files after use. In a related matter, the FORTRAN V NTAB$ was replaced with an equivalent ASCII FORTRAN F2FRT.

The segmentation structure carried over surprisingly intact. One necessary change was that the ASCII FORTRAN diagnostic routings (FTNPMD) were too large to remain in the main segment. They were put, along with RETRNO, in a higher segment.

As part of the conversion, a neutral graphics concept was introduced into NASCAP. NASCAP now writes a sequence of dummy graphics calls on file 2. A postprocessor (NASCAP*PLOTREAD.) reads these dummy calls and interfaces to the user's graphics library. This feature is discussed in more detail later in this report. Another added feature was automatic assignment of scratch files.

The ASCII FORTRAN version of NASCAP was compiled and tested at S-Cubed using level 9R1 of ASCII FORTRAN. All routines were compiled with the options FZE. In one instance the compiler generated bad code. The problem was corrected by rewriting the line. The code was installed at NASA/LeRC under level 7R1. It was found that:

1. Many routines required minor syntactical changes.
2. Some routines caused the compiler to guard mode if the Z-option was used.
3. Some routines caused the compiler to loop if the Z-option was not used.
4. A successful collection (@MAP) required that the bulk of routines be compiled with the Z option and without the F option.
5. The ERR= branch on I/O and DECODE statements was highly unreliable.
6. Several routines generated incorrect code when compiled with the Z option. The conditions were corrected by substituting the V option.

As a result, there is no uniform set of compilation options under level 7R1. We conclude that level 7R1 of ASCII FORTRAN is totally unsatisfactory.

2.2 NASCAP POCKET GUIDE

Early in the contract period we issued a NASCAP Pocket Guide to serve as a convenient memory aid to NASCAP options and syntaxes. The Guide has proved extremely worthwhile. Here we reprint the Guide, together with some errata and updates. Card-stock copies of the Guide are available on request from Systems, Science and Software.

2.2.1 NASCAP Pocket Guide

NASCAP

POCKET GUIDE

NOVEMBER 1, 1980

This document is a quick reference guide for the experienced user of NASCAP—the NASA Charging Analyzer Program It contains common NASCAP syntax and examples

There are also several interactive computer programs for easy pre- and post-processing of NASCAP information For descriptions of these and further NASCAP documentation, see NASA publications CR-159417 (NASCAP Users Manual) and CR-159595 (Final Report 1979)

USER OPTIONS—FILE 26

Supplied in file 26—OPT file In this section, "#" indicates integers "< >" indicates optional input Ellipses " " indicate continue on same line The most important options are RESTART, DELTA, LONGTIMESTEP, NCYC, and MESH Options are set sequentially as read They are remembered throughout the steps of a NASCAP execution, and may be changed by RODPT calls at any time

SYNTAX	MEANING	DEFAULT	EXAMPLE
3D-VIEW x y z	new SATPLT view	3 default views	3D-VIEW 4 2 4 9 8
3D VIEW NONE	clear view table	3 default views	3D-VIEW NONE
APRT grids#	number grids potential print	1	APRT 2
BFIELD bx by bz	constant mag field—Webers/m²	0, 0, 0	BFIELD 01 1 E 5 1 E-5
BIAS cond# volts	conductor bias relative to conductor 1	no bias	BIAS 2 -500
CIJ conda# condb# farads	mutual conductor capacitance	stray capacitance only	CIJ 3 4 1 E 4
COMMENT <anything>	comment—no effect	none	COMMENT SEPT 25 CHANGES
CONTOURS NONE	clear contour table	no contours	CONTOURS NONE
CONTOURS STANDARD	3 center cuts	no contours	CONTOURS STANDARD
CONTOURS $\binom{x}{y}_{z}$ cut# <GRIDS ng# MOD mod#>	additional contour cut	no contours	CONTOURS Y -1 GRIDS 3 MOD 4
CONTOURS $\binom{x}{y}_{z}$ cut# OFF	clear specific cut	no contours	CONTOURS X 0 OFF
CONVEX	convex object self shadowing only	HIDCEL must be called for nonzero sun intensity	CONVEX
CONVERGENCE PLOTS ON CONVERGENCE PLOTS OFF	potential solver printer plots	on	CONVERGENCE PLOTS ON CONVERGENCE PLOTS OFF
DEADLINE hhmmss#	finish before time of day	none	DEADLINE 234500
DEBYE	activates Debye screening	no screening	DEBYE
DELFAC factor	timestep = timestep * factor	1	DELFAC 1 5
DELTA timestep	initial timestep (seconds)	1	DELTA 01
DIPOLE MOMENT px py pz AT x y z	magnetic dipole moment (A – M²) and location	none	DIPOLE MOMENT 1 E-2, 1 E 2, 0 AT 0, 0 5
DISCHARGE relax	perform discharge analysis	no discharge analysis	DISCHARGE 5
EFFCON ON EFFCON OFF	effective surface conductivity	off	EFFCON ON EFFCON OFF
EMITTER unit#	activate particle emitter	NOEMIT	EMITTER 23
END	end of input file	none	END
FIXP cond# volts	fix conductor potential	conductor floats	FIXP 2 -3000
FLOAT	remove all previous FIXP and BIAS	previous status	FLOAT
FLOAT cond#	float previously fixed or biased conductor	previous status	FLOAT 3
IOUTER $\binom{0}{2}$	0—grounded outer boundary 2—monopole outer boundary	2 i e l/r potentials	IOUTER 2

SYNTAX	MEANING	DEFAULT	EXAMPLE
LONGTIMESTEP <dvlim>	implicit charging <voltage limit per timestep>	NOLONG	LONGTIMESTEP 2000
MATVIEW $\pm\begin{pmatrix}x\\y\\z\end{pmatrix}$ cuta# cutb#	additional material plot	6 default plots	MATVIEW −Z −5 +5
MATVIEW NONE	clears MATVIEW table	6 default plots	MATVIEW NONE
NCYC steps#	number timesteps to run	1	NCYC 5
NG grids#	number computational grids	2	NG 3
NOEMIT	turn off previously defined emitter	previous status	NOEMIT
NOLONG	see LONGTIMESTEP	explicit charging	NOLONG
NOPRINT modulename	see PRINT	no extra printout	NOPRINT POTENT
NOSCALE	see SCALE	SCALE	NOSCALE
NOSHEATH	see SHEATH	no sheath plot	NOSHEATH
NOTIME	see TIMER	no timer	NOTIME
NZ zdiv#	z grid size	33	NZ 29
OFFSET x# y# z#	moves coordinate origin	center of mesh (9 9 17)	OFFSET 0 0 0
POTCON decades	convergence of potential solver	8—CAPACI, 4—TRILIN	POTCON 3
PRINT modulename	diagnostic prints, modulename is LIMCEL POTENT HIDCEL, or OBJDEF	NOPRINT	PRINT POTENT
REPEAT times#	plot repetition factor (IGS only)	1	REPEAT 3
RESTART	next timestep—old problem	new problem	RESTART
SCALE	potential solver scales potential and boundary conditions	SCALE	SCALE
SECONDARY <EMISSION> ANGLE	secondary formulation	ANGLE	SECONDARY ANGLE
SECONDARY <EMISSION> NORMAL	secondary formulation	ANGLE	SECONDARY EMISSION NORMAL
SHEATH	plot space charge density	NOSHEATH	SHEATH
SUNDIR x y z	sun direction vector	1, 1, 1	SUNDIR 1, 0, 2 5
SUNINT intens	sun intensity	0	SUNINT 0 8
SURFACE CORNER x# y# z# <norx# nory# norz#>	surface cell of interest	none	SURFACE CORNER 3, 3, 2 −1, 0, 0
SURFACE CELL cell#	surface cell of interest	cell #1	SURFACE CELL 541
TANKCUR OFF TANKCUR ON	tank current contour plots	off	TANKCUR OFF TANKCUR ON
TANKTRAJ OFF TANKTRAJ ON	tank particle trajectory plots	off	TANKTRAJ OFF TANKTRAJ ON
TIMER	execution time each module	NOTIME	TIMER
XMESH unit	physical grid spacing (meters)	0 1	XMESH 03
ZTRUNCATE zlo# zhi#	truncation of outer grid	full grid, −16 to +16	ZTRUNCATE −12 +12

NASCAP COMMANDS

MNEMONIC	COMMAND WORD	IF NO UNIT SPECIFIED	ADDITIONAL INPUT	PREREQUISITE COMMAND
Read Options	RDOPT <unit>	Unit 26 assumed	Option keywords	None
Object Definition	OBJDEF <unit>	Unit 20 assumed	Object description	RDOPT
Satellite Plot	SATPLT	—	None	OBJDEF
Capacitance	CAPACI	—	None	OBJDEF
Trilinear Charge	TRILIN <unit>	Unit 22 assumed	Flux definition	CAPACI (HIDCEL)
Hidden Cells	HIDCEL	—	None	OBJDEF
Rotate with Time	ROTATE <unit>	Use 1 RPM about Z axis	(2 cards) radians/sec, initial sun vector	TRILIN
Spin Average	SPIN <unit>	Eight views about Z axis	(1 card) #views, spin axis vector	OBJDEF
Detector Enable	DETECT <unit>	Unit 5 (runstream) assumed	Detector keywords (see Manual)	TRILIN
New Material Parameters	NEWMAT <unit>	Error	(4 cards) material parameters	OBJDEF
End Run	END	—	None	RDOPT

TYPICAL UNIVAC RUNSTREAM

(RUN Card)

```
@ASG T     10
@ASG T     11
@ASG T     12
@ASG T     13
@ASG T     14
@ASG,T     15
@ASG T     16
@ASG T     17
@ASG T     21
@ASG T     25
@ASG,T     27
@ASG T     28 ///1000
@COPY prefix10  10
@COPY prefix15  15
@COPY prefix16  16
@COPY prefix17  17
@COPY prefix21  21
@COPY prefix27  27
@USE 20  prefixOBJ
@ASG A     20
@USE 22  prefixFLX
@ASG A     22
@USE       26  prefixOPT
@ASG A     26
@XQT NASCAP  NASCAP
RDOPT
TRILIN   NASCAP Commands
END
@PMD  EL
@COPY      10  prefix10
@COPY      15  prefix15
@COPY      16  prefix16
@COPY      17  prefix17
@COPY      21  prefix21
@COPY      27  prefix27
@FIN
```

SELF-CONTAINED RUNSTREAM

(RUN Card)

```
@ASG T     10
@ASG T     11
@ASG T     12
@ASG T     13
@ASG T     14
@ASG T     15
@ASG T     16
@ASG T     17
@ASG T     21
@ASG T     25
@ASG T     27
@ASG T     28 ///1000
@XQT NASCAP  NASCAP
RDOPT 5
  DELTA  01
  LONGTIMESTEP 1000
  NCYC 2
  XMESH  5
  END
OBJDEF 5
  OSPHERE
  CENTER 0  0  0
  DIAMETER 3
  SIDE 1
  MATERIAL SILVER
  ENDOBJ
  ENDSAT
CAPACI
TRILIN 5
  SINGLE MAXWELL
  1   CGS
  1 1 CGS
  3 5 KEV
  3   KEV
  END
END
@PMD  EL
@FIN
```

DEFAULT SURFACE MATERIALS

ALUMIN	KAPTON
AQUADG	NPAINT
CPAINT	SIO2
GOLD	SOLAR
INDOX	TEFLON
MAGNES	SILVER
SCREEN	

OBJECT DEFINITION—FILE 20

All integer input—except for "radius" and "materialname" See NASCAP Users Manual for information on material parameters

OBJECT DEFINITION SYNTAX	OBJECT DEFINITION EXAMPLES
RECTAN CORNER x y z DELTAS Δx Δy Δz (UP TO 6 SURFACE CARDS) ENDOBJ	RECTAN CORNER 3 −2 8 DELTAS 1 2 4 SURFACE +X ALUMINUM SURFACE −X ALUMINUM SURFACE +Y ALUMINUM SURFACE −Y ALUMINUM SURFACE +Z ALUMINUM SURFACE −Z ALUMINUM ENDOBJ
WEDGE CORNER x y z FACE materialname normal (type 110) LENGTH Δx Δy Δz (UP TO 4 SURFACE CARDS) ENDOBJ	WEDGE CORNER −3 2 1 FACE SIO2 −1 −1 0 LENGTH 1 1 3 SURFACE +X SIO2 SURFACE +Y SIO2 SURFACE +Z GOLD SURFACE −Z SIO2 ENDOBJ
TETRAH CORNER x y z FACE materialname normal (type 111) LENGTH Δx (UP TO 3 SURFACE CARDS) ENDOBJ	TETRAH CORNER −3 −2 8 FACE KAPTON 1 1 −1 LENGTH 2 SURFACE −X TEFLON SURFACE −Y KAPTON SURFACE −Z TEFLON ENDOBJ
OCTAGON AXIS x y z x' y' z' WIDTH w SIDE s (UP TO 3 SPECIAL SURFACE CARDS + − or C) ENDOBJ	OCTAGON AXIS 3 2 −6 3 2 −9 WIDTH 3 SIDE 1 SURFACE + SILVER SURFACE − SILVER SURFACE C MAGNES ENDOBJ
BOOM AXIS x y z x y z' RADIUS radius (floating point) SURFACE materialname ENDOBJ	BOOM AXIS 0 6 0 0 12 0 RADIUS 25 SURFACE ALUMINUM ENDOBJ
QSPHERE CENTER x y z DIAMETER d SIDE s MATERIAL materialname ENDOBJ	QSPHERE CENTER 0 0 0 DIAMETER 4 SIDE 2 MATERIAL NPAINT ENDOBJ

continued

OBJECT DEFINITION SYNTAX	OBJECT DEFINITION EXAMPLES
FIL111 CORNERLINE x y z x' y' z' FACE materialname normal (type 111) ENDOBJ	FIL111 CORNER 3 2 6 -5 4 6 FACE SOLAR −1 −1 −1 ENDOBJ
PLATE CORNER x y z DELTAS Δx Δy Δz TOP $\pm\begin{pmatrix}x\\y\\z\end{pmatrix}$ materialname BOTTOM $\pm\begin{pmatrix}x\\y\\z\end{pmatrix}$ materialname ENDOBJ	PLATE CORNER −1 −1 −10 DELTAS 2 2 0 TOP +Z CPAINT BOTTOM −Z CPAINT ENDOBJ
PATCHR CORNER x y z DELTAS Δx Δy Δz (UP TO 6 SURFACE CARDS) ENDOBJ	PATCHR CORNER 3 −2 8 DELTAS 1 0 1 SURFACE −Y SCREEN ENDOBJ
PATCHW CORNER x y z FACE materialname normal (type 110) LENGTH Δx Δy Δz (UP TO 4 SURFACE CARDS) ENDOBJ	PATCHW CORNER −3 2 7 FACE AQUADG −1 −1 0 LENGTH 1 1 1 ENDOBJ

NOTES normal is three values each either +1 0 or −1

SURFACE CARD has the following format

SURFACE $\pm\begin{pmatrix}x\\y\\z\end{pmatrix}$ materialname

SPECIAL SURFACE CARD is

SURFACE $\begin{pmatrix}+\\-\\C\end{pmatrix}$ materialname

OTHER OBJECT DEFINITION COMMANDS

ENDSAT	Must be last card in file
COMMENT	No effect
OFFSET i j k	Moves coordinate origin
CONDUCTOR n	Sets number of underlying conductors ($1 \leq n \leq 7$)
DELETE i j k	Deletes surfaces leaving empty cell
unrecognized word	Assumed to be name of new surface material Next card scanned for parameters

FLUX DEFINITION—FILE 22

SINGLE MAXWELLIAN SYNTAX

```
MAXWELL
eldens densityunits
prdens densityunits
eltemp tempunits
prtemp tempunits
END
```

DOUBLE MAXWELL SYNTAX

```
DOUBLE MAXWELL
ELECTRONS eldens densityunits eltemp tempunits
ELECTRONS eldens densityunits eltemp tempunits
PROTONS   prdens densityunits prtemp tempunits
PROTONS   prdens densityunits prtemp tempunits
END
```

SINGLE MAXWELLIAN EXAMPLE

```
MAXWELL
1 CGS
1 E6 MKS
3000 EV
3 5 KEV
END
```

DOUBLE MAXWELLIAN EXAMPLE

```
DOUBLE MAXWELL
ELECTRONS 0 3E6 MKS 10 KEV
ELECTRONS 0 7 CGS 500 EV
PROTONS 0 3 CGS 1 E6 KELVIN
PROTONS 0 7E6 MKS 1 E-15 JOULES
```

The densityunits are MKS or CGS and tempunits are JOULES EV KEV ERGS or KELVIN For test tank flux see Users Manual

DEFAULT FILE NUMBERS— FILE NAMES—FILE USAGE

USER INPUT FILES

26	prefix OPT	user options
20	prefix OBJ	object definition
22	prefix FLX	flux definition

RESTART FILES

10	IP	potential
15	IROUS	charge
16	IPQCND	TERMTALK information
17	ILTBL	element table
21	ICNOW	various—used everywhere
27	IAREA	booms

SCRATCH FILES

11	IAUN	conjugate gradient
12	IR	conjugate gradient
13	IU	conjugate gradient
14	ISPARE	conjugate gradient
25	IDIV	conjugate gradient
28	IPART	plots

2.2.2 Errata and Updates

User Options

(Heading) RODPT should be RDOPT.

APRT - change Default to 0.

Contours - add CONTOURS STANDARD MOD mod#.

Convergence Plots - change default to OFF.

Add DESTINATION dest

(meaning) plot destination

(default) NONE

(example) DEST ZETA

add FLASHOVER volts

(meaning) max voltage difference between adjacent cells before flashover

(default) 10000

(example) FLASHOVER 3000

SURFACE CORNER

Note that previous object definition is required.

add TANK AXIS dir

(meaning) axis of cylindrical tank

(default) Z

(example) TANK AXIS X

add TANK RADIUS r [METERS]

(meaning) radius of cylindrical tank (grid units)

(default) rectangular tank

(example) TANK RADIUS 15

TANK RADIUS 1.5 METERS

add TITLE title

(meaning) plot title (begin in column 9)

(default) NASCAP

(example) TITLEbbbbMY NASCAP RUN

add UPDATE ON

UPDATE OFF

(meaning) time dependent flux

(default) OFF

(examples) UPDATE ON

UPDATE OFF

NASCAP COMMANDS

Two New Commands:	COMMENT	TANK
Mnemonic	Ignore Card	Tank Gun Definition
Command Word	COMMENT	TANK <unit>
If no unit specified	-	Unit 22 assumed
Additional Input	none	Gun Definition
Prerequisite Command	none	RDOPT

RUNSTREAMS

Scratch files (11, 12, 13, 14, 25) need not be explicitly assigned for "Self-Contained Runstream". All @ASG,T's may be omitted.

OTHER OBJECT DEFINITION COMMANDS

omit plural on conductors

FLUX DEFINITION - FILE 22

add Other Flux Types:

Type 1 - Single gun test tank

Type 5 - Direct Integration

Type 6 - Multigun test tank

USER INPUT FILES

add 9 ISPECTR supplementary flux definition

2.3 OPTION REVISIONS

During this contract year the NASCAP options were revised with a view toward making them easier to use and to have more reasonable defaults. In many cases new syntaxes were added to perform in a superior fashion the functions of existing options, while retaining the older syntaxes for downward compatibility. In two cases (APRT and ICNVP) defaults were changed to eliminate non-useful printing. Also, new options were added to implement the NASCAP extensions developed under this contract. A list of new, revised, and obsolete option words is provided in Table 2.1.

2.3.1 Justifications for New Options

The new options break down into four categories: coordinate system, name changes, structural changes, and extensions.

COORDINATE SYSTEM - The original NASCAP coordinate system numbered each grid 1 to 17 in the X and Y directions, and 1 to 33 in the Z direction. The newer, more intuitive system puts the origin at grid center, so Z coordinates go from -16 to +16. These two incompatible systems coexist in NASCAP and confuse everybody. Some user options (e.g., SURFACE AT) required the user to use the 1-33 system. The new commands (e.g., SURFACE CORNER) allow a choice of coordinate systems, through the use of an OFFSET command.

NAMES - Some option names (e.g., ITCUR) gave the user only a foggy notion of what they were for. The new option names (e.g., TANKCUR) are more informative.

STRUCTURE - The plotting options NCON, NDIR, and NDIV were unnecessarily complicated and restrictive. The new options (CONTOURS, 3D-VIEW, and MATVIEW) give more control over plots and are easier to use.

TABLE 2.1. NEW, REVISED, AND OBSOLETE OPTION WORDS

NEW FLUX SPECIFICATIONS

MAXWELLIAN
DOUBLE MAXWELLIAN
TYPE 5 (Direct Integration)
TYPE 6 (Multigun Test Tank)

NEW OPTION KEYWORDS

1. Coordinate Systems

   DIPOLE MOMENT
   OFFSET
   SURFACE CORNER
   ZTRUNCATE

2. Mnemonic Names

   CONVERGENCE PLOTS
   TANKCUR
   TANKTRAJ

3. Structural Simplification

   CONTOURS
   MATVIEW
   3D-VIEW

4. Extensions

   DESTINATION
   FLASHOVER
   TANK AXIS
   TANK RADIUS
   TITLE
   UPDATE

EXCLUDED OPTION KEYWORDS

1. Superseded Keywords

   NGPLOT --> CONTOURS
   ICON --> CONTOURS
   ICNVP --> CONVERGENCE PLOTS
   ITPART --> TANKTRAJ
   ITCUR --> TANKCUR
   IROUSP --> SHEATH
   MAXITR --> POTCON
   NCON --> CONTOURS
   NDIR --> 3D-VIEW
   NDIV --> MATVIEW
   SURFACE AT --> SURFACE CORNER
   TANKSIZE --> ZTRUNCATE
   NGPRT --> APRT
   DIPOLE --> DIPOLE MOMENT

2. Rarely Used

   MCYC
   DSCALE
   SHEATH SELF CONSISTENT
   PROGID (CDC only)
   IP, IR, IDIV, IV, ISPARE, IROUS,
   IOBJ, IOBPLT, ISAT, IPQCND,
   ILTBL, ICNOW, IKEYWD, IFLUX,
   IAREA, IPART (file numbers)

3. Functionally Obsolete

   NX
   NY
   ICREST
   IPREST

EXTENSIONS - New options associated with the discharge revision, environment extensions, and plotting revisions.

2.3.1.1 Flux Definition. In addition to the new user options, two flux type specifications have been added. 'MAXWELLIAN' and 'DOUBLE MAXWELLIAN' will perform the same function as 'TYPE 2' and 'TYPE 4', respectively.

Test tank (Type 1) and particle pushing (Type 3) flux types were not included on the Pocket Guide for reasons of space. Direct integration (Type 5), multigun test tank (Type 6) postdated the Pocket Guide.

2.3.1.2 Options Not Documented. Several options from the NASCAP User's Manual were not included in the Pocket Guide. These option keywords were left out for any one of these reasons:

1. Superseded by another (e.g., MAXITR replaced by POTCON).
2. Rarely or never used (e.g., file number keywords).
3. Reference obsolete functions (e.g., ICREST).

2.3.2 Description of New Options

CONTOURS NONE
CONTOURS STANDARD <MOD mod#>

CONTOURS $\begin{pmatrix} X \\ Y \\ Z \end{pmatrix}$ cut# <GRIDS ng# MOD mod#>

CONTOURS $\begin{pmatrix} X \\ Y \\ Z \end{pmatrix}$ cut# OFF

Determines contours to be plotted after each potential cycle. Replaces NCON, ICON, NGPLOT and the additional cards following NCON. Allows complete user control over potential contour plots.

Each instance of 'CONTOURS $\begin{pmatrix} X \\ Y \\ Z \end{pmatrix}$ cut#' adds a single potential contour to the contours table. GRIDS ng specifies the number of grids to be shown. Contours will be plotted whenever the cycle number minus one is divisible by mod#. If GRIDS and MOD are omitted, the outermost grid and a mod# of 1 are assumed.

Each 'CONTOURS $\begin{pmatrix} X \\ Y \\ Z \end{pmatrix}$ cut# OFF' eliminates a single entry from the contours table. If no such entry exists, it has no effect.

'CONTOURS NONE' erases the contours table.

'CONTOURS STANDARD' adds to the contours table six standard center cuts. It is equivalent to these six cards:

```
CONTOURS  X    0   GRIDS   1   MOD 1
CONTOURS  X    0   GRIDS  ng   MOD 1
CONTOURS  Y    0   GRIDS   1   MOD 1
CONTOURS  Y    0   GRIDS  ng   MOD 1
CONTOURS  Z    0   GRIDS   1   MOD 1
CONTOURS  Z    0   GRIDS  ng   MOD 1
```

where ng represents the number of the outermost grid.

Cut# is affected by the OFFSET keyword. The total number of contours allowed in the contour table is 14. For detailed examination of potential contours, use the interactive post-processor POTPLT.

The CONTOURS keyword is a Structural Simplification.

CONVERGENCE PLOTS ON
CONVERGENCE PLOTS OFF

Replaces ICNVP flag. If 'ON' then printer plots of potential solver convergence are included in printed listing. The default has been changed to 'OFF'.

DESTINATION dest

A plot destination may be specified for transmittal to the NASCAP*PLOTREAD program. The destinations are site-dependent. The default is 'NONE'.

At S-Cubed, valid destinations are

NONE	Request user input; write COMPRS file if EOF encountered.
COMPRS	
CALComp	
TEKTronix	
ELECtrostatic	

At NASA/LeRC valid destinations are

NONE	Quicklook + 24X microfiche
24X	Quicklook + 24X microfiche
48X	Quicklook + 48X microfiche
FILM	Quicklook + microfilm
ZETA	Quicklook + Zeta plot
QUICK	Quicklook only

This facility results from extension of the plotting package.

DIPOLE MOMENT px py pz AT x y z

Replaces DIPOLE. Places a magnetic dipole with moment (px, py, pz) at location (x, y, z). Affected by OFFSET. Coordinate System.

FLAShover volts

This specifies the potential difference (in volts) between two neighboring surface cells which will cause surface flashover if a discharge analysis is requested. The default is 10 kV. This is a NASCAP extension.

MATVIEW $\pm \begin{pmatrix} X \\ Y \\ Z \end{pmatrix}$ cuta# cutb#

MATVIEW NONE

Determines material plot views. Replaces NDIV and 1 to 6 cards following NDIV with 1 to 11 entries each.

When SATPLT is called, material plots are automatically generated. If the MATVIEW keyword has not been used, six default views will be generated.

Each material plot shows all the surface one would see looking from the specified direction. Cuta# and cutb# give limits, outside of which all surfaces are made invisible. This is handy for examining concave objects.

'MATVIEW NONE' clears the material views table, eliminating the default views and any other previously defined views.

'MATVIEW $\pm \begin{pmatrix} X \\ Y \\ Z \end{pmatrix}$ cuta# cutb#' adds one view to the material views table, up to a maximum of five per direction, or 30 total. Cuta# and cutb# are affected by the OFFSET keyword.

Assuming that OFFSET has not been used, the following set of keywords is equivalent to not using MATVIEW at all:

```
MATVIEW   NONE
MATVIEW   +X     -8     8
MATVIEW   -X     -8     8
MATVIEW   +Y     -8     8
MATVIEW   -Y     -8     8
MATVIEW   +Z    -16    16
MATVIEW   -Z    -16    16
```

The MATVIEW keyword is a Structural Simplification.

OFFSET x# y# z#

New keyword option. Allows user to place coordinate origin for RDOPT options. Works just like OFFSET command in Object Definition file. OFFSET during OBJDEF has no effect on OFFSET during RDOPT. New origin location is specified in "absolute" (1-33) coordinates. For example, specifying 'OFFSET 0 0 0' sets up the old NASCAP (1-17, 1-17, 1-33) coordinate system. Default offset is at mesh center, i.e., 'OFFSET 9 9 17' for the usual mesh. OFFSET should be placed first, or near the front of the OPT file, before other options affected by it. Coordinate System.

SURFACE CORNER x# y# z# <norx# nory# norz#>

Replaces SURFACE AT. Specifies surface cell for extra charging printout. x, y, and z are the coordinates of the lower left corner of the volume element out of which the surface points. Optionally, a surface normal can be specified, to distinguish between cells on the same element. (For geometrically complex objects, use TERMTALK to find the cell number and use 'SURFACE CELL cell#'.) The coordinate system is as specified by OFFSET, with default the "centered" (-16 to +16) system. This is the only difference between SURFACE AT and SURFACE CORNER. SURFACE AT uses the 1 to 33 coordinate system exclusively. (Note: Either keyword can only be used if OBJDEF has already been called; e.g., in a RESTART run.) Coordinate System.

TANK AXIS $\begin{pmatrix} X \\ Y \\ Z \end{pmatrix}$

The axis for a cylindrical tank may be specified. The default is Z. This option results from a NASCAP extension.

TANKCUR ON
TANKCUR OFF

Replaces ITCUR flag. If 'ON' then test tank current contour plots are output on graphics device. Mnemonic Aid.

TANK RADIUS x <METERS>

The radius of a cylindrical tank may be specified in grid units or meters. The default is a rectangular tank. This option also guarantees a grounded outer boundary. This is a NASCAP extension.

TANKTRAJ ON
TANKTRAJ OFF

Replaces ITPART flag. If 'ON' then test tank particle trajectory plots are output on graphics device. Mnemonic Aid.

TITLE title

A title to appear on the first plot frame (along with the date and time) may be specified beginning in column 9 of the input line. The title may have up to 56 characters. The default title is 'NASCAP'. This option results from extension of the plotting package.

UPDATE

The update feature allows the description of the plasma spectrum used by the code to be changed automatically to the most recent one available, drawn from a list of spectra and their associated time periods. For example, given a list of double Maxwellian spectra associated with successive 209 periods, as the accumulated timesteps exceed multiples of 205, the active plasma spectrum is updated to the most recent in the list. UPDATE is a NASCAP extension.

ZTRUNCATE zlo# zhi#

Replaces TANKSIZE. Reduces the z dimension of the outermost computational grid. Default is -16 to +16. Smallest allowable size is -8 to +8 (edges of next inner grid). This keyword is affected by OFFSET. Coordinate System.

3D-VIEW x y z
3D-VIEW NONE

Determines viewpoint for 3D object illustration plots. Replaces NDIR and succeeding DIROPT cards.

When SATPLT is called, 3D object illustration plots are automatically generated. If the 3D-VIEW keyword has not been used, three default viewpoints will be assumed.

'3D-VIEW NONE' clears the viewpoints table, eliminating the default views and any other previously defined views.

The maximum number of viewpoints allowed is five. For a detailed examination of a NASCAP object use the interactive program OBJCHECK.

The following series of keywords gives the same set of views as not using 3D-VIEW at all:

```
3D-VIEW  NONE
3D-VIEW   5    8    -5
3D-VIEW  -5    8     5
3D-VIEW   2   -5     5
```

The 3D-VIEW keyword is a Structural Simplification.

2.4 OUTPUT REVISIONS

NASCAP's printed output was reviewed and revised in order to reflect more clearly the input, the final result, and the physical processes leading thereto. In particular:

a. The option summary routine, SUMOPT, was rewritten to summarize options in a more clearly organized fashion and to be more indicative as to the option words available (Figure 2.1).

b. The format of the surface cell potential list was improved. Also, its initial values are printed for a RESTART run.

c. The output was clarified as to when a timestep begins and ends. Fluxes and currents were better defined as to initial or average values.

d. Units of current and charge were better defined.

e. Initial values of low energy electron fluxes were printed with limiting taken into account.

f. Superfluous output in the LIMCEL section was made optional or expunged.

g. The defaults for convergence plot and grid potential array printouts were changed to off.

```
                                        NASA CHARGING ANALYZER PROGRAM
                                              OPTION SUMMARY

TITLE =NASCAP

GRID SIZE OPTIONS:    NX    NY    NZ    NG
                      17    17    33     2
          FULL OUTER GRID USED
          ADDITIONAL OPTION WORDS: OFFSET, TANKSIZE, ZTRUNC

LOGICAL UNIT NUMBERS

          INPUT FILES: IKEYWD    ISAT     IFLUX    ISPCTR
                         26       20       22        9

          RESTART FILES: IP    IROUS   IPOCNO   ILIBL   ICNOW   IAREA
                         10      15       16      17      21      27

          SCRATCH FILES: IAUN    IR    IDIV    IU    ISPARE   IOBJ   IOBPLT   IPART
                         11     12     25     13      14      18      19      28

RUN MODE OPTIONS: ICREST   IPREST   NCYC   MCYC
                     0        0       1      1

                    DELTA      DELFAC
                 1.00+000   1.00+000
          DEADLINE = NONE
          ADDITIONAL KEYWORD = [RESTART]

POTENTIAL SOLVER OPTIONS: POTCON     MAXITR    IOUTER    SCALE
                          NOTSET       99         2       SCAL
                    SCALING KEYWORDS: SCALE, NOSCALE, DSCALE
          AMBIENT SPACE CHARGE OPTION [KEYWORD DEBYE]=NONE

CONDUCTOR FIXING AND BIASING:KEYWORDS FIXP, BIAS, FLOAT

INTERCONDUCTOR CAPACITANCES:  KEYWORD CIJ
          THE CODE UNIT OF CHARGE IS    8.854-013 COULOMBS.
          THE CODE UNIT OF CAPACITANCE IS    8.85-013 FARADS.
          NO INTERCONDUCTOR CAPACITANCES SPECIFIED.

LONGTIMESTEP AND DISCHARGE OPTIONS
          KEYWORDS: LONGTIMESTEP, NOLONGTIMESTEP, DISCHARGE, FLASHOVER
          LONGTIMESTEP HAS NOT BEEN REQUESTED.
          DISCHARGE ANALYSIS OFF

ILLUMINATION SPECIFICATIONS:
          SUNINT=   .000      SUNDIR =    .577*    .577*    .577*
          SHADOWING FORMULATION [KEYWORD=CONVEX]=SHAD

ENVIRONMENT TYPE AND MESH SIZE
          ITYPE=    2      UPDATE=OFF       XMESH=  1.00-001

           SECONDARY EMISSION FORMULATION ='ANGL'
           EFFECTIVE PHOTOSHEATH CONDUCTIVITY [EFFCON] = OFF

OUTPUT OPTIONS:
                     NGPRT [APRT]     TIMER [NOTIMER]
                        0                NO
                     ICNVP [CONVERGENCE PLOTS]= 0
          PRINT [NOPRINT]:  POTENT     LIMCEL     OBJDEF     HIDCEL
                              NO          NO         SOME       NO

     1 SURFACE CELLS SPECIFIED FOR I/O:
                    1
          KEYWORDS: [SURFACE CELL], [SURFACE AT], [SURFACE CORNER]

PLOT OPTIONS:  TITLE=NASCAP
          NGPLOT     ICON       REPEAT     ITPART     ITCUR      IROUSP
             0          0          1          0          0          0
          DEST = NONE
          NCON       NDIR
             0          3
          ADDITIONAL KEYWORDS: TANKCUR TANKTRAJ 3D-VIEW MATVIEW CONTOUR

      NO. OF ADDITIONAL CONTOUR PLOT CUTS =      0

      NO. OF 3-D PLOT VIEWS =      3

     VECTORS FROM SATELLITE CENTER TOWARD VIEWER ARE

                                                        -.5000      .8000      .5000
                                                        -.5000      .8000      .5000
                                                         .2000     -.5000      .5000

      NO. OF MATERIAL PLOT VIEWS [NDIV] =      1     1     1     1     1     1

PARTICLE TRACKING OPTIONS:
          KEYWORDS: EMITTER, NOEMITTER, SHEATH, SHEATH SELF-CONSISTENT

           NO EMITTERS REQUESTED

MAGNETIC FIELD OPTIONS: KEYWORDS [BFIELD], [DIPOLE]
          CONSTANT MAGNETIC FIELD =(    .00        .00        .00     ) W/M**2.
          NO MAGNETIC DIPOLES
```

Figure 2.1. New format for NASCAP option summary, indicating default options.

2.5 SECONDARY ELECTRON REVIEW

2.5.1 A Reformulation of Secondary Electron Emission

NASCAP calculates the secondary electron emission yield, δ, using the empirical formula:[1]

$$\delta = C \int_0^R \left|\frac{dE}{dx}\right| e^{-\alpha x}\, dx \qquad (2.1)$$

where x is the depth of penetration of a primary electron beam into the material, and R is the "Range", or maximum penetration depth.

Equation (2.1) is based upon a simple physical model:[2]

a. The number of secondary electrons produced by the primary beam at a depth x is proportional to the energy loss of the beam or "stopping power" of the material, $|dE/dx|$.

b. The fraction of the secondaries that migrate to the surface and escape decreases exponentially with depth ($f = e^{\alpha x}$). Thus only those produced within a few multiples of the distance $1/\alpha$ (the depth of escape) from the surface contribute significantly to the observed yield.

The range increases with the initial energy, E_o, of the incident electrons in a way that approximates a simple "power law":[3]

$$R = b\, E_o^n \qquad (2.2)$$

where $1.0 < n < 2.0$.

Equation (2.2) implies a simple form for the stopping power S(E):

$$S(E) = \left|\frac{dE}{dx}\right| = \left|\frac{dR}{dE_0}\right|^{-1} = \frac{E^{1-n}}{nb} \qquad (2.3)$$

Because the primary beam loses energy as it passes through the material, both E, and hence $S(E_0,x)$, depend on the depth x. Integrating (2.3):

$$E^n(x) = E_0^n - \frac{x}{b} \qquad (2.4)$$

$$S(x) = \frac{1}{nb}\left(\frac{b}{R - x}\right)^{1-1/n} \qquad (2.5)$$

The stopping power $S(E_0,x)$ depends upon both the initial electron energy E_0, via R, and the depth x. Figure 2.2a shows schematically $S(E_0,x)$ plotted against x for several values of E_0. Inspection of Figure 2.2 and Eq. (2.5) illustrates the following points:

1. $S(E_0,x)$ increases with x, slowly at first, before reaching a singularity as x approaches R.
2. The initial value of $S(E_0,x)$ decreases with increasing initial energy E_0.

Both of these observations are due to the decrease in electron-atom collision cross-section with increasing energy.

The yield is only sensitive to the details of the stopping-power depth-dependence for initial energies with ranges of the same order as the escape depth, $R \sim 1/\alpha$ (i.e., about the maximum of the yield

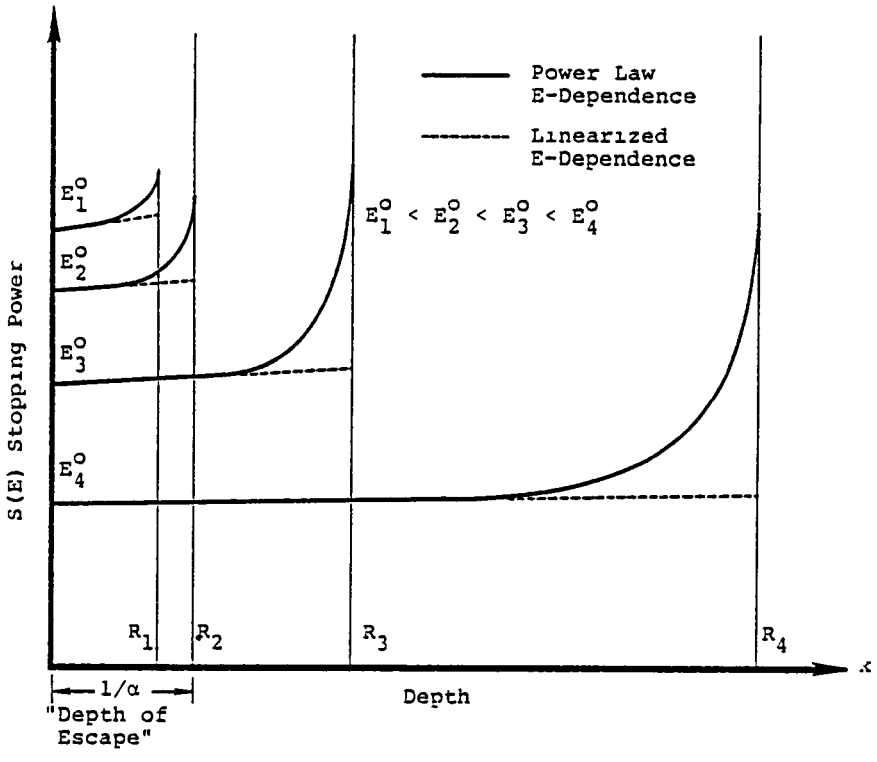

Figure 2.2a. Energy deposition profiles of primary electrons for incident energies E^o.

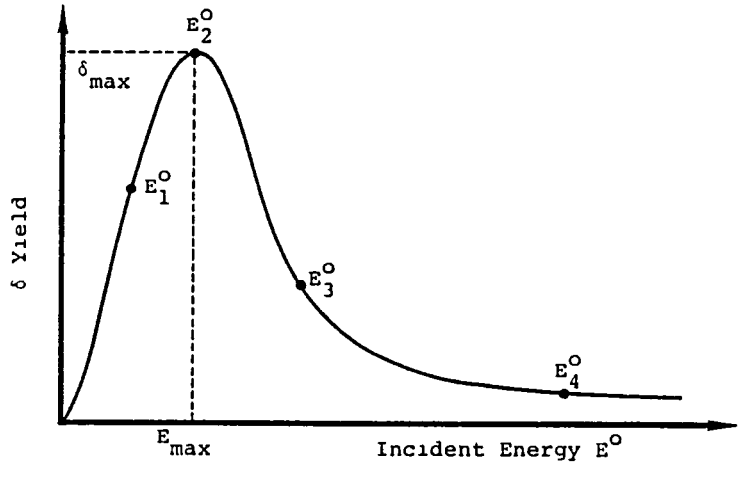

Figure 2.2b. Generalized yield curve.

curve). For lower energies, $R \ll 1/\alpha$, and essentially all of the primary energy is available for detectable secondary production, leading to a linear increase in yield with increasing E_0. At higher energies, where $R \gg 1/\alpha$, $S(E_0,x)$ remains almost constant, at its initial value, over the depth of escape and so, along with $S(E_0,x)$ the yield decreases as E_0 increases.

NASCAP takes this into account and approximates the stopping power by a linear expansion in x, about x = 0.

$$\frac{dE}{dx} = \left(\frac{dR}{dE_0}\right)^{-1} + \left(\frac{d^2R}{dE_0^2}\right)\left(\frac{dR}{dE_0}\right)^{-3} x \qquad (2.6)$$

NASCAP allows for a bi-exponential range law:

$$R = b_1 E_0^{n_1} + b_2 E_0^{n_2} \qquad (2.7)$$

involving four parameters b_1, b_2, n_1, n_2. The parameters are fit to reproduce range data as accurately as possible. For materials where no suitable data is available, a mono-exponential form is generated using Feldman's empirical relationships,[3] connecting b and n to atomic data. The stopping power is then obtained indirectly via Eq. (2.6). Recently good theoretical estimates of the stopping power for a number of materials have become available[4] (see below). Comparison of these values with those implied by the range data showed significant discrepancies, particularly for those materials fit using Feldman's formula.[3] A better approach is to fit the four parameters in (2.7) directly to the stopping power data.

$$S = \left(n_1 b_1 E^{n_1-1} + n_2 b_2 E^{n_2-1}\right)^{-1}$$

The method of fitting is described in Section 2.5.2.

Inspection of the tables of yields for the old and new input parameters shows that good agreement is found for most of the materials, particularly the metals. The major difference lies in the high energy "tail" of the kapton yield curve. The new version has a significantly damped high energy region compared with the old (e.g., the value at 50 keV is 3x higher for the old version). Damping also occurs for all but gold and teflon, by as much as 25 percent, in the high energy tail.

The effect of this will be to increase the charging rate of these materials (particularly kapton) for environments that sample these regions. Teflon is actually uniformly higher in the new version and so will charge at a slightly slower rate than before.

Experimental data[5] indicates that the original input parameters caused NASCAP to underestimate the rate of charging in some instances. These modified results may overcome this discrepancy.

The four parameters b_1, b_2, n_1, n_2, are fit to theoretical stopping power data rather than range data, providing a more direct contact between reliable information for $|dE/dx|$ and the yield.

2.5.2 Fitting of Four Parameter Form to Stopping Power Data

The form:

$$S(E) = \left(n_1 b_1 E^{n_1 - 1} + n_2 b_2 E^{n_2 - 1} \right)^{-1}$$

is fit to the available data using the following algorithm:

1. E = 1.0 keV is taken as a fixed point and

$$n_1 b_1 + n_2 b_2 = [S(E = 1.0)]^{-1}$$

2. Another fixed point is chosen - usually at or close to E_{max}. (If $E_{max} \sim 1.0$ keV another point further away is a better choice.)
3. All combinations of n_1 and n_2 between two limits and with a fixed step size are tried. The choice of n_1 and n_2 and the two equations above uniquely determine all four parameters.
4. The choice that minimizes the function:

$$Q = \left[\frac{(S_{fit} - S_{data})}{S_{data}}\right]^2$$

is found.

5. The fit can be weighted to various energy regions by including more points in these regions.

The fits tabulated below (Table 2.2) use the energies (keV) 0.1, 0.2, ... 1.0, 2.0, ... 10.0, 20.0, ... 50.0 where possible. For kapton and teflon data only up to 10 keV was available. However, using polystyrene as a test, the fit from 0.1-10.0 was found to give a reliable extrapolation to 50 keV. We use extrapolated values, therefore, for kapton and teflon. (Errors will tend to slightly overestimate S(E) for 10-50 keV.) It is also possible to fit the data to a three parameter form

$$S(E) = bE^{-(a+c \log_{10} E)}$$

This fit (Table 2.3) is compared to the four parameter fit for some of the materials in Table 2.4. Finally, Table 2.5 and Figures 2.3 and 2.4 compare the secondary yields for various materials using the old and new parameters.

TABLE 2.2. FOUR PARAMETER STOPPING POWER FITS

$$S = \left(n_1 b_1 E^{n_1 - 1} + n_2 b_2 E^{n_2 - 1} \right)^{-1}$$

Material	b_1	n_1	b_2	n_2
Au	88.79	0.92	53.48	1.73
Ag	84.46	0.82	79.43	1.74
Al	153.7	0.80	220.0	1.76
SiO_2	116.3	0.81	183.1	1.86
Polystyrene	88.42	0.67	371.7	1.79
Kapton	71.48	0.60	312.1	1.77
Teflon	45.37	0.40	217.6	1.77
Al_2O_3 (SOLAR)	77.5	0.45	156.1	1.73

TABLE 2.3. THREE PARAMETER STOPPING POWER FITS

$$S = bE^{-(a + c \log_{10} E)}$$

Material	$b(x10^{-3})$	a	c
Au	5.74	0.32	0.18
Ag	4.82	0.40	0.18
Cu	5.27	0.375	0.32
Ni	5.72	0.40	0.24
Si	1.98	0.58	0.17
Al	1.96	0.525	0.22
SiO_2	2.30	0.59	0.145
C_8H_8	1.38	0.66	0.11

TABLE 2.4. COMPARISON OF THREE AND FOUR PARAMETER FITS WITH ATAR[4]

$$S_3 = bE^{-(a + c \log_{10} E)}$$

$$S_4 = \left(n_1 B_1 E^{n_1 - 1} + n_2 B_2 E^{n_2 - 1} \right)^{-1}$$

Units of S = eV $\mathring{A}^{-1}$

1. GOLD

E	S_{ATAR}	S_4	S_3
0.1	7.94	8.66	7.92
0.2	8.20	8.23	7.85
0.3	7.79	7.79	7.53
0.5	7.01	7.04	6.90
1.0	5.74	5.74	5.74
2.0	4.37	4.33	4.43
3.0	3.75	3.56	3.68
5.0	2.84	2.69	2.80
10.0	1.75	1.77	1.82
50.0	0.60	0.60	0.50

2. SILVER

E	S_{ATAR}	S_4	S_3
0.1	7.04	7.69	8.00
0.2	7.20	7.43	7.49
0.3	6.91	7.00	6.97
0.5	6.27	6.20	6.13
1.0	4.82	4.82	4.82
2.0	3.44	3.42	3.51
3.0	2.80	2.71	2.83
5.0	2.09	1.97	2.07
10.0	1.26	1.24	1.27
50.0	0.39	0.39	0.30

TABLE 2.4. COMPARISON OF THREE AND FOUR PARAMETER FITS WITH ATAR (Continued)

3. ALUMINUM

E	S_{ATAR}	S_4	S_3
0.1	4.17	3.81	3.96
0.2	3.56	3.53	3.56
0.3	3.21	3.21	3.21
0.5	2.69	2.70	2.69
1.0	1.96	1.96	1.96
2.0	1.29	1.31	1.30
3.0	0.98	1.01	0.98
5.0	0.69	0.71	0.66
10.0	0.41	0.43	0.35
50.0	0.14	0.13	0.06

4. SiO_2

E	S_{ATAR}	S_4	S_3
0.1	4.62	5.18	6.41
0.2	4.71	4.69	5.05
0.3	4.20	4.18	4.27
0.5	3.37	3.39	3.36
1.0	2.30	2.30	2.30
2.0	1.48	1.43	1.48
3.0	1.12	1.05	1.11
5.0	0.77	0.70	0.76
10.0	0.46	0.40	0.42
50.0	0.09	0.10	0.09

5. POLYSTYRENE

E	S_{ATAR}	S_4	S_3
0.1	4.24	4.26	4.90
0.2	3.48	3.48	3.53
0.3	2.84	2.90	2.85
0.6	1.91	1.94	1.91
1.0	1.38	1.38	1.38
2.0	0.85	0.84	0.85
4.0	0.50	0.49	0.30
6.0	0.36	0.36	0.36
10.0	0.24	0.24	0.23
50.0	0.07	0.07	0.05

TABLE 2.4. COMPARISON OF THREE AND FOUR PARAMETER FITS WITH ATAR (Concluded)

6. KAPTON

E	S_{ATAR}	S_4	S_3
0.1	4.58	4.96	**
0.2	4.16	4.14	
0.3	3.44	3.47	
0.6	2.31	2.35	
1.0	1.68	1.68	
2.0	1.05	1.03	
4.0	0.63	0.61	
6.0	0.45	0.45	
10.0	0.30	0.31	
50.0	*	0.09	

* No Bethe data (readily) available.
** No three-parameter fit made.

7. TEFLON

E	S_{ATAR}	S_4	S_3
0.1	7.04	7.27	**
0.2	6.39	6.28	
0.3	5.27	5.27	
0.6	3.49	3.51	
1.0	2.48	2.48	
2.0	1.53	1.50	
4.0	0.91	0.89	
6.0	0.66	0.65	
10.0	0.44	0.44	
50.0	*	0.13	

* No Bethe data (readily) available.
** No three-parameter fit made.

TABLE 2.5. COMPARISON OF OLD AND NEW VERSION YIELDS

Old version uses old data, new version, new data. All data refers to a normal, monoenergetic beam.

1. GOLD $\delta_{max} = 0.88$, $E_{max} = 0.8$ keV.

E (kev)	δ_{old}	δ_{new}
0.1	0.234	0.266
0.2	0.432	0.472
0.3	0.590	0.624
0.5	0.792	0.806
1.0	0.858	0.778
2.0	0.613	0.650
3.0	0.475	0.521
5.0	0.346	0.388
10.0	0.225	0.253
50.0	0.083	0.085

2. SILVER $\delta_{max} = 1.000$, $E_{max} = 0.8$ keV.

E (kev)	δ_{old}	δ_{new}
0.1	0.266	0.289
0.2	0.490	0.518
0.3	0.670	0.692
0.5	0.900	0.908
1.0	0.975	0.937
2.0	0.696	0.692
3.0	0.540	0.532
5.0	0.393	0.379
10.0	0.256	0.236
50.0	0.094	0.075

3. ALUMINUM $\delta_{max} = 0.970$, $E_{max} = 0.3$ keV.

E (keV)	δ_{old}	δ_{new}
0.1	0.600	0.651
0.2	0.898	0.912
0.3	0.970	0.970
0.5	0.855	0.878
1.0	0.577	0.608
2.0	0.384	0.402
3.0	0.302	0.308
5.0	0.221	0.216
10.0	0.144	0.131
50.0	0.050	0.040

TABLE 2.5. COMPARISON OF OLD AND NEW VERSION YIELDS (Concluded)

4. SiO_2 $\delta_{max} = 2.4$, $E_{max} = 0.4$ keV.

E (keV)	δ_{old}	δ_{new}
0.1	1.094	1.233
0.2	1.875	1.960
0.3	2.287	2.308
0.5	2.325	2.339
1.0	1.507	1.565
2.0	0.887	0.994
3.0	0.662	0.686
5.0	0.462	0.454
10.0	0.285	0.256
50.0	0.094	0.065

5. KAPTON $\delta_{max} = 2.1$, $E_{max} = 0.15$ keV.

E (keV)	δ_{old}	δ_{new}
0.1	1.942	1.972
0.2	2.015	2.029
0.3	1.688	1.726
0.5	1.263	1.269
1.0	0.867	0.787
2.0	0.606	0.479
5.0	0.380	0.241
10.0	0.267	0.142
50.0	0.118	0.041

6. TEFLON $\delta_{max} = 3.0$, $E_{max} = 0.3$ keV.

E (kev)	δ_{old}	δ_{new}
0.1	1.751	1.971
0.2	2.737	2.798
0.3	3.000	3.000
0.5	2.546	2.615
1.0	1.495	1.514
2.0	0.875	0.889
3.0	0.642	0.650
5.0	0.433	0.439
10.0	0.250	0.257
50.0	0.065	0.075

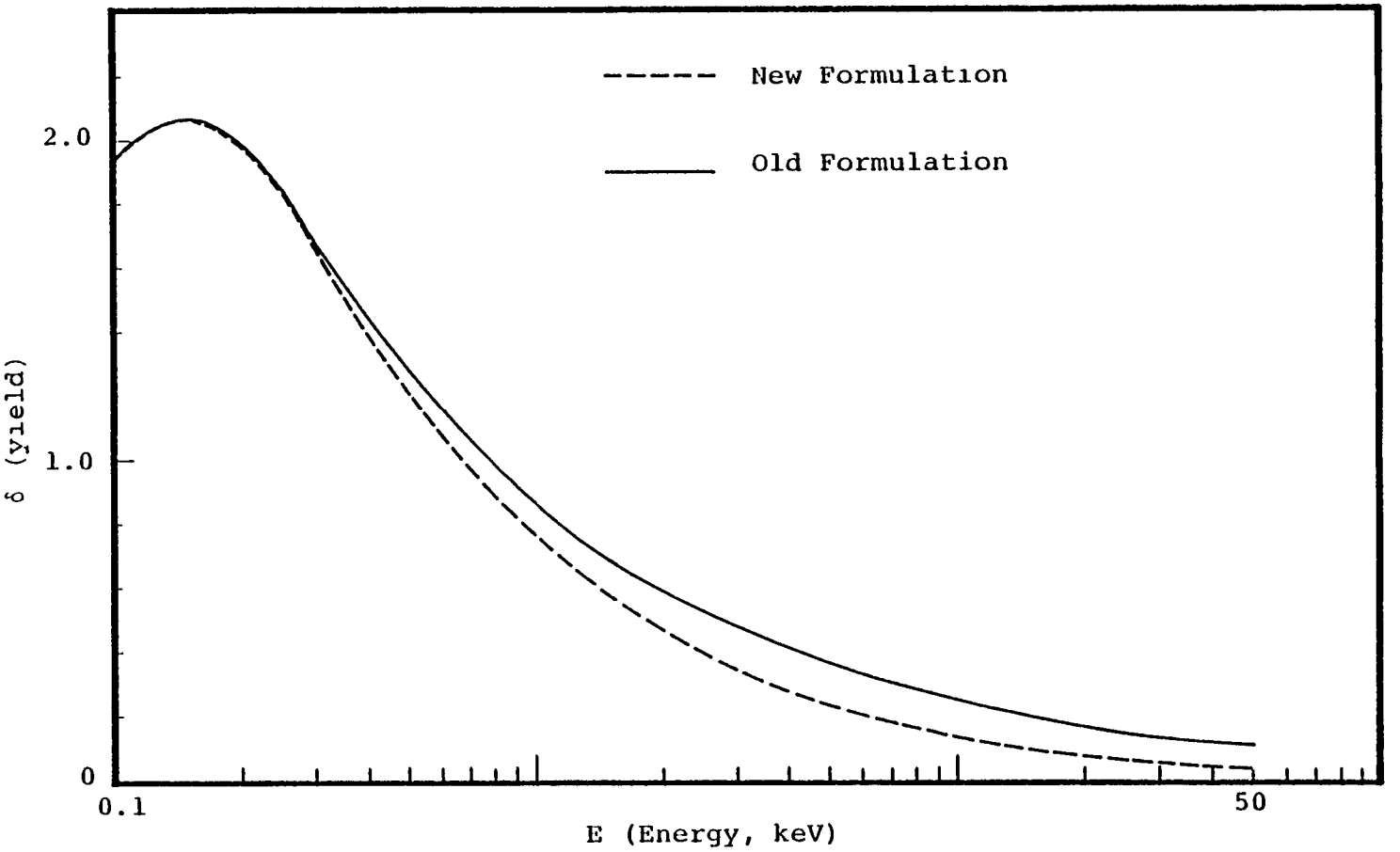

Figure 2.3. Comparison of new and old MATCHG yields for kapton.

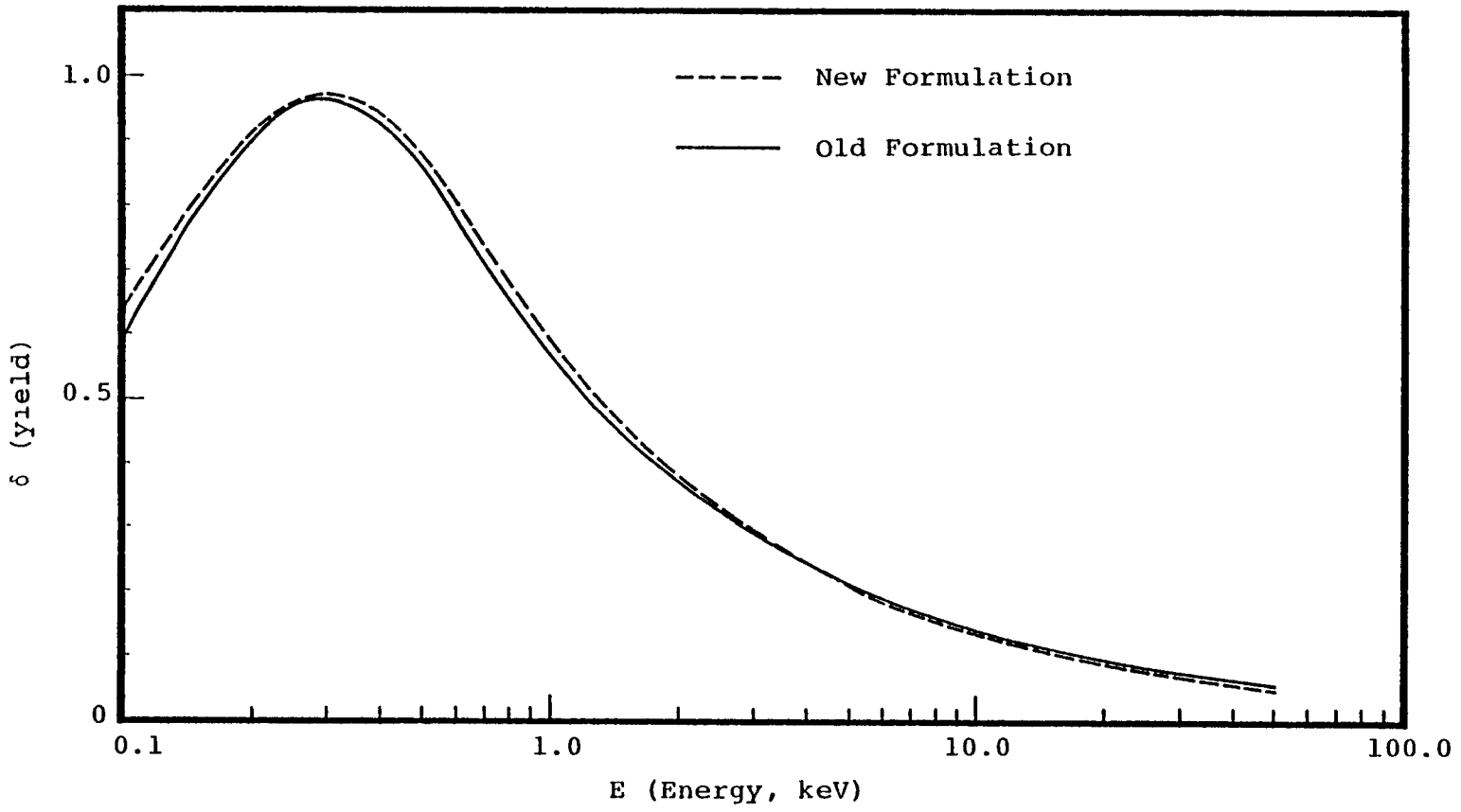

Figure 2.4. Comparison of new and old MATCHG yields for aluminum.

2.5.3 Ion-Induced Secondary Electron Emission

The NASCAP model assumes that all positively charged species in the plasma environment are protons H^+. Measurements made in geosynchronous orbit indicate in fact that often up to 80 percent of the ions present are O^+ rather than H^+. This observation calls into question the ion-impact induced, secondary electron current, calculated by the code assuming a purely proton environment.

Secondary emission of electrons following ion-surface impact can occur via two mechanisms.

a. Potential Emission

   This occurs via transfer of ion potential energy to lattice electrons at metal surfaces. Electrons tunnel into the potential well formed by the adsorption of the ion on the surface, neutralizing the ion, which then auto-ionizes. It is a low energy phenomenon (<20 eV) and is unimportant in most of the energy regime associated with NASCAP (0-50 keV).

b. Kinetic Emission

   Here emission results from the direct transfer of ion-kinetic energy to lattice electrons, and depends, in a complicated way, on the projectile/target atomic collision cross-section. It is the dominant mechanism in the energy range of interest.

The yield for both mechanisms does not appear to depend in any predictable way upon atomic number. The mechanism for potential emission is almost chemical in nature and depends much more upon electronic structure than nuclear mass. The most identifiable trend appears to be an increasing yield for projectile ions having greater electron affinities.

While the collision cross-section central to kinetic emission increases with atomic number of the projectile ion, the yield of escaping secondary electrons involves a trade-off between factors such as the efficiency of energy transfer per collision and the depth of penetration of the ion. This is rather poorly understood and experimental studies with rare gas ions impinging on clean metal surfaces show an irregular dependence of yield upon atomic number. For example, the energy/yield curves for Kr and Xe incident on Mo cross twice within the range 6-10 keV.

A table of secondary yields for ions of 1 keV incident on Mo is shown below.

TABLE 2.6. SECONDARY YIELD FOR 1 keV IONS ON Mo.

Ion	Yield (at 1 keV)
H^+	0.250
He^+	0.276
O^+	0.172

In this case the yields for H^+ and O^+ are of a similar magnitude. Very little additional data is available. The data that is available is often subject to large errors because of the sensitivity of measurements to the nature of the test surface. This coupled with the fairly large uncertainties in the measurement of O^+/H^+ ratios in space at any particular time leads us to the conclusion that adjustment of the code and/or data to take the presence of O^+ into account is not justified at this time. The magnitude of the adjustments to be made are smaller than the additional uncertainties that would be introduced.

3. NASCAP/GEO EXTENSIONS

3.1 OBJDEF EXTENSION

It is now possible to divide a square cell into two right triangles, either by superseding part of a square cell or by defining two complementary wedges. In particular, it is now possible to supersede a portion of an octagonal surface with a smaller octagon of different material. The extension involved changes to subroutines OBJDEF, WEDGE, CUBE56, NIOWGE, TETRAH, NIOTET, CONDUC, TRNGLS, CMPRSS, SPECEL, DELETE, RECTAN, NIOOBJ, PLATE, and new subroutines NORMSK, RTSUP, WRDSRT, SQUARE. Examples of previously illegal objects are shown in Figures 3.1 and 3.2.

3.2 NEW DISCHARGE CAPABILITY

The NASCAP discharge capability has been revised to be more realistic both as to the triggering configuration and the charge blowoff and redistribution. The old "discharge to space" has been expunged, and a flashover capability added. Reasonable estimates of blowoff of charge to space and to other surfaces have been included. The general principles and specific implementation are presented below.

3.2.1 General Principles Governing Discharges

1. A discharge analysis takes place at the end of the LIMCEL routine when DISCHArge d [$0 < d \leq 1$] has been specified in the RDOPT file.
2. Subroutine DISCHG looks for the "most severe" discharge, with punchthroughs taking priority over flashovers.
   a. A punchthrough takes place when the potential between an insulating surface and its underlying conductor exceeds (in absolute value) material property 16. The "severity" is measured by the ratio of differential voltage to discharge threshold.

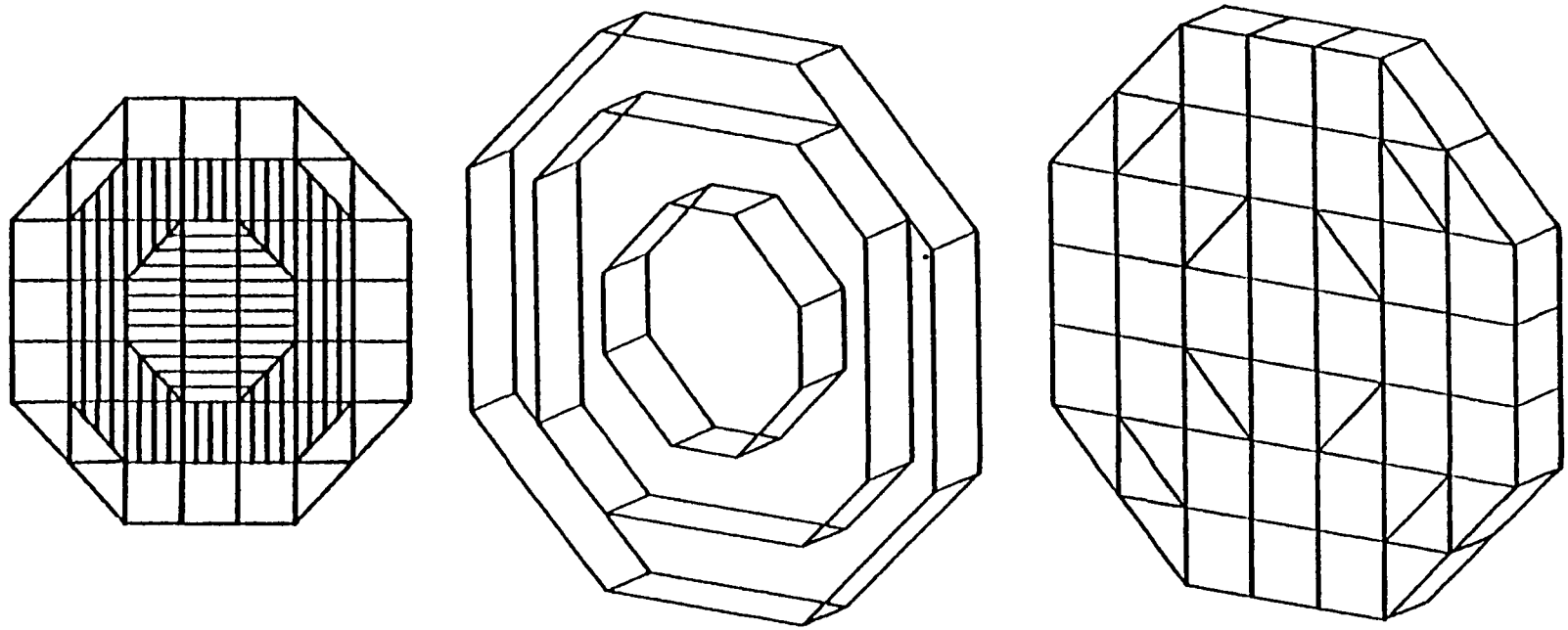

Figure 3.1. Three nested octagons.

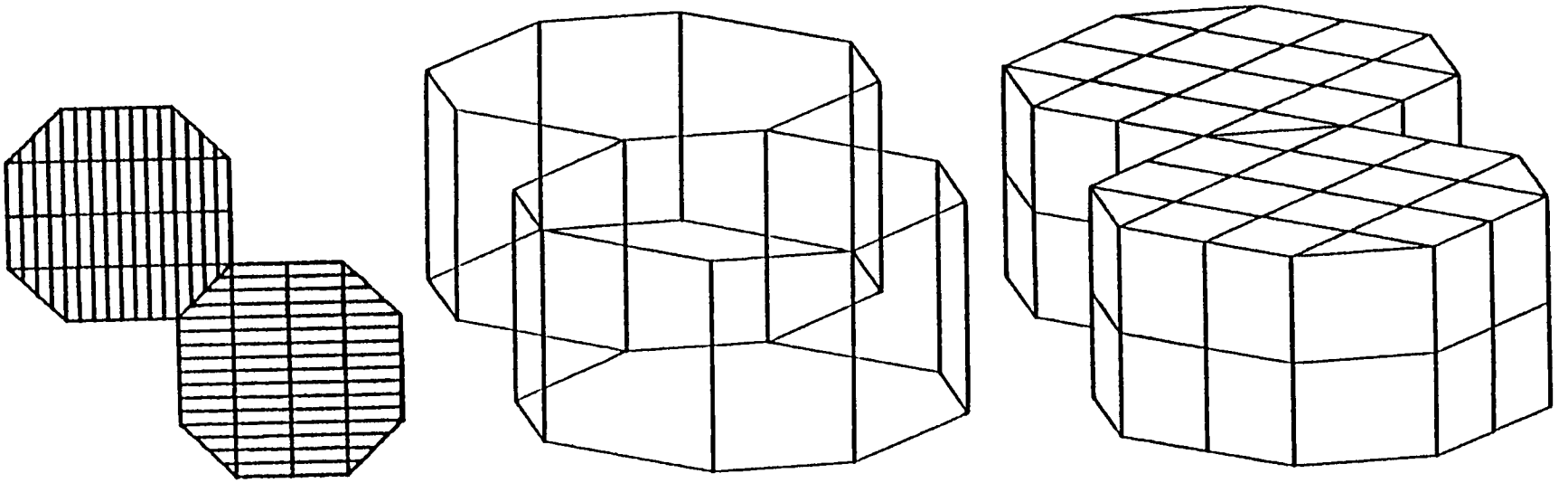

Figure 3.2. Two octagons meeting at a slanted side.

b. A flashover takes place when two cells sharing a common node differ in potential by more than the flashover threshold, entered in the RDOPT file through the keyword 'FLASHOver volts' (default 10 kV). Severity is similar to above.

c. After each discharge, charge is redistributed according to the rules below. New potentials are estimated by subroutine VPRED, and DISCHG is called again. The loop repeats, discharging one cell at a time until no further discharge conditions exist.

3. Charge Redistribution - General Rules

a. Under "fixed" potential conditions all charge lost by a negative dielectric is considered "blown off". This charge is immediately and implicitly replaced.

b. Negligible charge is assumed to flow through a punchthrough, with the exception of punchthrough of a positively charged dielectric, in which case all charge flows through the damage spot.

c. Under floating conditions charge lost by a negative dielectric is immediately blown off to the extent needed to bring the cell near zero potential. Remaining charge is distributed to more positive cells. This process takes $\sim 10^{-6}$ seconds, and typically leaves the satellite well above its "floating potential". Relaxation (typically taking $\sim 10^{-2}$ seconds) occurs during the next timestep(s).

3.2.2 Charge Redistribution - Specific Cases

Symbols:

- ΔQ - charge transferred from surface
- V_c - potential of relevant conductor
- V_{old} - cell potential before discharge
- V_{new} - cell potential after discharge, calculated as if conductor fixed
- V_{pt} - punchthrough threshold potential
- d - discharge relaxation factor
- V_{fl} - flashover threshold potential
- B - blowoff
- C_L - capacitance, cell to conductor
- C_S - cell capacitance to tank or plasma ground
- C_{TOT} - object capacitance

a. Punchthrough, negative dielectric, fixed potential

$V_{new} = V_c - d\ V_{pu}$

$\Delta Q = C_L\ (V_{old} - V_{new})$

$B = \Delta Q$

b. Punchthrough, negative dielectric, floating potential

$V_{new} = V_c - d\ V_{pu}$

$\Delta Q = C_L\ (V_{old} - V_{new})$

$B = C_{TOT}\ V_{old}\ (V_{old} < 0)$

$\Delta Q - B$ distributed to cells with $V > V_{new}$

c. Punchthrough, positive dielectric

$$V_{new} = V_c + d\,V_{pu}$$

$$\Delta Q = C_L\,(V_{old} - V_{new})$$

$$B = \begin{cases} 0 & V_{new} > 0 \text{ or fixed} \\ C_{TOT}\,V_{new} & V_{new} < 0 \text{ and floating} \end{cases}$$

d. Flashover, negative dielectric to conductor, fixed potential

$$V_{new} = V_c$$

$$\Delta Q = C_L\,(V_{old} - V_{new})$$

$$B = \Delta Q$$

e. Flashover, negative dielectric to conductor, floating potential

$$V_{new} = V_c$$

$$\Delta Q = C_L\,(V_{old} - V_{new})$$

$$B = C_{TOT}\,V_{old} \text{ (for } V_{old} < 0)$$

$\Delta Q - B$ distributed to cells with $V > V_{new}$

f. Flashover, positive dielectric to conductor

$$V_{new} = V_c + d\,V_{fl}$$

$$\Delta Q = C_L\,(V_{old} - V_{new})$$

$$B = 0$$

ΔQ transferred from dielectric to conductor

g. Flashover between two insulating cells - fixed potential

$V^i < V^j$

$V^i_{new} = V^j_{old} - d\ V_{fl}$

$\Delta Q = C^i_L\ (V^i_{old} - V^i_{new})$

$B = \Delta Q$

ΔQ transferred to conductor underlying i

h. Flashover between two insulating cells - floating potential

$V^i < V^j$

$$\Delta Q = \left(V^i_{old} - V^j_{old}\right) \Big/ \left[\left(C^i_L\right)^{-1} + \left(C^j_L\right)^{-1}\right]$$

$B = C_{TOT}\ V_{old}$

ΔQ - B distributed to more positive cells

i. Flashover between two conductors

$\Delta Q = C_{ij}\ (V^i_c - V^j_c)$

$B = 0$

(simple charge transfer)

3.3 MULTIPLE TEST TANK ENVIRONMENT

3.3.1 Theory

The existing versions of NASCAP model ground test experiments by using particle pushing techniques to simulate an electron gun. With this method the beam electron trajectories are approximated by calculating the actual trajectories of representative beam particles. While, in principle, enough particles could be followed to make the results as accurate as desired, in practice, computer time used to calculate each representative orbit places severe restrictions on the number of test particles followed. As a result, even for the present single gun, monoenergetic electron beam simulation, the particle pushing was taking upwards of a minute of CPU time per code timestep. The present technique, as implemented, had the added shortcoming of not correctly accounting for many cases of particle shadowing.

Using particle tracking to determine current density would quickly become unmanageable for a multi-gun, multi-energy simulation. If the present technique were used to simulate five guns of variable energy, it would easily take an hour of CPU time per code timestep. Following the basic philosophy that has been successful throughout NASCAP we opted instead to use a simplified representation of the space potentials which allows direct integration of particle orbit. Particle shadowing is included in an approximate manner using HIDCEL with the "viewer" located at the gun position.

The potential is modeled by keeping only one monopole term in the multipole expansion. This is a reasonable approximation for gun to satellite distance large compared to satellite radius.

To implement the proposed method of approach, consider a point source at a distance r_0 from the center of force (Figure 3.3). The rate at which the source emits electrons with kinetic energy E_0 into the interval dE_0 and the solid angle $d\Omega_0$ is denoted by

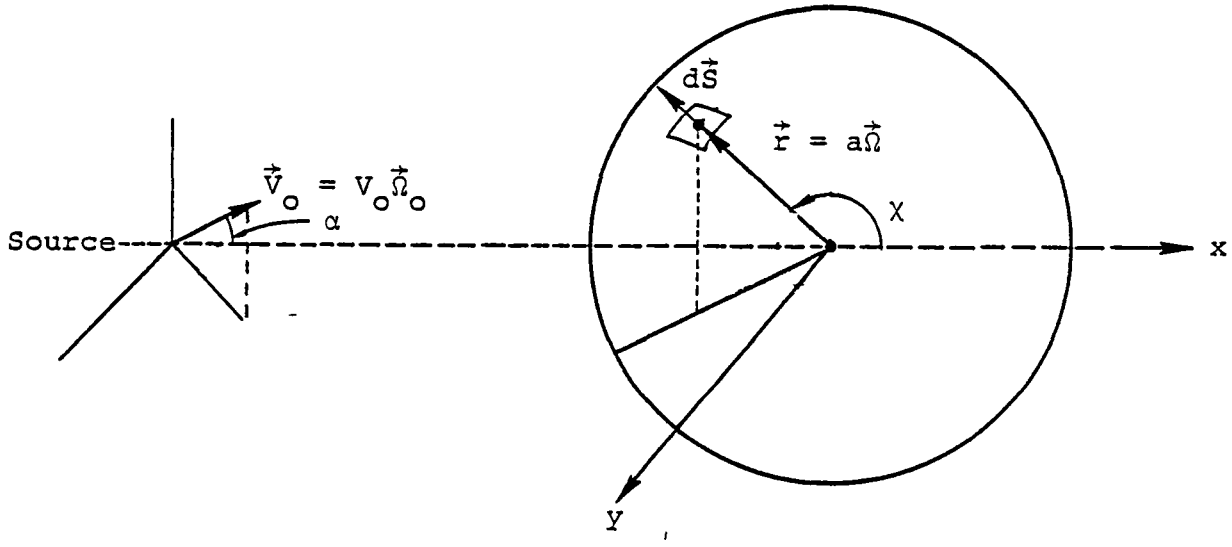

Figure 3.3. Geometry for electron gun aimed at a sphere.

$$\frac{d^2I}{dE_o d\Omega_o}(E_o,\vec{\Omega}_o)\, dE_o\, d\Omega_o \tag{3.1}$$

Particles leaving the source in the range $dE_o\ d\Omega_o$ about $(E_o,\vec{\Omega}_o 0)$ cross a surface element of area $d\vec{S}$ about the point $\vec{r} = \vec{r}(E_o,\vec{\Omega}_o)$ on a sphere of radius a with energies in the range dE. In a steady state particle conservation requires that

$$\int_{(\Delta E_o,\Delta\Omega_o)} \frac{d^2I}{dE_o d\Omega_o}\, dE_o d\Omega_o = \int_{(\Delta E,\Delta S)} \vec{j}\cdot d\vec{S}\, dE$$

$$= a^2 \int_{(\Delta E,\Delta\Omega)} \vec{j}\cdot\vec{n}\, dE\, d\Omega \tag{3.2}$$

where $\vec{j}$ is the current density per unit energy at $\vec{r},\Delta\Omega = \Delta S/a^2$ in the solid angle subtended by ΔS at the center of force, and $\vec{\Omega} = \vec{n} = \vec{r}/r$ is the unit vector normal to the surface of the sphere of radius r with center at the center of force. Since ΔE_o and $\Delta\Omega_o$ are arbitrary

$$|j\cdot n| = \frac{1}{a^2}\frac{d^2I}{dE_o d\Omega_o}\frac{1}{|J|} \tag{3.3}$$

where

$$J = \frac{\partial}{\partial}\left(\frac{E,\vec{\Omega}}{E_o\vec{\Omega}_o}\right) \tag{3.4}$$

Once $|j \cdot n|$ is determined, the current density $\vec{j}$ per unit energy follows from

$$\vec{j} = |\vec{j} \cdot n| \frac{\vec{V}}{\vec{V} \cdot \vec{\Omega}} \tag{3.5}$$

where $\vec{V} = \vec{V}(E_o, \vec{\Omega}_o)$ is the velocity at $\vec{r} = \vec{r}(E_o, \vec{\Omega})$.

The primary problem in the determination of $\vec{j}$ is the evaluation of the Jacobian. Consider first the case of no magnetic field and a repulsive potential $V = k/r$. The particles follow a hyperbolic path with the center of force at the focus. The geometry of the encounter is shown in Figure 3.4 where we also introduce the angular coordinate θ in terms of which the orbit is given by[6]

$$\frac{1}{r} = - \frac{mk}{\ell^2} (1 + \varepsilon \cos\theta) \ . \tag{3.6}$$

Here θ is measured from the symmetry axis of the orbit, m is the particle mass, $\ell = mv_o r_o \sin\alpha = (2mE_o)^{1/2} r_o \sin\alpha$ is the angular momentum, and

$$\varepsilon = \left[1 + 4 \left(1 + \frac{E_o}{V_o} \right) \frac{E_o}{V_o} \sin^2\alpha \right]^{1/2} \tag{3.7}$$

where $V_o = k/r_o$. In the following we shall use the orbit equation in the form

$$\cos\theta = - \frac{1}{\varepsilon} \left(\frac{2E_o}{V_o} \frac{\sin^2\alpha}{x} + 1 \right) \tag{3.8}$$

with $x = r/r_o$.

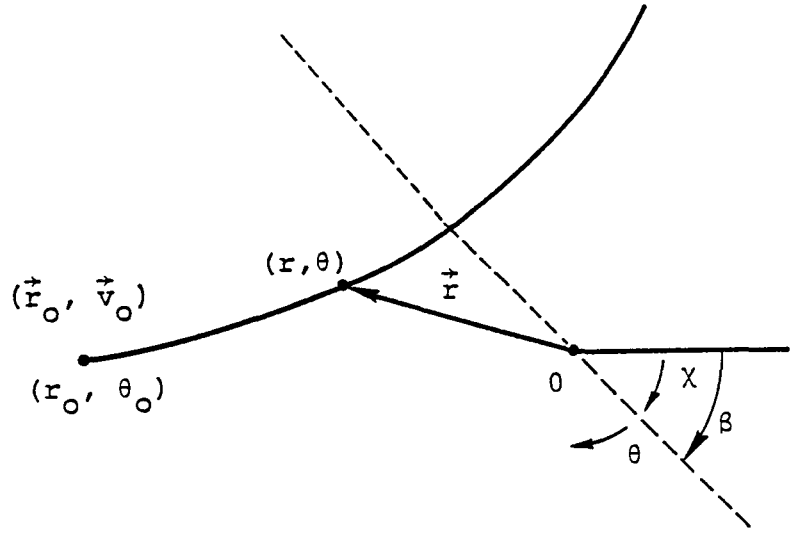

Figure 3.4. Geometrical quantities used to calculate current density.

For the present problem the required Jacobian is

$$J = \frac{\partial(\cos\chi)}{\partial\mu}$$

where

$$\cos\chi = -\cos(\theta-\theta_0)$$

$$= -(\cos\theta\cos\theta_0 + \sin\theta\sin\theta_0)$$

$$\mu = \cos\alpha$$

and $\cos\theta_0$ is obtained from Eq. (3.8) with x = 1. We find

$$J = -\frac{1}{\varepsilon}\left[\left(-\frac{\partial\varepsilon}{\partial\mu}\cos\theta + \frac{4E_0}{V_0}\frac{\mu}{x}\right)(\cos\theta_0 - \sin\theta_0\,\mathrm{ctn}\theta)\right.$$

$$\left. + \left(-\frac{\partial\varepsilon}{\partial\mu}\cos\theta_0 + \frac{4E_0}{V_0}\mu\right)(\cos\theta - \sin\theta\,\mathrm{ctn}\theta_0)\right]$$

with

$$\frac{\partial\varepsilon}{\partial\mu} = -\frac{4}{\varepsilon}\left(1 + \frac{E_0}{V_0}\right)\frac{E_0}{V_0}\mu$$

In the presence of a constant magnetic field, $\vec{B}$, spherical symmetry of the force field is lost and the simple analytic expressions for the particle orbit are not known. The problem simplifies considerably however if the magnetic field is small in a sense that will become clear as we consider the motion observed in a system rotating at a constant angular velocity $\vec{\omega}$. In the rotating

system the effective force is[7]

$$F_{eff} = q\left[\vec{E} + \frac{\vec{V}_s x \vec{B}}{c}\right] - 2m(\omega x \vec{V}_r) - m\vec{\omega}x(\vec{\omega}x\vec{r})$$

where

$$\vec{V}_r = \vec{V}_s - \omega x \vec{r}$$

and $\vec{V}_s$ and $\vec{V}_r$ are the velocities of the particle relative to the space and rotating axes respectively. If we choose

$$\vec{\omega} = -\frac{q\vec{B}}{2mc}$$

then

$$\vec{F}_{eff} = q\vec{E} + m\vec{\omega}x(\vec{\omega}x\vec{r})$$

Neglecting terms of second and higher order in the $\vec{B}$ field, the equation of motion in the rotating system becomes

$$m\frac{d\vec{V}_r}{dt} = q\vec{E} \ .$$

Thus, to the considered degree of approximation, in the rotating frame the effects of the magnetic field vanish and to the rotating observer the particle moves in a 1/r potential.

To find where a given particle strikes the body we can consider that during the particle's flight time the body rotates with constant angular velocity $-\vec{\omega}$. The magnitude of the rotation requires a knowledge of the flight time, which to the required order of accuracy

is given by

$$t = \int_{r}^{r_o} \frac{dr}{|\dot{r}|}$$

where

$$|\dot{r}| = \left[\frac{2}{m}\left(E_o - V_o\left(1 - \frac{r_o}{r}\right) - E_o \frac{r_o^2}{r^2} \sin^2\alpha\right)\right]^{1/2}$$

The foregoing expressions have been programmed to determine where a particle of given initial energy and direction strike the object that is being charged. The magnitude of the current striking the body is calculated as if there were no magnetic field. Corrections for the effect of $\vec{B}$ on the current striking the object could be made, but in view of the rough nature of the initial monopole approximation, such corrections are not warrented.

3.3.2 Implementation

3.3.2.1 General Considerations. NASCAP now has the capability of modeling exposure of an object in a test tank to several ion and electron guns. The guns may be arbitrarily located and directed, and their currents and angular widths are readily specified. A single gun may shoot a multi-energy beam, for a total of up to thirty beams. Because the incident fluxes and angles to each surface cell are calculated analytically (see above) rather than with particle tracking, this mode of calculation is fast-running and not subject to statistical noise. Optical shadowing is included for non-convex objects. The approximations work well for objects without excessive differential charging, and whose aspect ratios are not too large. Even for cases which do not meet the above criteria, qualitatively correct results may be expected.

3.3.2.2 Usage. The new test tank mode operates as flux type (ITYPE) 6. However, because an optical shadowing calculation (for non-convex objects) must be performed for each gun (requiring use of the HIDCEL routines) the flux definition must occur in a special code module, TANK, rather than being called from TRILIN. Also, this shadowing calculation destroys any previous HIDCEL information, so that the call to HIDCEL must follow the call to TANK (unless 'NOSHADOW' is specified). Of course, HIDCEL need not be invoked for simulations having no solar or ultraviolet illumination.

Some typical runstreams might be (in part)

1.
```
@USE  22,multiplegundefinitionfile
  .
  .
  .
@XQT  NASCAP
RDOPT
OBJDEF
CAPACI
TANK
TRILIN
END
```

or

2.
```
@XQT  NASCAP
RDOPT
TANK 5
@ADD  multiplegundefinitionfile
HIDCEL
TRILIN
END
```

or

```
3.  @ASG,A  prefix19
    @USE    19, prefix19
      .
      .
      .
    @XQT  NASCAP
    RDOPT
    TRILIN
    END
```

In all the above examples, the specification 'ITYPE 6' must be included in the options input file. The first example is appropriate to a new run, with an object exposed to particle beams in the dark. The second example allows the possibility of exposure to sunlight or an ultraviolet source. The third example takes advantage of previous storage of the gun shadowing information in file 19.

3.3.2.3 Gun Definition Input Specification. The TANK module consists of two major subroutines, INGUNS and GUNSHD. INGUNS reads user input and writes the gun specifications through subroutine CELLIO. GUNSHD performs a shadowing calculation using the gun location as a viewpoint, and writes the visibility factors on file IOBPLT [19]. If the object has been declared CONVEX, a visibility factor of unity is assigned to each surface cell.

The permissible gun definition input cards are:

OFFSET ix iy iz

Should be first card in file. Defines position relative to which gun locations are defined. Default is mesh center. OFFSET 0 0 0 will make gun positions defined in "absolute" grid location.

GUN AT x y z

ELECTRON GUN AT x y z

ION GUN AT x y z

Defines position and type of gun. If gun type not specified, electron gun is assumed.

ENERGY } $e_1 \ldots e_n$ unit
ENERGIES }

Defines beam energies of gun. Unit is 'EV' or 'KEV'. The default unit is 'KEV'.

BEAMWIDTH(S) $b_1 \ldots b_n$ unit

Defines half-angle of beam. Unit is assumed to be radians, unless 'DEGREES' is specified.

ALL BEAMWIDTHS b unit

Assigns b as the beamwidth for all beams of this gun.

CURRENT(S) $c_1 \cdots c_n$

Specifies beam currents in amperes.

ALL CURRENTS c

Assign c as current for all beams of this gun.

NOSHADOW

Indicates that file IOBPLT [19] already exists for guns at these locations.

ION MASS m unit

Defines mass for an ion gun. Unit is assumed kilograms unless 'AMU' is specified.

DIRECTION x y z

Specifies direction in which gun is pointing.

END

Ignore subsequent cards.

3.3.2.4 Examples. The first example defines four guns pointing at the mesh center, each from a distance of 22.6 grid units. After echoing the gun definition input (which concludes with an 'END' card or end-of-file condition), the gun characteristics are echoed for each gun, and for each beam. It is then indicated that a shadowing calculation is being performed for each gun.

The second example defines an ion gun. As the 'NOSHADOW' specification is included, the purpose of this input is presumably to change the beamwidth, current, or energy.

Example 3 defines a two-beam electron gun with different current and beamwidth for each energy. Example 4 defines a three-beam electron gun with equal currents and beamwidths.

```
 1.                    GUN AT 0 16 16
 2.                    ENERGY 6. KEV
 3.                    CURRENT 5.E-6
 4.                    BEAMWIDTH 30 DEGREES
 5.                    DIRECTION 0 -1 -1
 6.                    GUN AT 0 -16 16
 7.                    ENERGY 6. KEV
 8.                    CURRENT 5.E-6
 9.                    BEAMWIDTH 30 DEGREES
10.                    DIRECTION 0 1 -1
11.                    GUN AT 0 -16 -16
12.                    ENERGY 6. KEV
13.                    CURRENT 5.E-6
14.                    BEAMWIDTH 30 DEGREES
15.                    DIRECTION 0 1 1
16.                    GUN AT 0 16 -16
17.                    ENERGY 6. KEV
18.                    CURRENT 5.E-6
19.                    BEAMWIDTH 30 DEGREES
20.                    DIRECTION 0 -1 1
21.                    END
```

Gun definition input for example 1.

```
 1.                    ION GUN AT -44., 0.5, 6.2
 2.                    NOSHADOW
 3.                    ION MASS 14 AMU
 4.                    BEAMWIDTH 20 DEGREES
 5.                    CURRENT 5.E-6
 6.                    ENERGY 5000 EV
 7.                    DIRECTION 3. 0. 1.
 8.                    END
```

Gun definition input for example 2.

```
 1.                    ELECTRON GUN AT -20 0. 0.
 2.                    DIRECTION 1 0 0
 3.                    ENERGIES 0.1  10 KEV
 4.                    BEAMWIDTHS  40  10  DEGREES
 5.                    CURRENTS 1.E-6  0.5E-6
 6.                    END
```

Gun definition input for example 3.

```
 1.                    ELECTRON GUN AT 50 35 4
 2.                    DIRECTION -2 -1 0
 3.                    ENERGIES 5 10 20 KEV
 4.                    ALL BEAMWIDTHS 25 DEGREES
 5.                    ALL CURRENTS 1.E-6
 6.                    END
```

Gun definition input for example 4.

```
******TANK 5

  OBJECT DEFINITION INFORMATION BEING READ FROM FILE

A SHADOWING TABLE WAS PREVIOUSLY GENERATED
 FOR THIS OBJECT USING THE GUNS OPTION
GUN AT 0 16 16
ENERGY 6. KEV
CURRENT 5.E-6
BEAMWIDTH 30 DEGREES
DIRECTION 0 -1 -1
GUN AT 0 -16 16
ENERGY 6. KEV
CURRENT 5.E-6
BEAMWIDTH 30 DEGREES
DIRECTION 0 1 -1


GUN AT 0 -16 -16
ENERGY 6. KEV
CURRENT 5.E-6
BEAMWIDTH 30 DEGREES
DIRECTION 0 1 1
GUN AT 0 16 -16
ENERGY 6. KEV
CURRENT 5.E-6
BEAMWIDTH 30 DEGREES
DIRECTION 0 -1 1
END

 GUN DEFINITION ------
GUN  1 HAS BEEN DEFINED AS AN ELECTRON GUN
GUN IS LOCATED AT GRID COORDINATES   9.00  25.00  25.00
GUN DIRECTION IS     .00  -1.00  -1.00
BEAM  1: ENERGY=  6.00+003 EV    CURRENT=  5.00-006 AMPS   CUT-OFF ANGLE= 30.0000 DEGREES

 GUN DEFINITION ------
GUN  2 HAS BEEN DEFINED AS AN ELECTRON GUN
GUN IS LOCATED AT GRID COORDINATES   9.00  -7.00  25.00
GUN DIRECTION IS     .00   1.00  -1.00
BEAM  1: ENERGY=  6.00+003 EV    CURRENT=  5.00-006 AMPS   CUT-OFF ANGLE= 30.0000 DEGREES

 GUN DEFINITION ------
GUN  3 HAS BEEN DEFINED AS AN ELECTRON GUN
GUN IS LOCATED AT GRID COORDINATES   9.00  -7.00  -7.00
GUN DIRECTION IS     .00   1.00   1.00
BEAM  1: ENERGY=  6.00+003 EV    CURRENT=  5.00-006 AMPS   CUT-OFF ANGLE= 30.0000 DEGREES

 GUN DEFINITION ------
GUN  4 HAS BEEN DEFINED AS AN ELECTRON GUN
GUN IS LOCATED AT GRID COORDINATES   9.00  25.00  -7.00
GUN DIRECTION IS     .00  -1.00   1.00
BEAM  1: ENERGY=  6.00+003 EV    CURRENT=  5.00-006 AMPS   CUT-OFF ANGLE= 30.0000 DEGREES
SHADOWING BEING CALCULATED FOR GUN   1
 DISTANCE EQUALS  22.627417

FINAL NA1 =    20
SHADOWING BEING CALCULATED FOR GUN   2
 DISTANCE EQUALS  22.627417

FINAL NA1 =    20
SHADOWING BEING CALCULATED FOR GUN   3
 DISTANCE EQUALS  22.627417

FINAL NA1 =    20
SHADOWING BEING CALCULATED FOR GUN   4
 DISTANCE EQUALS  22.627417

FINAL NA1 =    20
```

Gun definition (INGUNS and GUNSHD) output for example 1.

```
******TANK 5
ION GUN AT -44., 0.5, 6.2
NOSHADOW
ION MASS 14 AMU
BEAMWIDTH 20 DEGPEES
CURRENT 5.E-6
ENERGY 5000 EV
DIRECTION 3. 0. 1.
END


 GUN DEFINITION ------
GUN  1 HAS BEEN DEFINED AS AN ION GUN WITH AN ION MASS=  2.34-026 KILOGRAMS.
GUN IS LOCATED AT GRID COORDINATES -35.00   9.50  15.20
GUN DIRECTION IS   3.00     .00    1.00
BEAM  1: ENERGY=  5.00+003 EV    CURRENT=  5.00-006 AMPS   CUT-OFF ANGLE= 20.0000 DEGREES
```

Gun definition (INGUNS and GUNSHD) output for example 2.

```
******TANK 5
ELECTRON GUN AT -20 0. 0.
DIRECTION 1 0 0
ENERGIES 0.1  10 KEV
BEAMWIDTHS  40  10  DEGREES
CURRENTS 1.E-6  0.5E-6
END

 GUN DEFINITION ------
GUN  1 HAS BEEN DEFINED AS AN ELECTRON GUN
GUN IS LOCATED AT GRID COORDINATES -11.00   9.00   9.00
GUN DIRECTION IS   1.00     .00     .00
BEAM  1: ENERGY=  1.00+002 EV    CURRENT=  1.00-006 AMPS   CUT-OFF ANGLE= 40.0000 DEGREES
BEAM  2: ENERGY=  1.00+004 EV    CURRENT=  5.00-007 AMPS   CUT-OFF ANGLE= 10.0000 DEGREES
SHADOWING BEING CALCULATED FOR GUN   1
 DISTANCE EQUALS  20.000000

FINAL NA1 =    16
```

Gun definition (INGUNS and GUNSHD) output for example 3.

```
******TANK 5
ELECTRON GUN AT 50 35 4
DIRECTION -2 -1 0
ENERGIES 5 10 20 KEV
ALL BEAMWIDTHS 25 DEGREES
ALL CURRENTS 1.E-6
END

 GUN DEFINITION ------
GUN  1 HAS BEEN DEFINED AS AN ELECTRON GUN
GUN IS LOCATED AT GRID COORDINATES  59.00  44.00  13.00
GUN DIRECTION IS  -2.00  -1.00     .00
BEAM  1: ENERGY=  5.00+003 EV    CURRENT=  1.00-006 AMPS   CUT-OFF ANGLE= 25.0000 DEGREES
BEAM  2: ENERGY=  1.00+004 EV    CURRENT=  1.00-006 AMPS   CUT-OFF ANGLE= 25.0000 DEGREES
BEAM  3: ENERGY=  2.00+004 EV    CURRENT=  1.00-006 AMPS   CUT-OFF ANGLE= 25.0000 DEGREES
SHADOWING BEING CALCULATED FOR GUN   1
 DISTANCE EQUALS  61.163713

FINAL NA1 =    28
```

Gun definition (INGUNS and GUNSHD) output for example 4.

3.3.3 Cylindrical Tank

The Cylindrical Tank option has now been implemented in NASCAP. This mode is invoked by the option file input cards

```
TANK RADIUS x [METERS]
TANK AXIS   a
```

where a is 'X', 'Y', or 'Z'. The default tank axis is Z. If the word 'METERS' is omitted, x is assumed given in inner grid units; if 'METERS' is specified, the value is immediately converted to grid units using the current value of XMESH. The default tank radius is 'NOPE'.

When the cylindrical tank is requested, the RDOPT subroutine sets IOUTER = 0 and POTSCL = 'NOSCALE'. This is needed because the total charge (found by QSUMER) will not be correct, as the electric field will be integrated only over the end walls of the tank. On contour plots, the tank wall is drawn as a double blue circle for cuts normal to the axis, and as two sets of double blue lines for cuts parallel to the tank axis. (See Figures 3.5-3.6.)

Examples

```
TANK RADIUS   12.
TANK AXIS     Z
```

Defines a tank with radius 12 inner grid units about Z-axis.

```
XMESH   0.3
TANK RADIUS   5 METERS
TANK AXIS   Y
```

Defines a tank with radius 16.7 grid units about Y-axis.

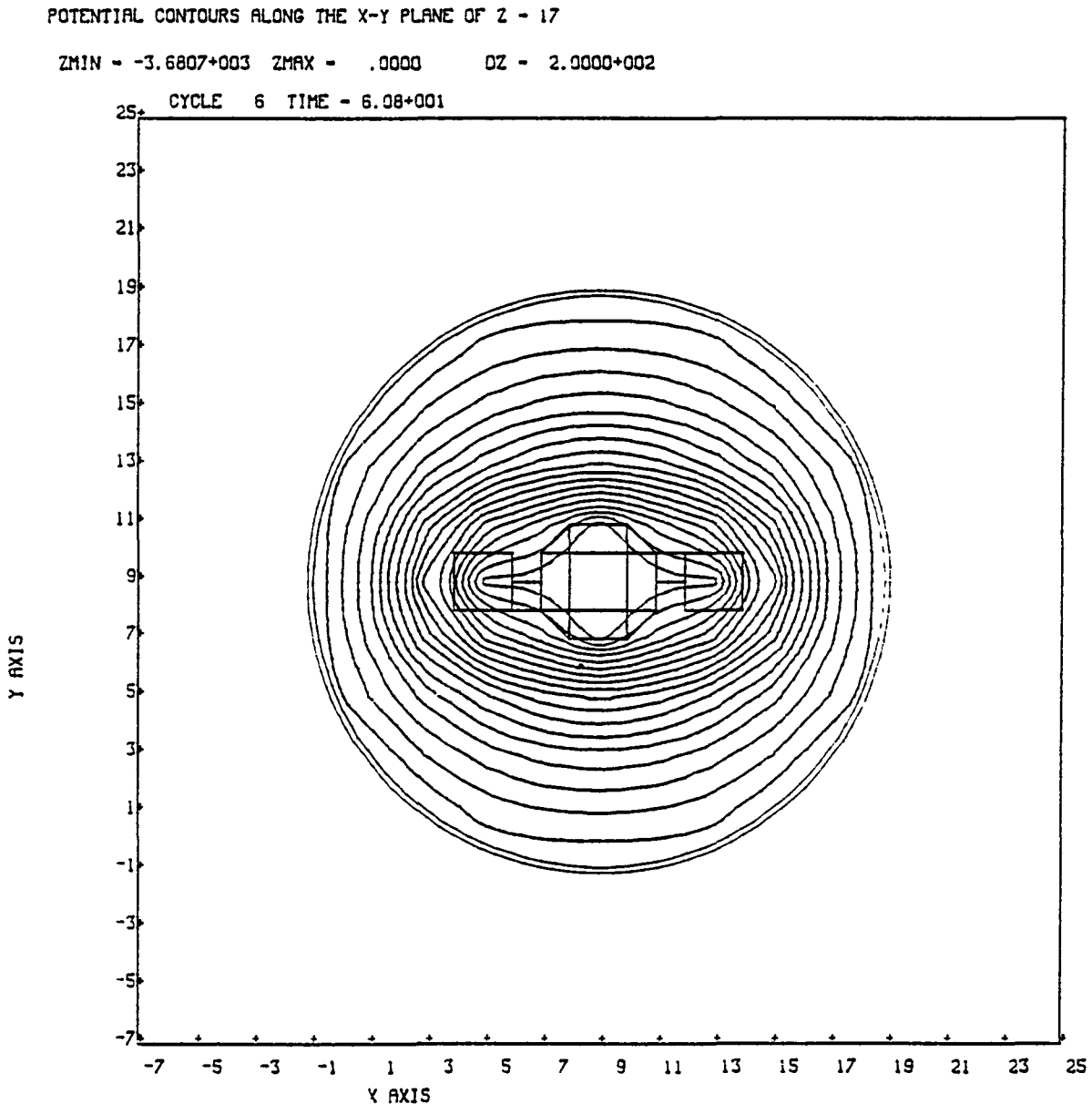

Figure 3.5. Potential contours — cylindrical tank of radius 10 grid units about Z-axis.

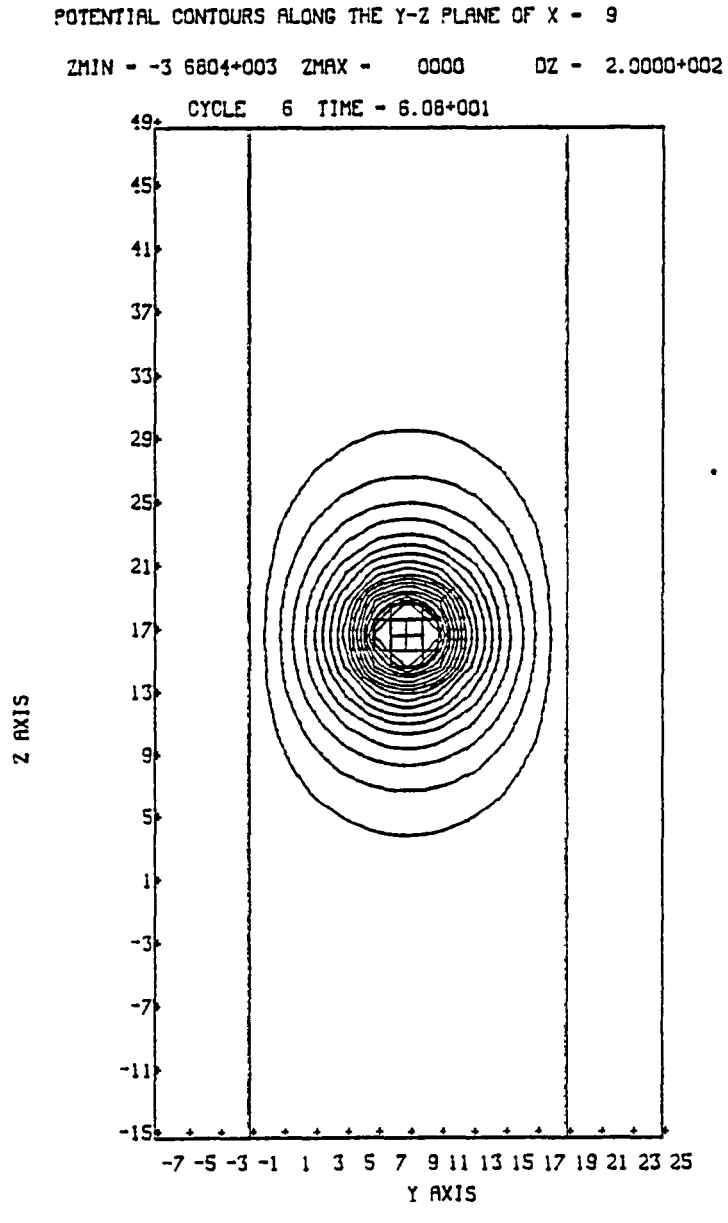

Figure 3.6. Potential contours — cylindrical tank of radius 10 grid units about Z-axis.

3.4 SPACE ENVIRONMENT

3.4.1 Anisotropic Flux

The NASCAP model formerly allowed only for incident electron and ion fluxes that are isotropic; i.e., all incident directions are considered equally likely. This is not usually true for orbiting satellites.

Injection of a charged particle into a static magnetic field causes the particle to follow a spiraling trajectory about the magnetic lines of force. The component of its velocity $\vec{v}_{||}$ along the field direction is unchanged and the radius of the spiral trajectory r_L depends on the perpendicular component $\vec{v}_{\perp}$

$$r_L = \frac{mv_{\perp}}{qB}$$

Thus for a fixed velocity magnitude, $|v|$, injection of a flux of charged particles into a magnetic field will lead to fast moving particles (in the field direction) with small Larmor radii (r_L), and slower particles with large radii.

Similar events occur in the earth's magnetic field. Plasma is injected into normally low-density regions and the particles begin an orbiting trajectory along the field lines. A satellite bathed in this orbiting plasma will experience a flux with two principal components:

a. A background, essentially isotropic, flux consisting of the pre-existing low density plasma, and particles from the injected plasma, that have r_L much greater than the spacecraft's dimensions.

b. A directional flux, aligned with the terrestrial field, consisting of particles with r_L smaller than the spacecraft dimensions. This can be a negative contribution. If some of the injected plasma has passed the poles several times, the faster moving particles will have been "filtered out" leaving a reduced flux in the field direction (a "loss-cone").

This model is too simplistic to account for all of the varied magnetic phenomena that can occur in earth orbit. However, it does illustrate the features that are desirable in a model incorporating anisotropic flux distribution.

The form introduced into the NASCAP model consists of a background isotropic component and a $\cos^2\theta$ distribution aligned with the field direction. The shape of such a form depends on just one parameter: the ratio of integrated flux for each component, R.

3.4.1.1 The Coordinate System. The most convenient coordinate system in which to represent the aligned component is the "fan"-like system shown in Figure 3.7. The angle of incidence β of an incoming vector $\vec{r}$ is related to the two angles of rotation shown, θ and ϕ, by the relationship

$$\cos\beta = \cos\theta \cos\phi$$

Rotating the "fan" from a plane containing the surface normal to a plane containing the vector $\vec{r}$ only partially defines the angle θ. The choice of θ becomes unique when the second rotation (ϕ) within the plane of the "fan", to reach $\vec{r}$, is specified. The coordinate system is chosen so that the magnetic field direction $\vec{B}$ has $\phi = 0$. This provides a reference point for all other vectors in the space above the surface, and hence fully defines the θ, ϕ coordinate system.

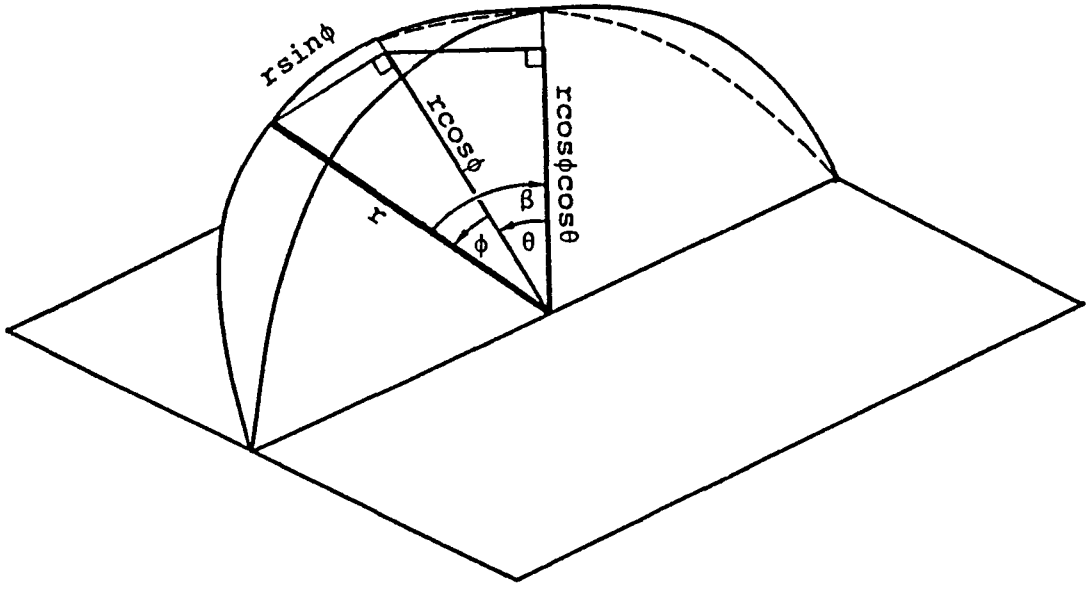

Figure 3.7. The projection of an incident vector $\vec{r}$ upon the surface normal, in the "fan-like" coordinated system.

3.4.1.2 Angular Distribution Function. The angular distribution function is assumed to be symmetric about the field direction, and so the aligned component depends only upon the angle ψ made between a vector $\vec{r}$ and $\vec{B}$, the field direction

$$\cos\psi = \cos(\theta-\theta_0)\cos\phi$$

The form we choose for the aligned component is simply $\cos^2\psi$, i.e., the angular distribution function $f(\theta,\phi)$ becomes

$$f(\theta,\phi) = a + b\cos^2(\theta-\theta_0)\cos^2\phi$$

Integration over the half-sphere must be normalized to 2π.

$$\int_{1/2} f(\theta,\phi)d\omega = 2\pi$$

In the "fan" coordinate system:

$$d\omega = \cos\phi\, d\phi\, d\theta$$

$$\therefore \int_{-\pi/2}^{\pi/2}\int_{-\pi/2}^{\pi/2} \left(a + b\cos^2(\theta-\theta_0)\cos^2\phi\right)\cos\phi\, d\theta\, d\phi = 2\pi$$

$$\therefore 2\pi a + \frac{2\pi b}{3} = 2\pi$$

i.e.,

$$a + \frac{b}{3} = 1$$

We define the ratio of integrated fluxes R as

$$R = b/3a$$

$$\therefore \quad a = 1/(1 + R)$$

$$b = 3R/(1 + R)$$

Thus overall the angular distribution function depends only upon two parameters:

1. The angle θ_o between the field direction $\vec{n}_B$ and the surface normal $\vec{n}$.
   $\cos\theta_o = \vec{n}_B \cdot \vec{n}$.
2. The ratio R.

While this form for $f(\theta,\phi)$ cannot represent exactly all possible angular distributions it does, in a simple way, model the most commonly observed situations of enhancement of flux incident along the field lines (R is positive) and a "loss-cone" along the field direction (R is negative).

NASCAP allows for a table of R(E) values for different incident energies to be entered. The code then automatically takes the variation in anisotropy as a function of energy into account when calculating currents.

3.4.1.3 Current Collection. For particles incident with an energy E, the incoming current FIN(E) is given by:

$$FIN(E) = F(E) \int_{-\pi/2}^{\pi/2} \int_{-\pi/2}^{\pi/2} \left(a(E)+b(E)\cos^2(\theta-\theta_o)\cos^2\phi\right) \cos\theta\cos^2\phi \, d\theta \, d\phi$$

where for a Maxwellian

$$F(E) = \frac{N}{\pi}\left(\frac{T}{2\pi m}\right)^{1/2} e^{-E/T}$$

Integrating gives

$$FIN(E) = F(E)\left[a(E) + \frac{3b(E)}{8}\left(1 + \frac{\cos 2\theta_o}{3}\right)\right]$$

Integrating over the plasma energy spectrum gives the observed incident current FIN. The emitted current is more complex since all of the integrals cannot be performed analytically.

$$FOUT(E) = \frac{F(E)}{\pi}\int_{-\pi/2}^{\pi/2}\int_{-\pi/2}^{\pi/2} \delta(\beta)(E)\left[a(E)+b(E)\cos^2(\theta-\theta_o)\cos^2\phi\right]$$

$$\cos\theta \cos^2\phi \; d\theta \; d\phi$$

$$= 2\, F(E)\, A(E)\, \delta_{ISO}(E) + \kappa(E)$$

For secondary electron emission, expanding $\cos^2(\theta-\theta_o)\cos^2\phi$:

$$\kappa(E) = \kappa_1(E) + \kappa_2(E)$$

$$\kappa_1(E) = -2b(E)\cos(2\theta_o)F(E)C$$

$$\cdot\left[\frac{C1}{Q}\left(\frac{2}{Q^3} - e^{-Q}\left(\frac{1}{Q} + \frac{2}{Q^2} + \frac{2}{Q^3}\right) - \frac{1}{3}\right)\right.$$

$$\left. + \frac{C2}{Q^2}\left(\frac{3}{Q^2} - e^{-Q}\left(1 + \frac{3}{Q} + \frac{3}{Q^2}\right) - \frac{1}{2}\right)\right]$$

where

$$\delta(\beta) = C \cdot \left[C1 \left(\frac{1-e^{-Q\cos\beta}}{Q\cos\beta} \right) - C2 \left(\frac{1-\cos\beta+1)e^{-Q\cos\beta}}{Q^2\cos^2\beta} \right) \right]$$

$Q = \alpha R$ (R is the range of electrons of energy E).

$$K_2(E) = \sin^2\theta_o \frac{F(E)}{\pi} b(E)\, C\left[C1 \cdot I_1 + C2 \cdot I_2 \right]$$

The integrals I_1 and I_2 are integrated numerically and tabulated for various values of Q. Interpolation finds the value of each for an unknown Q.

$$I_1 = \int_{-\pi/2}^{\pi/2} \int_{-\pi/2}^{\pi/2} \left(\frac{1-e^{-Q}}{Q} \right) \cos^4\phi \cos\theta \, d\theta \, d\phi$$

$$I_2 = \int_{-\pi/2}^{\pi/2} \int_{-\pi/2}^{\pi/2} \left(\frac{1+(Q+1)e^{-Q}}{Q^2} \right) \cos^4\phi \cos\theta \, d\theta \, d\phi$$

By dividing the values of FOUT(E) so calculated by the incident current normalization ANGF(E)

$$\text{ANGF(E)} = \frac{\text{FIN(E)}}{\text{F(E)}} = a(E) + \frac{3b(E)}{8} \left(1 + \frac{\cos^2\theta_o}{3} \right)$$

we obtain the anisotropic yield for secondary emission

$$\delta_{\text{ANISO}} = \frac{\text{FOUT(E)}}{\text{ANGF(E)}}$$

The proton secondary emission is much simpler to calculate since FOUT(E) is independent of angle:

$$\delta^{proton}_{ANISO}(E) = \frac{FOUT(E)}{ANGF(E)} = \frac{FOUT_{ISO}(E)}{ANGF(E)}$$

The backscatter requires an additional tabulated integral:

$$\eta(\theta) = \eta_0 \, e^{-\log\eta_0} \, e^{\log\eta_0 \cos\beta}$$

$$\therefore \quad FOUT(E) = \frac{F(E)}{\pi} \, \eta_0(E) \, e^{-\log\eta_0(E)} \, \kappa_\eta$$

where

$$\kappa_\eta = \int_{-\pi/2}^{\pi/2} \int_{-\pi/2}^{\pi/2} e^{\gamma \cos\theta \cos\phi} \cos^2(\theta-\theta_0) \cos^4\phi \cos\theta \, d\phi \, d\theta$$

where

$$\gamma = \log\eta_0$$

Separating as before:

$$\kappa_\eta = J_1 + J_2$$

$$J_1 = 2 \cdot \cos 2\theta_0 \left[e^{\gamma} \left(\frac{6}{\gamma^4} - \frac{6}{\gamma^3} + \frac{3}{\gamma^2} - \frac{1}{\gamma} \right) - \frac{6}{\gamma^4} \right]$$

$$J_2 = \sin^2\theta_0 \int_{-\pi/2}^{\pi/2} \int_{-\pi/2}^{\pi/2} e^{\gamma \cos\theta \cos\phi} \cos^4\phi \cos\theta \, d\theta \, d\phi$$

J_2 is tabulated for values of η_0.

3.4.1.4 Fitting Data. Values for R(E) are obtained by fitting the observed distribution function data as a function of pitch angle, ψ, to the form

$$f(\psi) = N\left[\frac{1}{(1+R)} + \frac{3R\cos^2\psi}{(1+R)}\right]$$

where N is the value of the distribution function close to a pitch angle of 90 degrees.

Some examples of $f(\phi)$ are shown in Figures 3.8-3.12 for different values of R. The figures show a cross-section through the full three-dimensional distribution function, obtained by rotation about the field direction axis.

As R increases from -0.35 to 0.5 from Figure 3.8 to Figure 3.12 the distribution changes from the "doughnut" shaped loss-cone form to a "dumb-bell" aligned flux form. Figure 3.10 corresponds to the isotropic spherical distribution.

In conclusion, this simple one parameter representation is flexible enough to provide an adequate model for the angular distributions of electron and ion fluxes found in earth orbit. In addition, it is simple enough to be included in the NASCAP numerical model without decreasing its speed or increasing its size to unmanageable levels.

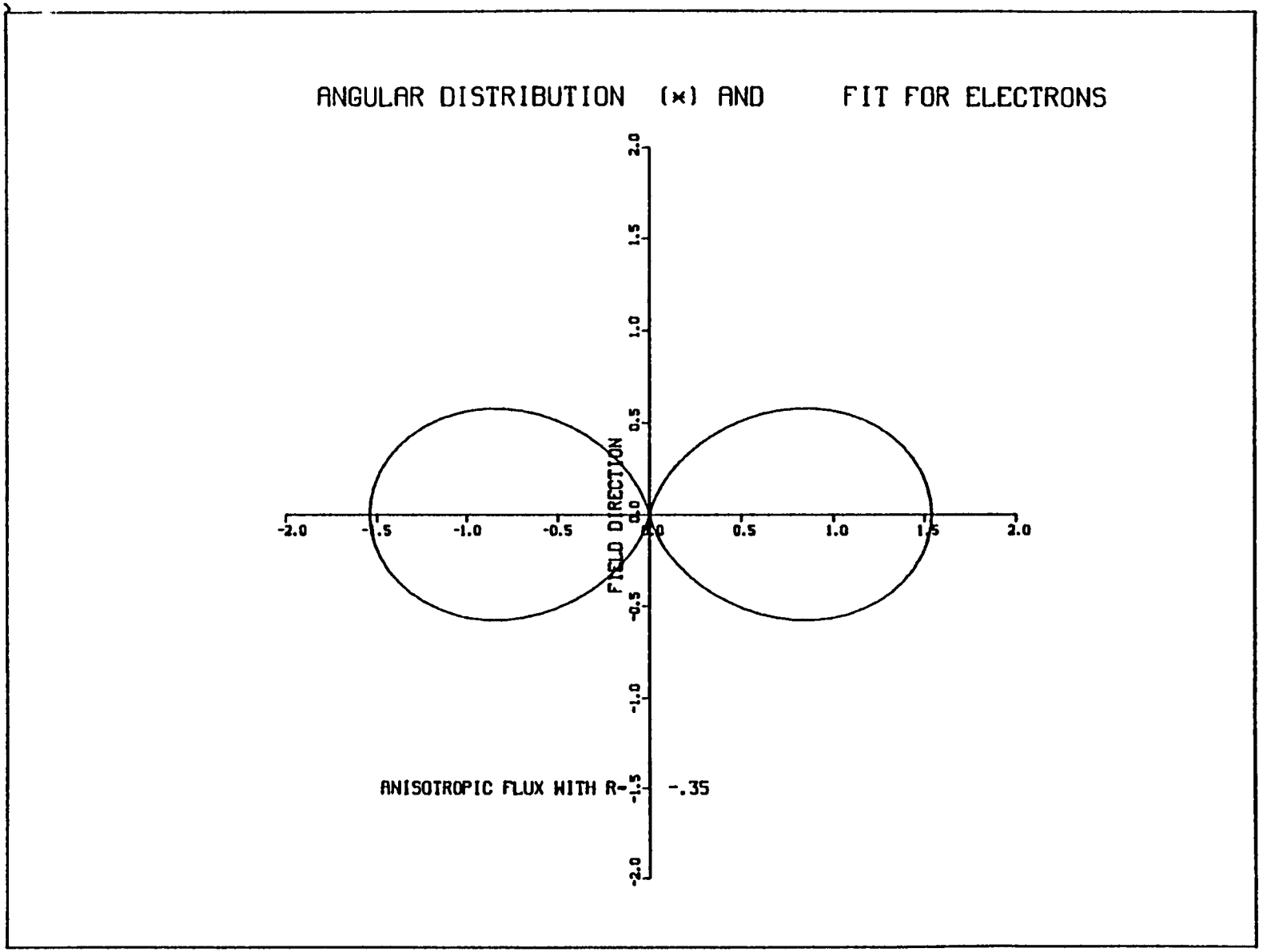

Figure 3.8. Anisotropic flux distribution with R = -0.35.

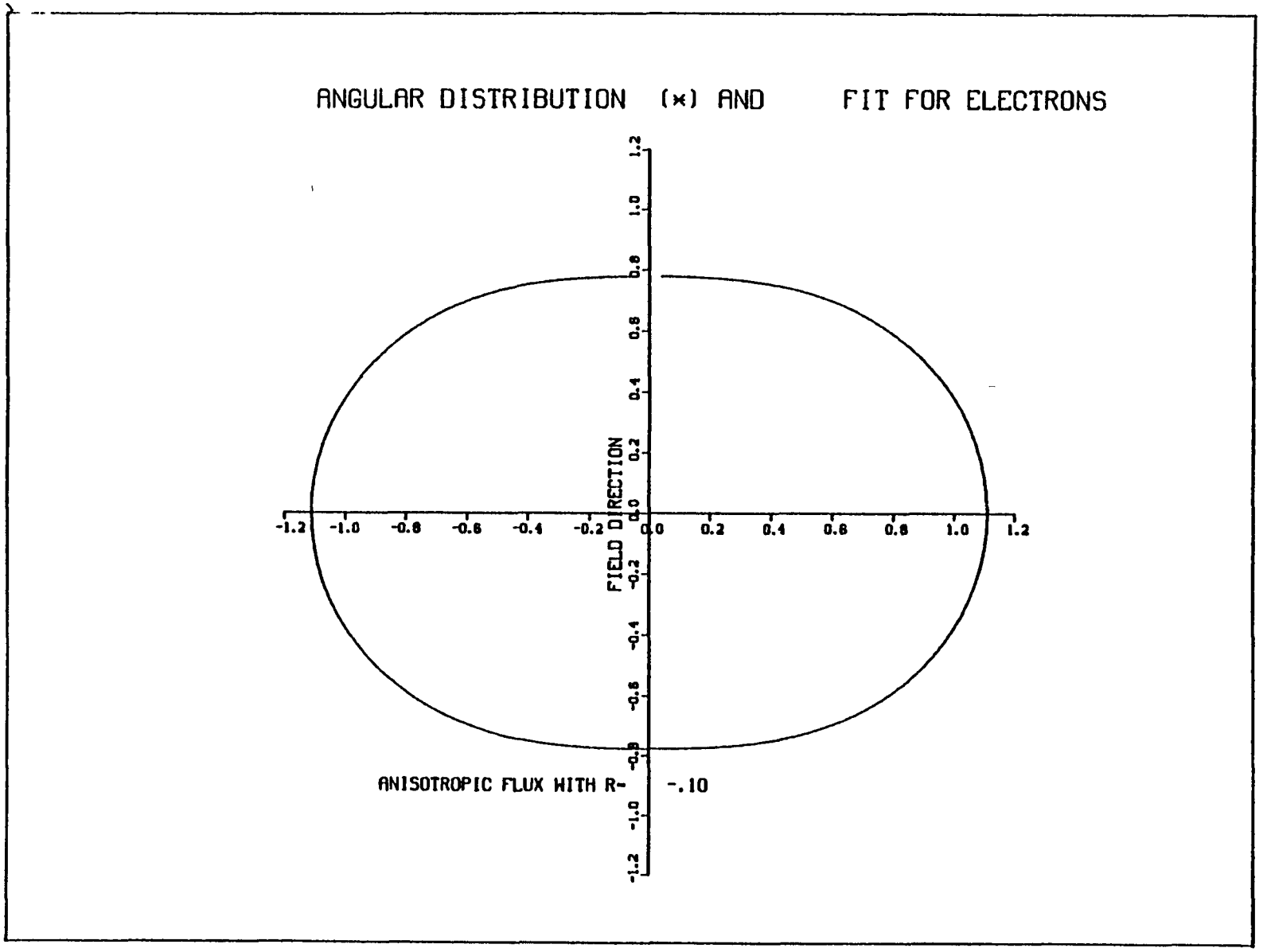

Figure 3.9. Anisotropic flux distribution with R = -0.10.

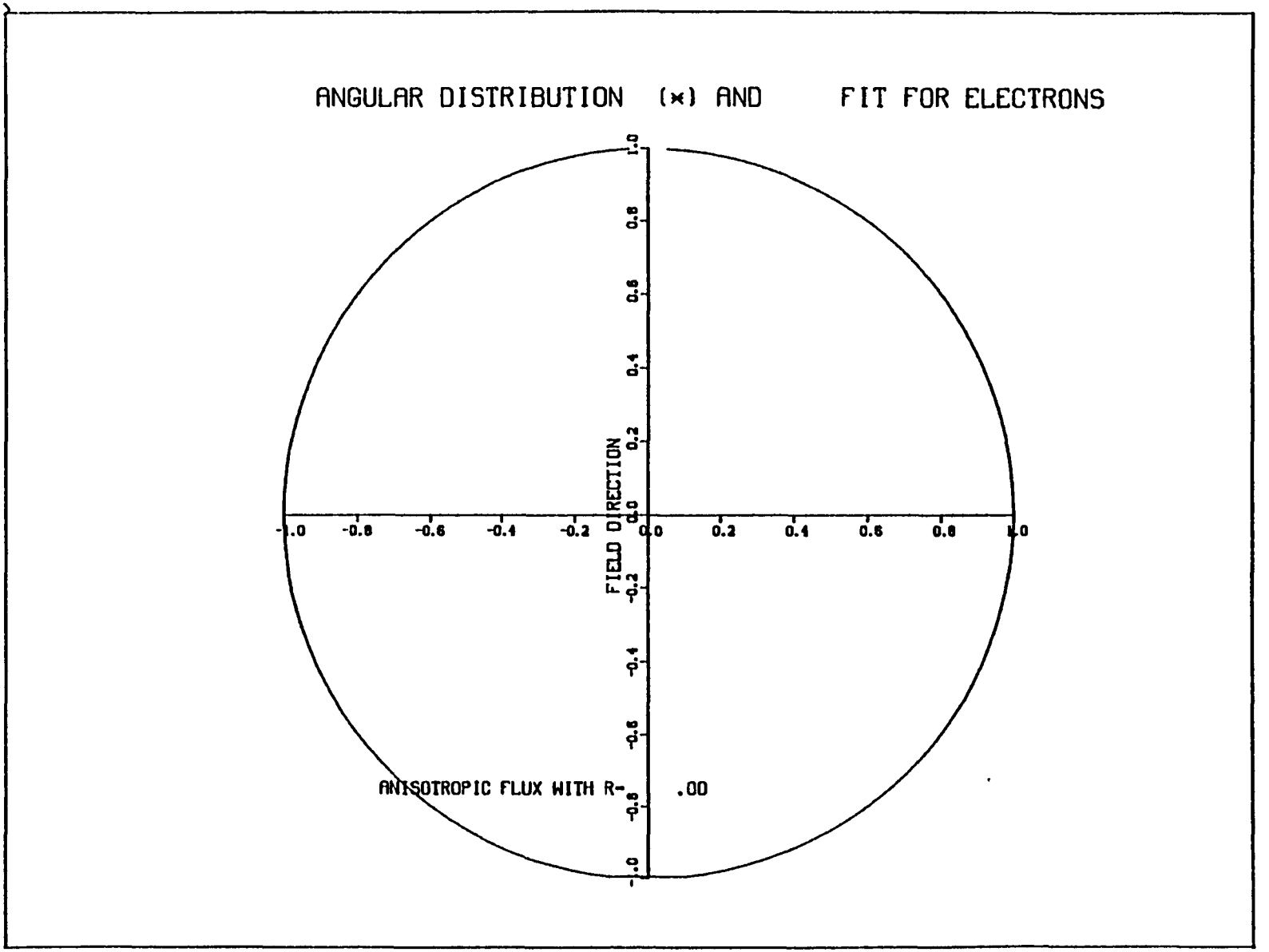

Figure 3.10. Isotropic flux distribution.

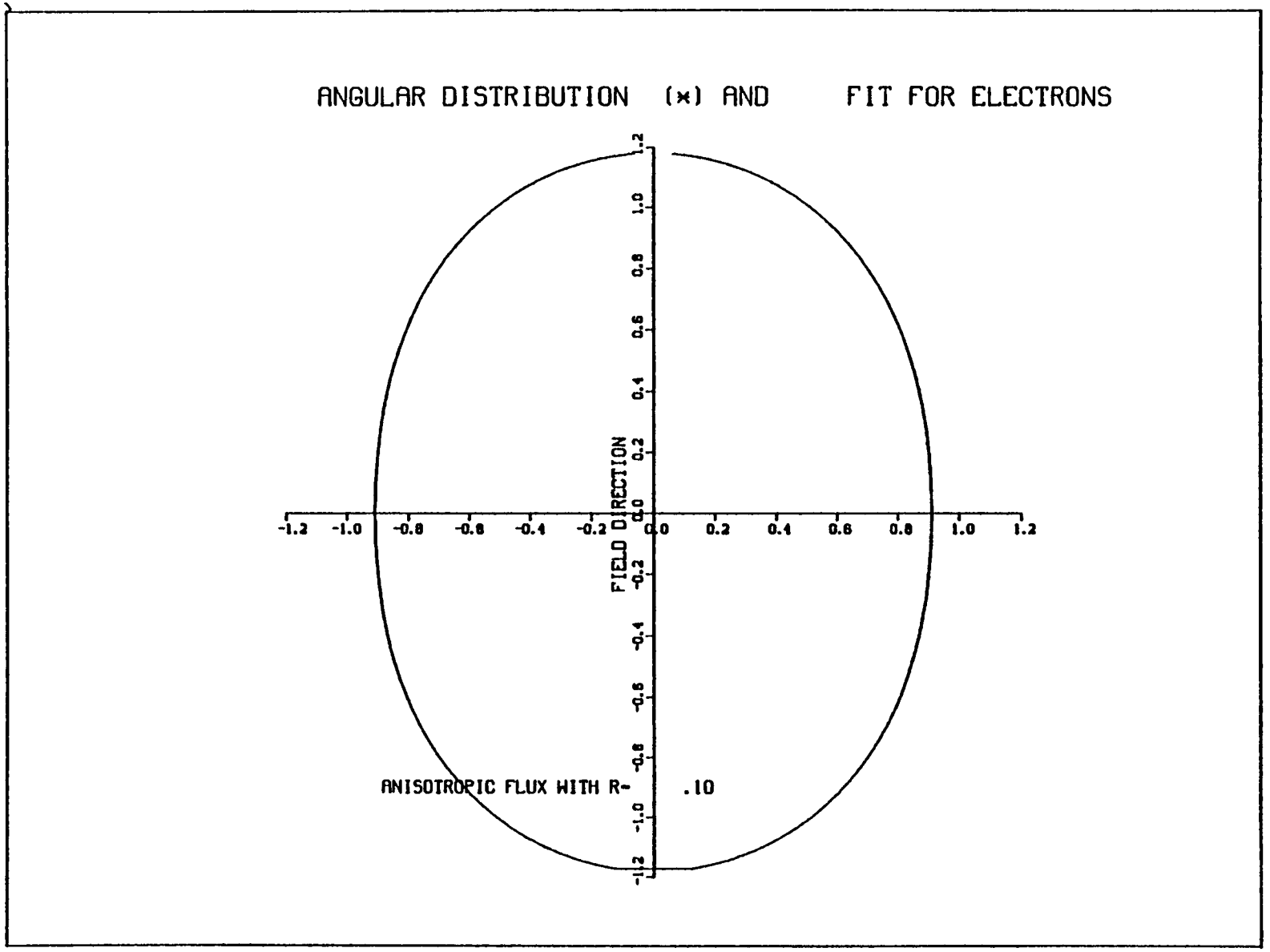

Figure 3.11. Anisotropic flux distribution with R = 0.10.

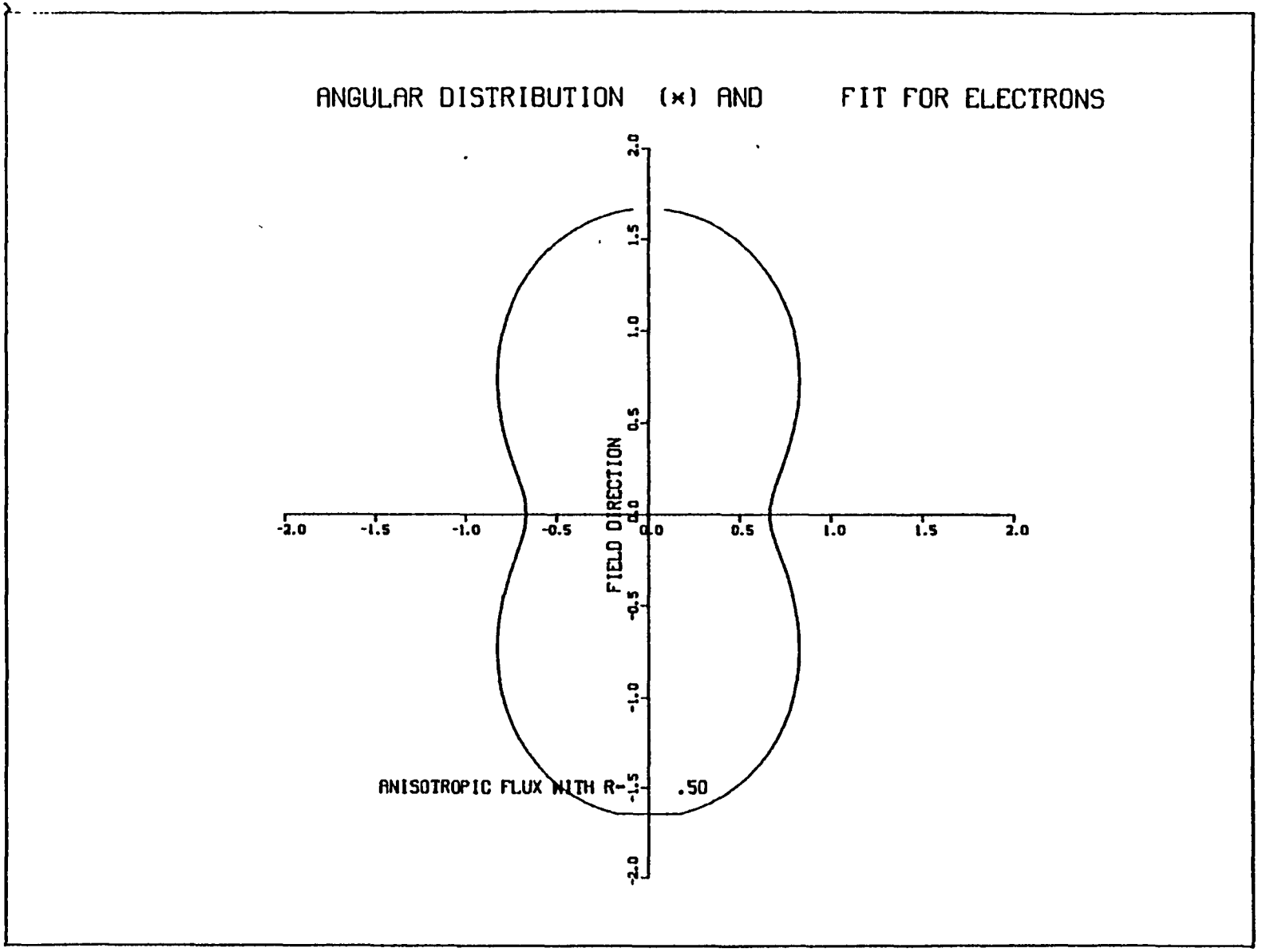

Figure 3.12. Anisotropic flux distribution with R = 0.50.

3.4.2 DIRECT and UPDATE

The model for the description of the plasma surrounding the spacecraft in NASCAP has been extended. Now, in addition to isotropic Maxwellian and double Maxwellian representations, tabulations of distribution function data, as observed experimentally, may be entered directly. The angular distribution function may also be entered, as a function of energy, for each species (electrons and ions).

In addition, as an aid to simulation of charging events over a period of time where several measurements of the environmental parameters are available, the UPDATE feature has been added. In this mode NASCAP continually updates the environment description to correspond to the latest available.

3.4.2.1 DIRECT. The direct input of a tabulation of distribution function data points has been added as a new flux definition type 5. It may be invoked with a flux definition card in the FLX file of the type 'ITYPE 5', or 'DIRECT'. Following this, three cards specifying 'YEAR', 'DAY', 'TIME' must be included to pinpoint the data set to be used; e.g.,

```
YEAR   1980.
DAY    87.
TIME   59630.
```

The order of the cards is unimportant. All values are real. The time is in seconds. Syntaxes are given in Table 3.1 and examples in Figure 3.13. The data itself must be in the standard format described in Section 3.4.3, and resides in a separate file ISPCTR. The default value of ISPCTR is 9.

TABLE 3.1. SYNTAX

a. Flux File Cards (or ISPCTR)

Syntax	Meaning	Example
DIRECT (ITYPE 5)	Flux type 5, direct input of data from ISPCTR	DIRECT
YEAR <year>	YEAR associated with data to be read under DIRECT	YEAR 1980.
DAY <day>	DAY associated with data to be read under DIRECT	DAY 146.
TIME <time>	TIME in seconds on day associated with data to be read under DIRECT	TIME 15216.
ANISOTROPIC <ianiso>	Read RATIO cards from unit IANISO and use ANISOTROPIC mode	ANISOTROPIC 19
<energy unit> <energy> ERATIO <ratio>	Value of ratio, R, for electrons of energy given	KEV 10. ERATIO 0.8
<energy unit> <energy> IRATIO <ratio>	Value of ratio, R, for ions of energy given	EV 1000. IRATIO - 0.2

b. Option File

Syntax	Meaning	Default	Example
UPDATE ON	Read flux data from ISPCTR and update where possible	OFF	UPDATE ON
UPDATE OFF	Read flux data from FLX. file in the normal way	OFF	UPDATE OFF
ISPCTR <ispctr>	Specify the unit for DIRECT mode — or the UPDATE file	9	ISPCTR 11

a. UPDATE OFF, ISPCTR = 9.

File 22

```
DIRECT
TIME 59001
DAY 87
YEAR 1979
ANISOTROPIC 25
END
```

File 25

```
KEV  0.1    ERATIO  0.9
KEV  0.5    ERATIO  0.5
KEV  2.0    ERATIO -0.2
KEV 10.0    ERATIO -0.01
KEV 50.0    ERATIO  0.0
EV  1000    IRATIO -0.2
EV  3000    IRATIO -0.05
EV  40000   IRATIO  0.06
END
```

b. UPDATE ON, ISPCTR = 9.

File 22

```
DOUBLE MAXWELLIAN
TIME 59050
END
```

File 9

```
TIME 59000
ELECTRONS  0.3E6 MKS 10 KEV
ELECTRONS  0.7 CGS 500 EV
PROTONS    0.3 CGS 1.E6 KELVIN
PROTONS    0.7 E6 MKS 1.E-15 JOULES
END
TIME 59100
ELECTRONS  etc.
etc.
```

For an example of file 9 see Section 3.4.3.

Figure 3.13. File examples for DETECT and ANISOTROPIC fluxes.

3.4.2.2 Anisotropic. The angular distribution function used by NASCAP has the form

$$f(\psi) = a + b \cos^2\psi$$

where

$$R = \frac{3b}{a} = \frac{\text{integrated aligned flux}}{\text{integrated isotropic flux}}$$

The theoretical model is discussed in more detail in Subsection 3.4.1.

The angle ψ is the angle between the incoming particle and the magnetic field direction. To include an anisotropic angular distribution in the description of the flux, two pieces of information are needed; the magnetic field direction and the value of R.

The magnetic field direction is defined by including a 'BFIELD' card in the options file.

BFIELD bx by bz

By choosing the absolute value of $\vec{B}$ to be small no unwanted magnetic effects are included in the calculation. The default magnetic field direction is along the Z axis.

The values of R are usually the last items to be included in the FLX. file before the 'END' card. They are preceded by the 'ANISOTROPIC' card; e.g.,

'ANISOTROPIC 19.'

The 'ANISOTROPIC' card switches NASCAP into the anisotropic mode and indicates which file the values of R are to be read from. If no file number is included the default is used. There are two defaults. In the usual operating mode the default is file 22, (the FLX. file), and the cards immediately following the 'ANISOTROPIC' statement are read. In the 'UPDATE' mode (see below) the default is the UPDATE file ISPCTR.

The cards defining the ratio R, whether following in the FLX. file, or in a separate file, must have the format

```
<energy unit>  <energy>   ERATIO      <R>
                            or
                          IRATIO
```

e.g., for electrons

```
'KEV 1.  ERATIO  0.5'
```

and for ions

```
'JOULES  9000.  IRATIO - 0.2'
```

The energy units allowed are keV, eV, joules, ergs, kelvin.

If more than one card is included for one species, NASCAP linearly interpolates the value of R between the energies when necessary. The values at zero and infinity are taken as the values for the lowest and highest energies known, respectively. A maximum of ten cards per species can be read. Syntaxes and examples are given in Table 3.1 and Figure 3.13.

3.4.2.3 UPDATE. 'UPDATE' is a new keyword that may appear in the options file.

```
'UPDATE ON'
'UPDATE OFF'
```

The default is 'OFF', when the code behaves as it always has.

When 'UPDATE' is 'ON' the flux is read from a new file ISPCTR. (The default value for this is 9.) The code searches ISPCTR for the most recent spectrum and updates the flux description correspondingly. For example, suppose a 60 second time step began at time 59803 seconds, the next time step begins at 59863. If ISPCTR contains data for times 59800 and 59850, then for the second time step, UPDATE will change the environment description from that measured at 59800 to 59850. UPDATE always looks backwards to the most "recent" data.

UPDATE operates for flux types 2 (single Maxwellian), 4 (double Maxwellian), and 5 (DIRECT). For the Maxwellian representation the FLX. file, 22, need contain only the flux type and the time, in seconds, of the beginning of the simulation. The DIRECT mode requires the YEAR and DAY additionally, e.g.,

```
SINGLE MAXWELLIAN
TIME 59803
```

or

```
TYPE 5.
YEAR 1979.
DAY  146.
TIME 59803.
```

The file in ISPCTR has the format described in Section 3.4.3 for DIRECT, and the following format for the Maxwellian representations:

```
TIME  <time in seconds>
DATA CARDS

TIME  <time in seconds>
DATA CARDS

and so on . . . .
```

The data cards have the same format as those usually found in the FLX. file when UPDATE is off; e.g., for a single Maxwellian

```
TIME 59800
1 CGS
1.E6 MKS
3000 EV
3.5 KEV
ANISOTROPIC
KEV 1.0  ERATIO 0.5
KEV 1.0  IRATIO 0.8
END.
TIME 59900
ETC.
. . . .
```

As shown in the above example, the angular distribution function of the flux can also be included in the update file just as in the FLX. file. The exception to this is the DIRECT mode: ANISOTROPIC and DIRECT cannot be used together in the UPDATE mode. The reason for this is that inserting RATIO cards in the files, carefully prepared according to the format shown in Section 3.4.3, would cause confusion and difficulty in reading the data in other operating modes.

3.4.2.4 Summary.

1. Direct input of spectral data points into NASCAP is now possible using ITYPE 5, the 'DIRECT' flux type.
2. The angular distribution function of flux types 'SINGLE MAXWELLIAN', 'DOUBLE MAXWELLIAN', and 'DIRECT' may be specified using the 'ANISOTROPIC' statement in the flux file.
3. Simulations over many timesteps, during a period when several characterizations of the environment are available, are made easier by the use of the UPDATE option. In this mode the code automatically changes the environmental description when appropriate, using data compiled in file ISPCTR. UPDATE may be used for flux types 'SINGLE MAXWELLIAN', 'DOUBLE MAXWELLIAN', and 'DIRECT'.

3.4.3 Format for Tabulated Spectral Data

For NASCAP operating in the DIRECT mode to be able to read in the tabulated data it must be prepared according to the following specifications and format:

1. Magnetic Tape Characteristics
   Spectra can be provided on a coded 9 track magnetic tape with the following characteristics:
   unlabelled
   1600 bpi
   EBCDIC or ASCII coded
   fixed length records: 80 characters per record
   fixed block size: 20 records per block
2. Each data tape will consist of header records followed by repeated series of data records. The data will be read by a FORTRAN program using the FORMAT statements indicated below:

HEADER RECORD 1. DETECTOR FORMAT (80A1)
Identifies the detector(s) used to obtain the data.

HEADER RECORD 2. SOURCE FORMAT (80A1)
Identifies the individual(s) responsible for preparing the data.

HEADER RECORDS 3. through 10. COMMENTS FORMAT (80A1)
Any relevant information regarding the data can be included here, such as date data tape was generated, detector mode of operation, and what corrections have been applied to the raw data.

HEADER RECORD 11. $YEAR_0$, DAY_0, SEC_0, $Year_1$, DAY_1, SEC_1 FORMAT (10F8.0)
$YEAR_0$, DAY_0, SEC_0 = time of earliest spectrum on tape
$YEAR_1$, DAY_1, SEC_1 = time of latest spectrum on tape
Each series of data records will represent a complete energy scan by the detector.

DATA RECORD 1. YEAR, DAY, SEC, NBINS, DELTA, VSAT, $|\vec{S}|$, SX, XY, SZ FORMAT (10F8.0)

YEAR, DAY, SEC = time energy scan was begun

NBINS = number of distinct energy bins in the scan

DELTA = time (seconds) between each data point in the scan of the spectrum

VSAT = satellite potential during scan (volts)

$|\vec{S}|$ = sun intensity (1.0 = full sun)

SX, SY, SZ = normalized sun direction vector components at start of scan

DATA RECORDS 2. through (NBINS+1). ENERGY, $\log_{10}(F_i)$, $\log_{10}(F_e$, Ω, α, BX, BY, BZ FORMAT (10F8.0)

Each of these records represents a data point on the scan of the energy range

ENERGY = energy (eV)

F_i = ion distribution function (sec^3/m^6)

F_e = electron distribuition function (sec^3/m^6)

Ω = detector view angle (degrees)

α = pitch angle (degrees)

BX, BY, BZ = magnetic field vector components ($nT = 10^{-9}$ W/m^2)

(The α value is redundant since it can be calculated from Ω and the magnetic field vector.)

DATA RECORD NBINS+2. (END OF DATA MARKER) FORMAT (10F8.0)

This record will contain any negative real number to indicate the end of the spectral scan. (This record is redundant since NBINS is known.)

The data records 1 through (NBINS+2) are then repeated for each spectrum. Some of the information above may not be available for each spectrum or each data point. The following conventions can be used to indicate that the data is to be ignored:

VSAT: any value greater than +10000

$|\vec{S}|$: any negative value

SX, SY, SZ: blank or zero

F_i, F_e: blank or zero

Ω, α: any value greater than 360

BX, BY, BZ: blank or zero

An example is shown in Table 3.2.

TABLE 3.2. EXAMPLE OF A DIRECT DATA FILE

```
inp!
 1:DETECTOR>NORTH/SOUTH ON SC-9
 2:SOURCE  >J. DAVID NICHOLS/ UCSD
 3:COMMENTS>BACKGROUND COUNT SET AT 100
 4:COMMENTS>POTENTIAL ESTIMATED FROM DISTRABUTION FUN
 5:COMMENTS>NO SUN VECTOR OR ABSOLUTE ATTITUDE INFORM
 6:COMMENTS>I TRIED TO GIVE MORE CLOSELY SPACED DATA WHEN
 7:COMMENTS>THE POTENTIAL IS CHANGING MOST RAPIDLY
 8:COMMENTS>WE COME OUT OF ECLIPSE ABOUT 17:15
 9:COMMENTS>FOR ABOUT 10 MINUTES AFTER THIS POTENTIALS ARE
10:COMMENTSONLY ROUGH ESTIMATES - HIGHLY UNCERTAIN
11:     1979      87   59400     1979      87   63053
12:     1979      87   59473       64    0.25       0.   -1.00     0.00     0.00     0.00
13:    -3.90    0.00    0.00     0.00   86.20  -12.09 -173.27    90.26
14:    -1.60    0.00    0.00     0.00   86.50  -11.80 -162.32   108.95
15:     1.00    0.00  -11.18     0.00   86.50  -11.80 -162.32   108.95
16:     4.00    0.00  -12.91     0.00   86.50  -11.80 -162.32   108.95
17:     7.40    0.00  -14.34     0.00   86.50  -11.80 -162.32   108.95
18:    11.40    0.00  -14.86     0.00   86.80  -11.80 -149.58   126.12
19:    16.00    0.00  -15.20     0.00   86.80  -11.80 -149.58   126.12
20:    21.20    0.00  -15.64     0.00   86.80  -11.80 -149.58   126.12
21:    27.20    0.00  -15.82     0.00   86.80  -11.80 -149.58   126.12
22:    34.00    0.00  -15.92     0.00   87.00  -12.09 -134.77   141.54
23:    41.90    0.00  -16.03     0.00   87.00  -12.09 -134.77   141.54
24:    50.90    0.00  -16.00     0.00   87.00  -12.09 -134.77   141.54
25:    61.30  -12.22  -16.08     0.00   87.00  -12.09 -134.77   141.54
26:    73.10    0.00  -16.14     0.00   87.20  -12.09 -118.75   155.79
27:    86.60  -12.52  -16.16     0.00   87.20  -12.09 -118.75   155.79
28:   102.20    0.00  -16.20     0.00   87.20  -12.09 -118.75   155.79
29:   119.90    0.00  -16.27     0.00   87.20  -12.09 -118.75   155.79
30:   140.30  -12.94  -16.31     0.00   87.50  -12.09 -100.98   167.95
31:   163.60  -12.77  -16.36     0.00   87.50  -12.09 -100.98   167.95
32:   190.30  -12.48  -16.32     0.00   87.50  -12.09 -100.98   167.95
33:   220.90  -13.33  -16.35     0.00   87.50  -12.09 -100.98   167.95
34:   255.90  -12.83  -16.37     0.00   87.70  -12.09  -82.02   178.04
35:   295.90  -12.96  -16.43     0.00   87.70  -12.09  -82.02   178.04
36:   341.80  -13.41  -16.47     0.00   87.70  -12.09  -82.02   178.04
37:   394.40  -12.97  -16.55     0.00   87.70  -12.09  -82.02   178.04
38:   454.60  -13.65  -16.59     0.00   87.90  -12.09  -62.18   185.80
39:   523.50  -13.28  -16.70     0.00   87.90  -12.09  -62.18   185.80
40:   602.40  -13.39  -16.85     0.00   87.90  -12.09  -62.18   185.80
41:   692.70  -13.19  -16.94     0.00   87.90  -12.09  -62.18   185.80
42:   796.20  -13.48  -17.03     0.00   88.10  -12.09  -41.71   194.44
43:   914.60  -13.71  -17.14     0.00   88.10  -12.09  -41.71   194.44
44:  1050.20  -13.59  -17.26     0.00   88.10  -12.09  -41.71   194.44
45:  1205.50  -13.63  -17.38     0.00   88.10  -12.09  -41.71   194.44
46:  1383.30  -13.52  -17.50     0.00   88.30  -12.09  -20.39   195.00
47:  1588.90  -13.83  -17.70     0.00   88.30  -12.09  -20.39   195.00
48:  1820.00  -13.62  -17.89     0.00   88.30  -12.09  -20.39   195.00
49:  2087.00  -13.51  -18.06     0.00   88.30  -12.09  -20.39   195.00
50:  2392.60  -13.63  -18.20     0.00   88.40  -12.39    1.05   196.19
51:  2742.50  -13.95  -18.33     0.00   88.40  -12.39    1.05   196.19
52:  3143.20  -14.07  -18.58     0.00   88.40  -12.39    1.05   196.19
53:  3602.00  -14.11  -18.80     0.00   88.40  -12.39    1.05   196.19
54:  4127.30  -14.01  -19.07     0.00   88.40  -12.69   22.37   195.00
55:  4729.70  -14.37  -19.32     0.00   88.40  -12.69   22.37   195.00
56:  5417.40  -14.33  -19.74     0.00   88.40  -12.69   22.37   195.00
57:  6208.00  -14.46  -19.85     0.00   88.40  -12.69   22.37   195.00
58:  7108.80  -14.46  -20.28     0.00   88.50  -12.98   43.40   194.44
59:  8142.70  -14.55  -20.73     0.00   88.50  -12.98   43.40   194.44
60:  9326.40  -14.59  -20.97     0.00   88.50  -12.98   43.40   194.44
61: 10681.70  -14.67  -20.96     0.00   88.50  -12.98   -3.40   194.44
62: 12233.60  -14.79  -21.22     0.00   88.50  -13.28   63.87   195.51
63: 14010.50  -14.89  -21.24     0.00   88.50  -13.28   63.87   195.51
64: 16045.00  -15.05  -21.48     0.00   88.50  -13.28   63.87   195.5
65: 18374.60  -15.37  -22.22     0.00   88.50  -13.28   63.87   195.51
66: 21041.90  -15.34  -21.91     0.00   88.40  -13.58   83.71   177.44
67: 24096.00  -15.49  -21.76     0.00   88.40  -13.58   83.71   177.44
68: 27592.90  -15.70  -21.78     0.00   88.40  -13.58   83.71   177.44
69: 31596.90  -15.80  -22.17     0.00   88.40  -13.58   83.71   177.44
70: 36181.50  -16.08    0.00     0.00   88.50  -13.58  102.96   167.06
71: 41430.90  -16.10  -22.88     0.00   88.50  -13.58  102.96   167.06
72: 47441.40  -16.02  -23.30     0.00   88.50  -13.58  102.96   167.06
73: 54323.40  -16.47  -22.69     0.00   88.50  -13.58  102.96   167.06
74: 62203.30  -16.65  -23.23     0.00   88.40  -13.87  120.48   154.90
75: 71225.30  -17.06    0.00     0.00   88.40  -13.87  120.48   154.90
76: 81550.60  -17.51  -23.28     0.00   88.40  -13.87  120.48   154.90
77:     -1.
78:     1979      87   59673       64    0.25       0.   -1.00     0.00     0.00     0.00
79:    -3.90    0.00    0.00     0.00   90.40    0.36 -174.39  -87.55
80:    -1.70    0.00    0.00     0.00   90.20    0.95 -163.43 -106.33
81:     1.00    0.00  -11.15     0.00   90.30    0.95 -163.43 -106.33
82:     4.00    0.00  -12.96     0.00   90.30    0.95 -163.43 -106.33
83:     7.40    0.00  -13.68     0.00   90.30    0.95 -163.43 -106.33
84:    11.40    0.00  -14.34     0.00   90.20    1.25 -150.40 -123.70
85:    16.00    0.00  -14.70     0.00   90.30    1.25 -150.40 -123.70
86:    21.20    0.00  -15.05     0.00   90.30    1.25 -150.40 -123.70
87:    27.20    0.00  -15.27     0.00   90.20    1.25 -150.40 -123.70
88:    34.00    0.00  -15.55     0.00   89.30    0.95 -135.38 -139.72
89:    41.90  -11.89  -15.72     0.00   89.30    0.95 -135.38 -139.72
90:    50.90    0.00  -15.90     0.00   89.30    0.95 -135.38 -139.72
91:    61.20    0.00  -16.04     0.00   89.30    0.95 -135.38 -139.72
```

4. PLOTTING EXTENSIONS - NASCAP*PLOTREAD

The graphics capability has always been one of the most time-consuming problems in NASCAP code maintenance and code installation. Among the repeatedly encountered problems associated with performing graphics directly were (1) significant amounts of core storage devoted to graphics instructions and data; (2) changes in locally implemented graphics software and hardware beyond our control; (2) non-transferability of absolute elements; (4) difficulties in making optimal use of hardware; (5) difficulties in developing and testing interface routines to new graphics packages. The problem became particularly serious with the need to use the DISSPLA package at S-Cubed, as the size of these routines did not permit any hope of including them directly in NASCAP. Thus it became necessary to develop a new graphics protocol for NASCAP.

Under the new protocol, the higher level data manipulation routines (contouring, shading, perspective projection) are considered part of NASCAP. However, lower level routines (draw lines; print letters) are coded in a manner to permit replication of subroutine calls. A list of these routines, together with their functions, is given in Table 4.1. Each routine produces a sequence of words consisting of:

Word 1: Number of words in plot call.

Words 2-3: Subroutine name.

Subsequent words: Subroutine arguments, as needed.

The key subroutine in this scheme is IGFBUF. IGFBUF maintains a buffer of 280 words, and is called by each pseudo-graphics routine. If the buffer has insufficient storage remaining to store the plot calls the buffer is written out to file 2 and reset. Then, IGFBUF enters the number of words and subroutine name into the buffer, and returns control to the subroutine to enter its arguments.

TABLE 4.1 NASCAP PSEUDO-GRAPHICS SUBROUTINES

SUBROUTINE	ARGUMENTS	FUNCTION
ADF	None	Eject current plot frame
APRNTV	(IDX,IDY,N,TEXT,IX,IY)	Print horizontal or vertical plot labels
AXISXV	(X,Y,XEND)	Draw horizontal line
AXISYV	(X,Y,YEND)	Draw vertical line
CONECT	(X1,X2,Y1,Y2,SL1,SL2,NLL)	Connect line segments for contours
CURVV	(N,X,JDX,Y,JDY,IDUM)	Draw connected line segments
DLINEV	(N,IX,IY)	N = 1: Draw line to raster position IX,IY N = 0: Move to raster position IX,IY N =-1: Draw increment IX,IY N =-2: Move increment IX,IY
DRAWV	(LINE,N,IX,IY,KEYPOS,KCSIZE)	Draw vector characters
FINSHV	None	Close plot file; process plot destination
IGFBUF	(NWDS,NAME)	Process plot buffer
LINEUV	(X1,Y1,X2,Y2)	Draw line between two points
LQUADV	(N,X,Y)	Fill in a quadrangle with solid lines
OUTLIN	None	Draw box around plot
PLOTCV	(N,X,Y,IC)	Plot a character (or dot) at listed points
SBLIN	(NN,KK)	Print scale values for linear baseline NN subdivisions KK Format 0 I6 1-5 F6.0 - F6.4 6-12 E12.1 - E12.7

TABLE 4.1 NASCAP PSEUDO-GRAPHICS SUBROUTINES (Continued)

SUBROUTINE	ARGUMENTS	FUNCTION
SETUAV	(XL,XR,YB,YT,IXL,IXR,IYB,IYT)	Define user area and establish raster coordinates
SETUPV	None	Open plot file
SLLIN	(NN,KK)	Print scale values for linear grid left line (See SBLIN)
SWPEN	(COLOR)	Switch pen color
TLINEV	(MODE,X2,Y2,LW)	MODE = 0 Set CP = X2, Y2 MODE = 1 Draw line to X2, Y2 with thickness 30 LW rasters
TYPEV	(ITEXT,N,IX,IY)	Write N letters of text starting at IX,IY

NASCAP*PLOTREAD contains a main routine (PLOT) which reconstructs each graphics call and calls an appropriate version of the subroutine which interfaces to the DISSPLA, IGS, or other library. The actual routines called by each graphics routine are shown in Table 4.2.

Two additional benefits of this implementation were plot destination options (implemented in subroutine SETUPV) and a plot editing capability, NASCAP*FRAME. An illustration of the advantage of this plotting protocol was the ease of conversion to Jet Propulsion Laboratory's PLOT*PLOT (FORTRAN V) graphics package. In fact, most of the effort in this conversion involved tracking down and correcting residual errors in NASCAP from the ASCII FORTRAN conversion.

TABLE 4.2 IGS AND DISSPLA ROUTINES CALLED BY NASCAP*PLOTREAD

SUBROUTINE	IGS CALLS	DISSPLA CALLS
ADF	METAZZ PAGEG	AREA2D ENDPL GRAF
APRNTV	LEGNDG SETSMG	SYMPLJ
AXISXV	LINESG	USEPLJ
AXISYV	LINESG	USEPLJ
CONECT	LINESG	USEPLJ
CURVV	LINESG	USEPLJ
DLINEV	LINESG SETSMG	INCHPJ MOVFRJ
DRAWV	FONT2 OBJCTG SETSMG SUBJEG VECIZ VECTZZ	
FINSHV	EXITG	DONEPL ENDPL
INCHPJ	--	CURVE
LINEUV	LINESG	USEPLJ
LQUADV	MLTPLG	USEPLJ
MOVFRJ	--	CURVE
OUTLIN	LINESG SETSMG	INCHPJ
PLOTCV	POINTG SETSMG	SYMPLJ USEIN
RESETV	--	AREA2D BGNPL GRAF NOBRDR PAGE

TABLE 4.2 IGS AND DISSPLA ROUTINES CALLED BY NASCAP*PLOTREAD (Continued)

SUBROUTINE	IGS CALLS	DISSPLA CALLS
SBLIN	--	--
SETCAL	--	AREA2D BGNPL BLOWUP GRAF NOBRDR PAGE
SETUAV	OBJCTG SUBJEG	--
SETUPV	METAZZ MODESG SETSMG	CMPRS S3PLOT TK
SLLIN	--	--
SWPEN	METAZZ	SETCLR
SYMPLJ	--	ANGLE HEIGHT MESSAG XPOSN YPOSN
TLINEV	LINESG SETSMG	--
TYPEV	LEGNDG SETSMG	SYMPLJ
USEPLJ	--	INCHPJ

5. NASCAP*MATCHG

MATCHG is a code that models the current collection and charging response of a conducting sphere covered with a particular material. The purpose of the code is to give the user of NASCAP a general idea of how a complex object will charge by examining the response of a single surface material to a specified flux. The command structure of MATCHG has been reformulated into menu-type format. Rather than the code questioning the user for information repetitively, the user tells the code directly what is desired. As a result, he can change parameters and obtain revised answers with just one or two commands at any time.

MATCHG commands are entered as a string of keywords separated by spaces. The first keyword in a string is one of commands listed below.

1. Input Commands ('LIST', 'CHANGE', 'PARAMETERS')
2. Output Commands ('PLOT', 'TABLE', 'RESULT')
3. Utility Commands ('HELP', 'EXIT')

Table 5.1 summarizes the command functions.
Table 5.2 summarizes the command syntax.

TABLE 5.1. MATCHG COMMANDS

	Command	Purpose	Type
1.	LIST	Display a specific set of parameters	INPUT
2.	CHANGE	Change a specific set of parameters	INPUT
3.	PARAMETERS	Summarize input parameters	INPUT
4.	PLOT	Display a result in graphical form	OUTPUT
5.	TABLE	Display a result in tabular form	OUTPUT
6.	RESULT	Summarize a specific result	OUTPUT
7.	HELP	Display user information and guide	UTILITY
8.	EXIT	Exit MATCHG	UTILITY

TABLE 5.2. COMMAND FORMATS

First Word	Second Word	Other Input	Function
PARAmeters			Summarizes parameters
LIST	MATErial		Display input material
LIST	PROPerty	<#> to <#> or ALL	List material properties
LIST	ENVIronment		Display input environment
LIST	ANGLe		Display angular distribution
LIST	EMISsion		List emission formulation
LIST	VBACk		Backplate potential
	VINIt		Initial sample potential
	VBEGin		IV plot beginning and ending potentials
	VEND		
CHANge	MATErial	<new material>	Changes input material
CHANge	PROPerty	<#> to <#> or ALL	Changes material properties
CHANge	ENVIronment	<new envi> or (<envi parameter><value>)	Changes environment
CHANge	ANGLe	<new angle> or (<angle parameter><value>)	Changes angular distribution
CHANge	EMISsion	ANGLe or NORMal	Changes emission formulation
CHANge	VBACk	<potential>	Same as LIST
	VINIt		
	VBEGin		
	VEND		

TABLE 5.2. COMMAND FORMATS (Continued)

First Word	Second Word	Other Input	Function
RESUlt	CHARge	FULL (optional)	Summarize final potential
RESUlt	CURRent	<potential>	Currents at this potential
TABLe	CHARge		Summarize potential calculation
TABLe	IV		Current versus potential
TABLe	SECOndary BACKscatter ION ALL		Yields for these processes
PLOT	(same as TABLe)		Graph format
HELP	<Category (optional)>		Assist user
EXIT			Leave MATCHG

5.1 PROGRAM STRUCTURE

Upon execution of MATCHG, the main program initializes the input parameters to a set of default values. These are listed in Table 5.3. The program is now ready to branch to seven different modules, including the HELP module, under the user's control at any time. Figure 5.1 shows the basic program structure of MATCHG. A table briefly describing the subroutines that handle user/code interfacing appears as Table 5.4. After entering EXIT, the user may obtain a hard copy of his run.

TABLE 5.3. INITIAL DEFAULT VALUES

Property	Value
Material	KAPT
Angle	Isotropic
Environment	Single
NE1, NI1	10^{6} m^{-3}
TE1, TI1	1. keV
Emission	Angle
VBACK	0. keV
VINIT	0. keV
VBEGIN	0. keV
VEND	5. keV
Logical Unit Numbers;	
Material Data File	8
Spectral Data File	9
Anisotropy Data File	10

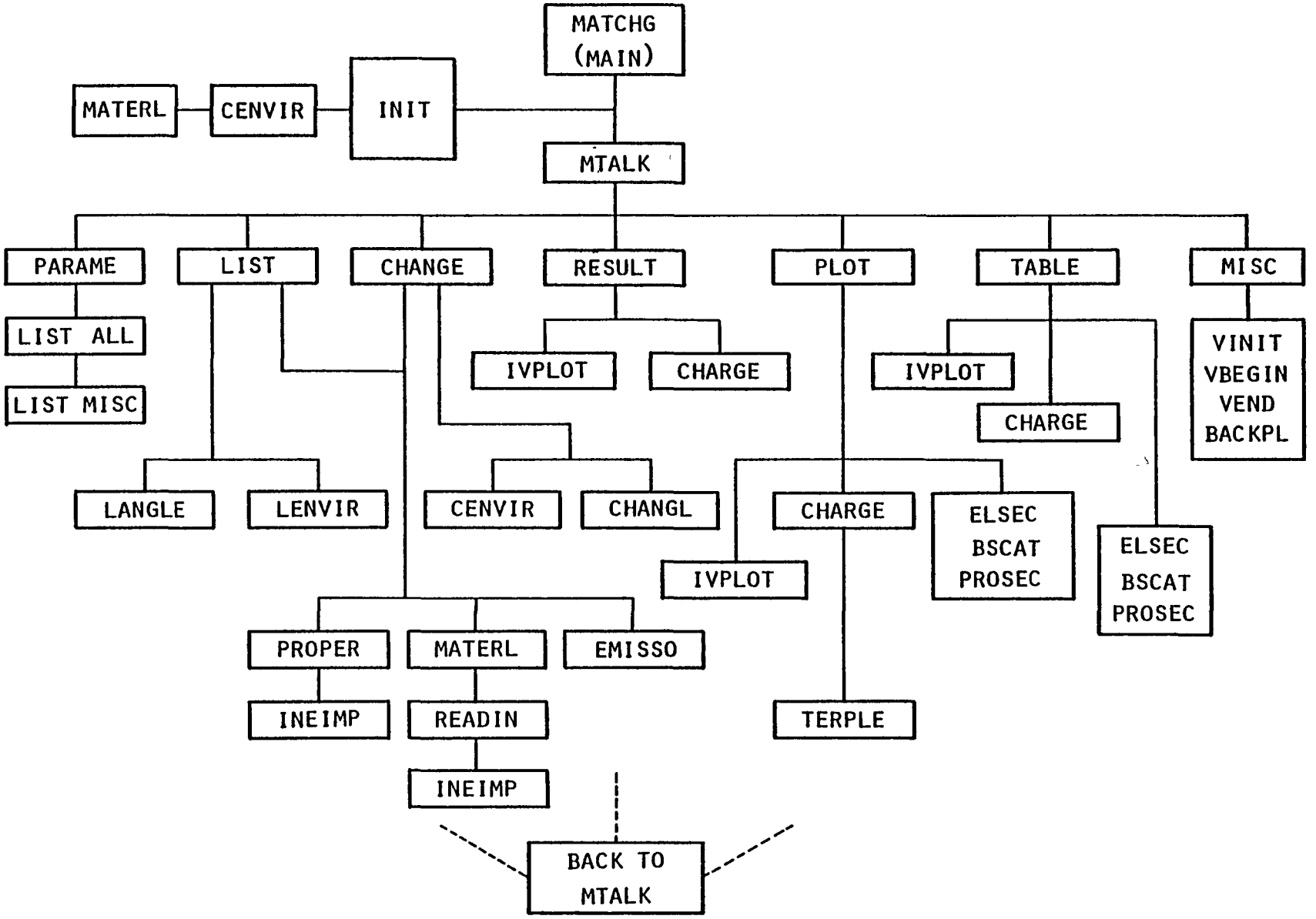

Figure 5.1. Block diagram of MATCHG.

TABLE 5.4. USER/CODE INTERFACING ROUTINES

Routine	Purpose	Called By
BACKPL	Lists/changes backplate potential	MTALK, PARAME
CENVIR	Changes environment parameters	CHANGE, INIT
CHANGE	Controls 'CHANGE' command	MTALK
CHANGL	Changes angular distribution parameters	CHANGE
CRETRN	Holds up output until user is ready	HELP
EMISSO	Lists/changes emission formulation	PARAME, LIST, CHANGE
FINISH	Hard copies MATCHG run	MATCHG
HELP	Gives interactive help to user	MTALK, CHANGE, LIST
INIKAP	Initializes input kappa values to code values	CENVIR
INIMAX	Initializes input Maxwellian values to code values	CENVIR
INIT	Initializes MATCHG/sets defaults	MATCHG
LANGLE	Lists angular distribution parameters	LIST, CHANGL
LENVIR	Lists environmental parameters	LIST, CENVIR
LIST	Controls 'LIST' command	MTALK
MATCHG	Main program	-
MATERL	Lists/changes material	INIT, LIST, CHANGE
MTALK	Interacts with user for commands	MATCHG

TABLE 5.4 USER/CODE INTERFACING ROUTINES (Continued)

Routine	Purpose	Called By
PARAME	Summarizes parameters	MTALK
PLOT	Controls 'PLOT' command	MTALK
PROPER	Lists/changes material properties	LIST, CHANGE
RESULT	Controls 'RESULT' command	MTALK
TABLE	Controls 'TABLE' command	MTALK
VBEGIN	Lists/changes beginning plot potential	MTALK, PARAME
VEND	Lists/changes ending plot potential	MTALK, PARAME
VINIT	Lists/changes initial sample voltage	MTALK, PARAME

5.2 MATCHG HELP

```
WELCOME TO 'MATCHG', A MATERIAL CHARGING
PROGRAM. TYPE 'HELP' AT ANY TIME FOR ASSISTANCE.
MATERIAL IS KAPT
ENVIRONMENT NOW SINGLE MAXWELLIAN

HELP

WELCOME TO HELP. CHOOSE ONE OF THE FOLLOWING
CATAGORIES BY ENTERING ONE OF THE 5 KEYWORDS SHOWN
1) SUMMARY
   (AN OVERVIEW OF MATCHG)

2) INPUT
   (WHAT GOES IN?: ENVIRONMENT, PROPERTIES
   ANGULAR DISTRIBUTION, AND MISC. PARAMETERS)

3) OUTPUT
   (WHAT COMES OUT?: CHARGING, CURRENTS,
   IV (CURRENTS VS. VOLTAGE), AND YIELDS)

4) COMMANDS
    (HOW DO I GET WHAT I WANT?:
   CHANGE, LIST, PARAMETERS, RESULT, TABLE, AND PLOT)

5) RETURN
   (BACK TO PROGRAM)
?
*** SUMMARY ***

 MATCHG MODELS THE RESPONSE OF A PARTICULAR MATERIAL
TO A SPECIFIED PLASMA ENVIRONMENT. THE PARAMETERS
DESCRIBE BOTH THE MATERIAL AND ENVIRONMENT, AND MAY
BE SUPPLIED BY THE USER. ALL HAVE BEEN GIVEN DEFAULT
VALUES. ON THE BASIS OF THIS INPUT, MATCHG WILL CAL-
CULATE POTENTIALS AND CURRENTS AS REQUESTED BY THE
USER

 MATCHG COMMANDS ARE ENTERED AS STRINGS OF KEYWORDS,
SEPARATED BY SPACES. THE FIRST KEYWORD IN A STRING
CORRESPONDS TO ONE OF THE FOLLOWING COMMANDS

       'LIST' - DISPLAY A SPECIFIC SET OF PARAMETERS.
     'CHANGE' - CHANGE A SPECIFIC SET OF PARAMETERS.
 'PARAMETERS' - DISPLAY A SUMMARY OF INPUT PARAMETERS.

       'PLOT' - DISPLAY A SPECIFIC RESULT IN GRAPH FORM.
      'TABLE' - DISPLAY A RESULT IN TABULAR FORM.
     'RESULT' - DISPLAY A PARTICULAR RESULT.
HIT RETURN <CR> TO CONTINUE
ALL KEYWORDS ARE SIGNIFICANT TO 4 CHARACTERS
(E.G. 'TABLE'='TABL') INTERNALLY. ADDING EXTRA
CHARACTERS HAS NO EFFECT. THE FIRST THREE COMMANDS
REFER TO USER INPUT. TYPE 'INPUT' FOR INFORMATION
CONCERNING THEIR USE.
```

```
THE LAST THREE REFER TO OUTPUT. TYPE 'OUTPUT' FOR
INFORMATION CONCERNING THESE.

TO EXIT AT ANY TIME, TYPE 'EXIT'. A HARD COPY OF
YOUR WORK CAN BE REQUESTED.
?
*** INPUT ***

 INPUT KEYWORDS FOLLOW 'LIST', AND 'CHANGE'
COMMANDS. THEY ARE:

1) ENVIRONMENT

   SPECIFIES THE PLASMA ENERGY SPECTRUM TYPE. IT IS
   ANOTHER OF THE FOLLOWING WORDS:

  A)      'TANK' - TEST TANK ENVIRONMENT
  B)    'SINGLE' - ONE COMPONENT MAXWELLIAN DISTRIBUTION
  C)    'DOUBLE' - TWO COMPONENT MAXWELLIAN DISTRIBUTION
  D)  'MULTIPLE' - MULT. MAXWELLIAN DISTRIBUTION (UP TO 5)
  E)     'KAPPA' - DISTRIBUTION (DESCRETIZED MAXWELLIAN)
  F)    'DIRECT' - INPUT OF TABULATED SPECTRAL DATA

FOR FURTHER INFORMATION ABOUT AN ENVIRONMENT, ENTER
THE RELEVANT KEYWORD, OR HIT RETURN TO CONTINUE.
?


2) ANGLE
REFERS TO THE ANGULAR DISTRIBUTION OF THE INCOMING
PLASMA FLUX. IT IS FOLLOWED BY ONE OF FOUR KEYWORDS:

 A) ISOTROPIC -
 B) ALIGNED - FIXED ANGLE OF INCIDENCE
 C) ANISOTROPIC - SUPERIMPOSED ISOTROPIC AND DIRECTED
    FLUX. PARAMETERS ARE ENTERED INTERACTIVELY
 D) FILE - ANISOTROPIC FLUX WHERE ENERGY DEPENDANT
    PARAMETERS ARE READ FROM A DATA FILE.

FOR FURTHER INFORMATION ABOUT AN ANGLE TYPE, ENTER
THE RELEVSNT KEYWORD, OR HIT RETURN TO CONTINUE
?

3) PROPERTY

 REFERS TO THE PROPERTIES OF THE MATERIAL CHOSEN.
THE  USER MAY ENTER A NEW MATERIAL BY TYPING:
'CHANGE MATERIAL <MATERIAL NAME>'
ANY NAME, SIGNIFICANT TO FOUR CHARACTERS, DEFINED
ON DATA FILE 8, MAY BE SPECIFIED. PARTICULAR PROP-
ERTIES ARE REFERED TO BY NUMBER (1-14). TO REVIEW
MATERIAL PROPERTIES, RETURN TO PROGRAM AND TYPE:
'LIST PROPERTIES ALL'.
```

```
4) MISCELLANEOUS PARAMETERS

  THE FOLLOWING PARAMETERS MAY ALSO BE SET BY THE USER:

 A) VBACK - UNDERLYING CONDUCTOR (BACKPLATE) VOLTAGE
 B) VINIT - INITIAL SURFACE POTENTIAL
 C) VBEGIN - BEGINNING POTENTIAL FOR IV PLOT OR TABLE
 D) VEND - ENDING POTENTIAL FOR IV PLOT OR TABLE
 E) EMISSION - DEFAULT IS 'ANGLE'. SET TI NORMAL, THE
    ANGULAR DEPENDANCE OF THE SECONDARY EMISSION IS
    SUPPRESSED
HIT RETURN <CR> TO CONTINUE
WELCOME TO HELP. CHOOSE ONE OF THE FOLLOWING
CATAGORIES BY ENTERING ONE OF THE 5 KEYWORDS SHOWN
1) SUMMARY
   (AN OVERVIEW OF MATCHG)

2) INPUT
   (WHAT GOES IN?: ENVIRONMENT, PROPERTIES
   ANGULAR DISTRIBUTION, AND MISC. PARAMETERS)

3) OUTPUT
   (WHAT COMES OUT?: CHARGING, CURRENTS,
   IV (CURRENTS VS. VOLTAGE), AND YIELDS)

4) COMMANDS
    (HOW DO I GET WHAT I WANT?:
   CHANGE, LIST, PARAMETERS, RESULT, TABLE, AND PLOT)

5) RETURN
   (BACK TO PROGRAM)
?
*** COMMANDS ***

  USER COMMANDS ARE MADE UP OF STRINGS OF KEY-
WORDS ORGANIZED UNDER THE FOLLOWING HEIRARCHY:

* FIRST WORDS *
     LIST - DISPLAY WHAT FOLLOWS
   CHANGE - CHANGE WHAT FOLLOWS
PARAMETER - SUMMARIZE  STATUS OF ALL PARAMETERS
   RESULT - SUMMARIZE THE RESULT OF WHAT FOLLOWS
     PLOT - PLOT THE RESULT OF WHAT FOLLOWS
    TABLE - DISPLAY IN TABULAR FORM WHAT FOLLOWS

* SECOND WORDS *
ENVIRONMENT - PERTAINS TO THE PLASMA ENERGY SPECTRUM
      ANGLE - PERTAINS TO PLASMA ANGULAR DISTRIBUTION
   EMISSION - EMISSION FORMULATION
   MATERIAL - NAME OF MATERIAL
 PROPERTIES - PERTAINS TO MATERIAL PROPERTIES
     CHARGE - PERTAINS TO POTENTIAL CALCULATION
    CURRENT - PERTAINS TO CALCULATION OF INCIDENT CURRENTS
```

```
        IV - PERTAINS TO CALCULATION OF CURRENTS AS A FUNC-
     TION OF SURFACE POTENTIALS
HIT RETURN <CR> TO CONTINUE

SECONDARY \
BACKSCATTER\  PERTAIN TO YIELDS FOR
ION        /  THESE PROCESSES
ALL       /

VBEGIN \  PERTAINS TO THE RANGE OF POTENTIALS
VEND   /  FOR 'IV' CALCULATIONS

VBACK \  PERTAINS TO INITIAL POTENTIAL IN A
VINIT /  CHARGE CALCULATION
HIT RETURN <CR> TO CONTINUE
* SUBSEQUENT WORDS AND DATA *
SOME COMMANDS CAN BE APPENDED WITH DATA STRINGS
AND/OR ADDITIONAL WORDS WHERE APPROPRIATE E.G.:

'CHANGE VBEGIN -2.'
(CHANGE THE PARAMETER VBEGIN TO -2. KEV)

'LIST PROPERTIES 2 7'
(LIST  THE VALUES OF MATERIAL PROPERTIES 2-7)

'RESULT CHARGE FULL'
(DISPLAY THE CHARGING RESULT OF THE SAMPLE, AND
 HAVE A 'FULL' SUMMARY OF CURRENTS AT EACH TIMESTEP)

'CHANGE ANGLE FILE 10'
(CHANGE ANGULAR DISTRIBUTION TO ANISOTROPIC PARAMETERS
 FROM FILE 10)

'CHANGE ENVIRONMENT TE1 2'
(CHANGE ENVIRONMENTAL ELECTRON TEMERATURE 1 TO 2 KEV)
HIT RETURN <CR> TO CONTINUE
WELCOME TO HELP. CHOOSE ONE OF THE FOLLOWING
CATAGORIES BY ENTERING ONE OF THE 5 KEYWORDS SHOWN
1) SUMMARY
   (AN OVERVIEW OF MATCHG)

2) INPUT
   (WHAT GOES IN?: ENVIRONMENT, PROPERTIES
   ANGULAR DISTRIBUTION, AND MISC. PARAMETERS)

3) OUTPUT
   (WHAT COMES OUT?: CHARGING, CURRENTS,
   IV (CURRENTS VS. VOLTAGE), AND YIELDS)

4) COMMANDS
    (HOW DO I GET WHAT I WANT?:
   CHANGE, LIST, PARAMETERS, RESULT, TABLE, AND PLOT)

5) RETURN
```

(BACK TO PROGRAM)
?
*** MAXWELLIAN **

'CHANGE ENVIRONMENT MULTI <N>'

CAUSES THE PLASMA SPECTRUM TO BE REPRESENTED BY <N> SUPERIMPOSED MAXWELLIAN COMPONENTS FOR EACH PLASMA SPECIES (IONS AND ELECTRONS) UP TO A MAXIMUM OF 5. EACH COMPONENT REQUIRES TEMPERATURES (TE, TI IN KEV) AND DENSITIES (NE, NI IN M**3) FOR ELECTRONS AND IONS RESPECTIVELY. FOR EXAMPLE:

'CHANGE ENVIRONMENT TE4 6.8'

CAUSES THE ELECTRON TEMPERATURE FOR THE FOURTH MAXWELLIAN COMPONENT TO BE CHANGED TO 6.8 KEV. THERE ARE TWO SPECIAL CASES:

1) 'CHANGE ENVIRONMENT SINGLE'
   SETS N TO ONE. ONLY TE1-TI1-NE1-NI1 NEED BE SET

2) 'CHANGE ENVIRONMENT DOUBLE'
   SETS N TO TWO. ONLY TE1-TE2-TI1-TI2-NE1-NE2-NI1-NI2 NEED BE SET.

*** KAPPA ***

THE SO-CALLED 'KAPPA' PLASMA SPECTRUM IS A DESCRETIZED MAXWELLIAN AND, AS SUCH, REQUIRES FIVE PARAMETERS TO BE SET. THEY ARE:

TE1 - ELECTRON TEMPERATURE IN KEV

TI1 - ION TEMPERATURE IN KEV

NE1 - ELECTRON DENSITY IN METERS**3

NI1 - ION DENSITY IN METERS**3

KAPPA - AN INTEGER >1

AS KAPPA BECOMES LARGER (>100), THE DISTRIBUTION TENDS TO BECOME LIKE A CONVENTIONAL MAXWELLIAN. LOWER VALUES GIVE AN INCREASINGLY NON-MAXWELLIAN HIGH ENERGY TAIL TO THE DISTRIBUTION.

*** TANK ***

IN THE 'TANK' MODE, MATCHG SIMULATES CHARGING VIA A SINGLE MONO-ENERGETIC ELECTRON BEAM IN A TEST TANK. THREE PARAMETERS SHOULD BE SET:

1) ENERGY - ENERGY OF THE BEAM IN KEV.

2) CURRENT - BEAM CURRENT DENSITY IN A/M**2

3) PREF - ANGLE OF INCIDENCE IN DEGREES.

'PREF' MUST BE SET VIA THE FOLLOWING COMMAND:

'CHANGE ENVI PREF <N>' N = ANGLE OF INCIDENCE

'TANK' SHOULD BE OPERATED WITH 'EMISSION' SET TO 'ANGLE'.

*** DIRECT ***

'CHANGE ENVIRONMENT DIRECT <N> '

CAUSES TABULATED SPECTRAL DATA TO BE READ FROM FILE N. FILE N MUST BE IN THE CORRECT FORMAT (SEE MATCHG DOCUMENTATION). EACH DATA SET IN THE FILE IS LABELLED WITH THE TIME (IN SECONDS) DAY AND YEAR WITH WHICH IT CORRESPONDS. YOU WILL BE PROMPTED FOR THIS INFORMATION. E.G. ENTER:

'59000 87 1980'

FOR THE DATA SET CORRESPONDING TO DAY 87, 1980 TAKEN AT 59000 SECONDS.

*** ANISOTROPIC ***

MATCHG ALLOWS FOR AN ANGULAR DISTRIBUTION MADE UP OF A DIRECTED COMPONENT (A COS**2 THETA DISTRIBUTION), AND AN ISOTROPIC BACKGROUND. THE RATIOS OF THESE COMPONENTS (ERAT, IRAT) MUST BE SET FOR ELECTRONS AND IONS. THEY RANGE FROM -1 TO INFINITY.

'CHANGE ANGLE FILE <N>'

CAUSES DIFFERENT VALUES OF 'ERAT' AND 'IRAT', FOR UP TO 10 ENERGIES EACH, TO BE READ IN FROM A FILE N (SEE MATCHG DOCUMENTATION FOR CORRECT FILE FORMAT). THIS ALLOWS THE ANISOTROPY RATIO TO DEPEND ON ENERGY. VALUES BETWEEN THOSE GIVEN ARE LINEARLY INTERPOLATED.

THE ORIENTATION OF THE DIRECTED COMPONENT (I.E. THE ANGLE BETWEEN THE SURFACE NORMAL AND THE PREFERRED DIRECTION) IS SPECIFIED WITH THE WORD 'PREF' E.G.

'CHANGE PREF 80.' - CHANGES THE ANGLE TO 80 DEGREES.

*** ALIGNED ***

AN 'ALIGNED' FLUX IS ONE WHERE ALL PARTICLES ARE INCIDENT WITH THE SAME ANGLE 'PREF' E.G.:

'CHANGE ANGLE PREF 80.'

```
  CHANGES THE ANGLE OF INCIDENT TO 80 DEGREES.
*** ISOTROPIC ***

  WHEN THE ANGLE TYPE IS ISOTROPIC, THE FLUX IS
INCIDENT WITH ALL ANGLES BEING EQUALLY PROBABLE.
NO ADDITIONAL PARAMETERS ARE IMPLIED.

EXIT

[EXIT]
```

5.3 INPUT

The MATCHG input parameters describe the physical properties of the material and the surrounding plasma environment. There are five basic types of input which may be specified.

1. 'ENVIRONMENT' - specifies the plasma energy spectrum
2. 'ANGLE' - angular distribution of incoming flux
3. 'MATERIAL' - surface material at hand (see Table 5.5).
4. 'PROPERTIES' - properties of the material (1-14)
5. 'MISCELLANEOUS' - potential parameters for the calculations: 'VBEGIN', 'VEND', 'VBACK', and 'VINIT'

One of these words must follow a 'LIST' or 'CHANGE' command word. (See HELP in Section 5.1.1 for more details.)

TABLE 5.5 MATERIAL PROPERTIES

MATERIAL = KAPT.

	PROPERTY	INPUT VALUE	CODE VALUE
1	DIELECTRIC CONSTANT	3.50+000 (NONE)	3.50+000 (NONE)
2	THICKNESS	1.27-004 METERS	1.27-004 MESH
3	CONDUCTIVITY	1.00-016 MHO/M	1.00-016 MHO/M
4	ATOMIC NUMBER	5.00+000 (NONE)	5.00+000 (NONE)
5	DELTA MAX>COEFF	2.10+000 (NONE)	4.06+001 (NONE)
6	E-MAX >DEPTH**-1	1.50-001 KEV	8.74-002 ANG-01
7	RANGE	7.15+001 ANG.	4.29+001 ANG.
8	EXPONENT> RANGE	6.00-001 (NONE)	5.52+002 ANG.
9	RANGE> EXPONENT	3.12+002 ANG.	6.00-001 (NONE)
10	EXPONENT	1.77+000 (NONE)	1.77+000 (NONE)
11	YIELD FOR 1KEV PROTONS	4.55-001 (NONE)	4.55-001 (NONE)
12	MAX DE/DX FOR PROTONS	1.40+002 KEV	1.40+002 KEV
13	PHOTOCURRENT	2.00-005 A/M**2	2.00-005 A/M**2
14	SURFACE RESISTIVITY	1.00+016 OHMS	8.85+004 V-S/Q

MATERIAL IS GOLD

MATERIAL = GOLD.

	PROPERTY	INPUT VALUE	CODE VALUE
1	DIELECTRIC CONSTANT	1.00+000 (NONE)	1.00+000 (NONE)
2	THICKNESS	1.00-003 METERS	1.00-003 MESH
3	CONDUCTIVITY	-1.00+000 MHO/M	-1.00+000 MHO/M
4	ATOMIC NUMBER	7.90+001 (NONE)	7.90+001 (NONE)
5	DELTA MAX>COEFF	8.80-001 (NONE)	2.93+000 (NONE)
6	E-MAX >DEPTH**-1	8.00-001 KEV	2.02-002 ANG-01
7	RANGE	8.88+001 ANG.	8.17+001 ANG.
8	EXPONENT> RANGE	9.20-001 (NONE)	9.25+001 ANG.
9	RANGE> EXPONENT	5.35+001 ANG.	9.20-001 (NONE)
10	EXPONENT	1.73+000 (NONE)	1.73+000 (NONE)
11	YIELD FOR 1KEV PROTONS	4.13-001 (NONE)	4.13-001 (NONE)
12	MAX DE/DX FOR PROTONS	1.35+002 KEV	1.35+002 KEV
13	PHOTOCURRENT	2.90-005 A/M**2	2.90-005 A/M**2
14	SURFACE RESISTIVITY	-1.00+000 OHMS	-8.85-012 V-S/Q

MATERIAL IS SOLA

MATERIAL = SOLA.

	PROPERTY	INPUT VALUE	CODE VALUE
1	DIELECTRIC CONSTANT	3.80+000 (NONE)	3.80+000 (NONE)
2	THICKNESS	1.79-004 METERS	1.79-004 MESH
3	CONDUCTIVITY	1.00-017 MHO/M	1.00-017 MHO/M
4	ATOMIC NUMBER	1.00+001 (NONE)	1.00+001 (NONE)
5	DELTA MAX>COEFF	2.05+000 (NONE)	1.31+001 (NONE)
6	E-MAX >DEPTH**-1	4.10-001 KEV	3.17-002 ANG-01
7	RANGE	7.75+001 ANG.	3.49+001 ANG.
8	EXPONENT> RANGE	4.50-001 (NONE)	2.70+002 ANG.
9	RANGE> EXPONENT	1.56+002 ANG.	4.50-001 (NONE)
10	EXPONENT	1.73+000 (NONE)	1.73+000 (NONE)
11	YIELD FOR 1KEV PROTONS	2.44-001 (NONE)	2.44-001 (NONE)
12	MAX DE/DX FOR PROTONS	2.30+002 KEV	2.30+002 KEV
13	PHOTOCURRENT	2.00-005 A/M**2	2.00-005 A/M**2
14	SURFACE RESISTIVITY	1.00+019 OHMS	8.85+007 V-S/Q

MATERIAL IS SCRE

MATERIAL = SCRE.

	PROPERTY	INPUT VALUE	CODE VALUE
1	DIELECTRIC CONSTANT	1.00+000 (NONE)	1.00+000 (NONE)
2	THICKNESS	1.00-003 METERS	1.00-003 MESH
3	CONDUCTIVITY	-1.00+000 MHO/M	-1.00+000 MHO/M
4	ATOMIC NUMBER	1.00+000 (NONE)	1.00+000 (NONE)
5	DELTA MAX>COEFF	.00 (NONE)	.00 (NONE)
6	E-MAX >DEPTH**-1	1.00+000 KEV	1.38-001 ANG-01
7	RANGE	1.00+001 ANG.	1.50+001 ANG.
8	EXPONENT> RANGE	1.50+000 (NONE)	.00 ANG.
9	RANGE> EXPONENT	.00 ANG.	1.50+000 (NONE)
10	EXPONENT	1.00+000 (NONE)	1.00+000 (NONE)
11	YIELD FOR 1KEV PROTONS	.00 (NONE)	.00 (NONE)
12	MAX DE/DX FOR PROTONS	1.00+000 KEV	1.00+000 KEV
13	PHOTOCURRENT	.00 A/M**2	.00 A/M**2
14	SURFACE RESISTIVITY	-1.00+000 OHMS	-8.85-012 V-S/Q

MATERIAL IS ASTR

MATERIAL = ASTR.

	PROPERTY	INPUT VALUE	CODE VALUE
1	DIELECTRIC CONSTANT	3.80+000 (NONE)	3.80+000 (NONE)
2	THICKNESS	2.75-004 METERS	2.75-004 MESH
3	CONDUCTIVITY	2.75-012 MHO/M	2.75-012 MHO/M
4	ATOMIC NUMBER	1.00+001 (NONE)	1.00+001 (NONE)
5	DELTA MAX>COEFF	2.40+000 (NONE)	1.46+001 (NONE)
6	E-MAX >DEPTH**-1	4.00-001 KEV	3.81-002 ANG-01
7	RANGE	6.75+001 ANG.	5.47+001 ANG.
8	EXPONENT> RANGE	8.10-001 (NONE)	1.97+002 ANG.
9	RANGE> EXPONENT	1.06+002 ANG.	8.10-001 (NONE)
10	EXPONENT	1.86+000 (NONE)	1.86+000 (NONE)
11	YIELD FOR 1KEV PROTONS	4.55-001 (NONE)	4.55-001 (NONE)
12	MAX DE/DX FOR PROTONS	1.40+002 KEV	1.40+002 KEV
13	PHOTOCURRENT	2.00-005 A/M**2	2.00-005 A/M**2
14	SURFACE RESISTIVITY	1.00+011 OHMS	8.85-001 V-S/Q

MATERIAL IS TEFL

MATERIAL = TEFL.

	PROPERTY	INPUT VALUE	CODE VALUE
1	DIELECTRIC CONSTANT	2.00+000 (NONE)	2.00+000 (NONE)
2	THICKNESS	1.27-004 METERS	1.27-004 MESH
3	CONDUCTIVITY	1.00-016 MHO/M	1.00-016 MHO/M
4	ATOMIC NUMBER	7.00+000 (NONE)	7.00+000 (NONE)
5	DELTA MAX>COEFF	3.00+000 (NONE)	2.27+001 (NONE)
6	E-MAX >DEPTH**-1	3.00-001 KEV	3.83-002 ANG-01
7	RANGE	4.54+001 ANG.	1.81+001 ANG.
8	EXPONENT> RANGE	4.00-001 (NONE)	3.85+002 ANG.
9	RANGE> EXPONENT	2.18+002 ANG.	4.00-001 (NONE)
10	EXPONENT	1.77+000 (NONE)	1.77+000 (NONE)
11	YIELD FOR 1KEV PROTONS	4.55-001 (NONE)	4.55-001 (NONE)
12	MAX DE/DX FOR PROTONS	1.40+002 KEV	1.40+002 KEV
13	PHOTOCURRENT	2.00-005 A/M**2	2.00-005 A/M**2
14	SURFACE RESISTIVITY	1.00+016 OHMS	8.85+004 V-S/Q

MATERIAL IS INDO

MATERIAL = INDO.

	PROPERTY	INPUT VALUE	CODE VALUE
1	DIELECTRIC CONSTANT	1.00+000 (NONE)	1.00+000 (NONE)
2	THICKNESS	1.00-003 METERS	1.00-003 MESH
3	CONDUCTIVITY	-1.00+000 MHO/M	-1.00+000 MHO/M
4	ATOMIC NUMBER	2.44+001 (NONE)	2.44+001 (NONE)
5	DELTA MAX>COEFF	1.40+000 (NONE)	3.02+000 (NONE)
6	E-MAX >DEPTH**-1	8.00-001 KEV	1.49-002 ANG-01
7	RANGE	-1.00+000 ANG.	1.57+002 ANG.
8	EXPONENT> RANGE	.00 (NONE)	.00 ANG.
9	RANGE> EXPONENT	7.18+000 ANG.	2.01+000 (NONE)
10	EXPONENT	5.55+001 (NONE)	1.00+000 (NONE)
11	YIELD FOR 1KEV PROTONS	4.90-001 (NONE)	4.90-001 (NONE)
12	MAX DE/DX FOR PROTONS	1.23+002 KEV	1.23+002 KEV
13	PHOTOCURRENT	3.20-005 A/M**2	3.20-005 A/M**2
14	SURFACE RESISTIVITY	-1.00+000 OHMS	-8.85-012 V-S/Q

MATERIAL IS ALUM

MATERIAL = ALUM.

	PROPERTY	INPUT VALUE	CODE VALUE
1	DIELECTRIC CONSTANT	1.00+000 (NONE)	1.00+000 (NONE)
2	THICKNESS	1.00-003 METERS	1.00-003 MESH
3	CONDUCTIVITY	-1.00+000 MHO/M	-1.00+000 MHO/M
4	ATOMIC NUMBER	1.30+001 (NONE)	1.30+001 (NONE)
5	DELTA MAX>COEFF	9.70-001 (NONE)	9.18+000 (NONE)
6	E-MAX >DEPTH**-1	3.00-001 KEV	3.00-002 ANG-01
7	RANGE	1.54+002 ANG.	1.23+002 ANG.
8	EXPONENT> RANGE	8.00-001 (NONE)	3.87+002 ANG.
9	RANGE> EXPONENT	2.20+002 ANG.	8.00-001 (NONE)
10	EXPONENT	1.76+000 (NONE)	1.76+000 (NONE)
11	YIELD FOR 1KEV PROTONS	2.44-001 (NONE)	2.44-001 (NONE)
12	MAX DE/DX FOR PROTONS	2.30+002 KEV	2.30+002 KEV
13	PHOTOCURRENT	4.00-005 A/M**2	4.00-005 A/M**2

```
 14      SURFACE RESISTIVITY          -1.00+000 OHMS          -8.85-012 V-S/Q
MATERIAL IS YGOL

    MATERIAL = YGOL.

     PROPERTY                          INPUT VALUE            CODE VALUE
  1      DIELECTRIC CONSTANT          1.00+000 (NONE)         1.00+000 (NONE)
  2      THICKNESS                    1.00-003 METERS         1.00-003 MESH
  3      CONDUCTIVITY                -1.00+000 MHO/M         -1.00+000 MHO/M
  4      ATOMIC NUMBER                4.20+001 (NONE)         4.20+001 (NONE)
  5      DELTA MAX>COEFF              1.49+000 (NONE)         5.00+000 (NONE)
  6      E-MAX >DEPTH**-1             4.80-001 KEV            4.52+000 ANG-01
  7      RANGE                       -1.00+000 ANG.           1.56+000 ANG.
  8      EXPONENT> RANGE               .00     (NONE)          .00     ANG.
  9      RANGE> EXPONENT              1.78+001 ANG.           2.27+000 (NONE)
 10      EXPONENT                     3.40+000 (NONE)         1.00+000 (NONE)
 11      YIELD FOR 1KEV PROTONS       4.13-001 (NONE)         4.13-001 (NONE)
 12      MAX DE/DX FOR PROTONS        1.35+002 KEV            1.35+002 KEV
 13      PHOTOCURRENT                 2.40-005 A/M**2         2.40-005 A/M**2
 14      SURFACE RESISTIVITY         -1.00+000 OHMS          -8.85-012 V-S/Q
MATERIAL IS AQUA

    MATERIAL = AQUA.

     PROPERTY                          INPUT VALUE            CODE VALUE
  1      DIELECTRIC CONSTANT          1.00+000 (NONE)         1.00+000 (NONE)
  2      THICKNESS                    1.00-003 METERS         1.00-003 MESH
  3      CONDUCTIVITY                -1.00+000 MHO/M         -1.00+000 MHO/M
  4      ATOMIC NUMBER                6.00+000 (NONE)         6.00+000 (NONE)
  5      DELTA MAX>COEFF              1.00+000 (NONE)         7.06+000 (NONE)
  6      E-MAX >DEPTH**-1             3.00-001 KEV            2.21-002 ANG-01
  7      RANGE                       -1.00+000 ANG.           5.80+002 ANG.
  8      EXPONENT> RANGE               .00     (NONE)          .00     ANG.
  9      RANGE> EXPONENT              2.00+000 ANG.           1.55+000 (NONE)
 10      EXPONENT                     1.20+001 (NONE)         1.00+000 (NONE)
 11      YIELD FOR 1KEV PROTONS       4.55-001 (NONE)         4.55-001 (NONE)
 12      MAX DE/DX FOR PROTONS        1.40+002 KEV            1.40+002 KEV
 13      PHOTOCURRENT                 2.10-005 A/M**2         2.10-005 A/M**2
 14      SURFACE RESISTIVITY         -1.00+000 OHMS          -8.85-012 V-S/Q
MATERIAL IS CPAI

    MATERIAL = CPAI.

     PROPERTY                          INPUT VALUE            CODE VALUE
  1      DIELECTRIC CONSTANT          3.50+000 (NONE)         3.50+000 (NONE)
  2      THICKNESS                    1.00-003 METERS         1.00-003 MESH
  3      CONDUCTIVITY                -1.00+000 MHO/M         -1.00+000 MHO/M
  4      ATOMIC NUMBER                5.00+000 (NONE)         5.00+000 (NONE)
  5      DELTA MAX>COEFF              2.10+000 (NONE)         4.06+001 (NONE)
  6      E-MAX >DEPTH**-1             1.50-001 KEV            8.74-002 ANG-01
  7      RANGE                        7.15+001 ANG.           4.29+001 ANG.
  8      EXPONENT> RANGE              6.00-001 (NONE)         5.52+002 ANG.
  9      RANGE> EXPONENT              3.12+002 ANG.           6.00-001 (NONE)
 10      EXPONENT                     1.77+000 (NONE)         1.77+000 (NONE)
```

11	YIELD FOR 1KEV PROTONS	4.55-001 (NONE)	4.55-001 (NONE)
12	MAX DE/DX FOR PROTONS	1.40+002 KEV	1.40+002 KEV
13	PHOTOCURRENT	2.00-005 A/M**2	2.00-005 A/M**2
14	SURFACE RESISTIVITY	-1.00+000 OHMS	-8.85-012 V-S/Q

MATERIAL IS YELO

MATERIAL = YELO.

	PROPERTY	INPUT VALUE	CODE VALUE
1	DIELECTRIC CONSTANT	3.50+000 (NONE)	3.50+000 (NONE)
2	THICKNESS	1.00-003 METERS	1.00-003 MESH
3	CONDUCTIVITY	-1.00+000 MHO/M	-1.00+000 MHO/M
4	ATOMIC NUMBER	5.00+000 (NONE)	5.00+000 (NONE)
5	DELTA MAX>COEFF	2.10+000 (NONE)	4.06+001 (NONE)
6	E-MAX >DEPTH**-1	1.50-001 KEV	8.74-002 ANG-01
7	RANGE	7.15+001 ANG.	4.29+001 ANG.
8	EXPONENT> RANGE	6.00-001 (NONE)	5.52+002 ANG.
9	RANGE> EXPONENT	3.12+002 ANG.	6.00-001 (NONE)
10	EXPONENT	1.77+000 (NONE)	1.77+000 (NONE)
11	YIELD FOR 1KEV PROTONS	4.55-001 (NONE)	4.55-001 (NONE)
12	MAX DE/DX FOR PROTONS	1.40+002 KEV	1.40+002 KEV
13	PHOTOCURRENT	2.00-005 A/M**2	2.00-005 A/M**2
14	SURFACE RESISTIVITY	-1.00+000 OHMS	-8.85-012 V-S/Q

MATERIAL IS ML12

MATERIAL = ML12.

	PROPERTY	INPUT VALUE	CODE VALUE
1	DIELECTRIC CONSTANT	1.00+000 (NONE)	1.00+000 (NONE)
2	THICKNESS	1.00-003 METERS	1.00-003 MESH
3	CONDUCTIVITY	-1.00+000 MHO/M	-1.00+000 MHO/M
4	ATOMIC NUMBER	6.00+000 (NONE)	6.00+000 (NONE)
5	DELTA MAX>COEFF	1.00+000 (NONE)	7.06+000 (NONE)
6	E-MAX >DEPTH**-1	3.00-001 KEV	2.21-002 ANG-01
7	RANGE	-1.00+000 ANG.	5.80+002 ANG.
8	EXPONENT> RANGE	.00 (NONE)	.00 ANG.
9	RANGE> EXPONENT	2.00+000 ANG.	1.55+000 (NONE)
10	EXPONENT	1.20+001 (NONE)	1.00+000 (NONE)
11	YIELD FOR 1KEV PROTONS	4.55-001 (NONE)	4.55-001 (NONE)
12	MAX DE/DX FOR PROTONS	1.40+002 KEV	1.40+002 KEV
13	PHOTOCURRENT	2.10-005 A/M**2	2.10-005 A/M**2
14	SURFACE RESISTIVITY	-1.00+000 OHMS	-8.85-012 V-S/Q

MATERIAL IS MAGN

MATERIAL = MAGN.

	PROPERTY	INPUT VALUE	CODE VALUE
1	DIELECTRIC CONSTANT	1.00+000 (NONE)	1.00+000 (NONE)
2	THICKNESS	1.00-003 METERS	1.00-003 MESH
3	CONDUCTIVITY	-1.00+000 MHO/M	-1.00+000 MHO/M
4	ATOMIC NUMBER	1.20+001 (NONE)	1.20+001 (NONE)
5	DELTA MAX>COEFF	9.20-001 (NONE)	7.02+000 (NONE)
6	E-MAX >DEPTH**-1	2.50-001 KEV	2.79-002 ANG-01
7	RANGE	-1.00+000 ANG.	6.96+002 ANG.

8	EXPONENT> RANGE	.00	(NONE)	.00	ANG.
9	RANGE> EXPONENT	1.74+000	ANG.	1.75+000	(NONE)
10	EXPONENT	2.43+001	(NONE)	1.00+000	(NONE)
11	YIELD FOR 1KEV PROTONS	2.44-001	(NONE)	2.44-001	(NONE)
12	MAX DE/DX FOR PROTONS	2.30+002	KEV	2.30+002	KEV
13	PHOTOCURRENT	4.00-005	A/M**2	4.00-005	A/M**2
14	SURFACE RESISTIVITY	-1.00+000	OHMS	-8.85-012	V-S/Q

MATERIAL IS NPAI

MATERIAL = NPAI.

PROPERTY		INPUT VALUE		CODE VALUE	
1	DIELECTRIC CONSTANT	3.50+000	(NONE)	3.50+000	(NONE)
2	THICKNESS	5.00-005	METERS	5.00-005	MESH
3	CONDUCTIVITY	5.90-014	MHO/M	5.90-014	MHO/M
4	ATOMIC NUMBER	5.00+000	(NONE)	5.00+000	(NONE)
5	DELTA MAX>COEFF	2.10+000	(NONE)	3.05+001	(NONE)
6	E-MAX >DEPTH**-1	1.50-001	KEV	3.41-002	ANG-01
7	RANGE	-1.00+000	ANG.	1.05+003	ANG.
8	EXPONENT> RANGE	.00	(NONE)	.00	ANG.
9	RANGE> EXPONENT	1.05+000	ANG.	1.51+000	(NONE)
10	EXPONENT	9.80+000	(NONE)	1.00+000	(NONE)
11	YIELD FOR 1KEV PROTONS	4.55-001	(NONE)	4.55-001	(NONE)
12	MAX DE/DX FOR PROTONS	1.40+002	KEV	1.40+002	KEV
13	PHOTOCURRENT	2.00-005	A/M**2	2.00-005	A/M**2
14	SURFACE RESISTIVITY	1.00+013	OHMS	8.85+001	V-S/Q

MATERIAL IS SILV

MATERIAL = SILV.

PROPERTY		INPUT VALUE		CODE VALUE	
1	DIELECTRIC CONSTANT	1.00+000	(NONE)	1.00+000	(NONE)
2	THICKNESS	1.00-003	METERS	1.00-003	MESH
3	CONDUCTIVITY	-1.00+000	MHO/M	-1.00+000	MHO/M
4	ATOMIC NUMBER	4.70+001	(NONE)	4.70+001	(NONE)
5	DELTA MAX>COEFF	1.00+000	(NONE)	3.09+000	(NONE)
6	E-MAX >DEPTH**-1	6.00-001	KEV	1.58-002	ANG-01
7	RANGE	8.45+001	ANG.	6.93+001	ANG.
8	EXPONENT> RANGE	8.20-001	(NONE)	1.38+002	ANG.
9	RANGE> EXPONENT	7.94+001	ANG.	8.20-001	(NONE)
10	EXPONENT	1.74+000	(NONE)	1.74+000	(NONE)
11	YIELD FOR 1KEV PROTONS	4.90-001	(NONE)	4.90-001	(NONE)
12	MAX DE/DX FOR PROTONS	1.23+002	KEV	1.23+002	KEV
13	PHOTOCURRENT	2.90-005	A/M**2	2.90-005	A/M**2
14	SURFACE RESISTIVITY	-1.00+000	OHMS	-8.85-012	V-S/Q

MATERIAL IS PDGO

MATERIAL = PDGO.

PROPERTY		INPUT VALUE		CODE VALUE	
1	DIELECTRIC CONSTANT	1.00+000	(NONE)	1.00+000	(NONE)
2	THICKNESS	1.00-003	METERS	1.00-003	MESH
3	CONDUCTIVITY	-1.00+000	MHO/M	-1.00+000	MHO/M
4	ATOMIC NUMBER	7.31+001	(NONE)	7.31+001	(NONE)

5	DELTA MAX>COEFF	1.03+000 (NONE)	3.89+000 (NONE)
6	E-MAX >DEPTH**-1	7.20-001 KEV	2.37-002 ANG-01
7	RANGE	9.88+001 ANG.	8.17+001 ANG.
8	EXPONENT> RANGE	9.20-001 (NONE)	9.25+001 ANG.
9	RANGE> EXPONENT	5.35+001 ANG.	9.20-001 (NONE)
10	EXPONENT	1.73+000 (NONE)	1.73+000 (NONE)
11	YIELD FOR 1KEV PROTONS	4.13-001 (NONE)	4.13-001 (NONE)
12	MAX DE/DX FOR PROTONS	1.35+002 KEV	1.35+002 KEV
13	PHOTOCURRENT	2.90-005 A/M**2	2.90-005 A/M**2
14	SURFACE RESISTIVITY	-1.00+000 OHMS	-8.85-012 V-S/Q

MATERIAL IS MTBO

MATERIAL = MTBO.

PROPERTY		INPUT VALUE	CODE VALUE
1	DIELECTRIC CONSTANT	2.00+000 (NONE)	2.00+000 (NONE)
2	THICKNESS	5.00-003 METERS	5.00-003 MESH
3	CONDUCTIVITY	1.00-015 MHO/M	1.00-015 MHO/M
4	ATOMIC NUMBER	6.34+001 (NONE)	6.34+001 (NONE)
5	DELTA MAX>COEFF	8.80-001 (NONE)	2.93+000 (NONE)
6	E-MAX >DEPTH**-1	8.00-001 KEV	2.02-002 ANG-01
7	RANGE	8.88+001 ANG.	8.17+001 ANG.
8	EXPONENT> RANGE	9.20-001 (NONE)	9.25+001 ANG.
9	RANGE> EXPONENT	5.35+001 ANG.	9.20-001 (NONE)
10	EXPONENT	1.73+000 (NONE)	1.73+000 (NONE)
11	YIELD FOR 1KEV PROTONS	4.13-001 (NONE)	4.13-001 (NONE)
12	MAX DE/DX FOR PROTONS	1.35+002 KEV	1.35+002 KEV
13	PHOTOCURRENT	2.72-005 A/M**2	2.72-005 A/M**2
14	SURFACE RESISTIVITY	1.00+011 OHMS	8.85-001 V-S/Q

MATERIAL IS WHIT

MATERIAL = WHIT.

PROPERTY		INPUT VALUE	CODE VALUE
1	DIELECTRIC CONSTANT	3.50+000 (NONE)	3.50+000 (NONE)
2	THICKNESS	5.00-005 METERS	5.00-005 MESH
3	CONDUCTIVITY	5.90-014 MHO/M	5.90-014 MHO/M
4	ATOMIC NUMBER	5.00+000 (NONE)	5.00+000 (NONE)
5	DELTA MAX>COEFF	2.10+000 (NONE)	4.06+001 (NONE)
6	E-MAX >DEPTH**-1	1.50-001 KEV	8.74-002 ANG-01
7	RANGE	7.15+001 ANG.	4.29+001 ANG.
8	EXPONENT> RANGE	6.00-001 (NONE)	5.52+002 ANG.
9	RANGE> EXPONENT	3.12+002 ANG.	6.00-001 (NONE)
10	EXPONENT	1.77+000 (NONE)	1.77+000 (NONE)
11	YIELD FOR 1KEV PROTONS	4.55-001 (NONE)	4.55-001 (NONE)
12	MAX DE/DX FOR PROTONS	1.40+002 KEV	1.40+002 KEV
13	PHOTOCURRENT	2.00-005 A/M**2	2.00-005 A/M**2
14	SURFACE RESISTIVITY	1.00+013 OHMS	8.85+001 V-S/Q

MATERIAL IS BLAC

MATERIAL = BLAC.

PROPERTY		INPUT VALUE	CODE VALUE
1	DIELECTRIC CONSTANT	3.50+000 (NONE)	3.50+000 (NONE)

```
  2      THICKNESS                      1.00-003 METERS        1.00-003 MESH
  3      CONDUCTIVITY                  -1.00+000 MHO/M        -1.00+000 MHO/M
  4      ATOMIC NUMBER                  5.00+000 (NONE)        5.00+000 (NONE)
  5      DELTA MAX>COEFF                2.10+000 (NONE)        4.06+001 (NONE)
  6      E-MAX >DEPTH**-1               1.50-001 KEV           8.74-002 ANG-01
  7      RANGE                          7.15+001 ANG.          4.29+001 ANG.
  8      EXPONENT> RANGE                6.00-001 (NONE)        5.52+002 ANG.
  9      RANGE> EXPONENT                3.12+002 ANG.          6.00-001 (NONE)
 10      EXPONENT                       1.77+000 (NONE)        1.77+000 (NONE)
 11      YIELD FOR 1KEV PROTONS         4.55-001 (NONE)        4.55-001 (NONE)
 12      MAX DE/DX FOR PROTONS          1.40+002 KEV           1.40+002 KEV
 13      PHOTOCURRENT                   2.00-005 A/M**2        2.00-005 A/M**2
 14      SURFACE RESISTIVITY           -1.00+000 OHMS         -8.85-012 V-S/Q
DO YOU WANT A HARD COPY OF THIS RUN??
[EXIT]


&BIG-NAME,N
BIG-NAME 2.2  11 MAR 81  12:02:43
```

5.4 OUTPUT

Using these input parameters MATCHG calculates equilibrium potentials ('CHARGE'), incident and emitted currents ('CURRENT'), secondary and surface emission yields, and current versus surface potential information.

'IV' - These results are displayed in summary ('RESULT'), tabular ('TABLE'), or graphical ('PLOT') form according to the command given, e.g.,

'TABLE CHARGE' - gives a table of surface potential to equilibrium potential as a function of time.

'PLOT CHARGE' - expresses the same information graphically. Similarly 'PLOT IV' gives a current-voltage plot.

The command 'RESULT' can only be used with 'CHARGE' or 'CURRENTS' <n> where it gives a breakdown of the incident and emitted currents to the surface at potential N. 'RESULT' CHARGE gives a similar breakdown for the first and last cycle in the equilibrium potential calculation. See Section 5.2 for more examples.

5.5 INSTRUCTIONS FOR USE

The most extensive documentation for MATCHG is internal to the program. It is accessed by typing 'HELP' for unspecified help, or 'HELP<CATEGORY>' for help on a specific topic. This gives the user a complete explanation of the commands and modes available. (See Section 5.2 for 'HELP' documentation.)

To use MATCHG on a UNIVAC computer, type '@ADD NASCAP* MATCHG.XQT'. The ADD file will assign all necessary files and execute MATCHG. Section 5.4.1 contains a sample MATCHG run. Although many command words are typed completely, remember that all words are significant to four characters (i.e., 'TABLE' ≡ 'TABL').

5.6 MATCHG Test Run

```
WELCOME TO 'MATCHG', A MATERIAL CHARGING
PROGRAM. TYPE 'HELP' AT ANY TIME FOR ASSISTANCE.
MATERIAL IS KAPT
ENVIRONMENT NOW SINGLE MAXWELLIAN

PARAMETERS

MATERIAL IS KAPT.
EMISSION FORMULATION IS ANGL.
VBACK  =     .00      KEV
VINIT  =     .00      KEV
VBEGIN =     .00      KEV
VEND   =  -5.00+000 KEV
ANGULAR DISTRIBUTION IS ISOTROPIC
ENVIRONMENT IS A SINGLE MAXWELLIAN

ELECTRONS: NE1 =  1.00+006 (M**-3)     TE1 =     1.000 KEV
IONS     : NI1 =  1.00+006 (M**-3)     TI1 =     1.000 KEV

LIST PROP ALL

    MATERIAL = KAPT.

     PROPERTY                          INPUT VALUE          CODE VALUE
  1     DIELECTRIC CONSTANT            3.50+000 (NONE)      3.50+000 (NONE)
  2     THICKNESS                      1.27-004 METERS      1.27-004 MESH
  3     CONDUCTIVITY                   1.00-016 MHO/M       1.00-016 MHO/M
  4     ATOMIC NUMBER                  5.00+000 (NONE)      5.00+000 (NONE)
  5     DELTA MAX>COEFF                2.10+000 (NONE)      4.06+001 (NONE)
  6     E-MAX >DEPTH**-1               1.50-001 KEV         8.74-002 ANG-01
  7     RANGE                          7.15+001 ANG.        4.29+001 ANG.
  8     EXPONENT> RANGE                6.00-001 (NONE)      5.52+002 ANG.
  9     RANGE> EXPONENT                3.12+002 ANG.        6.00-001 (NONE)
 10     EXPONENT                       1.77+000 (NONE)      1.77+000 (NONE)
 11     YIELD FOR 1KEV PROTONS         4.55-001 (NONE)      4.55-001 (NONE)
 12     MAX DE/DX FOR PROTONS          1.40+002 KEV         1.40+002 KEV
 13     PHOTOCURRENT                   2.00-005 A/M**2      2.00-005 A/M**2
 14     SURFACE RESISTIVITY            1.00+016 OHMS        8.85+004 V-S/Q

LIST ENVI

ENVIRONMENT IS A SINGLE MAXWELLIAN

ELECTRONS: NE1 =  1.00+006 (M**-3)     TE1 =     1.000 KEV
IONS     : NI1 =  1.00+006 (M**-3)     TI1 =     1.000 KEV

CHAN ENVI TE1 5.

ENVIRONMENT IS A SINGLE MAXWELLIAN

ELECTRONS: NE1 =  1.00+006 (M**-3)     TE1 =     5.000 KEV
IONS     : NI1 =  1.00+006 (M**-3)     TI1 =     1.000 KEV
```

```
CHAN ENVI TI1 5.

ENVIRONMENT IS A SINGLE MAXWELLIAN

ELECTRONS: NE1 =  1.00+006 (M**-3)      TE1 =      5.000 KEV
IONS     : NI1 =  1.00+006 (M**-3)      TI1 =      5.000 KEV

TABLE ALL
```

TABLE GENERATED USING ISOTROPIC INCIDENT FLUX

ENERGY(KEV)	EL. SEC.	EL. BKSCAT.	PP. SEC.
.100	2.484	.165	.036
.200	3.153	.230	.051
.300	3.033	.262	.062
.400	2.742	.282	.072
.500	2.460	.296	.090
.600	2.219	.307	.144
.700	2.019	.315	.201
.800	1.852	.322	.260
1.000	1.592	.333	.375
2.000	.965	.316	.865
3.000	.712	.302	1.236
4.000	.573	.290	1.535
5.000	.483	.280	1.787
6.000	.420	.272	2.007
7.000	.374	.265	2.202
8.000	.338	.259	2.378
9.000	.308	.254	2.538
10.000	.285	.250	2.686
20.000	.167	.234	3.561
30.000	.122	.232	4.105
40.000	.098	.232	4.476
50.000	.083	.232	4.741

PLOT SECO

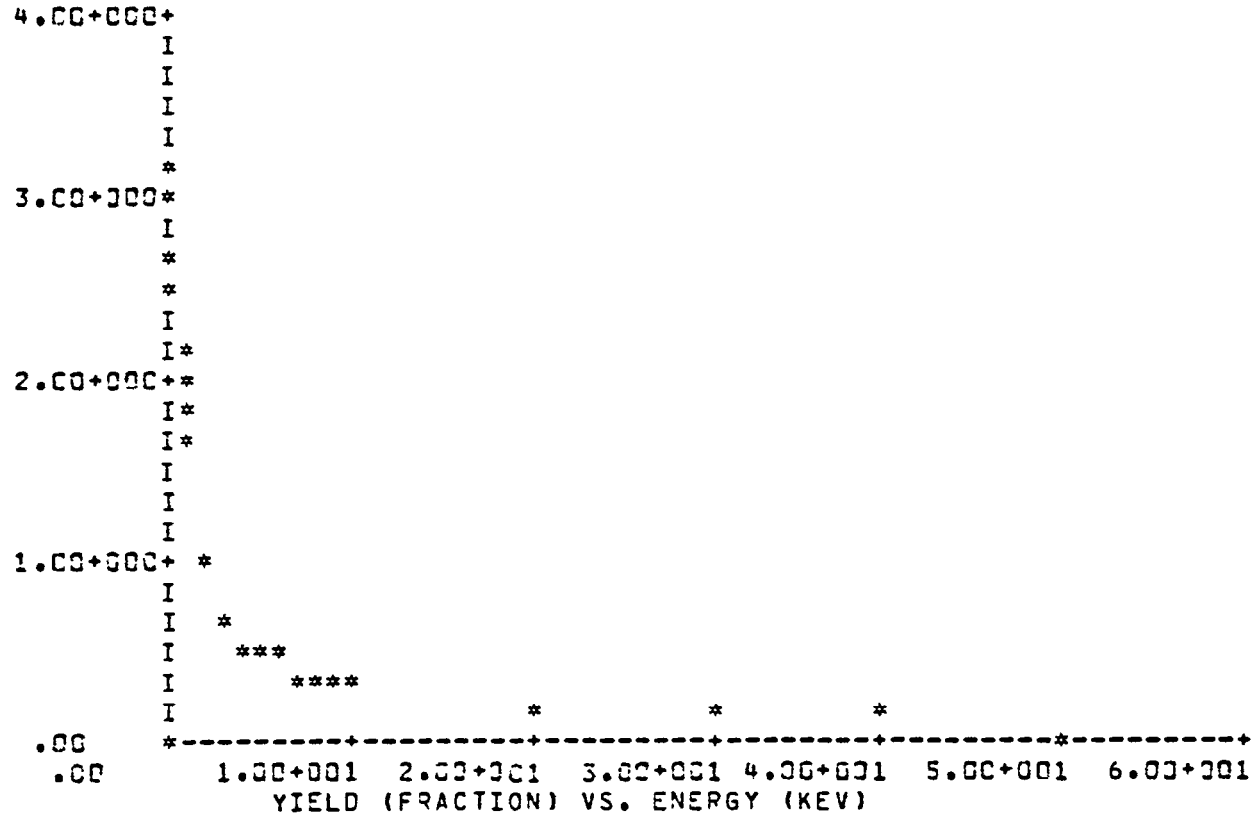
4.00+000
3.00+000
2.00+000
1.00+000
.00
.00
1.00+001 2.00+001 3.00+001 4.00+001 5.00+001 6.00+001
YIELD (FRACTION) VS. ENERGY (KEV)

PLOT BACK

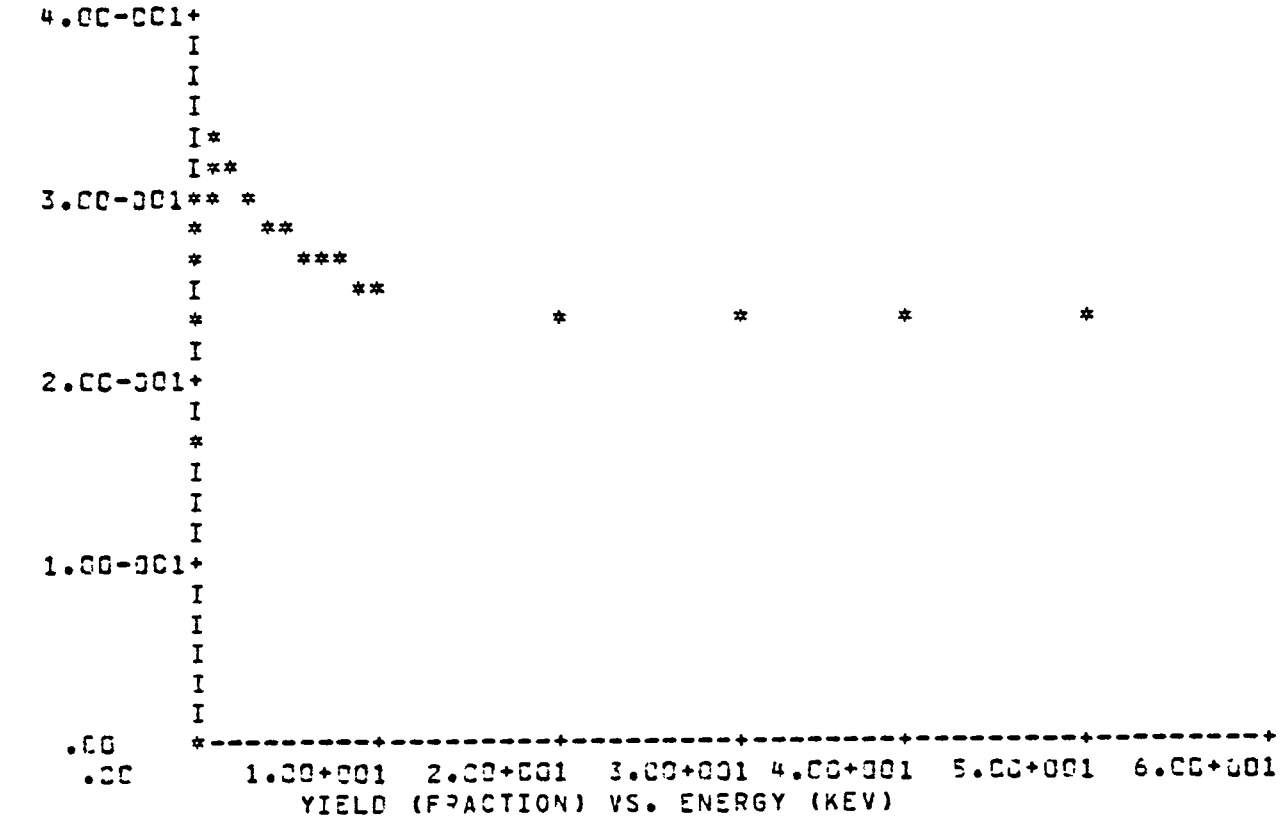
4.00-001
3.00-001
2.00-001
1.00-001
.00
.00
1.00+001 2.00+001 3.00+001 4.00+001 5.00+001 6.00+001
YIELD (FRACTION) VS. ENERGY (KEV)

PLOT ION

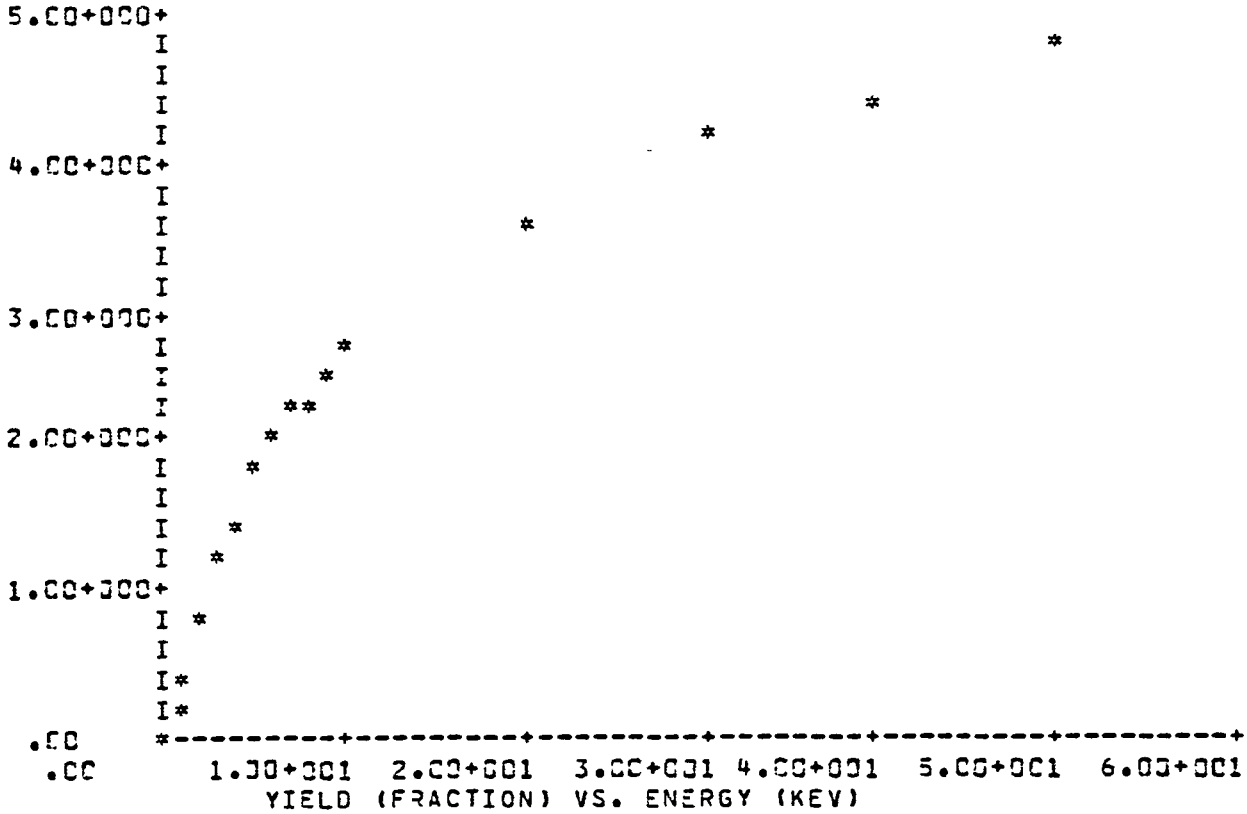


```
RESULT CHARGE

CYCLE    1   TIME   .00     SECONDS    POTENTIAL   .00     VOLTS

***TIME LEFT =131013 SECONDS***

INCIDENT ELECTRON CURRENT          -1.90-006
         SECONDARY ELECTRONS        8.13-007
         BACKSCATTERED ELECTRONS    5.00-007
INCIDENT PROTON CURRENT             4.43-008
         SECONDARY ELECTRONS        1.05-007
BULK CONDUCTIVITY CURRENT            .00
                                  -------------
                     NET CURRENT  -4.37-007  AMPS/M**2
CYCLE   78   TIME  2.74+004 SECONDS    POTENTIAL -3.64+003 VOLTS

***TIME LEFT =130997 SECONDS***

INCIDENT ELECTRON CURRENT          -9.17-007
         SECONDARY ELECTRONS        3.92-007
         BACKSCATTERED ELECTRONS    2.42-007
INCIDENT PROTON CURRENT             7.65-008
         SECONDARY ELECTRONS        2.04-007
BULK CONDUCTIVITY CURRENT            2.87-009
                                  -------------
```

NET CURRENT -8.63-011 AMPS/M**2

TABLE CHARGE

TIME LEFT =130997 SECONDS

TIME LEFT =130982 SECONDS

T (SEC)	V (VOLTS)	I(AMPS/M**2)
.00	.00	-4.37-007
5.59+002	-8.01+002	-3.24-007
1.12+003	-1.41+003	-2.46-007
1.68+003	-1.87+003	-1.90-007
2.23+003	-2.23+003	-1.48-007
2.79+003	-2.51+003	-1.17-007
3.35+003	-2.74+003	-9.22-008
3.91+003	-2.92+003	-7.33-008
4.47+003	-3.06+003	-5.85-008
5.03+003	-3.17+003	-4.68-008
5.59+003	-3.26+003	-3.76-008
6.14+003	-3.34+003	-3.02-008
6.70+003	-3.40+003	-2.43-008
7.26+003	-3.44+003	-1.96-008
7.82+003	-3.48+003	-1.58-008
8.38+003	-3.51+003	-1.27-008
8.94+003	-3.54+003	-1.03-008
9.50+003	-3.56+003	-8.29-009
1.01+004	-3.57+003	-6.70-009
1.06+004	-3.59+003	-5.41-009
1.12+004	-3.60+003	-4.37-009
1.17+004	-3.61+003	-3.53-009
1.23+004	-3.61+003	-2.86-009
1.28+004	-3.62+003	-2.31-009
1.34+004	-3.62+003	-1.87-009
1.40+004	-3.63+003	-1.51-009
1.45+004	-3.63+003	-1.22-009
1.51+004	-3.63+003	-9.88-010
1.56+004	-3.63+003	-8.00-010
1.62+004	-3.63+003	-6.47-010
1.68+004	-3.64+003	-5.23-010
1.73+004	-3.64+003	-4.23-010
1.79+004	-3.64+003	-3.42-010
1.84+004	-3.64+003	-2.77-010
1.90+004	-3.64+003	-2.24-010
1.95+004	-3.64+003	-1.81-010
2.01+004	-3.64+003	-1.47-010
2.07+004	-3.64+003	-1.19-010
2.12+004	-3.64+003	-9.59-011

```
PLOT CHARGE

***TIME LEFT =130981 SECONDS***

***TIME LEFT =130966 SECONDS***
```

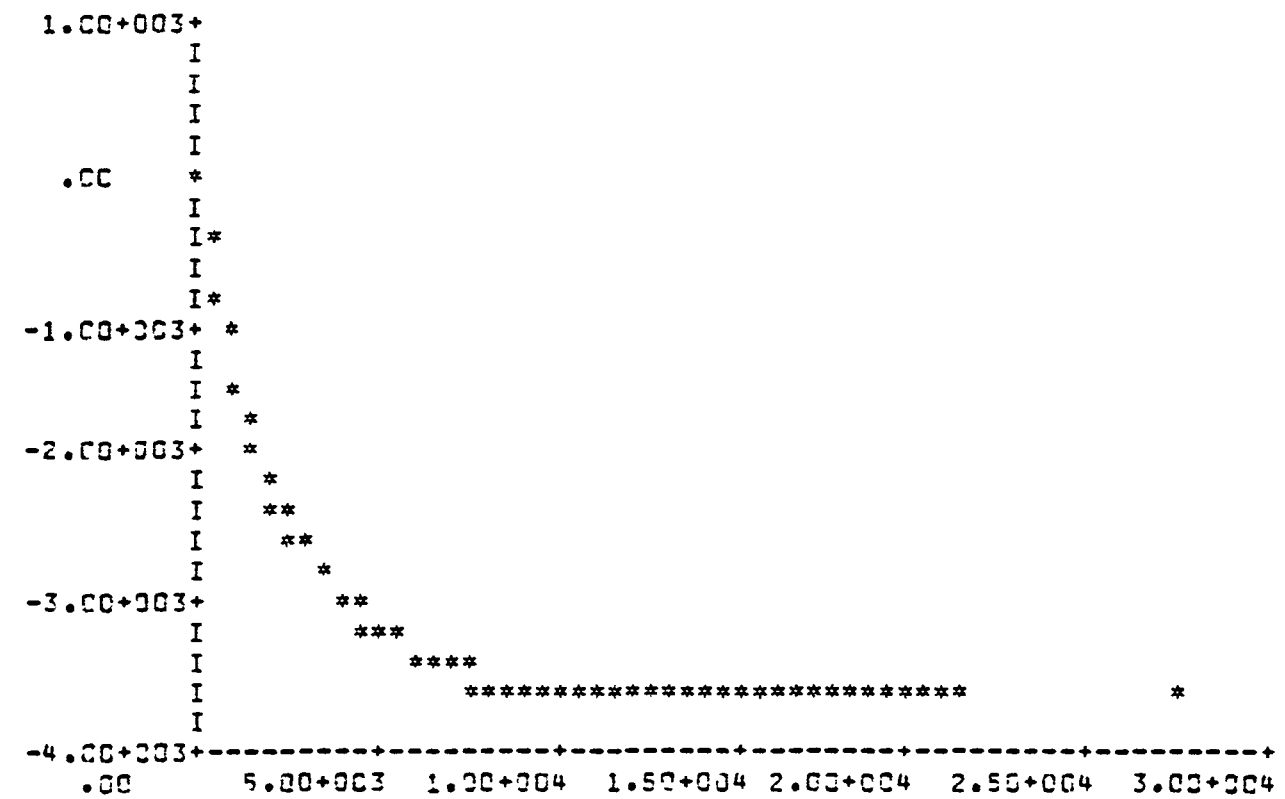
1.00+003
.00
-1.00+003
-2.00+003
-3.00+003
-4.00+003
.00
5.00+003
1.00+004
1.50+004
2.00+004
2.50+004
3.00+004
POTENTIAL (VOLTS) VS TIME (SECONDS)

PLOT IV

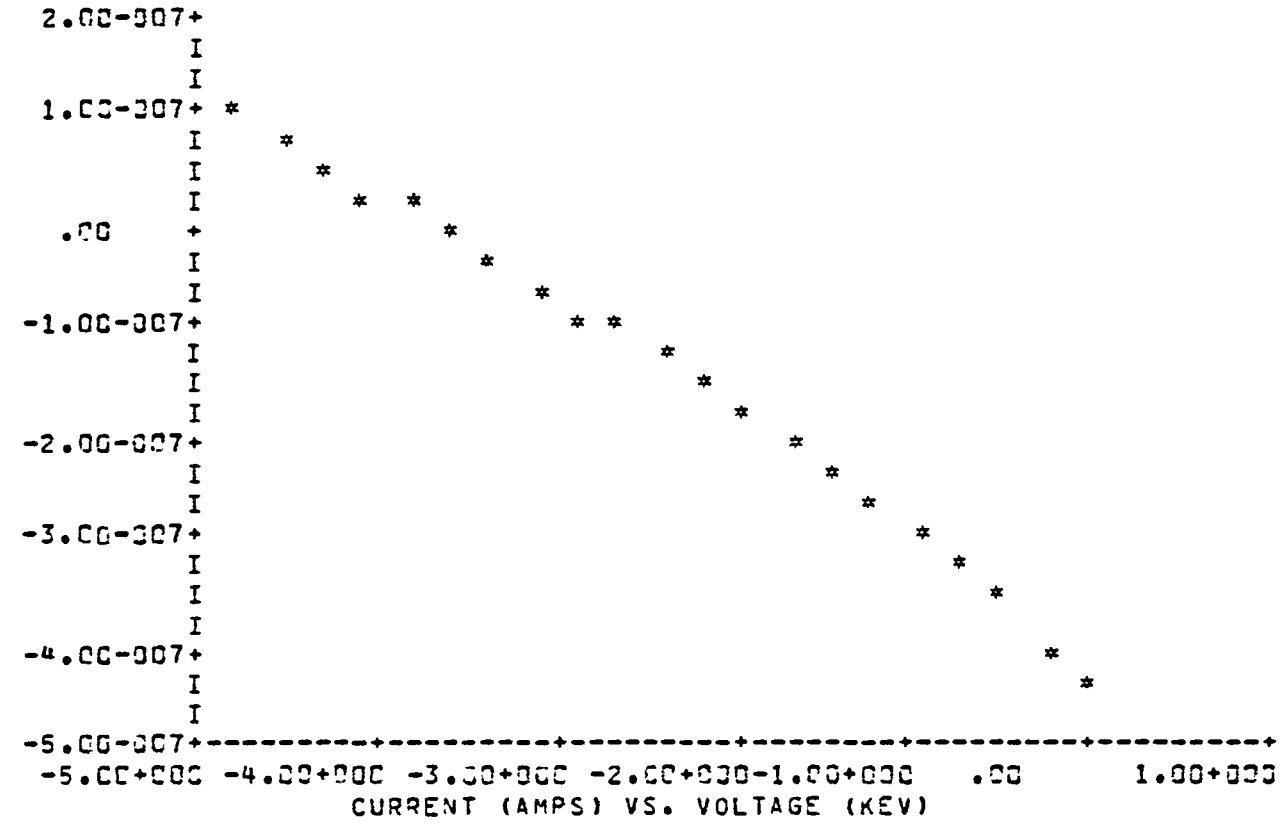
2.00-007
1.00-007
.00
-1.00-007
-2.00-007
-3.00-007
-4.00-007
-5.00-007
-5.00+000 -4.00+000 -3.00+000 -2.00+000 -1.00+000 .00 1.00+000
CURRENT (AMPS) VS. VOLTAGE (KEV)

TABLE IV

V	JTOT	JE	JSECE	JBSCAT	JI	JSECI
.CC	-4.37-CC7	-1.9C-CC6	8.13-CC7	5.CC-CC7	4.43-CC8	1.C5-CC7
-2.38-CC1	-4.C2-CC7	-1.81-CC6	7.75-CC7	4.77-CC7	4.64-CC8	1.1C-CC7
-4.76-CC1	-3.68-CC7	-1.73-CC6	7.39-CC7	4.55-CC7	4.85-CC8	1.16-CC7
-7.14-CC1	-3.36-CC7	-1.65-CC6	7.C5-CC7	4.34-CC7	5.C6-CC8	1.21-CC7
-9.52-CC1	-3.C4-CC7	-1.57-CC6	6.72-CC7	4.14-CC7	5.27-CC8	1.27-CC7
-1.19+CCC	-2.73-CC7	-1.5C-CC6	6.41-CC7	3.94-CC7	5.48-CC8	1.33-CC7
-1.43+CCC	-2.43-CC7	-1.43-CC6	6.11-CC7	3.76-CC7	5.7C-CC8	1.39-CC7
-1.67+CCC	-2.14-CC7	-1.36-CC6	5.82-CC7	3.59-CC7	5.9C-CC8	1.46-CC7
-1.9C+CCC	-1.86-CC7	-1.3C-CC6	5.55-CC7	3.42-CC7	6.12-CC8	1.52-CC7
-2.14+CCC	-1.58-CC7	-1.24-CC6	5.3C-CC7	3.26-CC7	6.33-CC8	1.59-CC7
-2.38+CCC	-1.31-CC7	-1.18-CC6	5.C5-CC7	3.11-CC7	6.54-CC8	1.66-CC7
-2.62+CCC	-1.C5-CC7	-1.13-CC6	4.81-CC7	2.96-CC7	6.75-CC8	1.73-CC7
-2.86+CCC	-7.97-CC8	-1.C7-CC6	4.59-CC7	2.83-CC7	6.96-CC8	1.8C-CC7
-3.1C+CCC	-5.48-CC8	-1.C2-CC6	4.38-CC7	2.69-CC7	7.17-CC8	1.87-CC7
-3.33+CCC	-3.C5-CC8	-9.75-CC7	4.17-CC7	2.57-CC7	7.38-CC8	1.94-CC7
-3.57+CCC	-6.86-CC9	-9.3C-CC7	3.98-CC7	2.45-CC7	7.59-CC8	2.C1-CC7
-3.81+CCC	1.63-CC8	-8.87-CC7	3.79-CC7	2.34-CC7	7.8C-CC8	2.C9-CC7
-4.C5+CCC	3.89-CC8	-8.45-CC7	3.62-CC7	2.23-CC7	8.C1-CC8	2.17-CC7
-4.29+CCC	6.11-CC8	-8.C6-CC7	3.45-CC7	2.12-CC7	8.22-CC8	2.24-CC7
-4.52+CCC	8.27-CC8	-7.69-CC7	3.29-CC7	2.C3-CC7	8.43-CC8	2.32-CC7
-4.76+CCC	1.C4-CC7	-7.33-CC7	3.14-CC7	1.93-CC7	8.64-CC8	2.4C-CC7

RESULT CURRENT -2.C7C

CURRENTS FOR POTENTIAL OF -2.C7+CCC KV

INCIDENT ELECTRON CURRENT	-1.26-CC6	
SECONDARY ELECTRONS	5.37-CC7	
BACKSCATTERED ELECTRONS	3.31-CC7	
INCIDENT PROTON CURRENT	6.26-CC8	
SECONDARY ELECTRONS	1.57-CC7	
BULK CONDUCTIVITY CURRENT	1.63-CC9	
NET CURRENT	-1.66-CC7	AMPS/M**2

CHANGE ENVI DIRECT 9

DATA IN FILE IS FROM 59CCC SECONDS ON DAY 87, 198C
TO 59CCC SECONDS ON DAY 87, 198C
SPECTRA FOUND FOR 59CCC SECONDS ON DAY 87, 198C
OBJECT POTENTIAL = -2CCC.C VOLTS
SINGLE MOMENT FIT GIVES N1= 984601. T1= 5111.78
SINGLE MOMENT FIT GIVES N1= .1CC257+CC7 T1= 5113.89

APPROXIMATE DENSITIES AND TEMPERATURES:

```
SPECIE      DENSITY(M-3)          TEMP(EV)
1( -1)          9.85+005          5.11+003
2(  1)          1.00+006          5.11+003

TABLE ALL
```

TABLE GENERATED USING ISOTROPIC INCIDENT FLUX

ENERGY(KEV)	EL. SEC.	EL. BKSCAT.	PR. SEC.
.100	2.484	.165	.036
.200	3.153	.230	.051
.300	3.033	.262	.062
.400	2.742	.282	.072
.500	2.460	.296	.090
.600	2.219	.307	.144
.700	2.019	.315	.201
.800	1.852	.322	.260
1.000	1.592	.333	.375
2.000	.965	.316	.865
3.000	.712	.302	1.236
4.000	.573	.293	1.535
5.000	.483	.280	1.787
6.000	.420	.272	2.007
7.000	.374	.265	2.202
8.000	.338	.259	2.378
9.000	.308	.254	2.538
10.000	.285	.250	2.686
20.000	.167	.234	3.561
30.000	.122	.232	4.105
40.000	.098	.232	4.476
50.000	.083	.232	4.741

PLOT SECO

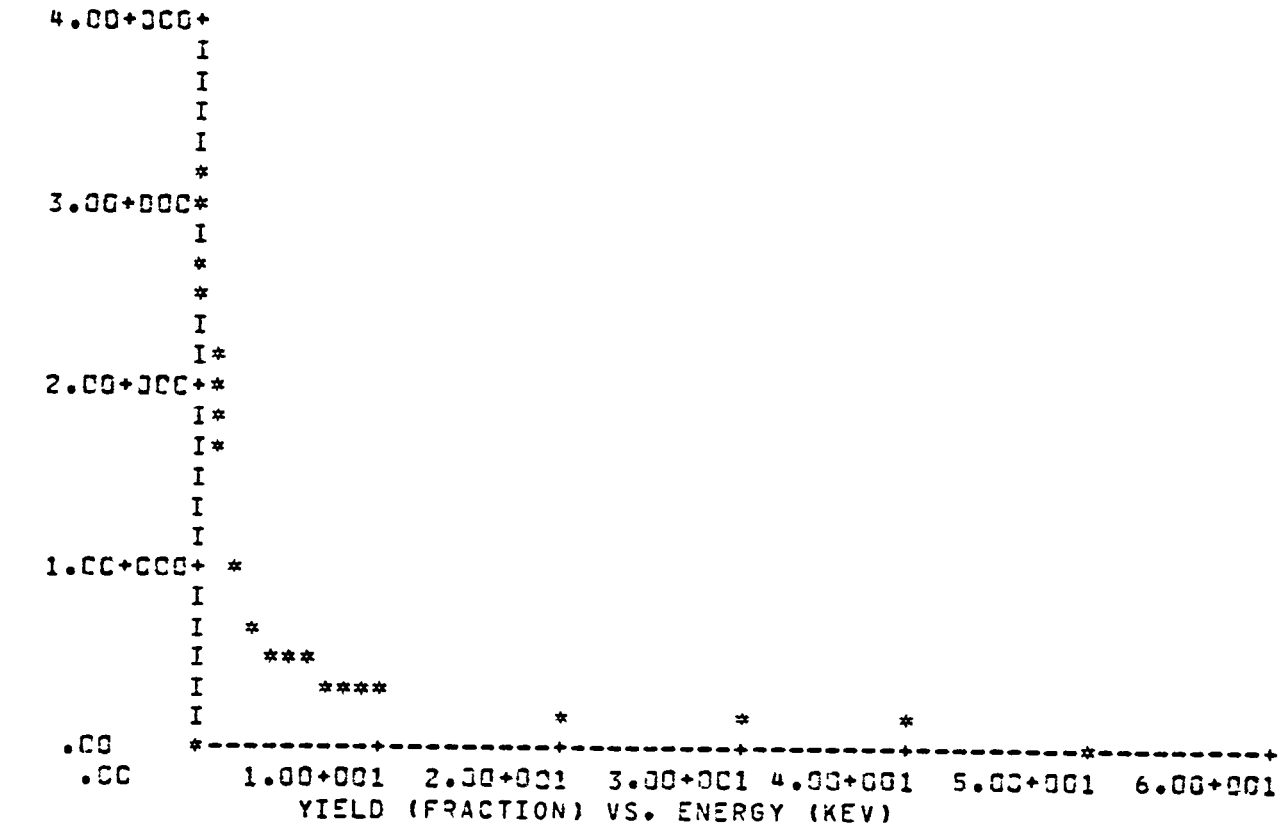
4.00+000
3.00+000
2.00+000
1.00+000
.00
.00
1.00+001 2.00+001 3.00+001 4.00+001 5.00+001 6.00+001
YIELD (FRACTION) VS. ENERGY (KEV)

PLOT BACK

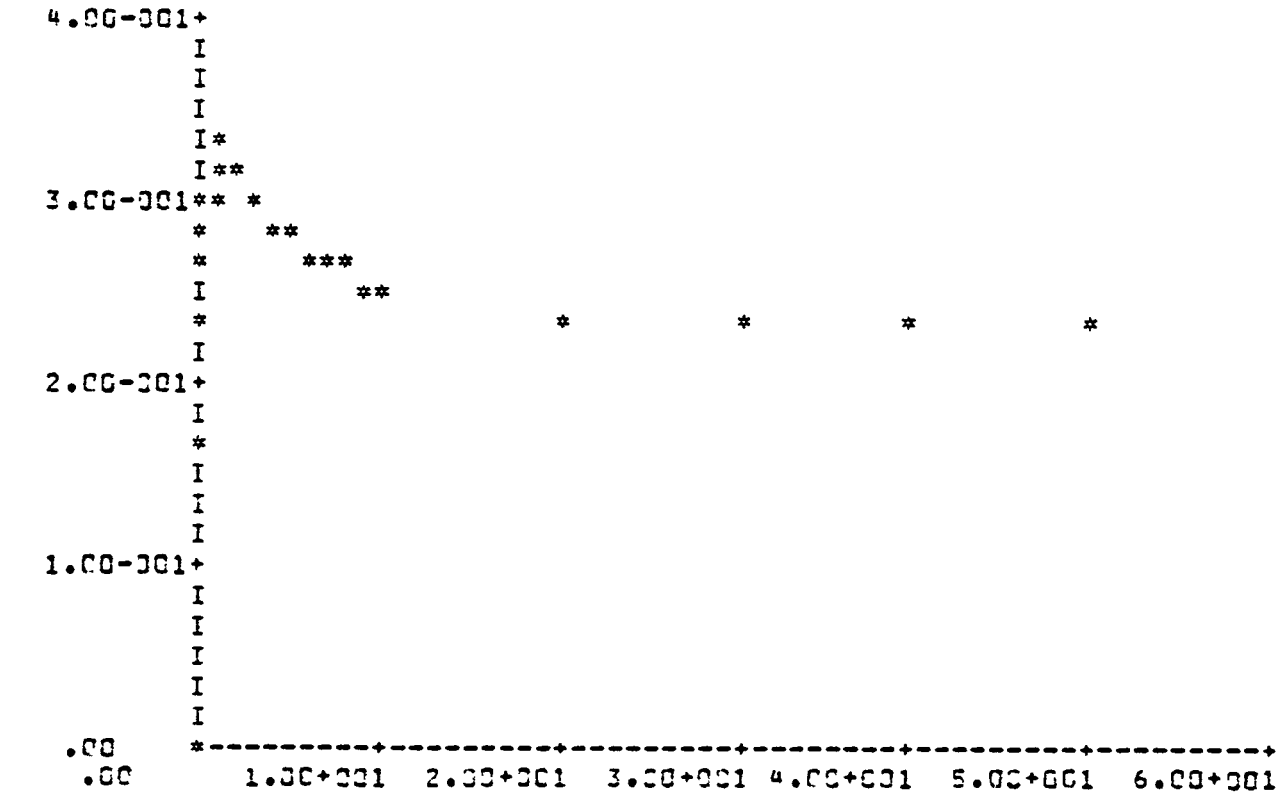
4.00-001
3.00-001
2.00-001
1.00-001
.00
.00
1.00+001 2.00+001 3.00+001 4.00+001 5.00+001 6.00+001
YIELD (FRACTION) VS. ENERGY (KEV)

```
PLOT ION
```

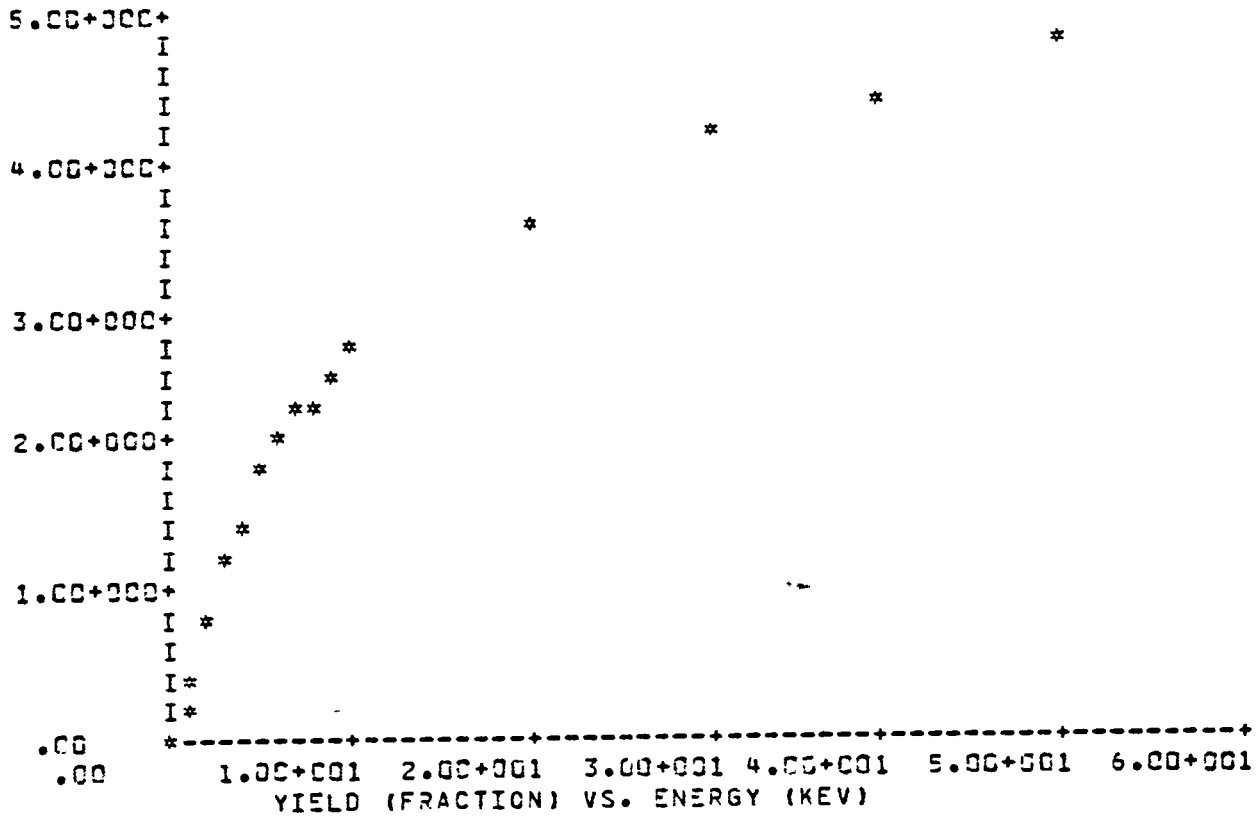


```
RESULT CHARGE

CYCLE    1   TIME    .00      SECONDS     POTENTIAL    .00      VOLTS

***TIME LEFT =130958 SECONDS***

INCIDENT ELECTRON CURRENT          -1.88-006
         SECONDARY ELECTRONS        8.27-007
         BACKSCATTERED ELECTRONS    4.98-007
INCIDENT PROTON CURRENT             4.42-008
         SECONDARY ELECTRONS        1.04-007
BULK CONDUCTIVITY CURRENT            .00
                                   ----------
                     NET CURRENT  -4.09-007  AMPS/M**2
CYCLE   72   TIME  2.98+004 SECONDS    POTENTIAL -3.48+003 VOLTS

***TIME LEFT =130948 SECONDS***

INCIDENT ELECTRON CURRENT          -9.45-007
         SECONDARY ELECTRONS        4.19-007
         BACKSCATTERED ELECTRONS    2.50-007
INCIDENT PROTON CURRENT             7.49-008
         SECONDARY ELECTRONS        1.98-007
BULK CONDUCTIVITY CURRENT           2.74-009
                                   ----------
```

NET CURRENT -9.37-011 AMPS/M**2

TABLE CHARGE

TIME LEFT =130948 SECONDS

TIME LEFT =130938 SECONDS

T (SEC)	V (VOLTS)	I(AMPS/M**2)
.00	.00	-4.09-007
6.09+002	-8.09+002	-2.99-007
1.22+003	-1.41+003	-2.24-007
1.83+003	-1.87+003	-1.70-007
2.44+003	-2.21+003	-1.31-007
3.05+003	-2.48+003	-1.01-007
3.65+003	-2.69+003	-7.87-008
4.26+003	-2.86+003	-6.14-008
4.87+003	-2.99+003	-4.84-008
5.48+003	-3.09+003	-3.82-008
6.09+003	-3.17+003	-3.02-008
6.70+003	-3.23+003	-2.40-008
7.31+003	-3.28+003	-1.90-008
7.92+003	-3.32+003	-1.51-008
8.53+003	-3.35+003	-1.21-008
9.14+003	-3.38+003	-9.60-009
9.75+003	-3.40+003	-7.65-009
1.04+004	-3.42+003	-6.10-009
1.10+004	-3.43+003	-4.86-009
1.16+004	-3.44+003	-3.88-009
1.22+004	-3.45+003	-3.09-009
1.28+004	-3.45+003	-2.47-009
1.34+004	-3.46+003	-1.97-009
1.40+004	-3.46+003	-1.57-009
1.46+004	-3.47+003	-1.25-009
1.52+004	-3.47+003	-1.00-009
1.58+004	-3.47+003	-7.98-010
1.64+004	-3.47+003	-6.37-010
1.71+004	-3.47+003	-5.08-010
1.77+004	-3.47+003	-4.06-010
1.83+004	-3.48+003	-3.24-010
1.89+004	-3.48+003	-2.58-010
1.95+004	-3.48+003	-2.06-010
2.01+004	-3.48+003	-1.65-010
2.07+004	-3.48+003	-1.31-010
2.13+004	-3.48+003	-1.05-010

PLOT CHARGE

```
***TIME LEFT =130938 SECONDS***

***TIME LEFT =130927 SECONDS***
```

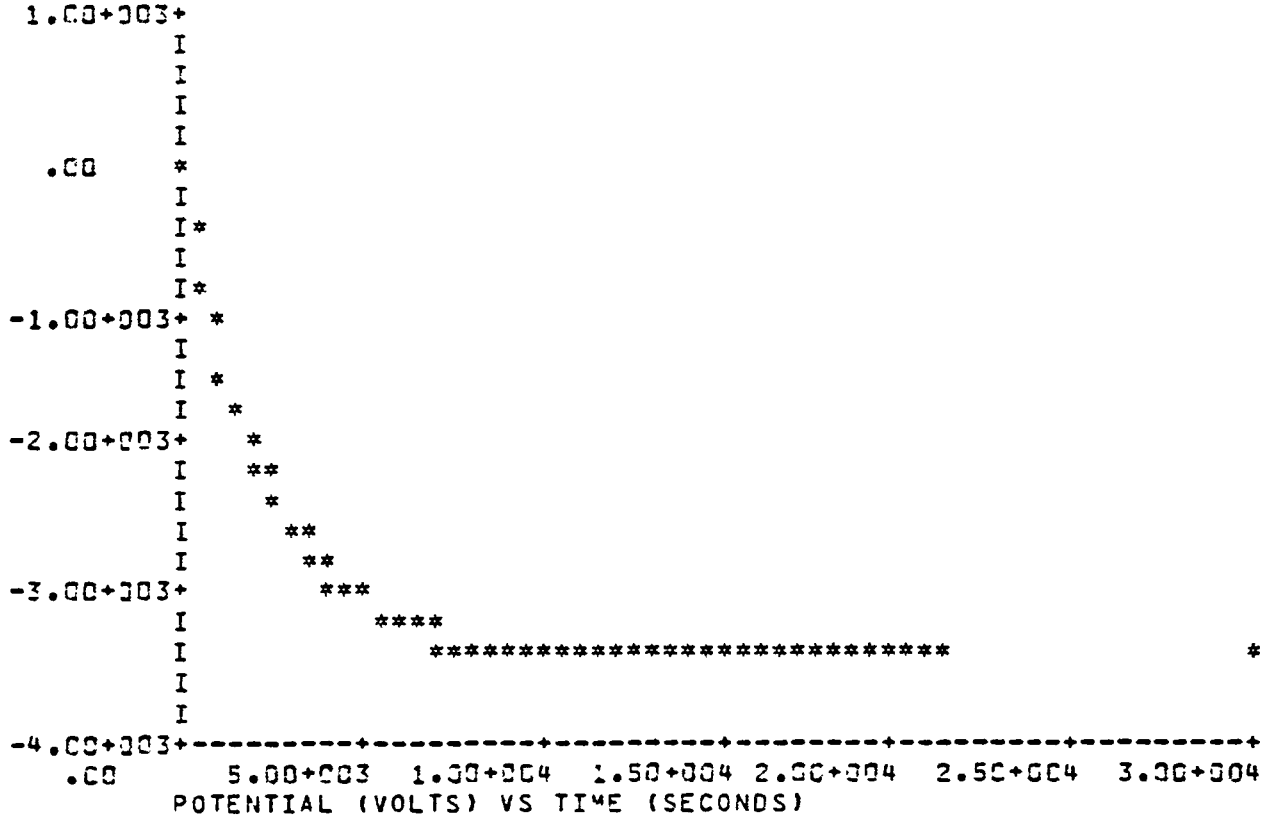
1.00+003
.00
-1.00+003
-2.00+003
-3.00+003
-4.00+003
.00
5.00+003
1.00+004
1.50+004
2.00+004
2.50+004
3.00+004
POTENTIAL (VOLTS) VS TIME (SECONDS)

PLOT IV

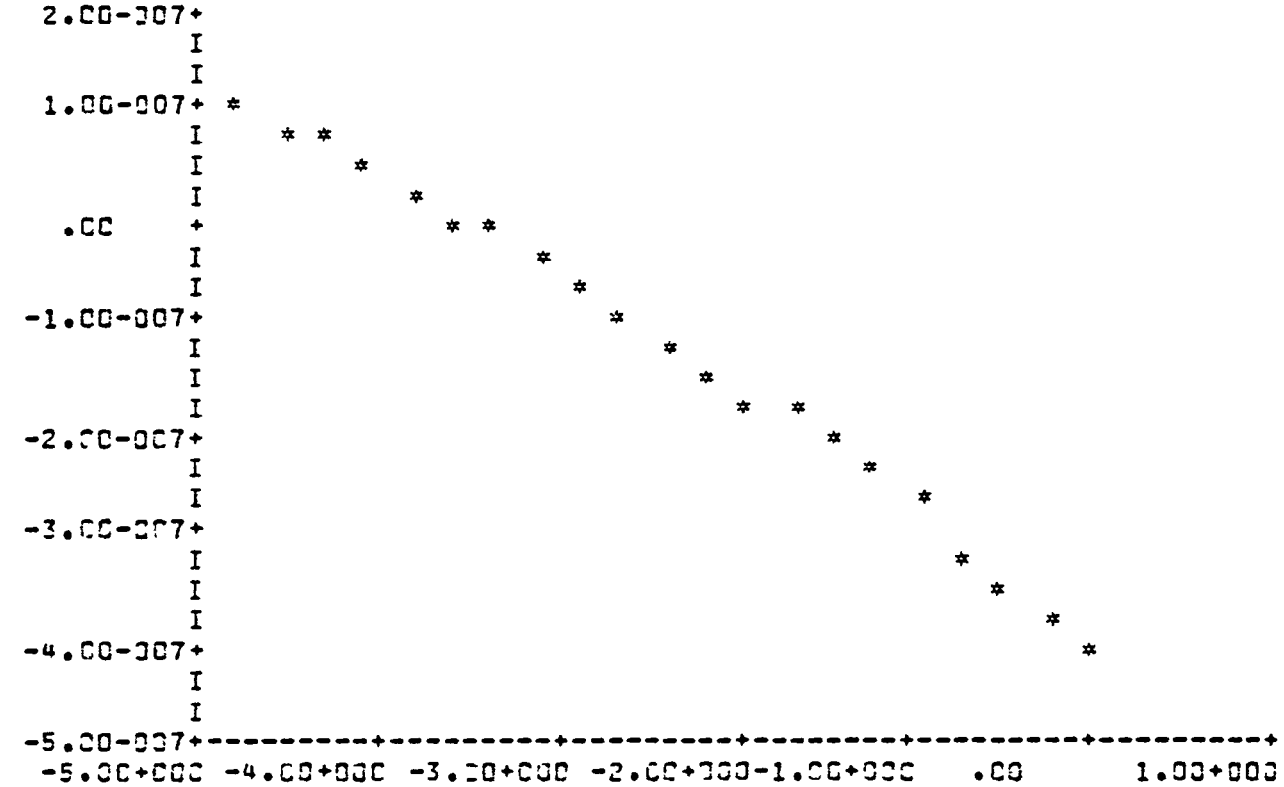
2.00-007
1.00-007
.00
-1.00-007
-2.00-007
-3.00-007
-4.00-007
-5.00-007
-5.00+000
-4.00+000
-3.00+000
-2.00+000
-1.00+000
.00
1.00+000
CURRENT (AMPS) VS. VOLTAGE (KEV)

TABLE IV

V	JTOT	JE	JSECE	JBSCAT	JI	JSECI
.00	-4.09-007	-1.88-006	8.27-007	4.98-007	4.42-008	1.04-007
-2.38-001	-3.76-007	-1.80-006	7.90-007	4.76-007	4.63-008	1.09-007
-4.76-001	-3.43-007	-1.71-006	7.54-007	4.54-007	4.84-008	1.15-007
-7.14-001	-3.11-007	-1.64-006	7.20-007	4.33-007	5.05-008	1.20-007
-9.52-001	-2.80-007	-1.56-006	6.87-007	4.13-007	5.26-008	1.26-007
-1.19+000	-2.50-007	-1.49-006	6.55-007	3.94-007	5.47-008	1.32-007
-1.43+000	-2.21-007	-1.42-006	6.25-007	3.76-007	5.68-008	1.39-007
-1.67+000	-1.93-007	-1.35-006	5.97-007	3.59-007	5.89-008	1.45-007
-1.90+000	-1.65-007	-1.29-006	5.70-007	3.42-007	6.10-008	1.52-007
-2.14+000	-1.39-007	-1.23-006	5.44-007	3.26-007	6.32-008	1.58-007
-2.38+000	-1.12-007	-1.18-006	5.19-007	3.11-007	6.53-008	1.65-007
-2.62+000	-8.67-008	-1.12-006	4.96-007	2.97-007	6.74-008	1.72-007
-2.86+000	-6.14-008	-1.07-006	4.74-007	2.84-007	6.95-008	1.79-007
-3.10+000	-3.74-008	-1.02-006	4.52-007	2.70-007	7.16-008	1.86-007
-3.33+000	-1.40-008	-9.73-007	4.31-007	2.58-007	7.37-008	1.94-007
-3.57+000	8.87-009	-9.28-007	4.11-007	2.46-007	7.58-008	2.01-007
-3.81+000	3.13-008	-8.85-007	3.92-007	2.34-007	7.79-008	2.08-007
-4.05+000	5.33-008	-8.44-007	3.74-007	2.24-007	8.00-008	2.16-007
-4.29+000	7.48-008	-8.04-007	3.57-007	2.13-007	8.21-008	2.24-007
-4.52+000	9.59-008	-7.67-007	3.40-007	2.03-007	8.42-008	2.32-007
-4.76+000	1.16-007	-7.31-007	3.24-007	1.94-007	8.63-008	2.40-007

RESULT CURRENT -2.000

CURRENTS FOR POTENTIAL OF -2.00+000 KV

INCIDENT ELECTRON CURRENT	-1.27-006
SECONDARY ELECTRONS	5.59-007
BACKSCATTERED ELECTRONS	3.36-007
INCIDENT PROTON CURRENT	6.19-008
SECONDARY ELECTRONS	1.54-007
BULK CONDUCTIVITY CURRENT	1.57-009
NET CURRENT	-1.55-007 AMPS/M**2

CHANGE ENVI SINGLE

ENVIRONMENT NOW SINGLE MAXWELLIAN
ENVIRONMENT IS A SINGLE MAXWELLIAN

ELECTRONS: NE1 = 1.00+006 (M**-3) TE1 = 5.000 KEV
IONS : NI1 = 1.00+006 (M**-3) TI1 = 5.000 KEV

CHANGE ANGLE ANISOTROPIC

ANISOTROPIC FLUX ASIGNED
ERATIO= 1.00+000 IRATIO= 1.00+000
PREFERED ANGLE= .000

```
CHANGE ANGLE ERAT 3.

ERATIO=    .00     IRATIO=   1.00+000

CHANGE ANGLE IRAT 0.

ERATIO=    .00     IRATIO=    .00

CHANGE ANGLE PREF 25.

PREFERED ANGLE=  25.000 DEGREES

PARAMETERS

MATERIAL IS KAPT.
EMISSION FORMULATION IS ANGL.
VBACK  =    .00     KEV
VINIT  =    .00     KEV
VBEGIN =    .00     KEV
VEND   =  -5.00+000 KEV
ANISOTROPIC FLUX
PREFERED DIRECTION=  25.000 DEGREES
ERATIO( 1) =    .00
IRATIO( 1) =    .00
ENVIRONMENT IS A SINGLE MAXWELLIAN

ELECTRONS: NE1 =  1.00+006 (M**-3)     TE1 =     5.000 KEV
IONS     : NI1 =  1.00+006 (M**-3)     TI1 =     5.000 KEV

TABLE ALL
```

```
TABLE GENERATED USING ANISOTROPIC INCIDENT FLUX AT  25.000+000 DEGREES

ENERGY(KEV)      EL. SEC.      EL. BKSCAT.      PR. SEC.
     .100          2.484           .165           .036
     .200          3.153           .230           .051
     .300          3.033           .262           .062
     .400          2.742           .282           .072
     .500          2.460           .296           .090
     .600          2.219           .307           .144
     .700          2.019           .315           .201
     .800          1.852           .322           .260
    1.000          1.592           .333           .375
    2.000           .965           .316           .865
    3.000           .712           .302          1.236
    4.000           .573           .290          1.535
    5.000           .483           .280          1.787
    6.000           .420           .272          2.007
    7.000           .374           .265          2.202
    8.000           .338           .259          2.378
    9.000           .308           .254          2.538
   10.000           .285           .250          2.686
   20.000           .167           .234          3.561
   30.000           .122           .232          4.105
   40.000           .098           .232          4.476
   50.000           .083           .232          4.741

RESULT CHARGE

CYCLE    1   TIME    .00     SECONDS    POTENTIAL    .00     VOLTS

***TIME LEFT =130922 SECONDS***

INCIDENT ELECTRON CURRENT          -1.90-006
         SECONDARY ELECTRONS        8.13-007
         BACKSCATTERED ELECTRONS    5.00-007
INCIDENT PROTON CURRENT             4.43-008
         SECONDARY ELECTRONS        1.05-007
BULK CONDUCTIVITY CURRENT            .00
                                  -----------
                     NET CURRENT  -4.37-007  AMPS/M**2
CYCLE   78   TIME  2.74+004 SECONDS    POTENTIAL -3.64+003 VOLTS

***TIME LEFT =130902 SECONDS***

INCIDENT ELECTRON CURRENT          -9.17-007
         SECONDARY ELECTRONS        3.92-007
         BACKSCATTERED ELECTRONS    2.42-007
INCIDENT PROTON CURRENT             7.65-008
         SECONDARY ELECTRONS        2.04-007
BULK CONDUCTIVITY CURRENT           2.87-009
                                  -----------
                     NET CURRENT  -8.63-011  AMPS/M**2

PLOT IV
```

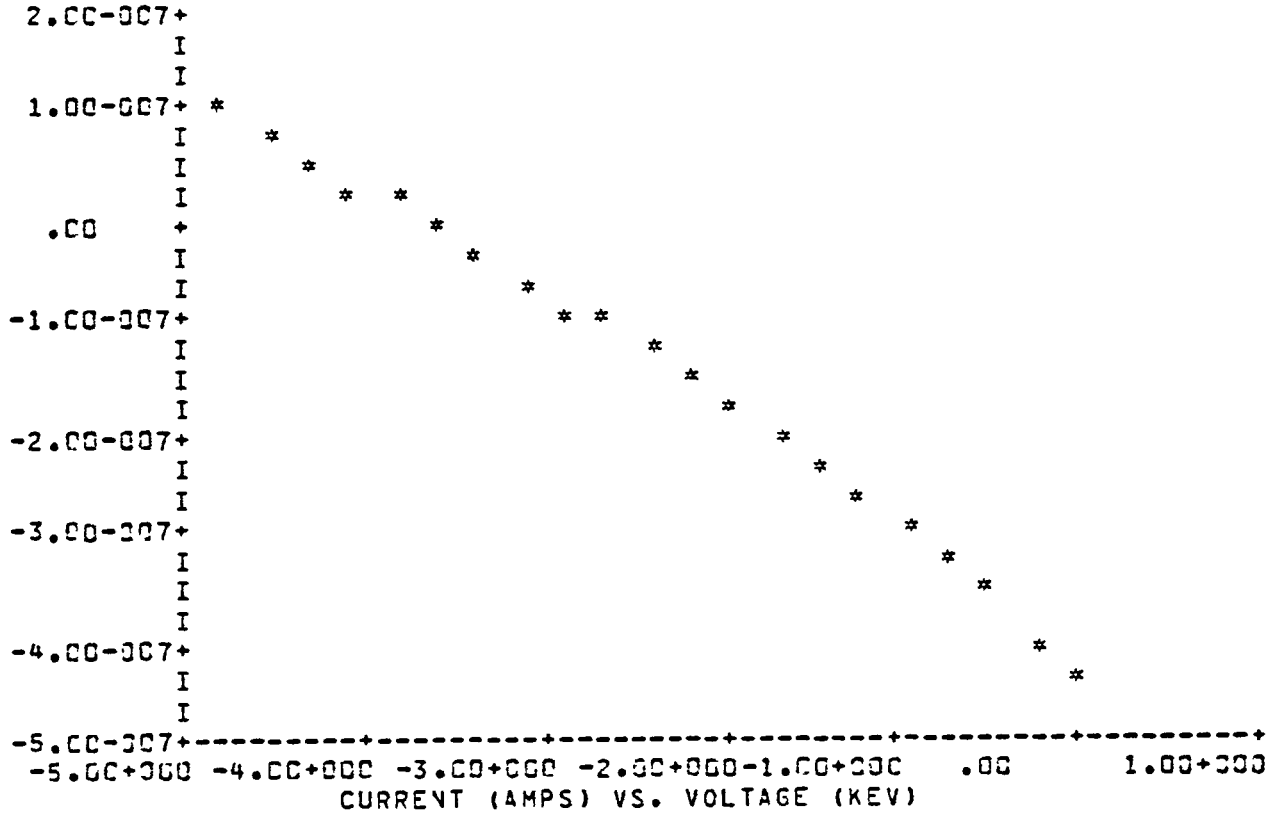
2.CC-CC7
1.CC-CC7
.CC
-1.CC-CC7
-2.CC-CC7
-3.CC-CC7
-4.CC-CC7
-5.CC-CC7
-5.CC+CCC -4.CC+CCC -3.CC+CCC -2.CC+CCC -1.CC+CCC .CC 1.CC+CCC
CURRENT (AMPS) VS. VOLTAGE (KEV)

TABLE IV

V	JTOT	JE	JSECE	JBSCAT	JI	JSECI
.00	-4.37-007	-1.90-006	8.13-007	5.00-007	4.43-008	1.05-007
-2.38-001	-4.02-007	-1.81-006	7.75-007	4.77-007	4.64-008	1.10-007
-4.76-001	-3.68-007	-1.73-006	7.39-007	4.55-007	4.85-008	1.16-007
-7.14-001	-3.36-007	-1.65-006	7.05-007	4.34-007	5.06-008	1.21-007
-9.52-001	-3.04-007	-1.57-006	6.72-007	4.14-007	5.27-008	1.27-007
-1.19+000	-2.73-007	-1.50-006	6.41-007	3.94-007	5.48-008	1.33-007
-1.43+000	-2.43-007	-1.43-006	6.11-007	3.76-007	5.70-008	1.39-007
-1.67+000	-2.14-007	-1.36-006	5.82-007	3.59-007	5.91-008	1.46-007
-1.90+000	-1.86-007	-1.30-006	5.55-007	3.42-007	6.12-008	1.52-007
-2.14+000	-1.58-007	-1.24-006	5.30-007	3.26-007	6.33-008	1.59-007
-2.38+000	-1.31-007	-1.18-006	5.05-007	3.11-007	6.54-008	1.66-007
-2.62+000	-1.05-007	-1.13-006	4.81-007	2.96-007	6.75-008	1.73-007
-2.86+000	-7.97-008	-1.07-006	4.59-007	2.83-007	6.96-008	1.80-007
-3.10+000	-5.48-008	-1.02-006	4.38-007	2.69-007	7.17-008	1.87-007
-3.33+000	-3.05-008	-9.75-007	4.17-007	2.57-007	7.38-008	1.94-007
-3.57+000	-6.86-009	-9.30-007	3.98-007	2.45-007	7.59-008	2.01-007
-3.81+000	1.63-008	-8.87-007	3.79-007	2.34-007	7.80-008	2.09-007
-4.05+000	3.89-008	-8.45-007	3.62-007	2.23-007	8.01-008	2.17-007
-4.29+000	6.11-008	-8.06-007	3.45-007	2.12-007	8.22-008	2.24-007
-4.52+000	8.27-008	-7.69-007	3.29-007	2.03-007	8.43-008	2.32-007
-4.76+000	1.04-007	-7.33-007	3.14-007	1.93-007	8.64-008	2.40-007

RESULT CURRENT -2.070

CURRENTS FOR POTENTIAL OF -2.07+000 KV

INCIDENT ELECTRON CURRENT	-1.26-006
SECONDARY ELECTRONS	5.37-007
BACKSCATTERED ELECTRONS	3.31-007
INCIDENT PROTON CURRENT	6.26-008
SECONDARY ELECTRONS	1.57-007
BULK CONDUCTIVITY CURRENT	1.63-009
NET CURRENT	-1.66-007 AMPS/M**2

CHANGE ANGLE ERAT 1.E4

ERATIO= 1.00+004 IRATIO= .00

CHANGE ANGLE IRAT 1.E4

ERATIO= 1.00+004 IRATIO= 1.00+004

CHANGE ANGLE PREF 0.

PREFERED ANGLE= .000 DEGREES

LIST ENVI

```
ENVIRONMENT IS A SINGLE MAXWELLIAN

ELECTRONS: NE1 =  1.00+006 (M**-3)     TE1 =     5.000 KEV
IONS     : NI1 =  1.00+006 (M**-3)     TI1 =     5.000 KEV

TABLE ALL
```

```
TABLE GENERATED USING ANISOTROPIC INCIDENT FLUX AT    .000     DEGREES

ENERGY(KEV)      EL. SEC.      EL. BKSCAT.      PP. SEC.
     .100          2.241           .393           .024
     .200          2.559           .151           .034
     .300          2.276           .180           .041
     .400          1.958           .199           .048
     .500          1.706           .213           .060
     .600          1.513           .224           .096
     .700          1.362           .232           .134
     .800          1.241           .239           .173
    1.000          1.060           .250           .250
    2.000           .639           .233           .577
    3.000           .472           .219           .824
    4.000           .380           .207          1.023
    5.000           .321           .198          1.192
    6.000           .279           .190          1.338
    7.000           .248           .183          1.468
    8.000           .224           .178          1.585
    9.000           .205           .173          1.692
   10.000           .189           .169          1.791
   20.000           .111           .155          2.374
   30.000           .082           .152          2.737
   40.000           .065           .152          2.984
   50.000           .055           .152          3.161

RESULT CHARGE

CYCLE    1   TIME    .00     SECONDS    POTENTIAL    .00     VOLTS

***TIME LEFT =130895 SECONDS***

INCIDENT ELECTRON CURRENT          -2.85-006
         SECONDARY ELECTRONS        8.14-007
         BACKSCATTERED ELECTRONS    5.19-007
INCIDENT PROTON CURRENT             6.65-008
         SECONDARY ELECTRONS        1.05-007
BULK CONDUCTIVITY CURRENT            .00
                                  -----------
                     NET CURRENT  -1.34-006  AMPS/M**2
CYCLE   99   TIME  8.89+003 SECONDS    POTENTIAL -6.14+003 VOLTS

***TIME LEFT =130870 SECONDS***

INCIDENT ELECTRON CURRENT          -8.35-007
         SECONDARY ELECTRONS        2.39-007
         BACKSCATTERED ELECTRONS    1.52-007
INCIDENT PROTON CURRENT             1.48-007
         SECONDARY ELECTRONS        2.87-007
BULK CONDUCTIVITY CURRENT           4.83-009
                                  -----------
                     NET CURRENT  -4.49-009  AMPS/M**2

TABLE CHARGE
```

TIME LEFT =130870 SECONDS

TIME LEFT =130845 SECONDS

T (SEC)	V (VOLTS)	I(AMPS/M**2)
.00	.00	-1.34-006
1.81+002	-8.47+002	-1.08-006
3.63+002	-1.54+003	-8.84-007
5.44+002	-2.11+003	-7.39-007
7.26+002	-2.60+003	-6.27-007
9.07+002	-3.01+003	-5.37-007
1.09+003	-3.37+003	-4.63-007
1.27+003	-3.68+003	-4.03-007
1.45+003	-3.95+003	-3.52-007
1.63+003	-4.19+003	-3.09-007
1.81+003	-4.40+003	-2.73-007
2.00+003	-4.58+003	-2.41-007
2.18+003	-4.75+003	-2.14-007
2.36+003	-4.89+003	-1.90-007
2.54+003	-5.02+003	-1.69-007
2.72+003	-5.14+003	-1.51-007
2.90+003	-5.24+003	-1.35-007
3.08+003	-5.34+003	-1.21-007
3.27+003	-5.42+003	-1.08-007
3.45+003	-5.49+003	-9.70-008
3.63+003	-5.56+003	-8.71-008
3.81+003	-5.62+003	-7.83-008
3.99+003	-5.67+003	-7.04-008
4.17+003	-5.72+003	-6.33-008
4.35+003	-5.76+003	-5.70-008
4.54+003	-5.80+003	-5.13-008
4.72+003	-5.84+003	-4.63-008
4.90+003	-5.87+003	-4.17-008
5.08+003	-5.90+003	-3.76-008
5.26+003	-5.93+003	-3.39-008
5.44+003	-5.95+003	-3.06-008
5.62+003	-5.97+003	-2.76-008
5.81+003	-5.99+003	-2.50-008
5.99+003	-6.01+003	-2.25-008
6.17+003	-6.02+003	-2.04-008
6.35+003	-6.04+003	-1.84-008
6.53+003	-6.05+003	-1.66-008
6.71+003	-6.06+003	-1.50-008
6.89+003	-6.07+003	-1.36-008
7.08+003	-6.08+003	-1.23-008
7.26+003	-6.09+003	-1.11-008
7.44+003	-6.10+003	-1.00-008
7.62+003	-6.10+003	-9.07-009

7.80+003	-6.11+003	-8.20-009
7.98+003	-6.11+003	-7.41-009
8.16+003	-6.12+003	-6.71-009
8.35+003	-6.12+003	-6.07-009
8.53+003	-6.13+003	-5.49-009
8.71+003	-6.13+003	-4.96-009
8.89+003	-6.14+003	-4.49-009

PLOT CHARGE

TIME LEFT =130845 SECONDS

TIME LEFT =130821 SECONDS

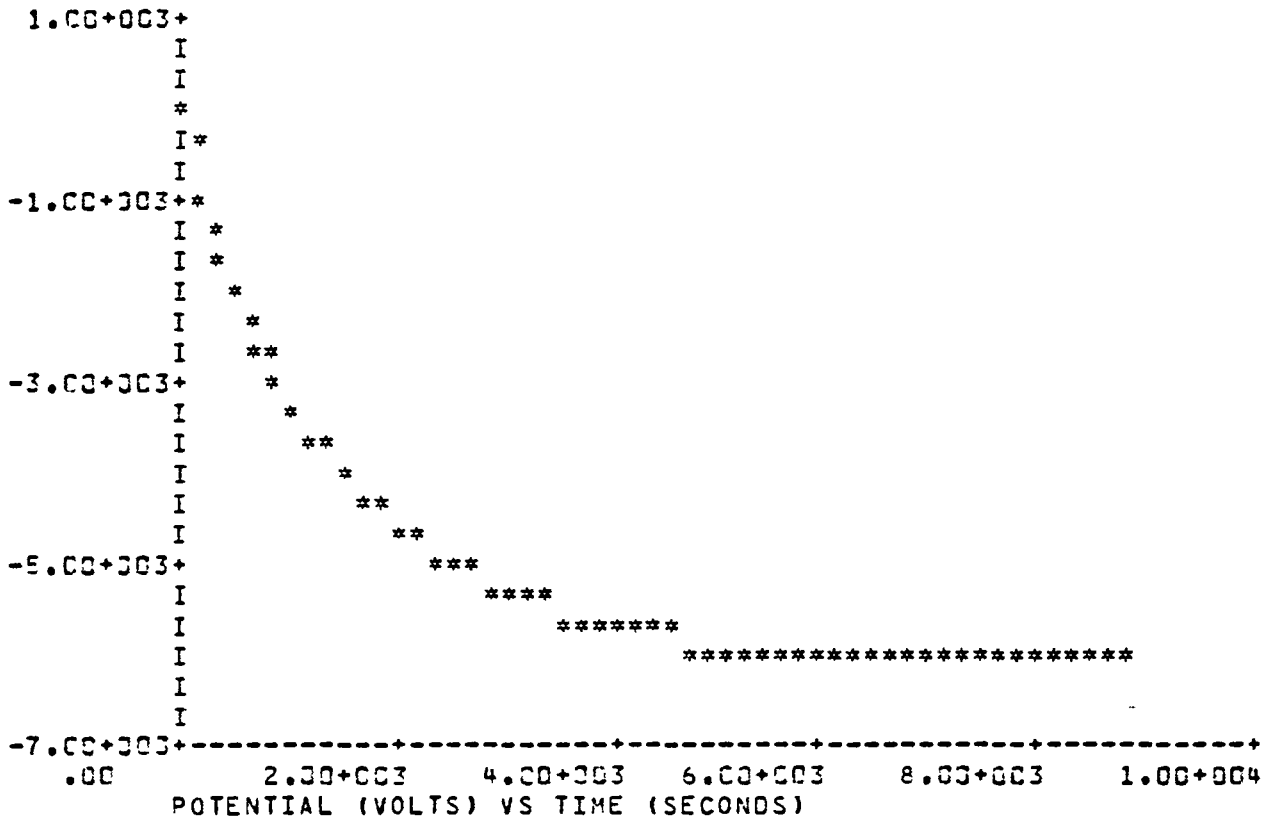
1.CC+CC3
-1.CC+CC3
-3.CC+CC3
-5.CC+CC3
-7.CC+CC3
.CC
2.CC+CC3
4.CC+CC3
6.CC+CC3
8.CC+CC3
1.CC+CC4
POTENTIAL (VOLTS) VS TIME (SECONDS)

PLOT IV

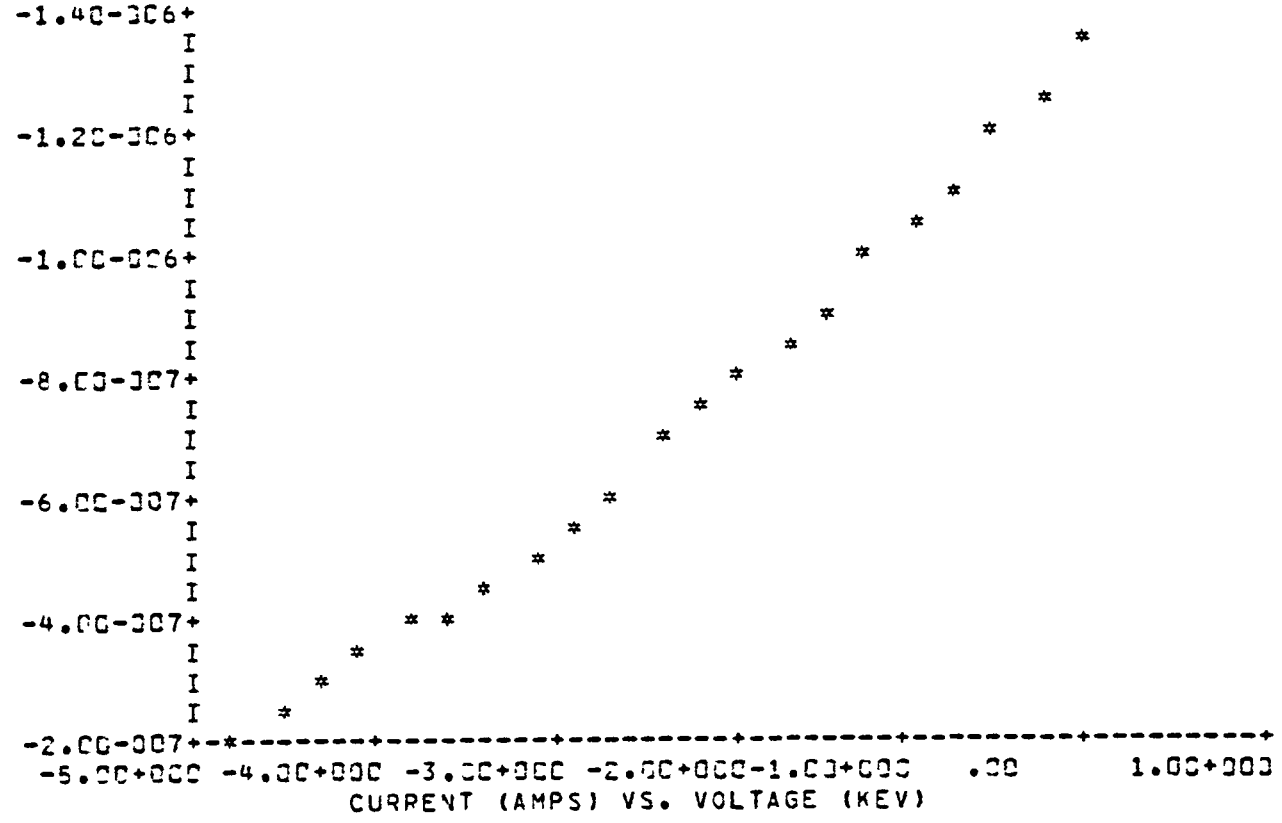
-1.40-006
-1.20-006
-1.00-006
-8.00-007
-6.00-007
-4.00-007
-2.00-007
-5.00+000
-4.00+000
-3.00+000
-2.00+000
-1.00+000
.00
1.00+003
CURRENT (AMPS) VS. VOLTAGE (KEV)

TABLE IV

V	JTOT	JE	JSECE	JBSCAT	JI	JSECI
.00	-1.34-006	-2.85-006	8.14-007	5.19-007	6.65-008	1.05-007
-2.38-001	-1.27-006	-2.72-006	7.76-007	4.95-007	6.97-008	1.10-007
-4.76-001	-1.19-006	-2.59-006	7.40-007	4.72-007	7.28-008	1.16-007
-7.14-001	-1.12-006	-2.47-006	7.06-007	4.50-007	7.60-008	1.21-007
-9.52-001	-1.05-006	-2.36-006	6.73-007	4.29-007	7.91-008	1.27-007
-1.19+000	-9.78-007	-2.25-006	6.42-007	4.09-007	8.23-008	1.33-007
-1.43+000	-9.13-007	-2.14-006	6.12-007	3.90-007	8.54-008	1.39-007
-1.67+000	-8.51-007	-2.04-006	5.83-007	3.72-007	8.86-008	1.46-007
-1.90+000	-7.90-007	-1.95-006	5.56-007	3.55-007	9.17-008	1.52-007
-2.14+000	-7.32-007	-1.86-006	5.30-007	3.38-007	9.49-008	1.59-007
-2.38+000	-6.76-007	-1.77-006	5.06-007	3.23-007	9.80-008	1.66-007
-2.62+000	-6.22-007	-1.69-006	4.82-007	3.08-007	1.01-007	1.73-007
-2.86+000	-5.70-007	-1.61-006	4.60-007	2.93-007	1.04-007	1.80-007
-3.10+000	-5.20-007	-1.53-006	4.38-007	2.80-007	1.07-007	1.87-007
-3.33+000	-4.71-007	-1.46-006	4.18-007	2.67-007	1.11-007	1.94-007
-3.57+000	-4.24-007	-1.39-006	3.98-007	2.54-007	1.14-007	2.01-007
-3.81+000	-3.79-007	-1.33-006	3.80-007	2.42-007	1.17-007	2.09-007
-4.05+000	-3.35-007	-1.27-006	3.62-007	2.31-007	1.20-007	2.17-007
-4.29+000	-2.92-007	-1.21-006	3.45-007	2.20-007	1.23-007	2.24-007
-4.52+000	-2.51-007	-1.15-006	3.29-007	2.10-007	1.26-007	2.32-007
-4.76+000	-2.12-007	-1.10-006	3.14-007	2.00-007	1.30-007	2.40-007

RESULT CURRENTS -4.100

CURRENTS FOR POTENTIAL OF -4.10+000 KV

INCIDENT ELECTRON CURRENT	-1.25-006
SECONDARY ELECTRONS	3.59-007
BACKSCATTERED ELECTRONS	2.29-007
INCIDENT PROTON CURRENT	1.21-007
SECONDARY ELECTRONS	2.18-007
BULK CONDUCTIVITY CURRENT	3.23-009
NET CURRENT	-3.25-007 AMPS/M**2

CHANGE ANGLE PREF 80.

PREFERED ANGLE= 80.000 DEGREES

PARAMETERS

MATERIAL IS KAPT.
EMISSION FORMULATION IS ANGL.
VBACK = .00 KEV
VINIT = .00 KEV
VBEGIN = .00 KEV
VEND = -5.00+000 KEV
ANISOTROPIC FLUX
PREFERED DIRECTION= 80.000 DEGREES

```
ERATIO( 1) =   1.00+004
IRATIO( 1) =   1.00+004
ENVIRONMENT IS A SINGLE MAXWELLIAN

ELECTRONS: NE1 =  1.00+006 (M**-3)      TE1 =      5.000 KEV
IONS     : NI1 =  1.00+006 (M**-3)      TI1 =      5.000 KEV

TABLE ALL
```

TABLE GENERATED USING ANISOTROPIC INCIDENT FLUX AT 80.000+000 DEGREES

ENERGY(KEV)	EL. SEC.	EL. BKSCAT.	PP. SEC.
.100	2.803	.205	.047
.200	3.698	.229	.066
.300	3.688	.289	.080
.400	3.442	.333	.093
.500	3.180	.367	.117
.600	2.901	.392	.187
.700	2.799	.410	.261
.800	2.525	.423	.336
1.000	2.128	.442	.486
2.000	1.256	.411	1.120
3.000	.923	.381	1.630
4.000	.741	.353	1.987
5.000	.625	.329	2.313
6.000	.544	.310	2.597
7.000	.484	.295	2.850
8.000	.437	.283	3.078
9.000	.399	.273	3.285
10.000	.368	.265	3.476
20.000	.216	.236	4.609
30.000	.158	.232	5.313
40.000	.127	.231	5.794
50.000	.107	.231	6.137

PLOT SECO

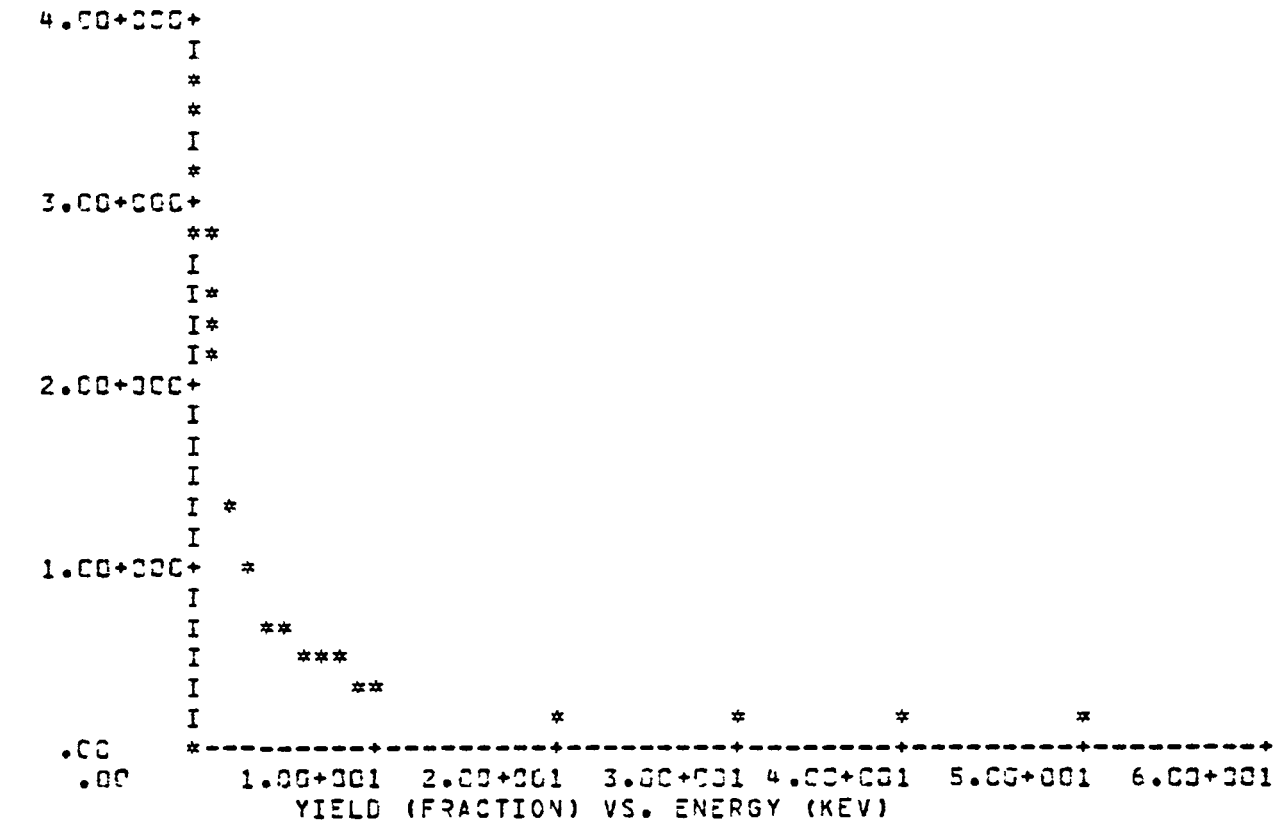
4.00+000
3.00+000
2.00+000
1.00+000
.00
.00
1.00+001 2.00+001 3.00+001 4.00+001 5.00+001 6.00+001
YIELD (FRACTION) VS. ENERGY (KEV)

PLOT BACK

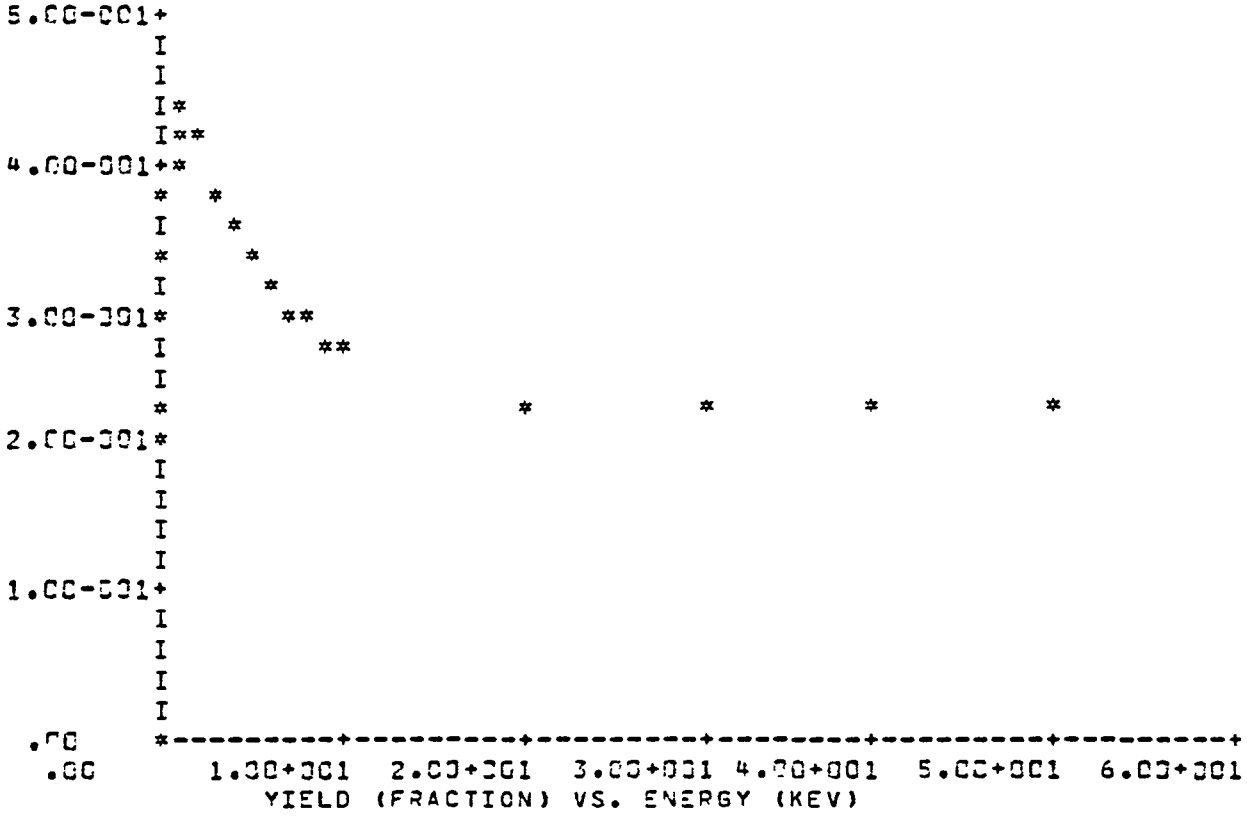
5.00-001
4.00-001
3.00-001
2.00-001
1.00-001
.00
.00
1.00+001 2.00+001 3.00+001 4.00+001 5.00+001 6.00+001
YIELD (FRACTION) VS. ENERGY (KEV)

PLOT ION

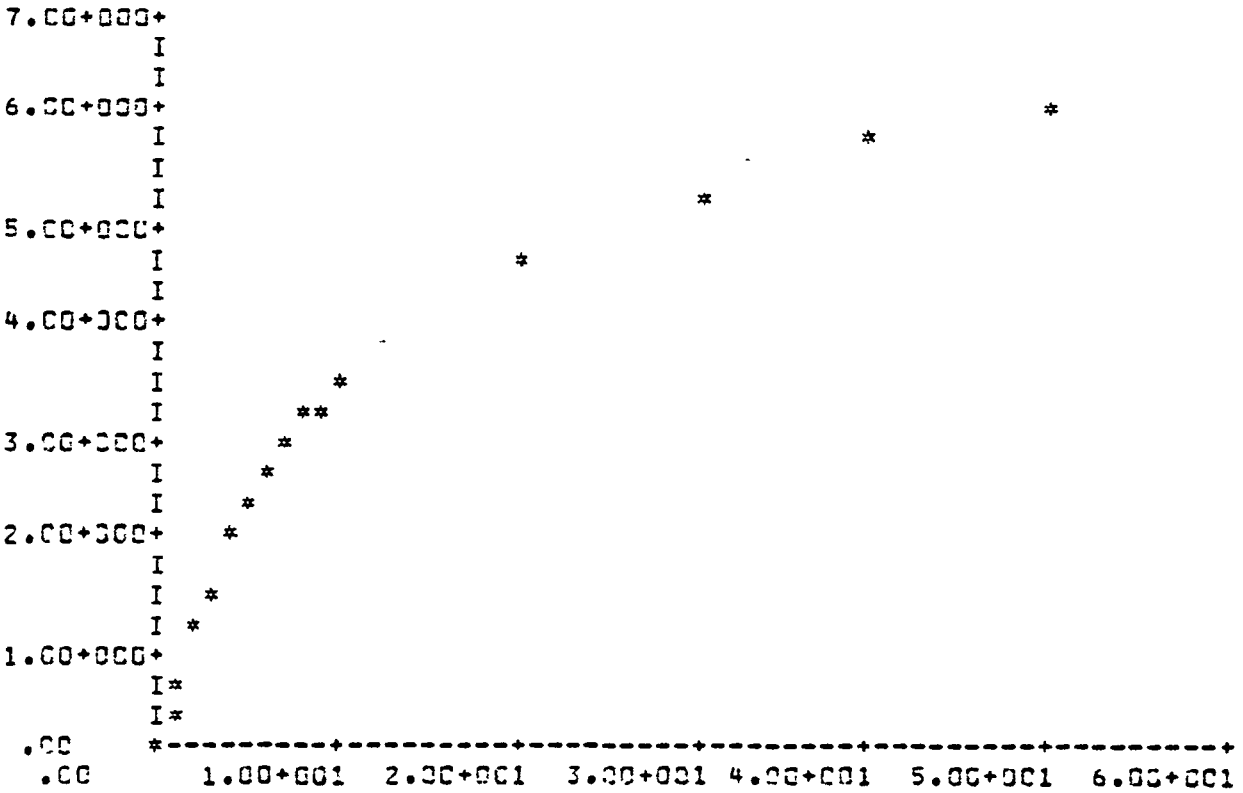

RESULT CHARGE

CYCLE 1 TIME .20 SECONDS POTENTIAL .00 VOLTS

TIME LEFT =130812 SECONDS

INCIDENT ELECTRON CURRENT	-1.47-006
SECONDARY ELECTRONS	8.15-007
BACKSCATTERED ELECTRONS	4.34-007
INCIDENT PROTON CURRENT	3.43-008
SECONDARY ELECTRONS	1.05-007
BULK CONDUCTIVITY CURRENT	.00
NET CURRENT	-7.97-008 AMPS/M**2

CYCLE 20 TIME 1.50+005 SECONDS POTENTIAL -1.13+003 VOLTS

TIME LEFT =130807 SECONDS

INCIDENT ELECTRON CURRENT	-1.17-006
SECONDARY ELECTRONS	6.49-007
BACKSCATTERED ELECTRONS	3.46-007
INCIDENT PROTON CURRENT	4.20-008
SECONDARY ELECTRONS	1.32-007
BULK CONDUCTIVITY CUPRENT	8.93-010

NET CURRENT -8.87-011 AMPS/M**2

TABLE CHARGE

TIME LEFT =130807 SECONDS

TIME LEFT =130802 SECONDS

T (SEC)	V (VOLTS)	I(AMPS/M**2)
.00	.00	-7.97-008
3.06+003	-5.84+002	-3.80-008
6.12+003	-8.66+002	-1.84-008
9.18+003	-1.00+003	-9.01-009
1.22+004	-1.07+003	-4.41-009
1.53+004	-1.10+003	-2.17-009
1.84+004	-1.12+003	-1.06-009
2.14+004	-1.13+003	-5.23-010
2.45+004	-1.13+003	-2.57-010
2.75+004	-1.13+003	-1.27-010

PLOT IV

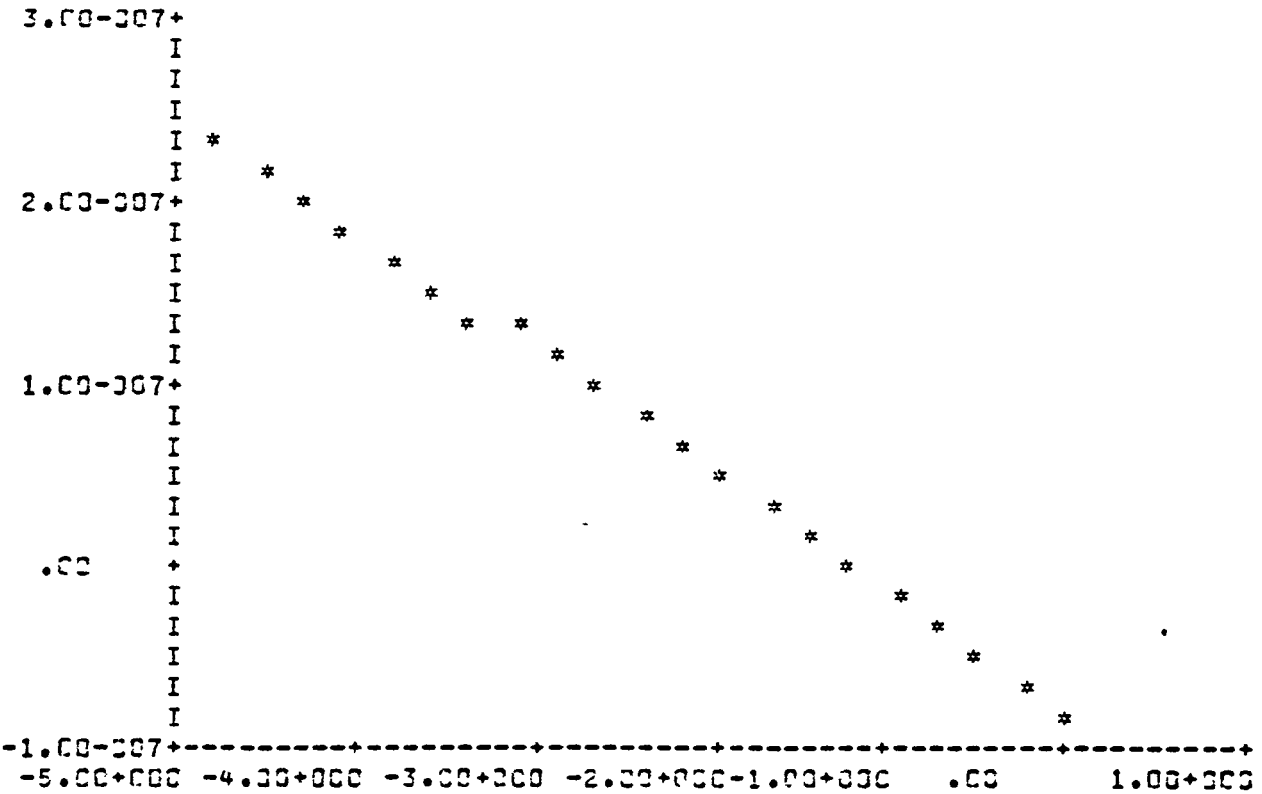


```
RESULT CURRENT -1.830



CURRENTS FOR POTENTIAL OF  -1.83+000 KV

INCIDENT ELECTRON CURRENT          -1.02-006
         SECONDARY ELECTRONS        5.65-007
         BACKSCATTERED ELECTRONS    3.01-007
INCIDENT PROTON CURRENT             4.67-008
         SECONDARY ELECTRONS        1.50-007
BULK CONDUCTIVITY CURRENT           1.44-009
                                  -------------
                     NET CURRENT    4.63-008  AMPS/M**2

LIST ENVI

ENVIRONMENT IS A SINGLE MAXWELLIAN

ELECTRONS: NE1 =  1.00+006 (M**-3)      TE1 =      5.000 KEV
IONS     : NI1 =  1.00+006 (M**-3)      TI1 =      5.000 KEV

CHANGE ANGLE ERAT .5
```

```
ERATIO=   5.00-001 IRATIO=   1.00+004
CHANGE ANGLE IRAT .5
ERATIO=   5.00-001 IRATIO=   5.00-001
TABLE ALL
```

TABLE GENERATED USING ANISOTROPIC INCIDENT FLUX AT 8[illegible].000+000 DEGREES

ENERGY(KEV)	EL. SEC.	EL. BKSCAT.	PR. SEC.
.100	2.573	.176	.039
.200	3.305	.230	.055
.300	3.216	.269	.067
.400	2.937	.296	.078
.500	2.661	.316	.098
.600	2.409	.331	.156
.700	2.236	.342	.218
.800	2.040	.350	.281
1.000	1.742	.363	.406
2.000	1.046	.342	.936
3.000	.771	.324	1.337
4.000	.620	.307	1.661
5.000	.523	.294	1.934
6.000	.455	.282	.2.171
7.000	.404	.273	2.383
8.000	.365	.266	2.573
9.000	.334	.259	2.747
10.000	.308	.254	2.906
20.000	.181	.235	3.853
30.000	.132	.232	4.441
40.000	.106	.232	4.843
50.000	.089	.232	5.130

PLOT SECO

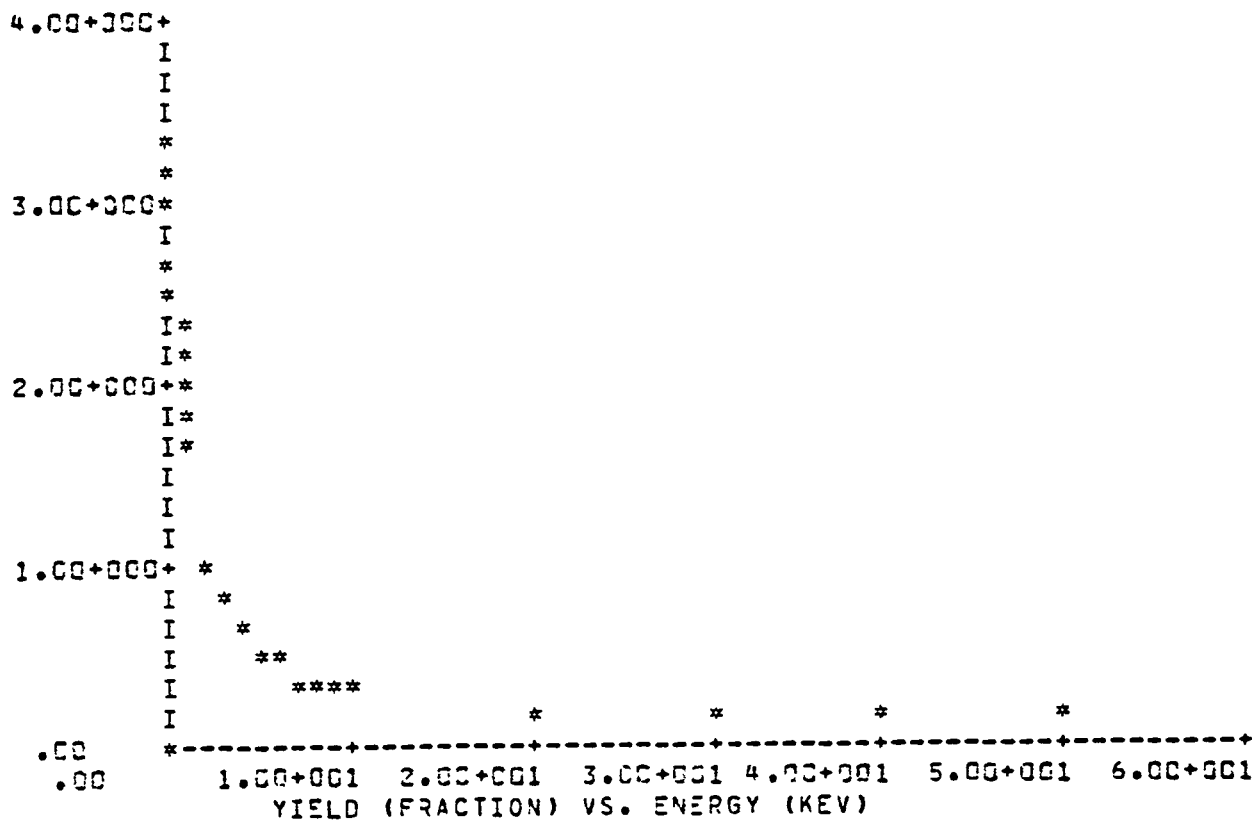
4.00+000
3.00+000
2.00+000
1.00+000
.00
.00
1.00+001
2.00+001
3.00+001
4.00+001
5.00+001
6.00+001
YIELD (FRACTION) VS. ENERGY (KEV)

PLOT BACK

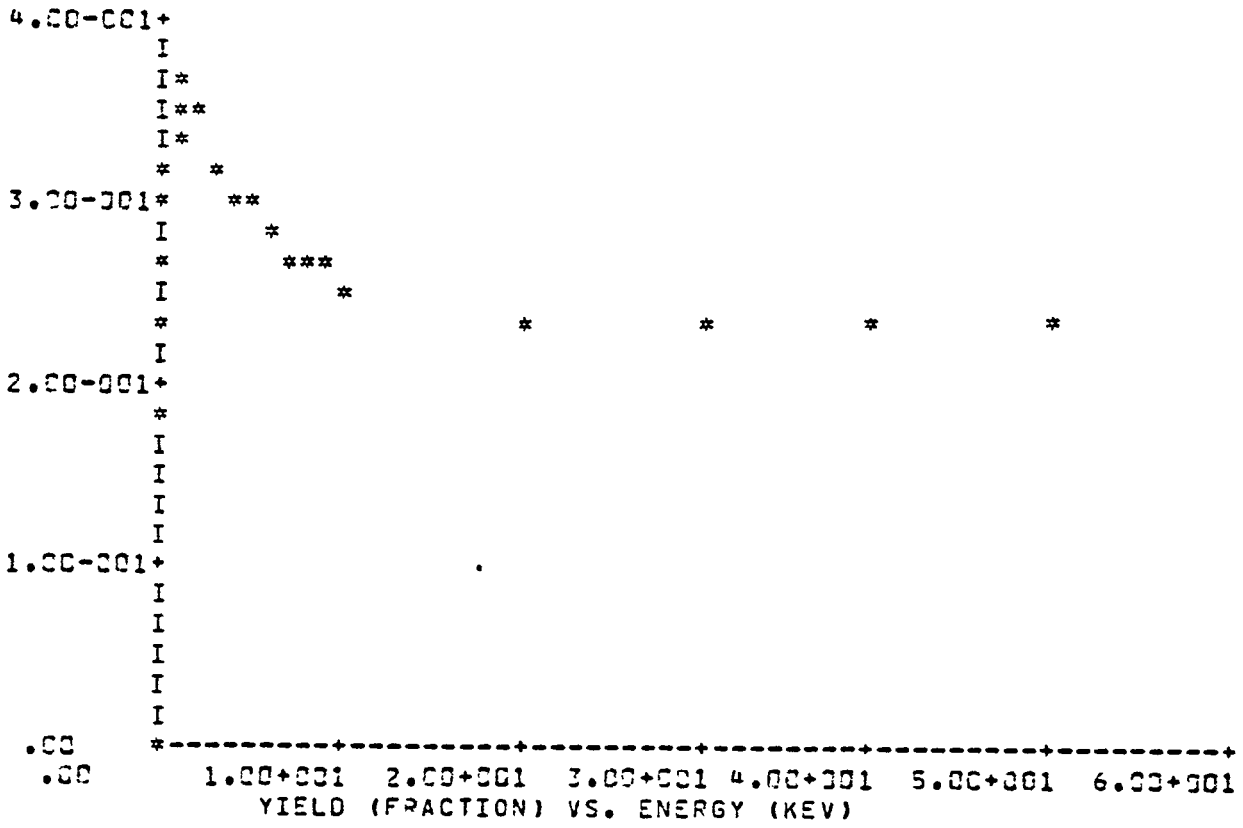
4.00-001
3.00-001
2.00-001
1.00-001
.00
.00
1.00+001 2.00+001 3.00+001 4.00+001 5.00+001 6.00+001
YIELD (FRACTION) VS. ENERGY (KEV)

PLOT ION

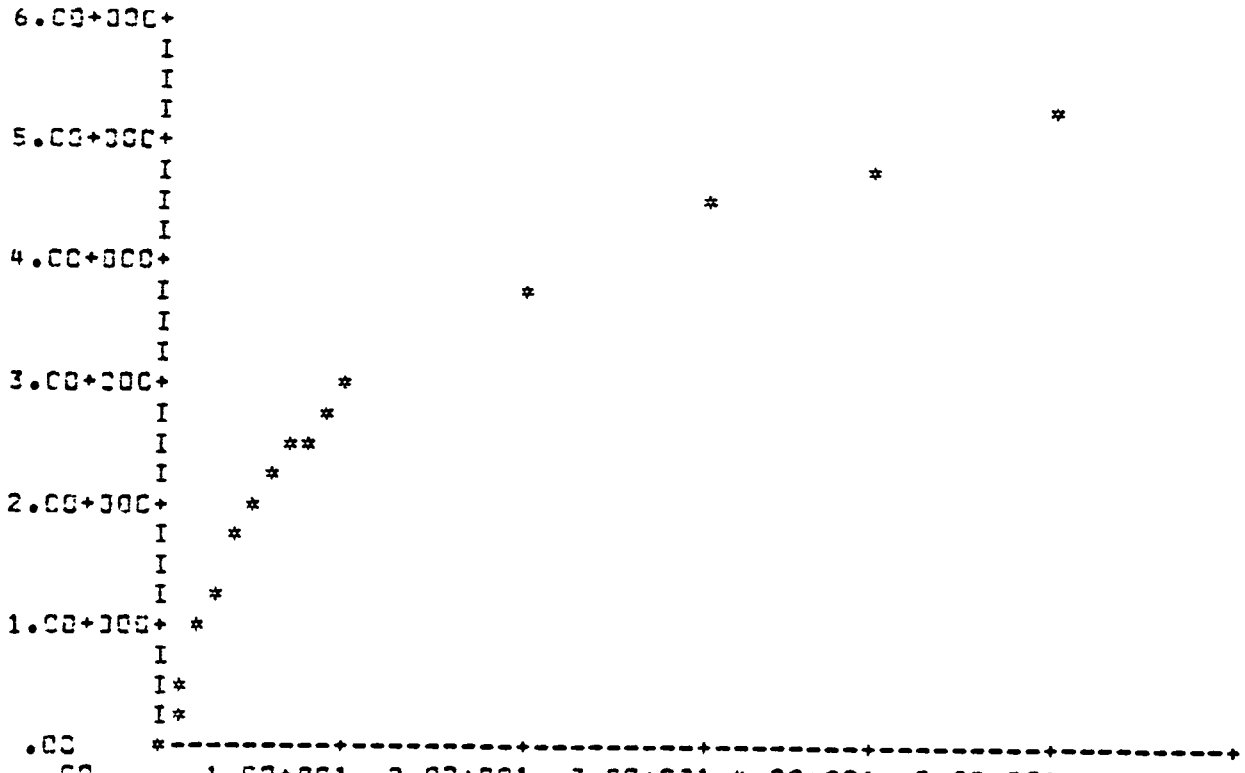


```
RESULT CHARGE

CYCLE    1   TIME   .00     SECONDS    POTENTIAL   .00     VOLTS

***TIME LEFT =130796 SECONDS***

INCIDENT ELECTRON CURRENT          -1.76-006
         SECONDARY ELECTRONS        8.14-007
         BACKSCATTERED ELECTRONS    4.78-007
INCIDENT PROTON CURRENT             4.10-008
         SECONDARY ELECTRONS        1.05-007
BULK CONDUCTIVITY CURRENT            .00
                                  -----------
                     NET CURRENT  -3.18-007  AMPS/M**2
CYCLE   61   TIME  3.76+004 SECONDS    POTENTIAL -3.03+003 VOLTS

***TIME LEFT =130780 SECONDS***

INCIDENT ELECTRON CURRENT          -9.58-007
         SECONDARY ELECTRONS        4.44-007
         BACKSCATTERED ELECTRONS    2.61-007
INCIDENT PROTON CURRENT             6.57-008
         SECONDARY ELECTRONS        1.85-007
BULK CONDUCTIVITY CURRENT           2.39-009
                                  -----------
```

NET CURRENT -8.63-011 AMPS/M**2

TABLE CHARGE

TIME LEFT =130780 SECONDS

TIME LEFT =130764 SECONDS

T (SEC)	V (VOLTS)	I(AMPS/M**2)
.00	.00	-3.18-007
7.68+002	-7.77+002	-2.26-007
1.54+003	-1.34+003	-1.65-007
2.30+003	-1.75+003	-1.22-007
3.07+003	-2.06+003	-9.10-008
3.84+003	-2.30+003	-6.84-008
4.61+003	-2.47+003	-5.17-008
5.37+003	-2.60+003	-3.93-008
6.14+003	-2.70+003	-2.99-008
6.91+003	-2.78+003	-2.26-008
7.68+003	-2.84+003	-1.74-008
8.45+003	-2.88+003	-1.33-008
9.21+003	-2.92+003	-1.02-008
9.98+003	-2.95+003	-7.80-009
1.07+004	-2.97+003	-5.98-009
1.15+004	-2.98+003	-4.58-009
1.23+004	-2.99+003	-3.51-009
1.31+004	-3.00+003	-2.69-009
1.38+004	-3.01+003	-2.07-009
1.46+004	-3.01+003	-1.59-009
1.54+004	-3.02+003	-1.22-009
1.61+004	-3.02+003	-9.34-010
1.69+004	-3.02+003	-7.17-010
1.77+004	-3.03+003	-5.50-010
1.84+004	-3.03+003	-4.22-010
1.92+004	-3.03+003	-3.24-010
2.00+004	-3.03+003	-2.49-010
2.07+004	-3.03+003	-1.91-010
2.15+004	-3.03+003	-1.46-010
2.23+004	-3.03+003	-1.12-010
3.76+004	-3.03+003	-8.63-011

PLOT IV

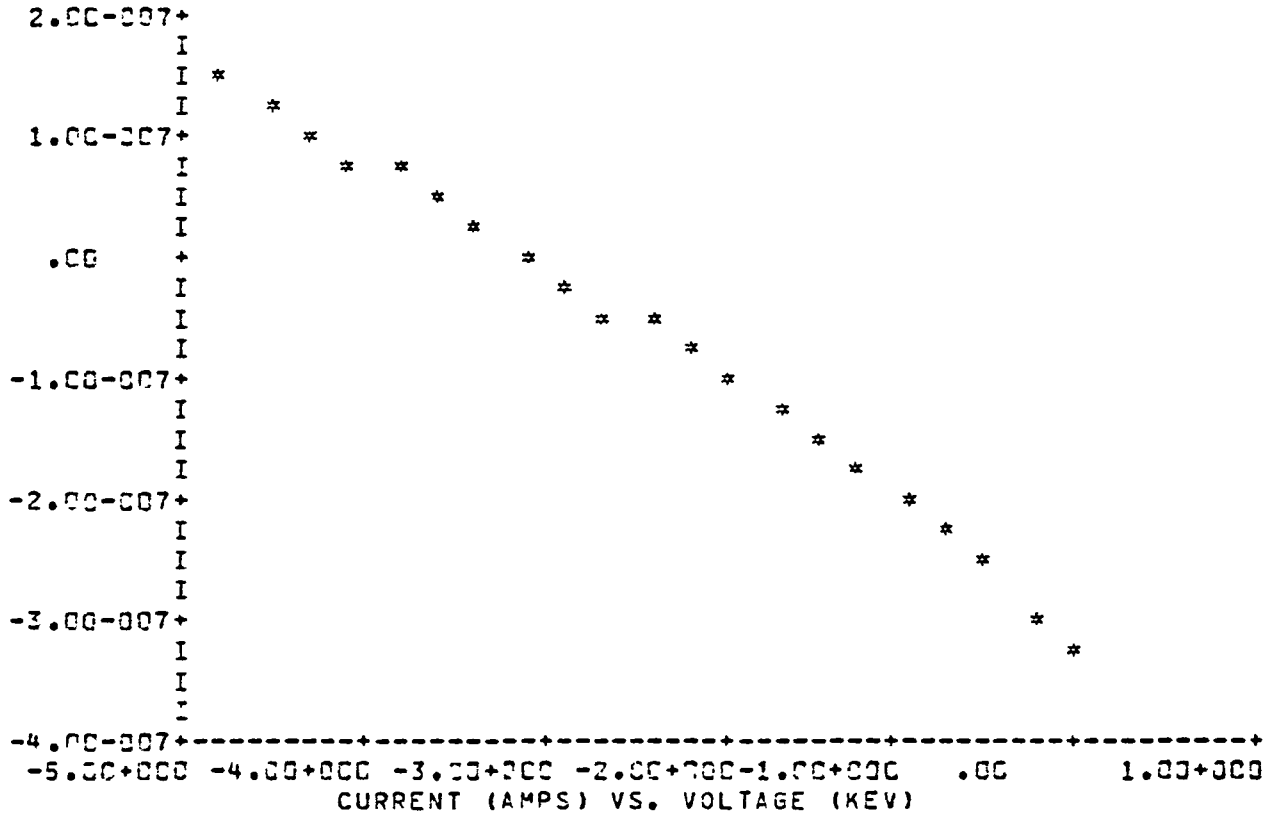
2.00-007
1.00-007
.00
-1.00-007
-2.00-007
-3.00-007
-4.00-007
-5.00+000
-4.00+000
-3.00+000
-2.00+000
-1.00+000
.00
1.00+000
CURRENT (AMPS) VS. VOLTAGE (KEV)

TABLE IV

V	JTOT	JE	JSECE	JBSCAT	JI	JSECI
.CC	-3.18-CC7	-1.76-CC6	8.14-CC7	4.78-CC7	4.1C-CC8	1.C5-CC7
-2.38-3C1	-2.89-CC7	-1.67-3C6	7.76-CC7	4.56-CC7	4.29-CC8	1.1C-3C7
-4.76-CC1	-2.61-CC7	-1.6C-3C6	7.4C-CC7	4.35-CC7	4.49-CC8	1.16-CC7
-7.14-CC1	-2.33-CC7	-1.52-CC6	7.C5-CC7	4.15-CC7	4.68-CC8	1.21-CC7
-9.52-3C1	-2.C7-CC7	-1.45-CC6	6.72-CC7	3.95-CC7	4.87-CC8	1.27-CC7
-1.19+CCC	-1.81-CC7	-1.38-CC6	6.41-CC7	3.77-CC7	5.C7-CC8	1.33-CC7
-1.43+CCC	-1.55-CC7	-1.32-CC6	6.11-CC7	3.59-CC7	5.26-CC8	1.39-CC7
-1.67+CCC	-1.31-CC7	-1.26-CC6	5.83-CC7	3.43-CC7	5.46-CC8	1.46-CC7
-1.9C+CCC	-1.C7-CC7	-1.2C-CC6	5.56-CC7	3.27-CC7	5.65-CC8	1.52-CC7
-2.14+CCC	-8.32-CC8	-1.14-CC6	5.3C-CC7	3.12-CC7	5.85-CC8	1.59-CC7
-2.38+CCC	-6.C2-CC8	-1.C9-CC6	5.C5-CC7	2.97-CC7	6.C4-CC8	1.66-CC7
-2.62+CCC	-3.78-CC8	-1.C4-CC6	4.82-CC7	2.83-CC7	6.23-CC8	1.73-CC7
-2.86+CCC	-1.58-CC8	-9.91-CC7	4.59-CC7	2.7C-CC7	6.43-CC8	1.8C-CC7
-3.1C+CCC	5.67-CC9	-9.45-CC7	4.38-CC7	2.57-CC7	6.62-CC8	1.87-CC7
-3.33+CCC	2.67-CC8	-9.C1-CC7	4.18-CC7	2.46-CC7	6.82-CC8	1.94-CC7
-3.57+CCC	4.73-CC8	-8.59-CC7	3.98-CC7	2.34-CC7	7.C1-CC8	2.C1-CC7
-3.81+CCC	6.75-CC8	-8.2C-CC7	3.8C-CC7	2.23-CC7	7.21-CC8	2.C9-CC7
-4.C5+CCC	8.73-CC8	-7.81-CC7	3.62-CC7	2.13-CC7	7.4C-CC8	2.17-CC7
-4.29+CCC	1.C7-CC7	-7.45-CC7	3.45-CC7	2.C3-CC7	7.59-CC8	2.24-CC7
-4.52+CCC	1.26-CC7	-7.1C-CC7	3.29-CC7	1.93-CC7	7.79-CC8	2.32-CC7
-4.76+CCC	1.45-CC7	-6.77-CC7	3.14-CC7	1.84-CC7	7.98-CC8	2.4C-CC7

RESULT CURRENT -1.99C

CURRENTS FOR POTENTIAL OF -1.99+CCC KV

INCIDENT ELECTRON CURRENT	-1.18-CC6	
SECONDARY ELECTRONS	5.46-CC7	
BACKSCATTERED ELECTRONS	3.21-CC7	
INCIDENT PROTON CURRENT	5.72-CC8	
SECONDARY ELECTRONS	1.55-CC7	
BULK CONDUCTIVITY CURRENT	1.57-CC9	
NET CURRENT	-9.82-CC8	AMPS/M**2

CHAN ENVI DIRECT 9

DATA IN FILE IS FROM 59CC3 SECONDS ON DAY 87, 198C
TO 59CC3 SECONDS ON DAY 87, 198C
SPECTRA FOUND FOR 59CCC SECONDS ON DAY 87, 198C
OBJECT POTENTIAL = -2CCC.3 VOLTS
SINGLE MOMENT FIT GIVES N1= 984601. T1= 5111.78
SINGLE MOMENT FIT GIVES N1= .1CC257+CC7 T1= 5112.89

APPROXIMATE DENSITIES AND TEMPERATURES:

```
SPECIE      DENSITY(M-3)          TEMP(EV)
1( -1)          9.85+005          5.11+003
2(  1)          1.00+006          5.11+003

TABLE ALL
```

TABLE GENERATED USING ANISOTROPIC INCIDENT FLUX AT 80.000+000 DEGREES

ENERGY(KEV)	EL. SEC.	EL. BKSCAT.	PR. SEC.
.100	2.573	.176	.039
.200	3.305	.230	.055
.300	3.216	.269	.067
.400	2.937	.296	.078
.500	2.661	.316	.098
.600	2.409	.331	.156
.700	2.236	.342	.218
.800	2.040	.350	.281
1.000	1.742	.363	.406
2.000	1.046	.342	.936
3.000	.771	.324	1.337
4.000	.620	.307	1.661
5.000	.523	.294	1.934
6.000	.455	.282	2.171
7.000	.404	.273	2.383
8.000	.365	.266	2.573
9.000	.334	.259	2.747
10.000	.308	.254	2.906
20.000	.181	.235	3.853
30.000	.132	.232	4.441
40.000	.106	.232	4.843
50.000	.089	.232	5.130

RESULT CHARGE

CYCLE 1 TIME .00 SECONDS POTENTIAL .00 VOLTS

TIME LEFT =130757 SECONDS

INCIDENT ELECTRON CURRENT	-1.74-006
SECONDARY ELECTRONS	8.29-007
BACKSCATTERED ELECTRONS	4.77-007
INCIDENT PROTON CURRENT	4.09-008
SECONDARY ELECTRONS	1.04-007
BULK CONDUCTIVITY CURRENT	.00
NET CURRENT	-2.90-007 AMPS/M**2

CYCLE 54 TIME 4.21+004 SECONDS POTENTIAL -2.82+003 VOLTS

TIME LEFT =130748 SECONDS

INCIDENT ELECTRON CURRENT	-9.96-007
SECONDARY ELECTRONS	4.79-007
BACKSCATTERED ELECTRONS	2.73-007
INCIDENT PROTON CURRENT	6.39-008
SECONDARY ELECTRONS	1.78-007
BULK CONDUCTIVITY CURRENT	2.22-009
NET CURRENT	-8.89-011 AMPS/M**2

TABLE CHARGE

TIME LEFT =130748 SECONDS

TIME LEFT =130740 SECONDS

T (SEC)	V (VOLTS)	I(AMPS/M**2)
.00	.00	-2.90-007
8.60+002	-7.80+002	-2.01-007
1.72+003	-1.33+003	-1.43-007
2.58+003	-1.73+003	-1.03-007
3.44+003	-2.01+003	-7.52-008
4.30+003	-2.23+003	-5.51-008
5.16+003	-2.38+003	-4.06-008
6.02+003	-2.49+003	-3.00-008
6.88+003	-2.58+003	-2.22-008
7.74+003	-2.64+003	-1.64-008
8.60+003	-2.69+003	-1.22-008
9.46+003	-2.72+003	-9.04-009
1.03+004	-2.75+003	-6.71-009
1.12+004	-2.77+003	-4.98-009
1.20+004	-2.78+003	-3.69-009
1.29+004	-2.79+003	-2.74-009
1.38+004	-2.80+003	-2.03-009
1.46+004	-2.81+003	-1.51-009
1.55+004	-2.81+003	-1.12-009
1.63+004	-2.81+003	-8.31-010
1.72+004	-2.82+003	-6.17-010
1.81+004	-2.82+003	-4.58-010
1.89+004	-2.82+003	-3.40-010
1.98+004	-2.82+003	-2.52-010
2.06+004	-2.82+003	-1.87-010
2.15+004	-2.82+003	-1.39-010
2.24+004	-2.82+003	-1.03-010

PLOT IV

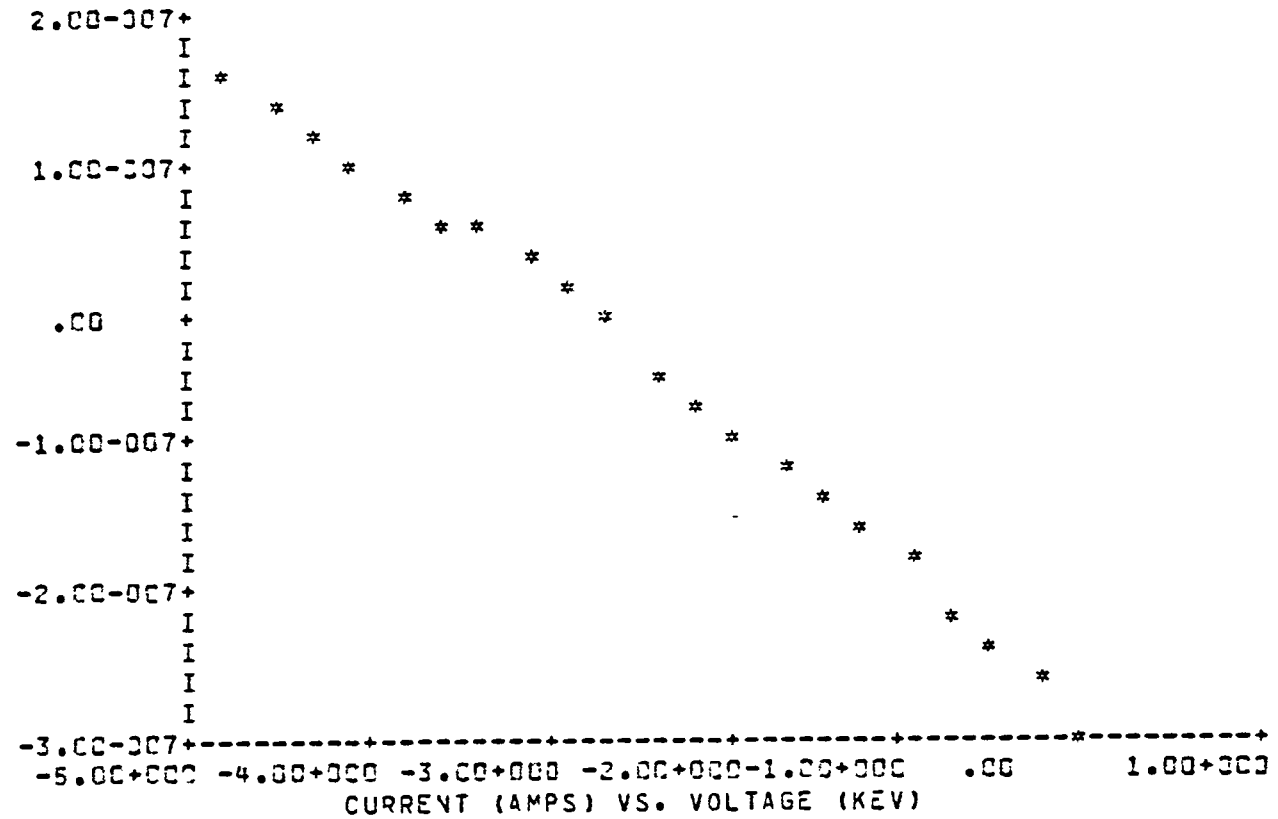
2.00-007
1.00-007
.00
-1.00-007
-2.00-007
-3.00-007
-5.00+000
-4.00+000
-3.00+000
-2.00+000
-1.00+000
.00
1.00+000
CURRENT (AMPS) VS. VOLTAGE (KEV)

TABLE IV

V	JTOT	JE	JSECE	JBSCAT	JI	JSECI
.00	-2.90-007	-1.74-006	8.29-007	4.77-007	4.09-008	1.04-007
-2.38-001	-2.62-007	-1.66-006	7.91-007	4.55-007	4.28-008	1.09-007
-4.76-001	-2.35-007	-1.58-006	7.55-007	4.34-007	4.48-008	1.15-007
-7.14-001	-2.08-007	-1.51-006	7.21-007	4.14-007	4.67-008	1.20-007
-9.52-001	-1.83-007	-1.44-006	6.88-007	3.95-007	4.86-008	1.26-007
-1.19+000	-1.57-007	-1.37-006	6.57-007	3.77-007	5.06-008	1.32-007
-1.43+000	-1.33-007	-1.31-006	6.27-007	3.60-007	5.25-008	1.39-007
-1.67+000	-1.09-007	-1.25-006	5.98-007	3.43-007	5.45-008	1.45-007
-1.90+000	-8.58-008	-1.19-006	5.71-007	3.27-007	5.64-008	1.52-007
-2.14+000	-6.30-008	-1.14-006	5.45-007	3.12-007	5.84-008	1.58-007
-2.38+000	-4.06-008	-1.09-006	5.21-007	2.98-007	6.03-008	1.65-007
-2.62+000	-1.86-008	-1.04-006	4.97-007	2.84-007	6.23-008	1.72-007
-2.86+000	3.17-009	-9.89-007	4.75-007	2.71-007	6.42-008	1.79-007
-3.10+000	2.39-008	-9.43-007	4.53-007	2.59-007	6.61-008	1.86-007
-3.33+000	4.40-008	-8.99-007	4.32-007	2.47-007	6.81-008	1.94-007
-3.57+000	6.37-008	-8.57-007	4.12-007	2.35-007	7.00-008	2.01-007
-3.81+000	8.32-008	-8.18-007	3.93-007	2.24-007	7.20-008	2.08-007
-4.05+000	1.02-007	-7.80-007	3.75-007	2.14-007	7.39-008	2.16-007
-4.29+000	1.21-007	-7.43-007	3.57-007	2.04-007	7.59-008	2.24-007
-4.52+000	1.40-007	-7.09-007	3.41-007	1.94-007	7.78-008	2.32-007
-4.76+000	1.58-007	-6.75-007	3.25-007	1.85-007	7.97-008	2.40-007

```
CHAN ENVI KAPPA

ENVIRONMENT NOW KAPPA

CHAN ENVI KAPPA 300

ELECTRONS: NE1 =  1.00+006 (M**-3)      TE1 =      5.000 KEV
IONS     : NI1 =  1.00+006 (M**-3)      TI1 =      5.000 KEV
KAPPA= 300


LIST ENVI

ELECTRONS: NE1 =  1.00+006 (M**-3)      TE1 =      5.000 KEV
IONS     : NI1 =  1.00+006 (M**-3)      TI1 =      5.000 KEV
KAPPA= 300


TABLE ALL
```

```
TABLE GENERATED USING ANISOTROPIC INCIDENT FLUX AT  80.000+000 DEGREES

ENERGY(KEV)      EL. SEC.      EL. BKSCAT.      PR. SEC.
     .100          2.573           .176           .039
     .200          3.335           .230           .055
     .300          3.216           .269           .067
     .400          2.937           .296           .078
     .500          2.661           .316           .098
     .600          2.409           .331           .156
     .700          2.236           .342           .218
     .800          2.040           .350           .281
    1.000          1.742           .363           .406
    2.000          1.046           .342           .936
    3.000           .771           .324          1.337
    4.000           .620           .307          1.661
    5.000           .523           .294          1.934
    6.000           .455           .282          2.171
    7.000           .404           .273          2.383
    8.000           .365           .266          2.573
    9.000           .334           .259          2.747
   10.000           .308           .254          2.906
   20.000           .181           .235          3.853
   30.000           .132           .232          4.441
   40.000           .106           .232          4.843
   50.000           .089           .232          5.130

RESULT CHARGE

CYCLE    1   TIME    .00     SECONDS    POTENTIAL    .00     VOLTS

***TIME LEFT =130735 SECONDS***

INCIDENT ELECTRON CURRENT          -1.75-006
         SECONDARY ELECTRONS        8.40-007
         BACKSCATTERED ELECTRONS    4.80-007
INCIDENT PROTON CURRENT             4.09-008
         SECONDARY ELECTRONS        1.04-007
BULK CONDUCTIVITY CURRENT            .00
                                  -----------
                     NET CURRENT  -2.86-007  AMPS/M**2
CYCLE   56   TIME  4.18+004 SECONDS    POTENTIAL -2.85+003 VOLTS

***TIME LEFT =130727 SECONDS***

INCIDENT ELECTRON CURRENT          -9.93-007
         SECONDARY ELECTRONS        4.76-007
         BACKSCATTERED ELECTRONS    2.72-007
INCIDENT PROTON CURRENT             6.41-008
         SECONDARY ELECTRONS        1.79-007
BULK CONDUCTIVITY CURRENT           2.24-009
                                  -----------
                     NET CURRENT  -8.93-011  AMPS/M**2

TABLE CHARGE
```

TIME LEFT =13C727 SECONDS

TIME LEFT =13C719 SECONDS

T (SEC)	V (VOLTS)	I(AMPS/M**2)
.CC	.C3	-2.86-3C7
8.54+3C2	-7.68+3C2	-2.0C-3C7
1.71+3C3	-1.32+3C3	-1.43-3C7
2.56+3C3	-1.71+3C3	-1.04-3C7
3.42+3C3	-2.00+3C3	-7.66-3C8
4.27+3C3	-2.22+3C3	-5.66-3C8
5.12+3C3	-2.38+3C3	-4.2C-3C8
5.98+3C3	-2.49+3C3	-3.13-3C8
6.83+3C3	-2.58+3C3	-2.34-3C8
7.69+3C3	-2.65+3C3	-1.75-3C8
8.54+3C3	-2.7C+3C3	-1.31-3C8
9.39+3C3	-2.73+3C3	-9.84-3C9
1.C2+3C4	-2.76+3C3	-7.39-3C9
1.11+3C4	-2.78+3C3	-5.55-3C9
1.2C+3C4	-2.8C+3C3	-4.17-3C9
1.28+3C4	-2.81+3C3	-3.14-3C9
1.37+3C4	-2.82+3C3	-2.36-3C9
1.45+3C4	-2.83+3C3	-1.77-3C9
1.54+3C4	-2.83+3C3	-1.33-3C9
1.62+3C4	-2.84+3C3	-1.CC-3C9
1.71+3C4	-2.84+3C3	-7.55-31C
1.79+3C4	-2.84+3C3	-5.68-31C
1.88+3C4	-2.84+3C3	-4.27-31C
1.96+3C4	-2.84+3C3	-3.21-31C
2.C5+3C4	-2.84+3C3	-2.42-31C
2.13+3C4	-2.84+3C3	-1.82-31C
2.22+3C4	-2.85+3C3	-1.37-31C
2.31+3C4	-2.85+3C3	-1.C3-31C

PLOT IV

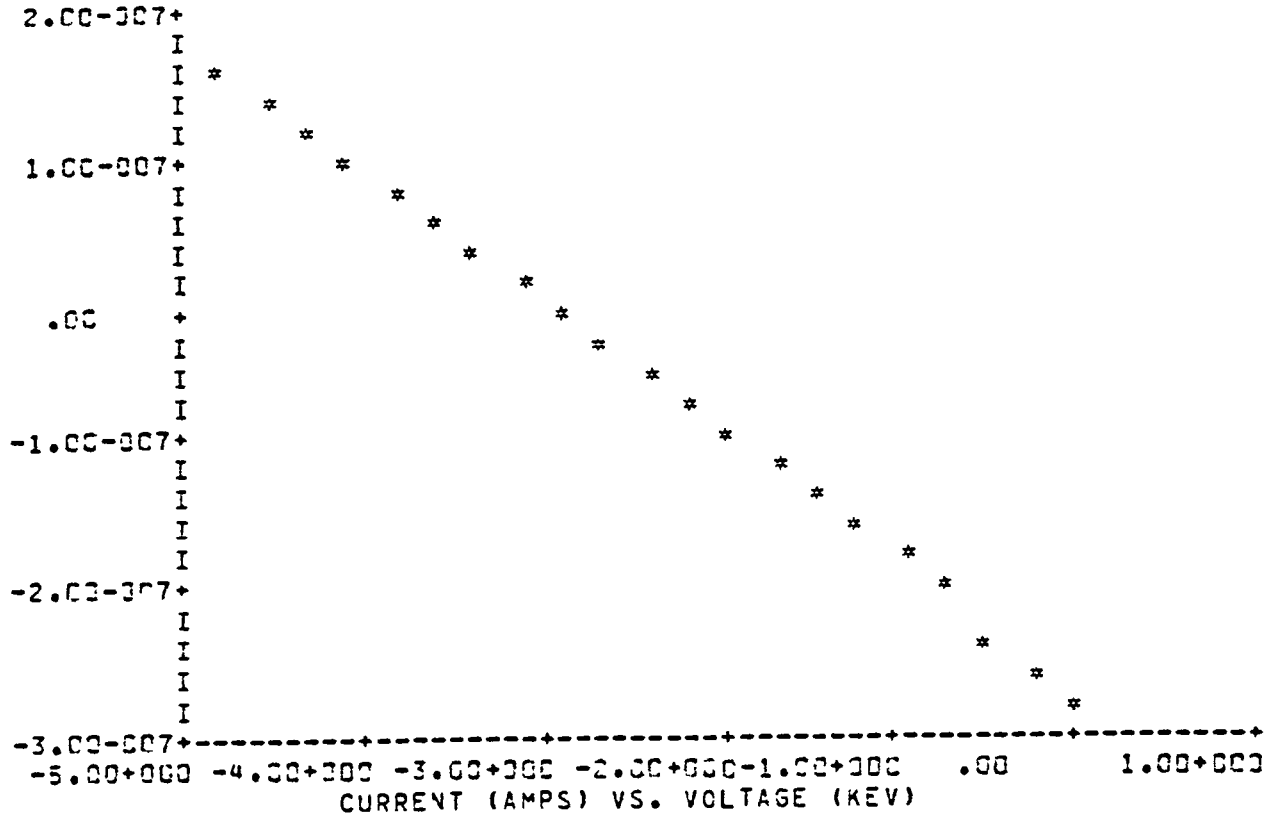
2.00-007
1.00-007
.00
-1.00-007
-2.00-007
-3.00-007
-5.00+000 -4.00+000 -3.00+000 -2.00+000 -1.00+000 .00 1.00+000
CURRENT (AMPS) VS. VOLTAGE (KEV)

TABLE IV

V	JTOT	JE	JSECE	JBSCAT	JI	JSECI
.00	-2.86-007	-1.75-006	8.40-007	4.80-007	4.09-008	1.04-007
-2.38-001	-2.58-007	-1.67-006	8.01-007	4.58-007	4.28-008	1.09-007
-4.76-001	-2.32-007	-1.59-006	7.64-007	4.37-007	4.47-008	1.15-007
-7.14-001	-2.06-007	-1.52-006	7.28-007	4.16-007	4.67-008	1.21-007
-9.52-001	-1.81-007	-1.45-006	6.95-007	3.97-007	4.86-008	1.26-007
-1.19+000	-1.56-007	-1.38-006	6.62-007	3.79-007	5.06-008	1.32-007
-1.43+000	-1.32-007	-1.32-006	6.32-007	3.61-007	5.25-008	1.39-007
-1.67+000	-1.09-007	-1.26-006	6.02-007	3.44-007	5.44-008	1.45-007
-1.90+000	-8.58-008	-1.20-006	5.74-007	3.28-007	5.64-008	1.52-007
-2.14+000	-6.34-008	-1.14-006	5.48-007	3.13-007	5.83-008	1.58-007
-2.38+000	-4.15-008	-1.09-006	5.22-007	2.99-007	6.03-008	1.65-007
-2.62+000	-2.01-008	-1.04-006	4.98-007	2.85-007	6.22-008	1.72-007
-2.86+000	8.80-010	-9.91-007	4.75-007	2.72-007	6.41-008	1.79-007
-3.10+000	2.14-008	-9.45-007	4.53-007	2.59-007	6.61-008	1.86-007
-3.33+000	4.16-008	-9.02-007	4.32-007	2.47-007	6.80-008	1.93-007
-3.57+000	6.14-008	-8.60-007	4.12-007	2.36-007	7.00-008	2.01-007
-3.81+000	8.08-008	-8.20-007	3.93-007	2.25-007	7.19-008	2.08-007
-4.05+000	9.99-008	-7.82-007	3.75-007	2.14-007	7.39-008	2.16-007
-4.29+000	1.19-007	-7.46-007	3.57-007	2.04-007	7.58-008	2.24-007
-4.52+000	1.37-007	-7.11-007	3.41-007	1.95-007	7.77-008	2.32-007
-4.76+000	1.55-007	-6.79-007	3.25-007	1.86-007	7.97-008	2.39-007

```
CHANGE ANGLE FILE 10

ANISOTROPY TABLE READ FROM UNIT  10

                    KEV 1.  ERATIO  0.5
                    EV  2000.    IRATIO     10.
                    END
SUMMARY OF ANISOTROPY TABLES

       ENERGY            RATIO(ELECTRONS)
  1.000000+000   5.000000-001
       ENERGY            RATIO(IONS)
  2.000000+000   1.000000+001

TABLE ALL
```

TABLE GENERATED USING ANISOTROPIC INCIDENT FLUX AT 80.000+000 DEGREES

ENERGY(KEV)	EL. SEC.	EL. BKSCAT.	PP. SEC.
.100	2.573	.176	.045
.200	3.305	.230	.064
.300	3.216	.269	.078
.400	2.937	.296	.090
.500	2.661	.316	.114
.600	2.409	.331	.182
.700	2.236	.342	.254
.800	2.040	.350	.328
1.000	1.742	.363	.473
2.000	1.046	.342	1.091
3.000	.771	.324	1.558
4.000	.620	.307	1.935
5.000	.523	.294	2.253
6.000	.455	.282	2.530
7.000	.404	.273	2.776
8.000	.365	.266	2.998
9.000	.334	.259	3.200
10.000	.308	.254	3.386
20.000	.181	.235	4.489
30.000	.132	.232	5.174
40.000	.106	.232	5.643
50.000	.089	.232	5.977

RESULT CHARGE

CYCLE 1 TIME .00 SECONDS POTENTIAL .00 VOLTS

TIME LEFT =130715 SECONDS

INCIDENT ELECTRON CURRENT	-1.75-006
SECONDARY ELECTRONS	8.40-007
BACKSCATTERED ELECTRONS	4.80-007
INCIDENT PROTON CURRENT	3.51-008
SECONDARY ELECTRONS	1.04-007
BULK CONDUCTIVITY CURRENT	.00
NET CURRENT	-2.91-007 AMPS/M**2

CYCLE 58 TIME 4.10+004 SECONDS POTENTIAL -2.95+003 VOLTS

TIME LEFT =130707 SECONDS

INCIDENT ELECTRON CURRENT	-9.73-007
SECONDARY ELECTRONS	4.66-007
BACKSCATTERED ELECTRONS	2.67-007
INCIDENT PROTON CURRENT	5.57-008
SECONDARY ELECTRONS	1.82-007
BULK CONDUCTIVITY CURRENT	2.30-009
NET CURRENT	-9.30-011 AMPS/M**2

CHANGE ENVI TANK

```
ENVIRONMENT TYPE IS TANK.
THE BEAM ENERGY IS  2.0+000KEV
THE BEAM CURRENT IS   1.0-005 AMPS/M**2
AND THE GUN ANGLE IS  80.000 DEGREES

CHANGE ENVI PREF 0.

ENVIRONMENT TYPE IS TANK.
THE BEAM ENERGY IS  2.0+000KEV
THE BEAM CURRENT IS   1.0-005 AMPS/M**2
AND THE GUN ANGLE IS    .000 DEGREES

CHANGE ENVI ENERGY 20.

ENVIRONMENT TYPE IS TANK.
THE BEAM ENERGY IS  2.0+001KEV
THE BEAM CURRENT IS   1.0-005 AMPS/M**2
AND THE GUN ANGLE IS    .000 DEGREES

CHANGE VEND -20.

VEND   =  -2.00+001 KEV

CHANGE EMISSION NORMAL

EMISSION FORMULATION IS NORM.

CHANGE ANGLE ALIGNED

FLUX ALIGNED    .000 DEGREES OFF-NORMAL

TABLE ALL
```

TABLE GENERATED USING ALIGNED INCIDENT FLUX AT .00 DEGREES

ENERGY(KEV)	EL. SEC.	EL. BKSCAT.	PR. SEC.
.100	1.955	.042	.036
.200	2.021	.084	.051
.300	1.712	.107	.062
.400	1.453	.123	.072
.500	1.264	.135	.086
.600	1.122	.144	.118
.700	1.012	.151	.151
.800	.924	.157	.182
1.000	.790	.166	.242
2.000	.479	.152	.481
3.000	.354	.139	.656
4.000	.285	.129	.797
5.000	.241	.121	.917
6.000	.210	.115	1.020
7.000	.187	.109	1.113
8.000	.168	.105	1.196
9.000	.154	.101	1.273
10.000	.142	.098	1.343
20.000	.084	.086	1.780
30.000	.061	.085	2.052
40.000	.049	.085	2.238
50.000	.041	.085	2.371

RESULT CHARGE

CYCLE 1 TIME .00 SECONDS POTENTIAL .00 VOLTS

TIME LEFT =130705 SECONDS

INCIDENT ELECTRON CURRENT	-1.00-005
SECONDARY ELECTRONS	8.35-007
BACKSCATTERED ELECTRONS	8.64-007
INCIDENT PROTON CURRENT	.00
SECONDARY ELECTRONS	.00
BULK CONDUCTIVITY CURRENT	.00
NET CURRENT	-8.30-006 AMPS/M**2

CYCLE 23 TIME 5.76+003 SECONDS POTENTIAL -1.91+004 VOLTS

TIME LEFT =130705 SECONDS

INCIDENT ELECTRON CURRENT	-1.00-005
SECONDARY ELECTRONS	8.35-006
BACKSCATTERED ELECTRONS	1.63-006
INCIDENT PROTON CURRENT	.00
SECONDARY ELECTRONS	.00
BULK CONDUCTIVITY CURRENT	1.50-008
NET CURRENT	-7.12-010 AMPS/M**2

TABLE CHARGE

TIME LEFT =130705 SECONDS

TIME LEFT =130705 SECONDS

T (SEC)	V (VOLTS)	I(AMPS/M**2)
.00	.00	-8.30-006
1.18+002	-3.94+003	-8.12-006
2.35+002	-7.76+003	-7.85-006
3.53+002	-1.14+004	-7.38-006
4.70+002	-1.46+004	-6.52-006
5.88+002	-1.72+004	-4.86-006
7.05+002	-1.85+004	-2.42-006
8.23+002	-1.90+004	-6.88-007
9.40+002	-1.91+004	-1.35-007
1.06+003	-1.91+004	-2.41-008
1.18+003	-1.91+004	-4.16-009
5.76+003	-1.91+004	-7.12-010

PLOT IV

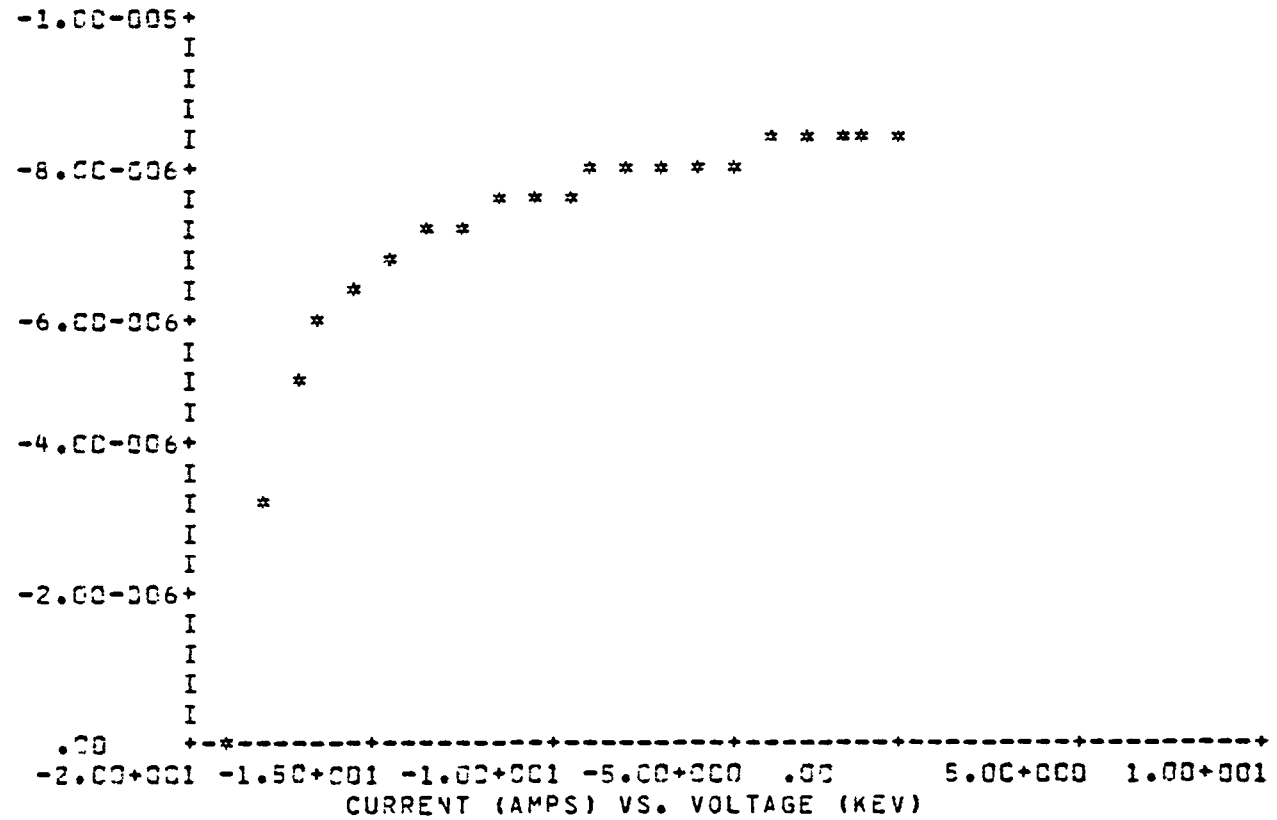
-1.00-005+
-8.00-006+
-6.00-006+
-4.00-006+
-2.00-006+
.00
-2.00+001 -1.50+001 -1.00+001 -5.00+000 .00 5.00+000 1.00+001
CURRENT (AMPS) VS. VOLTAGE (KEV)

TABLE IV

V	JTOT	JE	JSECE	JBSCAT	JI	JSECI
.00	-8.30-006	-1.00-005	8.35-007	8.64-007	.00	.00
-9.52-001	-8.26-006	-1.00-005	8.67-007	8.68-007	.00	.00
-1.90+000	-8.22-006	-1.00-005	9.02-007	8.72-007	.00	.00
-2.86+000	-8.18-006	-1.00-005	9.40-007	8.78-007	.00	.00
-3.81+000	-8.13-006	-1.00-005	9.82-007	8.85-007	.00	.00
-4.76+000	-8.07-006	-1.00-005	1.03-006	8.93-007	.00	.00
-5.71+000	-8.01-006	-1.00-005	1.08-006	9.03-007	.00	.00
-6.67+000	-7.94-006	-1.00-005	1.14-006	9.15-007	.00	.00
-7.62+000	-7.86-006	-1.00-005	1.21-006	9.30-007	.00	.00
-8.57+000	-7.76-006	-1.00-005	1.28-006	9.47-007	.00	.00
-9.52+000	-7.65-006	-1.00-005	1.37-006	9.69-007	.00	.00
-1.05+001	-7.52-006	-1.00-005	1.47-006	9.94-007	.00	.00
-1.14+001	-7.37-006	-1.00-005	1.60-006	1.03-006	.00	.00
-1.24+001	-7.18-006	-1.00-005	1.75-006	1.06-006	.00	.00
-1.33+001	-6.94-006	-1.00-005	1.94-006	1.11-006	.00	.00
-1.43+001	-6.65-006	-1.00-005	2.18-006	1.16-006	.00	.00
-1.52+001	-6.26-006	-1.00-005	2.50-006	1.23-006	.00	.00
-1.62+001	-5.72-006	-1.00-005	2.96-006	1.31-006	.00	.00
-1.71+001	-4.90-006	-1.00-005	3.67-006	1.41-006	.00	.00
-1.81+001	-3.50-006	-1.00-005	4.96-006	1.53-006	.00	.00
-1.90+001	-1.59-007	-1.00-005	8.18-006	1.64-006	.00	.00

EXIT

[EXIT]

6. NASCAP*TERMTALK

TERMTALK has been revised to display SINGLE cell information in the same manner as NASCAP. The new SINGLE keyword, 'SUMMAR', causes TERMTALK to give the user a breakdown of the incident currents for a particular surface cell. To make this possible NASCAP has been modified to write this new information on file 21. Using NASCAP data files that have been generated from older versions will lead to a warning, stating that the 'SUMMAR' option in the SINGLE module may not be used. The SINGLE module will, however, handle all other cell information as before.

The new TERMTALK output, in the single mode, is shown below.

```
0 CHOOSE ANY MODULE
  HELP IS ALWAYS AVAILABLE - TYPE 'HELP'
 >SINGLE
0 SINGLE COMMAND OR MODE SET ?
 >EVERY
 MODE RESET
0 SINGLE COMMAND OR MODE SET ?
 >2
 ------------------------------------------------------------------------
0  SURFACE CELL NO.    2
                                    CODE            3104C5166C43
                                    CENTERED AT      -5.C   -3.5   -2.5
                                    MATERIAL IS  *HIT
                                    NORMAL          -1  0  0
                                    SHAPE IS SQUARE
                      POTENTIAL =-1.375+003 VOLTS
                      INTERNAL FIELD STRESS =-2.118+002  VOLTS/METER
                      EXTERNAL ELECTRIC FIELD =-1.323+003  VOLTS/METER
                      DELTA V =-1.359-002 VOLTS
                      UNDERLYING CONDUCTOR IS NUMBER 1
                      UNDERLYING CONDUCTOR POTENTIAL =-1.375+003 VOLTS
                      ANGLE *ITH ANISOTROPIC DIRECTION    45.003 DEGS
   FLUXES IN A/M**2
         INCIDENT ELECTRONS              1.98-006
              RESULTING SECONDARIES      4.07-007
              RESULTING BACKSCATTER      4.92-007
         INCIDENT PROTONS                4.43-008
              RESULTING SECONDARIES      5.32-008
         BULK CONDUCTIVITY              -1.25-011
         PHOTOCURRENT                     .00
                                        ----------
       NET FLUX AFTER LONG-TIME-STEP    -7.57-007
0 SINGLE COMMAND OR MODE SET ?
 >EXIT
```

New TERMTALK

7. NASCAP/LEO

7.1 GENERAL

The BIGLEO and BIGFINE codes are designed to study the electrostatic potential and sheath structure in the vicinity of a large, high-voltage spacecraft, and consequent current collection by the spacecraft, given specified fixed spacecraft potentials with respect to the surrounding plasma. BIGLEO performs the calculation for a large spacecraft, and has mirror plane capability. BIGFINE performs the calculation for the region above a periodic surface (e.g., a solar array module) and takes potential and current boundary conditions from the BIGLEO code.

BIGLEO and BIGFINE are written in FORTRAN V for UNIVAC 1100 series computers. They share many routines in common (BIGFINE has only twelve (12) unique subroutines) and utilize numerous NASCAP routines. Object definition, options, and control statements retain great similarity to NASCAP. Current trajectory plots are generated directly by BIGLEO and BIGFINE with some degree of flexibility. Object plots may be generated by OBJCHECK or NASCAP, and potential contours by POTPLT. Both codes write restart information on files 15 and 21. Additionally, file 16 contains information passed from BIGLEO to BIGFINE.

7.2 MAIN CODE MODULES

The major code modules in the BIGLEO and BIGFINE codes are

```
RDOPT          [lun]
OBJDEF         [lun]
POTENT         [lun]
CURRENt        [lun]
MOVEP          [lun]
APRT         [n name]
END
```

As with NASCAP, RDOPT must be executed first in any run. Repeat calls to RDOPT will (unlike in NASCAP) begin by resetting options to their initial values. The OBJDEF module requires input similar to NASCAP's OBJDEF. POTENT solves a nonlinear Poisson's equation, and CURRENt calculates the current to various parts of the object and generates plots if requested. APRT is used to print the potential array, and MOVEP moves the potential array from file 15 to another file.

7.3 RDOPT MODULE

The RDOPT module reads the run options from file lun (default 5, i.e., runstream). Available options for these codes are:

END	End of input.
NZ nz	Z-dimension of mesh; default = 17.
NG ng	Number of nested grids; default = 1.
XMESH x	Physical mesh spacing (m); default = 1.
ERRLIM v	Error parameter for potent (q.v.); default = 0.5 volts.
PDAMP f	For each major potential iteration, mix f of previous iterate with (1-f) of current iterate; default: f = 0.
ITERMX m	Maximum number of major potential iterations; default: m = 100.
COARSCale	(Fine code only.) Resolve screening length to value appropriate to coarse code (16 x XMESH); default: resolve to XMESH.
PCOND icon	Specify potential of conductor icon in volts; default: v = 1000*icon.
DEBYE LENGTH d	Ambient plasma Debye length (m); default: 1 m.
SATVEL vx vy vz	Spacecraft velocity (m/sec); default: 0.
BIAS icon v	Bias conductor icon v volts relative to conductor 1 (see PCOND).

IONMAS mass [AMU]	Ion mass in kg or amu; default: 1.67×10^{-27} kg.
TEMPER t	Plasma temperature (eV); default: 1 eV.
PLOT UNIT [lun]	Perform plots using unit lun as a scratch file. Default is no plots. If lun is omitted, it is set to 28. If lun < 0, plots are made from previously saved file |lun|.
PRINT CURRNT PRINT TRAJEC PRINT SHEATH PRINT OBJDEF NOPRINT OBJDEF	Options for diagnostic print.
SHEATH BOUNDARY v	Potential at sheath boundary to be used by CURRENt module of BIGLEO code; default = 100 V.
LIMIT PLOTS xmin, xmax, ymin, ymax, zmin, zmax	Plotting limits in grid units. For trajectories projected on the Y-Z plane, only segments between xmin and xmax are plotted, etc.; default: plot full trajectories.
NSTP n	Maximum steps per trajectory; default: 100.
LUNPQV lun	Unit number of fill to be used to write (read) fine cell particle information; default: 16.
MIRROR plane	Plane = '+X', '-X', '+Y', '-Y', '+Z', '-Z'. Establish mirror plane on specified boundary of inner grid.
FINE CELL icell	(BIGLEO) Output information for cell icell for use by BIGFINE. Maximum of ten (10) cells. (BIGFINE) Retrieve information appropriate to cell icell from previous BIGLEO run.
FINE MESH xmesh	(BIGLEO only.) Resolution of previously specified fine cell; default = XMESH/16.
IZBOT i	(BIGFINE only.) z-value for "bottom" of space, i.e., height of cell = NZ-IZBOT. Used in calculating VTOP.

NEMITX n

NEMITY n

(BIGFINE only.) Allows coarsening for current emission, i.e., number of mesh units apart for particle emission points. Number of particle emission points

$$= \frac{NX-1}{NEMITX} \times \frac{NY-1}{NEMITY}$$

default: NEMITX = NEMITY = 1.

VECODE v

(BIGFINE only.) Code velocity of emitted particles at surface; default: 0.1.

7.4 OBJDEF MODULE

The OBJDEF module is invoked by the specification OBJDEF lun, where lun (default = 5) is the logical unit number of the OBJDEF input. The input differs from standard NASCAP input in the following ways:

1. The only allowed building blocks are RECTAN, PLATE, PATCHR, and PATCHW.
2. All materials are assumed conducting.
3. For the BIGLEO code, surfaces lying in a mirror plane should remain undefined. This will result in numerous warnings. It should be verified that the warnings refer to points in the mirror plane.
4. Similarly, for the BIGFINE code surfaces on the x- and y-boundary planes should remain undefined. There should be no surfaces on the z-boundary planes.

7.5 POTENT MODULE

The POTENT module solves the equation

$$\varepsilon_0 \nabla^2 \phi + \rho(n,\theta,\phi) = 0 \ ,$$

where ρ, the charge density, is a function of the local potential, density, and temperature. The function used,

$$\rho/\varepsilon_0 = - \frac{\phi}{D^2} \left[1 + (\phi/T)^{3/2} \right]^{-1} \ ,$$

$$D = \max(\lambda_D, 0.7L) \ ,$$

$$T = (k\theta/e) \ (4\pi)^{-1/3} \ (D/\lambda_D)^{4/3} \ ,$$

$$\lambda_D^2 = \frac{\varepsilon_0 k\theta}{ne^2} \ ,$$

reduces to Debye screening (within the code resolution, L) for low potentials, and to the density associated with the one-sided plasma thermal current at high potentials. At present, the input only allows for a constant ambient density and temperature. However, it is easy to modify the code to use an analytic formula for density and temperature as a function of position. The boundary conditions, for the BIGLEO code, are zero potential at boundaries and zero normal field at mirror planes. For the BIGFINE code, periodic boundaries are used in the x- and y-directions. User-specified potentials (which should average to the potential, VBOT, for that cell in the BIGLEO code) are used at the lower z-boundary, and at the upper boundary

VTOP = VBOT + (NZ-IZBOT)*XMESH*EZ

where EZ is the normal field taken from the BIGLEO code. (It should be noted that the BIGFINE code, with its small mesh spacing, can provide far more screening than the BIGLEO code, so that the user may

need to specify a small value of NZ. As a rule, NZ should not be much greater than the scale of potential variation at the cell bottom.)

POTENT solves the nonlinear equation $\varepsilon_0 \nabla^2 \phi + \rho(\phi) = 0$ by successive linearizations about the previous iterate. The scheme goes as follows:

1. Given iterate $\underset{\sim}{\phi}^{(n)}$, write

$$\rho_i^{(n+1)}\left(\phi_i^{(n+1)}\right) = \phi_i^{(n+1)} \left.\frac{\partial \rho_i}{\partial \phi_i}\right|_{\phi_i^{(n)}} + \rho_i\left(\phi_i^{(n)}\right)$$

$$- \phi_i^{(n)} \left.\frac{\partial \rho_i}{\partial \phi_i}\right|_{\phi_i^{(n)}}$$

2. Using the finite element formulation and scaled conjugate gradient equation solver, minimize (to solve for $\phi^{(n+1)}$)

$$\int \left\{ \frac{\varepsilon_0}{2} \left| \nabla \phi^{(n+1)} \right|^2 + \frac{1}{2} \left.\frac{\partial \rho}{\partial \phi}\right|_{\phi_i^{(n)}} \phi^{(n+1)2} \right.$$

$$\left. - \phi^{(n+1)} \left[\rho\left(\phi^{(n)}\right) + \phi^{(n)} \left.\frac{\partial \rho}{\partial \phi}\right|_{\phi^{(n)}} \right] \right\} \, dV.$$

Require two orders of magnitude convergence.

3. Calculate the root-mean-square change

$$E = \left[\frac{\sum_i \left(\phi_i^{(n)} - \phi_i^{(n+1)} \right)^2}{\sum_i 1} \right]^{1/2}$$

If $E \leq$ ERRLIM, finish.
If $E >$ ERRLIM, return to (1).

This scheme usually converges in 3-10 major iterations.

7.6 CURRENt MODULE

The CURRENt module calculates the current incident upon, and power loss by, each conducting segment of the test object. In the BIGLEO code this module operates as follows:

1. Define the sheath boundary as $|\phi| = \phi_B$, where ϕ_B is the sheath boundary potential.
2. Determine the electron (for $\phi > 0$) or ion (for $\phi < 0$) current through each sheath segment, taking account of thermal and primitive ram effects. (See below.)
3. Track appropriate particles inward from each sheath segment.
4. Summarize results; make particle plots as requested.

In the BIGFINE code, the particles which hit the surface cell in the coarse code are duplicated

$$\frac{NX-1}{NEMITX} \times \frac{NY-1}{NEMITY}$$

times and emitted above the finely resolved surface.

7.7 MOVEP MODULE

The MOVEP module writes the potentials on logical unit lun (default = 10). The intent is to enable use of POTPLT to generate potential contour plots.

7.8 APRT MODULE

APRT prints the values for n gridsworth of array 'name'. The default is to print the potential for one grid.

7.9 INTERFACING THE BIGLEO AND BIGFINE CODES

If the BIGFINE code is to be used on selected surface cells, those cells should be identified by number in the options file of the BIGLEO code. Up to ten cells may be specified. Potential information for these cells will be written on file 21, and particle information on file LUNPQV [16]. Before invoking the BIGFINE code, files 16 and 21 should be copied over. The mean surface potential of the module specified in the fine code object definition and options should equal the potential of that cell in the coarse code. The potential and particle information will be retrieved upon specification of the coarse code cell number.

7.10 TREATMENT OF RAM EFFECTS IN BIGLEO CODE

The BIGLEO code only includes an estimate of ram effects on sheath boundary currents. Ram effects are not included in sheath or shielded region densities. Thus this treatment is extremely primitive and should be employed only with great care.

Notation:

ρ	-	plasma density (m^{-3})
θ	-	plasma temperature (eV)
$\vec{V}_s$	-	spacecraft velocity (relative to plasma)
$\vec{E}$	-	electric field
$\hat{E}$	-	electric field direction
$\hat{n}$	-	outward normal to sheath
v_{th}	-	thermal velocity
m	-	particle mass (kg)
J	-	current density (A/m^2) in spacecraft reference
$f(\vec{v})$	-	distribution function ($sec^3\ m^{-6}$)
j_{th}	-	one-sided thermal current
ϕ	-	sheath boundary potential
q	-	particle electric charge
$\vec{v}$	-	particle velocity

A fundamental quantity in the LEO code is the one-sided current of an attracted particle species through the sheath surface. This is given by

$$\vec{J}\cdot\hat{n} = \hat{n} \cdot \int_{\Omega} e\vec{v}\, f(\vec{v})\, d^3\vec{v}$$

where $\vec{v} \in \Omega$ iff $\vec{v}\cdot\hat{n} < 0$. Now

$$f(\vec{v}) = f_0(\vec{v})\, e^{-1/2\, m[\vec{v} + \vec{V}_s)^2 - \vec{v}^2]/e\theta} \quad .$$

It follows that

$$\vec{J}\cdot\hat{n} = -j_{th}\int_{-\infty}^{0} v\, e^{-1/2\, m(v+\vec{V}_s\cdot\hat{n})^2/e\theta}\, dv \Big/ \int_{-\infty}^{0} v\, e^{-1/2\, m\, v^2/e\theta}\, dv$$

$$= -j_{th}\int_{-Z}^{\infty} (z+Z)\, e^{-z^2/2}\, dz$$

where

$$Z = \vec{V}_s\cdot\hat{n}(m/e\theta)^{1/2}$$

$$\frac{-\vec{J}\cdot\hat{n}}{j_{th}} = \begin{cases} 2 - \exp(-Z^2/2) + Z(\pi/2)^{1/2}\left(1 + \operatorname{erf}(Z/\sqrt{2})\right) & Z < 0 \\ \exp(-Z^2/2) + Z(\pi/2)^{1/2}\left(1 - \operatorname{erf}(-Z/\sqrt{2})\right) & Z < 0 \end{cases}$$

For $n = 10^{12}$, $\hat{n}\cdot\vec{V}_s = \pm 7500$ or 0, these formulae give the following values for $|\vec{J}\cdot\hat{n}|$:

θ	$\hat{n}\cdot\vec{V}_s$	e^-	H^+	O^+
0.1	-7500	7.9×10^{-3}	1.8×10^{-6}	2.0×10^{-25}
0.1	0	8.5×10^{-3}	2.0×10^{-4}	4.9×10^{-5}
0.1	7500	9.1×10^{-3}	1.6×10^{-3}	1.3×10^{-3}
1.0	-7500	2.62×10^{-2}	2.0×10^{-4}	1.5×10^{-7}
1.0	0	2.68×10^{-2}	6.3×10^{-4}	1.6×10^{-4}
1.0	+7500	2.74×10^{-2}	1.7×10^{-3}	1.5×10^{-3}

The above values are calculated from subroutine DISMAX (DISplaced MAXwellian), and are used by subroutine FLUX to return current density and initial velocity of the sheath particle as follows:

Provisionally:

$$\vec{v} = -\vec{V}_s + [2e(\theta + |\phi|)/m]^{1/2} \frac{q}{e} \hat{E} .$$

If

$$\vec{v} \cdot \frac{q}{e} \hat{E} < v_{th}$$

then

$$\vec{v} = v_{th} \frac{q}{e} \hat{E} .$$

7.11 SAMPLE RUN OF BIGLEO AND BIGFINE CODES

```
        ELT    * LEOTEST *

@ELT,LS       LEOTEST
ELT 8R1-S3C S74Q1C 02/10/81 10:03:24 (5)
     1.          01      @RUN MJM,11155-00,MANDELL-M,15
     2.          01      @BIG-NAME,P
     3.          01      LEO TEST
     4.          01      BOX 24
     5.          01      @MSG,N     ASSIGN FILES FOR BIGLEO CODE
     6.          01      @ASG,A SEPS15.
     7.          01      @USE 15,SEPS15
     8.          01      @ASG,A SEPS21.
     9.          01      @USE 21,SEPS21
    10.          04      @USE 16,SEPS16.
    11.          01      @ASG,A SEPS16.
    12.          01      @MSG,N       EXECUTION OF BIGLEO
    13.          05      @XQT BIGLEO.LEO
    14.          05      @OOPT 5
    15.          05      @ADD SEPSOPT.
    16.          05      OBJDEF 5
    17.          05      @ADD SEPSOBJ.
    18.          05      POTENT
    19.          05      CURRENT
    20.          05      END
    21.          01      @PMD,EL
    22.          01      @MSG,N      FREE COARSE CODE FILES AND ASSIGN FINE CODE FILES
    23.          01      @FREE 15.
    24.          01      @FREE 21.
    25.          01      @FREE 16.
    26.          01      @ASG,A FINE15.
    27.          01      @USE 15,FINE15
    28.          01      @ASG,A FINE21.
    29.          01      @USE 21,FINE21
    30.          02      @USE 16,FINE16
    31.          01      @ASG,A FINE16.
    32.          01      @MSG,N      INTERFACE FINE CODE TO COARSE CODE
    33.          01      @COPY SEPS21.,21.
    34.          01      @COPY SEPS16.,16.
    35.          01      @MSG,N     EXECUTE FINE CODE
    36.          01      @XQT BIGFINE.FINE
    37.          01      @OOPT 5
    38.          01      @ADD FINEOPT.
    39.          01      OBJDEF 5
    40.          03      @ADD FINEOBJ.
    41.          01      POTENT
    42.          01      CURRENT
    43.          01      END
    44.          01      @PMD,EL
    45.          01      @BIG-NAME,P
    46.          01      END
    47.          01      BOX 24
    48.          01      @FIN

END ELT.  ERRORS: NONE. TIME:  0.080 SEC. IMAGE COUNT: 48

@HDG          ELT    * SEPSOPT *
```

Runstream for sample run.

```
        ELT    * SEPSOPT *

@ELT,LS       SEPSOPT
ELT 8R1-S3C S74Q1C 02/10/81 15:03:24 (0)
     1.                  FINE CELL 300
     2.                  FINE CELL 400
     3.                  NOPRINT OBJDEF
     4.                  NZ 33
     5.                  MIRROR -Z
     6.                  NG 2
     7.                  ERPLIM .1
     8.                  PCOND 1 -198.
     9.                  BIAS 2 0.
    10.                  BIAS 3 100.
    11.                  BIAS 4 200.
    12.                  BIAS 5 0.
    13.                  BIAS 6 100.
    14.                  BIAS 7 150.
    15.                  XMESH .3
    16.                  PLOT UNIT 29
    17.                  LIMIT PLOTS 9. 10. 9. 10. 17. 18.
    18.                  DEBYE LENGTH .000
    19.                  TEMPERATURE .1
    20.                  SHEATH BOUNDARY 1.
    21.                  IONMASS 16 AMU
    22.                  SATVEL 0. 7500. 0.
    23.                  END

END ELT.  ERRORS: NONE. TIME:  0.059 SEC. IMAGE COUNT. 23

@HDG
```

Options input for coarse code sample run.

```
          ELT    * FINEOPT *

$ELT,LS      FINEOPT
ELT $R1-S3C S74QIC 02/10/81 15:07:24 (C)
     1.                    COARSCALE
     2.                    NSTP +00
     3.                    VECODE .2
     4.                    FINE CELL 300
     5.                    XMESH .21675
     6.                    IZBGT 2
     7.                    NOPRINT OBJDEF
     8.                    NZ 47
     9.                    NB 1
    10.                    ERRLIM .1
    11.                    PCOND 1 2
    12.                    PCOND 2 2
    13.                    PCOND 3 -3
    14.                    PCOND 4 2
    15.                    PCOND 5 7
    16.                    DEBYE LENGTH .003
    17.                    TEMPERATURE .1
    18.                    IONMASS 16 AMU
    19.                    SATVEL 0.  7500. 0.
    20.                    END

END-ELT.  ERRORS: NONE.  TIME:  0.057 SEC.  IMAGE COUNT: 20

$HDG          ELT    * LEOTEST *
```

Options input for fine code sample run.

```
          LEO HIGH-VOLTAGE CURRENT COLLECTION CODE


**********ROOPT 5
FINE CELL 300
FINE CELL 400
NOPRINT OBJDEF
NZ 33
MIRROR -Z
NC 2
ERRLIM .1
PCOND 1 -198.
BIAS 2 0.                          PCOND( 2) =   -1.98+02 VOLTS.
BIAS 3 100.                        PCOND( 3) =   -9.90+01 VOLTS.
BIAS 4 200.                        PCOND( 4) =    2.00+00 VOLTS.
BIAS 5 0.                          PCOND( 5) =   -1.98+02 VOLTS.
BIAS 6 100.                        PCOND( 6) =   -9.80+01 VOLTS.
BIAS 7 150.                        PCOND( 7) =   -4.80+01 VOLTS.
XMESH .3
PLOT UNIT 28
LIMIT PLOTS 9. 10. 9. 10. 17. 18.
DEBYE LENGTH .003
TEMPERATURE .1
SHEATH BOUNDARY 1.
IONMASS 16 AMU
SATVEL 0.  7500. 0.
END
LAMBDA=   3.00-03 M      T=   1.00-01 EV       SHEATH BOUNDARY=   1.00+00 EV
 PLASMA DENSITY =   6.14+11 M**(-3)      ION MASS=   2.68-26 KG.
  SATELLITE VELOCITY=(   0.00       7.50+03   0.00   ) M/SEC.

        2 FINE CELL(S) CHOSEN:
       1      CELL NO.   300          .0188 METER RESOLUTION
       2      CELL NO.   400          .0188 METER RESOLUTION

**********ORJDEF 5
```

Coarse code output — option specifications.

```
 ASGFIL: FILE 17              ISTAT= 000000000000

OFFSET 0 0 0

CONDUCTOR 1

RECTAN
 OBJECT NO= DEFINED.
                              9<X< 12
                              7<Y< 11
                              1<Z<  3

SURFACE +X GOLD
SURFACE -X GOLD
SURFACE +Y GOLD
SURFACE -Y GOLD
SURFACE +Z GOLD
ENDOBJ

RECTAN
 OBJECT NO= DEFINED.
                             12<X< 16
                              8<Y< 10
                              1<Z<  2

SURFACE +X GOLD
SURFACE -X GOLD
SURFACE +Y GOLD
SURFACE -Y GOLD
SURFACE +Z GOLD
ENDOBJ

PLATE
 THIN PLATE NO= DEFINED.
                             14<X< 14
                              6<Y< 12
                              1<Z<  4

TOP -X GOLD
BOTTOM +X GOLD
ENDOBJ

PLATE
 THIN PLATE NO= DEFINED.
                              9<X< 12
                              6<Y< 12
                              1<Z<  1

TOP +Z GOLD
ENDOBJ

RECTAN
 OBJECT NO= DEFINED.
                             10<X< 11
                              5<Y< 13
                              4<Z<  5

SURFACE +X GOLD
SURFACE -X GOLD
SURFACE +Y GOLD
SURFACE +Z GOLD
SURFACE -Y GOLD
SURFACE -Z GOLD
ENDOBJ

PLATE
 THIN PLATE NO= DEFINED.
                              9<X<  9
                              7<Y< 11
                              1<Z<  4

TOP +X GOLD
BOTTOM -X GOLD
ENDOBJ

CONDUCTOR 2

PLATE
 THIN PLATE NO= DEFINED.
                             11<X< 11
                              5<Y< 13
                              4<Z< 13

BOTTOM -X GOLD
ENDOBJ

CONDUCTOR 3

PLATE
 THIN PLATE NO= DEFINED.
                             11<X< 11
                              5<Y< 13
                             13<Z< 23

BOTTOM -X GOLD
ENDOBJ

CONDUCTOR 4

PLATE
 THIN PLATE NO= DEFINED.
                             11<X< 11
                              5<Y< 13
                             23<Z< 33

BOTTOM -X GOLD
```

BIGLEO object definition output.

```
ENDOBJ

CONDUCTOR 5

PLATE
 THIN PLATE NOW DEFINED.
                                11<X< 11
                                 5<Y< 13
                                 4<Z< 13

TOP +X GOLD
ENDOBJ

CONDUCTOR 6

PLATE
 THIN PLATE NOW DEFINED.
                                11<X< 11
                                 5<Y< 13
                                13<Z< 23

TOP +X GOLD
ENDOBJ

CONDUCTOR 7

PLATE
 THIN PLATE NOW DEFINED.
                                11<X< 11
                                 5<Y< 13
                                23<Z< 33

TOP +X GOLD
ENDOBJ

ENDSAT

       550 VOLUME CELLS NUMBERED BY NUMLTB.
CALLING GENMTL
*ARNING --- SCCYC ERROR IN ANALYSIS OF SURFACE AROUND VERTEX 110601
 CODE:  1
*ARNING --- SCCYC ERROR IN ANALYSIS OF SURFACE AROUND VERTEX 110701
 CODE:  2
*ARNING --- SCCYC ERROR IN ANALYSIS OF SURFACE AROUND VERTEX 111001
 CODE:  2
*ARNING --- SCCYC ERROR IN ANALYSIS OF SURFACE AROUND VERTEX 111101
 CODE:  2
*ARNING --- SCCYC ERROR IN ANALYSIS OF SURFACE AROUND VERTEX 111201
 CODE:  2
*ARNING --- SCCYC ERROR IN ANALYSIS OF SURFACE AROUND VERTEX 111301
 CODE:  2
*ARNING --- SCCYC ERROR IN ANALYSIS OF SURFACE AROUND VERTEX 111401
 CODE:  1
*ARNING --- SCCYC ERROR IN ANALYSIS OF SURFACE AROUND VERTEX 120601
 CODE:  2
*ARNING --- SCCYC ERROR IN ANALYSIS OF SURFACE AROUND VERTEX 121401
 CODE:  2
*ARNING --- SCCYC ERROR IN ANALYSIS OF SURFACE AROUND VERTEX 130601
 CODE:  2
*ARNING --- SCCYC ERROR IN ANALYSIS OF SURFACE AROUND VERTEX 131401
 CODE:  2
*ARNING --- SCCYC ERROR IN ANALYSIS OF SURFACE AROUND VERTEX 140601
 CODE:  1
*ARNING --- SCCYC ERROR IN ANALYSIS OF SURFACE AROUND VERTEX 140701
 CODE:  2
*ARNING --- SCCYC ERROR IN ANALYSIS OF SURFACE AROUND VERTEX 141001
 CODE:  2
*ARNING --- SCCYC ERROR IN ANALYSIS OF SURFACE AROUND VERTEX 141201
 CODE:  2
*ARNING --- SCCYC ERROR IN ANALYSIS OF SURFACE AROUND VERTEX 141301
 CODE:  2
*ARNING --- SCCYC ERROR IN ANALYSIS OF SURFACE AROUND VERTEX 141401
 CODE:  1
*ARNING --- SCCYC ERROR IN ANALYSIS OF SURFACE AROUND VERTEX 151001
 CODE:  2
*ARNING --- SCCYC ERROR IN ANALYSIS OF SURFACE AROUND VERTEX 151201
 CODE:  2
*ARNING --- SCCYC ERROR IN ANALYSIS OF SURFACE AROUND VERTEX 161001
 CODE:  2
*ARNING --- SCCYC ERROR IN ANALYSIS OF SURFACE AROUND VERTEX 161201
 CODE:  2
*ARNING --- SCCYC ERROR IN ANALYSIS OF SURFACE AROUND VERTEX 171001
 CODE:  2
*ARNING --- SCCYC ERROR IN ANALYSIS OF SURFACE AROUND VERTEX 171201
 CODE:  2
*ARNING --- SCCYC ERROR IN ANALYSIS OF SURFACE AROUND VERTEX 201001
 CODE:  2
*ARNING --- SCCYC ERROR IN ANALYSIS OF SURFACE AROUND VERTEX 201101
 CODE:  2
*ARNING --- SCCYC ERROR IN ANALYSIS OF SURFACE AROUND VERTEX 201201
 CODE:  2

  INSLST --     0 INSULATING SURFACE CELLS FOUND

 NO SURFACE CONDUCTIVITY

          1 ENTRIES IN REVISED VTXL

         NC DETERMINED BY CETNC TO BE  7
END GENMTL
```

BIGLEO object definition (continued). Note warnings for points on mirror plane, for which edges have surfaces on one side only.

```
**********POTENT

 ASGFIL: FILE 17                ISTAT= 100000000000
AT ITER     1 DRDOTR=  1.69+005
AT ITER     2 DRDOTR=  1.21+004
AT ITER     3 DRDOTR=  2.10+003
AT ITER     4 DRDOTR=  1.91+002

 SCG -- DRDOTR/DR1=   1.91+02/   1.69+05 IN   4 ITERATIONS.

 RMS ERROR =   1.1+01 AT ITER=   1
AT ITER     1 DRDOTR=  3.23+004
AT ITER     2 DRDOTR=  4.56+003
AT ITER     3 DRDOTR=  1.10+003
AT ITER     4 DRDOTR=  8.88+001

 SCG -- DRDOTR/DR1=   8.88+01/   3.23+04 IN   4 ITERATIONS.

 RMS ERROR =   4.2+00 AT ITER=   2
AT ITER     1 DRDOTR=  1.61+003
AT ITER     2 DRDOTR=  1.63+002
AT ITER     3 DRDOTR=  2.83+001
AT ITER     4 DRDOTR=  2.16+000

 SCG -- DRDOTR/DR1=   2.16+00/   1.61+03 IN   4 ITERATIONS.

 RMS ERROR =   7.4-01 AT ITER=   3
AT ITER     1 DRDOTR=  1.40+001
AT ITER     2 DRDOTR=  2.78+000
AT ITER     3 DRDOTR=  5.46-001
AT ITER     4 DRDOTR=  4.88-002

 SCG -- DRDOTR/DR1=   4.88-02/   1.40+01 IN   4 ITERATIONS.

 RMS ERROR =   7.2-02 AT ITER=   4

FINE CELL   300          .0188 METER RESOLUTION
                VBOT=      2.00 VOLTS, E=(       .09,       .13,      5.66) V/M

FINE CELL   400          .0188 METER RESOLUTION
                VBOT=   -198.00 VOLTS, E=(     -6.85,    -15.36,   -266.75) V/M
```

BIGLEO code potential calculation. For this case, convergence was achieved after four major iterations each consisting of four minor iterations. Note also output of fine cell potentials and fields.

```
 ASGFIL: FILE 10                ISTAT= 000000000000
SHAPE WROTE    9537 ELEMENTS TO FILE  10  # OF NON-ZERO FLUXES =    2288
CONDUCTOR      POTENTIAL (VOLTS)      CURRENT (AMPS)      POWER (WATTS)

      1          -1.980000+02           4.216193-03          -8.348062-01
      2          -1.980000+02           2.666272-03          -5.279219-01
      3          -9.800000+01           2.946982-03          -2.888042-01
      4           2.000000+00          -1.896886-02          -3.793772-02
      5          -1.980000+02           3.135605-03          -6.208499-01
      6          -9.800000+01           2.857887-03          -2.800729-01
      7          -4.800000+01           2.617382-03          -1.256343-01

TOTAL CURRENT TO CELLS =  -5.285503-04 AMPS   TOTAL POWER DISSIPATED BY ALL CELLS =  -2.716027+00 WATTS

 AVERAGE COLLECTION POTENTIAL VBAR =  5.13863+03 VOLTS

SUMMARY OF PARTICLE TRACKING RESULTS




CURRENT TO OBJECT   =  -5.297-04 AMPS
CURRENT ESCAPING    =   1.850-03 AMPS
CURRENT UNASSIGNED  =   0.000    AMPS


IUP=    15860  IDOWN=      197  NEST=     4929

NUMBER OF PARTICLES EMITTED IN GRID  1 =       5332
NUMBER OF PARTICLES EMITTED IN GRID  2 =        246
READQV FOUND      6 PARTICLES ON FILE    16  FOR CELL INDEX      1

    6 PARTICLES HIT COARSE CELL   300


K= 1 KCELLS=  300 XCEL=  1.87500-02 VBOT=  2.00000+00 EFLD=   9.24899-02   1.32516-01   5.65502+00
J=   1  V=   3.3208+05  -1.2180+04   9.0896+05 M/SEC   CURRENT= -1.1873-04 AMPS
J=   2  V=   6.6498+03  -1.5803+04   8.6541+05 M/SEC   CURRENT= -1.1706-04 AMPS
J=   3  V=   8.9619+03  -2.1374+04   8.5978+05 M/SEC   CURRENT= -1.1706-04 AMPS
J=   4  V=   5.0694+03  -2.0079+04   8.6637+05 M/SEC   CURRENT= -1.1709-04 AMPS
J=   5  V=   7.2821+03  -2.2701+04   8.6075+05 M/SEC   CURRENT= -1.1708-04 AMPS
J=   6  V=   8.0273+01  -3.5078+05   8.0528+05 M/SEC   CURRENT= -1.2265-04 AMPS
READQV FOUND      2 PARTICLES ON FILE    16  FOR CELL INDEX      2

    2 PARTICLES HIT COARSE CELL   400


K= 2 KCELLS=  400 XCEL=  1.87500-02 VBOT= -1.98000+02 EFLD=  -6.85342+00  -1.53620+01  -2.66750+02
J=   1  V=  -1.8695+04  -7.7830+03  -4.4821+04 M/SEC   CURRENT=  8.8075-06 AMPS
J=   2  V=  -1.7047+04  -6.0231+03  -4.4961+04 M/SEC   CURRENT=  3.6991-06 AMPS

***TIME LEFT =   592 SECONDS***


CALLING PLTPAR WITH LUNPLT = 28
IN PLTPAR IG=   2 NTRAJ=        5578 GSCALE=   5.0000000-01 IVIEW=   1
IN PLTPAR IG=   2 NTRAJ=        5578 GSCALE=   5.0000000-01 IVIEW=   1
IN PLTPAR IG=   2 NTRAJ=        5578 GSCALE=   5.0000000-01 IVIEW=   1

***TIME LEFT =   402 SECONDS***


YOU HAVE CREATED      5 FRAMES OF MICROFILM

**********END
```

BIGLEO CURRENt module output. (Listing of currents to individual cells has been omitted.) This object is near its floating potential, with electrons incident on conductor 4 balancing the total ion current. Note also output of particles hitting fine cells.

```
          LEO HIGH-VOLTAGE CURRENT COLLECTION CODE

                    FINE HIGH RESOLUTION PERIODIC SECTION

**********RDOPT 5

        2 FINE CELL(S) AVAILABLE:
        1       CELL NO.    300          .0188 METER RESOLUTION
        2       CELL NO.    400          .0188 METER RESOLUTION
COARSCALE
NSTP 400
VECODE .3
FINE CELL 300
XMESH .01875
IZBOT 2
NOPRINT OBJDEF
NZ 17
NG 1
ONLY NG=1 PERMITTED FOR THIS PERIODIC CODE.
ERRLIM .1
PCOND 1 2
PCOND 2 2
PCOND 3 -3
PCOND 4 2
PCOND 5 7
DEBYE LENGTH .003
TEMPERATURE .1
IONMASS 16 AMU
SATVEL 0.  7500. 0.
END
LAMBDA=   3.0D-03 M      T=   1.00-01 EV       SHEATH BOUNDARY=   1.0D+02 EV
 PLASMA DENSITY =   6.14+11 M**(-3)      ION MASS=   2.68-26 KG.
  SATELLITE VELOCITY=(   0.00       7.5D+03    0.00   ) M/SEC.

**********OBJDEF 5
```

Fine code output — option specifications.

```
 ASGFIL: FILE 17                ISTAT= 1000000000000

 OFFSET 0 0 1

 CONDUCTOR 1

 PLATE
  THIN PLATE NOW DEFINED.
                                    1<X< 17
                                    1<Y< 17
                                    2<Z<  2

 TOP +Z COPPER
 BOTTOM -Z COPPER
 ENDOBJ

 CONDUCTOR 2

 PLATE
  THIN PLATE NOW DEFINED.
                                    1<X< 17
                                   13<Y< 17
                                    2<Z<  2

 TOP +Z ALUMINUM
 ENDOBJ

 CONDUCTOR 3

 PLATE
  THIN PLATE NOW DEFINED.
                                    1<X< 17
                                    9<Y< 13
                                    2<Z<  2

 TOP +Z GOLD
 ENDOBJ

 CONDUCTOR 4

 PLATE
  THIN PLATE NOW DEFINED.
                                    1<X< 17
                                    5<Y<  9
                                    2<Z<  2

 TOP +Z SILVER
 ENDOBJ

 CONDUCTOR 5

 PLATE

 THIN PLATE NOW DEFINED.
                                   1<X< 17
                                   1<Y<  5
                                   2<Z<  2

TOP +Z MAGNESIUM
ENDOBJ

ENDSAT

       512 VOLUME CELLS NUMBERED BY NUMLTP.
CALLING GENMTL

  INSLST --    0 INSULATING SURFACE CELLS FOUND

 NO SURFACE CONDUCTIVITY

          2 ENTRIES IN REVISED VTXL

         NC DETERMINED BY CETNC TO BE  5
END GENMTL
```

BIGFINE code object definition output.

```
**********POTENT

 ASGFIL: FILE 17                ISTAT= 100000000000

MODELLING CELL   300 WITH     .0188 METER RESOLUTION.
                    TOP POTENTIAL =       .41 VOLTS.
 AT ITER     1 DRDOTR=  2.19+002
 AT ITER     2 DRDOTR=  7.99+001
 AT ITER     3 DRDOTR=  3.50+001
 AT ITER     4 DRDOTR=  1.69+001
 AT ITER     5 DRDOTR=  9.94+000
 AT ITER     6 DRDOTR=  5.14+000
 AT ITER     7 DRDOTR=  3.24+000
 AT ITER     8 DRDOTR=  2.27+000
 AT ITER     9 DRDOTR=  1.73+000

  SCG -- DRDOTR/DR1=   1.73+07/   2.19+02 IN   9 ITERATIONS.

  RMS ERROR =   8.5-01 AT ITER=   1
 AT ITER     1 DRDOTR=  8.79-001
 AT ITER     2 DRDOTR=  9.13-001
 AT ITER     3 DRDOTR=  9.50-001
 AT ITER     4 DRDOTR=  9.62-001
 AT ITER     5 DRDOTR=  6.54-001
 AT ITER     6 DRDOTR=  6.33-001
 AT ITER     7 DRDOTR=  3.00-001
 AT ITER     8 DRDOTR=  1.36-001
 AT ITER     9 DRDOTR=  7.73-002
 AT ITER    10 DRDOTR=  1.50-002
 AT ITER    11 DRDOTR=  1.39-002
 AT ITER    12 DRDOTR=  5.25-003

  SCG -- DRDOTR/DR1=   5.25-03/   8.79-01 IN  12 ITERATIONS.

  RMS ERROR =   2.4-01 AT ITER=   2
 AT ITER     1 DRDOTR=  2.57-003
 AT ITER     2 DRDOTR=  1.57-003
 AT ITER     3 DRDOTR=  1.13-003
 AT ITER     4 DRDOTR=  2.90-004
 AT ITER     5 DRDOTR=  1.67-004

  SCG -- DRDOTR/DR1=   1.67-04/   2.57-03 IN   5 ITERATIONS.

  RMS ERROR =   3.7-03 AT ITER=   3

**********CURPENT

***TIME LEFT =   342 SECONDS***

***TIME LEFT =   342 SECONDS***
```

BIGFINE code potential section output.

```
* * * * *  NASCAP-LEO FINE PARTICLE TRAJECTORY CODE * * * * *

 NEXTRA=     0

 EFPREP --     1 GRIDS OUT OF    1 READ IN.

 FREFIL: FILE 16                ISTAT= 000000000000

 PRMFIL: FILE 16                ISTAT= 000000000000
FNCURR FOUND AVG POT (POT1)=  2.00000+00  POT2=  4.09526-01  XMESH=  1.87500-02 FOR COARSE CELL    300
READQV FOUND      6 PARTICLES ON FILE     16  FOR CELL INDEX      1
FNCURR WROTE      0 TRAJECTORIES ON FILE      0

 NON-ZERO SURFACE CELL CURRENT CONTRIBUTIONS FROM PLASMA COLLECTION.   SUM OF CELL CURRENTS=   -7.082934-04 AMPS

 DFLUX( 258)=  -9.5820-07      DFLUX( 259)=  -9.5820-07      DFLUX( 260)=  -4.6167-06      DFLUX( 262)=  -9.5820-07
 DFLUX( 263)=  -1.4155-06      DFLUX( 264)=  -4.6167-06      DFLUX( 266)=  -4.7910-07      DFLUX( 267)=  -1.4373-06
 DFLUX( 268)=  -2.7875-06      DFLUX( 271)=  -1.9164-06      DFLUX( 272)=  -2.7875-06      DFLUX( 275)=  -1.9164-06
 DFLUX( 276)=  -2.7875-06      DFLUX( 279)=  -1.9164-06      DFLUX( 280)=  -2.7875-06      DFLUX( 283)=  -1.9164-06
 DFLUX( 284)=  -2.7875-06      DFLUX( 287)=  -2.3802-06      DFLUX( 288)=  -2.7875-06      DFLUX( 291)=  -1.9164-06
 DFLUX( 292)=  -2.7875-06      DFLUX( 295)=  -1.9164-06      DFLUX( 296)=  -2.7875-06      DFLUX( 299)=  -1.9164-06
 DFLUX( 300)=  -2.7875-06      DFLUX( 303)=  -1.9164-06      DFLUX( 304)=  -2.7875-06      DFLUX( 307)=  -1.9164-06
 DFLUX( 306)=  -2.7875-06      DFLUX( 310)=  -4.7910-07      DFLUX( 311)=  -1.4373-06      DFLUX( 312)=  -2.7875-06
 DFLUX( 314)=  -9.5820-07      DFLUX( 315)=  -9.5820-07      DFLUX( 316)=  -4.1595-06      DFLUX( 318)=  -1.4220-06
 DFLUX( 319)=  -9.5820-07      DFLUX( 320)=  -5.0740-06      DFLUX( 385)=  -1.8293-06      DFLUX( 388)=  -9.1465-07
 DFLUX( 389)=  -9.1464-07      DFLUX( 391)=  -1.8294-06      DFLUX( 392)=  -4.5727-07      DFLUX( 393)=  -4.5735-07
 DFLUX( 394)=  -4.5728-07      DFLUX( 395)=  -9.1462-07      DFLUX( 397)=  -4.6379-07      DFLUX( 398)=  -4.5727-07
 DFLUX( 399)=  -2.2866-06      DFLUX( 407)=  -1.8293-06      DFLUX( 411)=  -1.8293-06      DFLUX( 415)=  -1.8358-06
 DFLUX( 416)=  -4.6379-07      DFLUX( 419)=  -1.3848-06      DFLUX( 422)=  -4.6379-07      DFLUX( 423)=  -1.8293-06
```

BIGFINE code CURRENt section output.

```
 DFLUX( 427)=  -1.8293-06      DFLUX( 431)=  -1.3720-06      DFLUX( 435)=  -4.5727-07      DFLUX( 437)=  -9.1464-07
 DFLUX( 439)=  -1.8293-06      DFLUX( 440)=  -4.5727-07      DFLUX( 441)=  -1.8293-06      DFLUX( 442)=  -4.6379-07
 DFLUX( 443)=  -1.3721-06      DFLUX( 445)=  -2.2865-06      DFLUX( 447)=  -2.2865-06      DFLUX( 448)=  -1.3720-06
 DFLUX( 449)=  -9.2528-06      DFLUX( 450)=  -8.7867-06      DFLUX( 451)=  -7.3801-06      DFLUX( 452)=  -7.7938-06
 DFLUX( 453)=  -8.7956-06      DFLUX( 454)=  -9.7078-06      DFLUX( 455)=  -7.8591-06      DFLUX( 456)=  -8.2512-06
 DFLUX( 457)=  -1.0161-05      DFLUX( 458)=  -9.7078-06      DFLUX( 459)=  -9.7014-06      DFLUX( 460)=  -8.2511-06
 DFLUX( 461)=  -1.0625-05      DFLUX( 462)=  -1.0178-05      DFLUX( 463)=  -8.7521-06      DFLUX( 464)=  -8.7302-06
 DFLUX( 465)=  -1.0161-05      DFLUX( 466)=  -1.0657-05      DFLUX( 467)=  -8.2730-06      DFLUX( 468)=  -8.7302-06
 DFLUX( 469)=  -9.7037-06      DFLUX( 470)=  -1.0172-05      DFLUX( 471)=  -9.2093-06      DFLUX( 472)=  -8.7367-06
 DFLUX( 473)=  -9.7037-06      DFLUX( 474)=  -1.0635-05      DFLUX( 475)=  -9.2093-06      DFLUX( 476)=  -8.7520-06
 DFLUX( 477)=  -9.7037-06      DFLUX( 478)=  -1.0172-05      DFLUX( 479)=  -9.2093-06      DFLUX( 480)=  -8.2729-06
 DFLUX( 481)=  -9.7037-06      DFLUX( 482)=  -1.0635-05      DFLUX( 483)=  -9.2093-06      DFLUX( 484)=  -8.2729-06
 DFLUX( 485)=  -9.7037-06      DFLUX( 486)=  -1.0172-05      DFLUX( 487)=  -9.2093-06      DFLUX( 488)=  -8.7520-06
 DFLUX( 489)=  -9.7037-06      DFLUX( 490)=  -1.0172-05      DFLUX( 491)=  -9.2093-06      DFLUX( 492)=  -8.2729-06
 DFLUX( 493)=  -1.0161-05      DFLUX( 494)=  -1.0193-05      DFLUX( 495)=  -8.7368-06      DFLUX( 496)=  -8.7302-06
 DFLUX( 497)=  -1.0161-05      DFLUX( 498)=  -9.2505-06      DFLUX( 499)=  -8.2947-06      DFLUX( 500)=  -9.1875-06
 DFLUX( 501)=  -9.7038-06      DFLUX( 502)=  -1.0172-05      DFLUX( 503)=  -6.9228-06      DFLUX( 504)=  -7.7938-06
 DFLUX( 505)=  -8.7890-06      DFLUX( 506)=  -1.0172-05      DFLUX( 507)=  -9.7100-06      DFLUX( 508)=  -7.8003-06
 DFLUX( 509)=  -7.8745-06      DFLUX( 510)=  -1.0172-05      DFLUX( 511)=  -7.3737-06      DFLUX( 512)=  -7.7938-06

 ASGFIL: FILE 10               ISTAT= 100000000000
SHARE WROTE    4913 ELEMENTS TO FILE  10  # OF NON-ZERO FLUXES =     528
CONDUCTOR     POTENTIAL (VOLTS)     CURRENT (AMPS)     POWER (WATTS)

      1          2.000000+00          0.000000          0.000000
      2          2.000000+00         -8.396384-05      -1.679277-04
      3         -3.000000+00          0.000000          0.000000
      4          2.000000+00         -3.708798-05      -7.417596-05
      5          7.000000+00         -5.872416-04      -4.110691-03
      6          6.000000+00          0.000000          0.000000
      7          7.000000+00          0.000000          0.000000

TOTAL CURRENT TO CELLS =  -7.082934-04 AMPS   TOTAL POWER DISSIPATED BY ALL CELLS =  -4.352795-03 WATTS

 AVERAGE COLLECTION POTENTIAL VPAR =  6.14547+00 VOLTS

SUMMARY OF PARTICLE TRACKING RESULTS

CURRENT TO OBJECT   =  -7.083-04 AMPS
CURRENT ESCAPING    =   0.000    AMPS
CURRENT UNNASSIGNED =   0.000    AMPS
CURRENT INCOMPLETE  =  -1.379-06 AMPS


TOTAL CURRENT = -7.09669-04 AMPS

***WARNING***  NRING =      3  NRESC=      0

***TIME LEFT =   707 SECONDS***

**********END
```

BIGFINE code CURRENt section output (concluded).

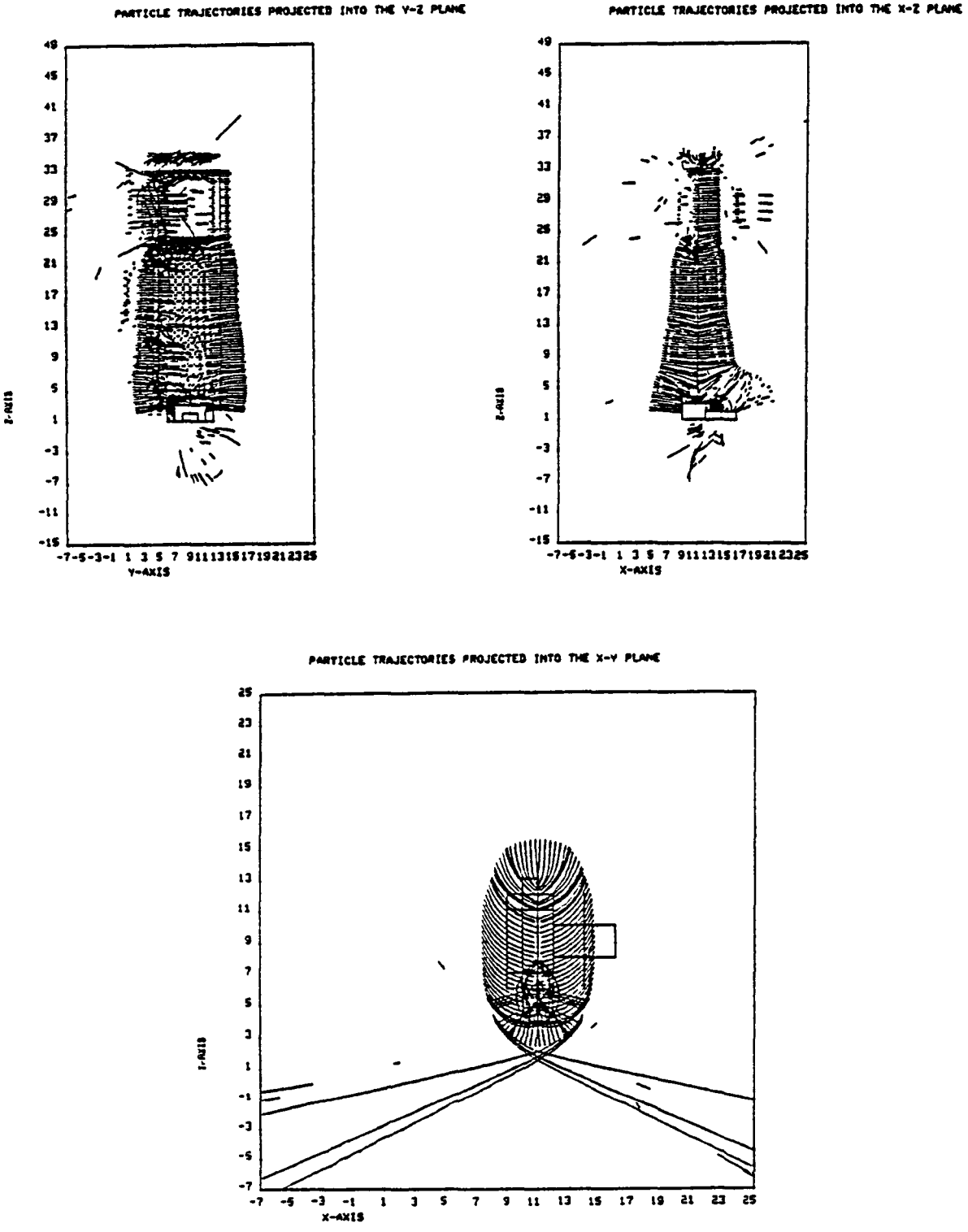

Sheath illustrations produced by BIGLEO sample run.

APPENDIX A

NASCAP BIBLIOGRAPHY

We provide here a list of publications referencing the NASCAP and NASCAP/LEO computer codes. For the reader's convenience, we have separated the major S-CUBED reports (which collectively provide thorough NASCAP documentation) from articles published in technical journals and conference proceedings. Numerous monthly, topical, and interim reports and technical memoranda from S-CUBED and NASA/Lewis Research Center have been intentionally omitted. The authors' apologize for any other omissions or inaccuracies.

S-CUBED Reports

Katz, I., D. E. Parks, M. J. Mandell, J. M. Harvey, D. H. Brownell, S. S. Wang and M. Rotenberg, "A Three Dimensional Dynamic Study of Electrostatic Charging in Materials," NASA CR-135256, August 1977.

Mandell, M. J., J. M. Harvey and I. Katz, "NASCAP User's Manual," NASA CR-135259, August 1977.

Cassidy, J. J., "NASCAP User's Manual - 1978," NASA CR-159417, August 1978.

Katz, I., J. J. Cassidy, M. J. Mandell, G. W. Schnuelle, P. G. Steen, D. E. Parks, M. Rotenberg and J. H. Alexander, "Extension, Validation and Application of the NASCAP Code," NASA CR-159595, January 1979.

Stannard, P. R., I. Katz, M. J. Mandell, J. J. Cassidy, D. E. Parks, M. Rotenberg and P. G. Steen, "Analysis of the Charging of the SCATHA (P78-2) Satellite," NASA CR-165348, December 1980.

Katz, I., J. J. Cassidy, M. J. Mandell, D. E. Parks, G. W. Schnuelle, P. R. Stannard and P. G. Steen, "Additional Application of the NASCAP Code, Volume I: NASCAP Extension," NASA CR-165349, February 1981.

Katz, I., J. J. Cassidy, M. J. Mandell, D. E. Parks, G. W. Schnuelle, P. R. Stannard and P. G. Steen, "Additional Application of the NASCAP Code, Volume II: SEPS, Ion Thruster Neutralization and Electrostatic Antenna Model," NASA CR-165350, February 1981.

Mandell, M. J., I. Katz and P. R. Stannard, "Additional Extensions to the NASCAP Computer Code, Volume I," NASA CR-167855, October 1981.

Stannard, P. R., I. Katz and M. J. Mandell, "Additional Extensions to the NASCAP Computer Code, Volume II," NASA CR-167856, February 1982.

Mandell, M. J. and D. L. Cooke, "Additional Extensions to the NASCAP Computer Code, Volume III," NASA CR-167857, August 1981.

Published Papers

Katz, I., D. E. Parks, M. J. Mandell, J. M. Harvey, D. H. Brownell, S. S. Wang and M. Rotenberg, "A Three Dimensional Dynamic Study of Electrostatic Charging in Materials," NASA CR-135256, August 1977.

Mandell, M. J., I. Katz, G. W. Schnuelle and P. G. Steen, "The Decrease in Effective Photocurrents Due to Saddle Points in Electrostatic Potentials Near Differentially Charged Spacecraft," IEEE Transactions on Nuclear Science, NS-25, p. 1313, 1978.

Katz, I., J. J. Cassidy, M. J. Mandell, G. W. Schnuelle, P. G. Steen and J. C. Roche, "The Capabilities of the NASA Charging Analyzer Program," Spacecraft Charging Technology-1978, NASA CP-2071, AFGL-TR-79-0082, p. 101, 1979.

Mandell, M. J., I. Katz and G. W. Schnuelle, "Photoelectron Charge Density and Transport Near Differentially Charged Spacecraft," IEEE Transactions on Nuclear Science, NS-26, p. 5107, 1979.

O'Donnell, E. E., "Spacecraft Charging Modeling Development and Validation Study," Spacecraft Charging Technology-1978, p. 797, 1979.

Roche, J. C. and C. K. Purvis, "Comparison of NASCAP Predictions with Experimental Data," Spacecraft Charging Technology-1978, NASA CP-2071, AFGL-TR-79-0082, p. 144, 1979.

Schnuelle, G. W., D. E. Parks, I. Katz, M. J. Mandell, P. G. Steen, J. J. Cassidy and A. G. Rubin, "Charging Analysis of the SCATHA Satellite," Spacecraft Charging Technology-1978, NASA CP-2071, AFGL-TR-79-0082, p. 123, 1979.

Stevens, N. J. and J. C. Roche, "NASCAP Modeling of Environmental-Charging-Induced Discharges in Satellites," IEEE Transactions on Nuclear Science, NS-26, p. 5112, 1979.

Mandell, M. J., I. Katz and G. W. Schnuelle, "The Effect of Solar Array Voltage Patterns on Plasma Power Losses," IEEE Transactions on Nuclear Science, NS-27, p. 1797, 1980.

Olsen, R. C., "Differential and Active Charging Results from the ATS Spacecraft." University of California (San Diego) Ph.D. Dissertation, 1980.

Purvis, C. K., "Configuration Effects on Satellite Charging Response," AIAA Paper No. 80-0040, 1980.

Rubin, A. G., I. Katz, M. J. Mandell, G. W. Schnuelle, P. G. Steen, D. E. Parks and J. J. Cassidy, "A Three-Dimensional Spacecraft Charging Computer Code," H. B. Garrett and C. P. Pike, editors, Space Systems and Their Interaction with Earth's Space Environment, New York, AIAA, 1980.

Stevens, N. J., "Modeling of Environmentally Induced Discharges in Geosynchronous Satellites," IEEE Transactions on Nuclear Science, NS-27, p. 1792, 1980.

Katz, I., M. J. Mandell, G. W. Schnuelle, D. E. Parks and P. G. Steen, "Plasma Collection by High-Voltage Spacecraft in Low Earth Orbit," Journal of Spacecraft and Rockets, 18, p. 79, 1981.

Mandell, M. J., I. Katz and D. E. Parks, "NASCAP Simulation of Laboratory Spacecraft Charging Tests Using Multiple Electron Guns," IEEE Transactions on Nuclear Science, NS-28, p. 4568, 1981.

Newell, D. M. and W. E. Waters, "Spacecraft Charge Protection of Large 3-Axis Stabilized Communications Satellites-INTELSAT V," IEEE Transactions on Nuclear Science, NS-28, p. 4505, 1981.

Olsen, R. C., C. E. McIlwain and E. C. Whipple, Jr., "Observations of Differential Charging Effects on ATS-6," Journal of Geophysical Research, 86, p. 6809, 1981.

Olsen, R. C., "Modification of Spacecraft Potentials by Thermal Electron Emission on ATS-5," Journal of Spacecraft and Rockets, 18, p. 527, 1981.

Purvis, C. K. and J. V. Staskus, "SSPM Charging Response: Comparison of Ground Test and Flight Data to NASCAP Predictions for Eclipse Conditions," Spacecraft Charging Technology-1980, NASA CP-2182, p. 592, 1981.

Rubin, A. G., H. A. Cohen, D. A. Hardy, M. F. Tautz and N. A. Saflekos, "Computer Simulation of Spacecraft Charging on SCATHA," Spacecraft Charging Technology-1980, NASA CP-2182, p. 632, 1981.

Saflekos, N. A., M. F. Tautz, A. G. Rubin, D. A. Hardy and P. M. Mizera, "Three Dimensional Analysis of Charging Events on Days 87, and 114, 1979 from SCATHA," Spacecraft Charging Technology-1980, NASA CP-2182, p. 608, 1981.

Sanders, N. L. and G. T. Inouye, "NASCAP Charging Calculations for a Synchronous Orbit Satellite," Spacecraft Charging Technology-1980, NASA CP-2182, p. 684, 1981.

Schnuelle, G. W., P. R. Stannard, I. Katz and M. J. Mandell, "Simulation of the Charging Response of the SCATHA (P78-2) Satellite," Spacecraft Charging Technology-1980, NASA CP-2182, p. 580, 1981.

Stang, D. B. and C. K. Purvis, "Comparison of NASCAP Modeling Results With Lumped-Circuit Analysis," Spacecraft Charging Technology-1980, NASA CP-2182, p. 665, 1981.

Stannard, P. R., I. Katz and D. E. Parks, "Bootstrap Charging of Surfaces Composed of Multiple Materials," IEEE Transactions on Nuclear Science, NS-28, p. 4563, 1981.

Stannard, P. R., G. W. Schnuelle, I. Katz and M. J. Mandell, "Representation and Material Charging Response of GEO Plasma Environments," Spacecraft Charging Technology-1980, NASA CP-2182, p. 560, 1981.

Staskus, J. V. and J. C. Roche, "Testing of a Spacecraft Model in a Combined Environment Simulator," IEEE Transactions on Nuclear Science, NS-28, p. 4509, 1981.

Stevens, N. J., "Use of Charging Control Guidelines for Geosynchronous Satellite Design Studies," Spacecraft Charging Technology-1980, NASA CP-2182, p. 789, 1981.

Stevens, N. J., "Review of Biased Solar Array-Plasma Interaction Studies," AIAA Paper No. 81-0738, 1981.

Stevens, N. J., H. E. Mills and L. Orange, "Voltage Gradients in Solar Array Cavities as Possible Breakdown Sites in Spacecraft-Charging Induced Discharges," IEEE Transactions on Nuclear Science, NS-28, p. 4558, 1981.

Stannard, P. R., I. Katz, L. Gedeon, J. C. Roche, A. G. Rubin and M. F. Tautz, "Validation of the NASCAP Model Using Spaceflight Data," AIAA 82-0269, 1982.

APPENDIX B

NASCAP SIMULATION OF LABORATORY SPACECRAFT CHARGING TESTS USING MULTIPLE ELECTRON GUNS

M. J. Mandell, I. Katz and D. E. Parks

IEEE Transactions on Nuclear Science, NS-28, p. 4568, 1981.

NASCAP SIMULATION OF LABORATORY SPACECRAFT CHARGING TESTS USING MULTIPLE ELECTRON GUNS*

M. J. Mandell, I. Katz, D. E. Parks
Systems, Science and Software
La Jolla, CA 92038

Summary

NASCAP calculations have been performed simulating exposure of a spacecraft-like model to multiple electron guns. The results agree well with experiment. It is found that magnetic field effects are fairly small, but substantial differential charging can result from electron gun placement. Conditions for surface flashover are readily achieved.

There is a great current interest in multibeam electron irradiation of spacecraft-like objects (or actual spacecraft) for spacecraft charging/SGEMP studies. Experiments at NASA/Lewis Research Center[1] have shown that, under appropriate conditions, charging and discharging behavior akin to that believed to occur in space can be simulated. A far more powerful simulation capability is planned for inclusion in the proposed Satellite X-Ray Test Facility (SXTF).[2,3] A recent addition to the NASCAP[4] code is the ability to numerically simulate such experiments. The calculations we present here are in good agreement with the Lewis results. They illustrate that angular effects are extremely important and can lead to potential configurations on a satellite very different from what would be expected in space. Magnetic field effects are noticeable but, at least for an experiment of this size, relatively minor. The effect of potential barriers can also be seen in this type of experiment.

The first series of calculations involved a simplified version of the Lewis experiment. The geometry is shown in Figure 1. The test object is an octagonal cylinder uniformly covered with 0.005 inch kapton. The code resolution was 0.1 m. Thus any nonuniformity of charging is atrributable to the experiment rather than to any "real" effects to be expected in space.

Under floating conditions and irradiation by four 10 keV beams, the potential develops in time as shown in Figure 2. The object initially (∿1 sec) develops a uniform potential of ∿-7200 V. As time proceeds, the surface irradiated by obliquely incident electrons charge positive relative to normally irradiated surfaces due to increased backscatter and secondary electron emission.[5,6] After six minutes the object develops over 2 kV of differential charging. Figure 3 shows the asymmetry caused by a 0.7 gauss magnetic field in the 0 1 $\bar{1}$ direction. The electrons incident on the 0 1 1 face are deflected downward (toward -x). Thus the surfaces below the belly are hit more obliquely than those above, causing the observed asymmetry. The maximum differential charging was slightly higher with the magnetic field on.

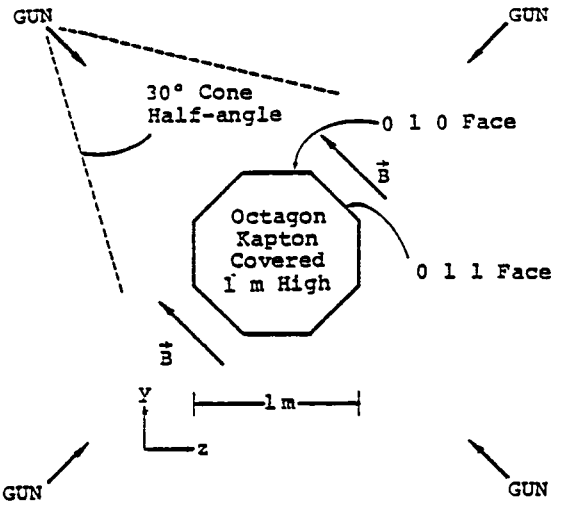

Figure 1. Geometry for simplified model of NASA/Lewis Research Center multigun irradiation experiment.

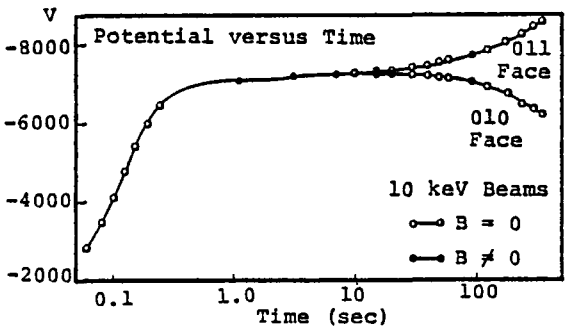

Figure 2. Potential versus time for irradiation of kapton covered cylinder by four 10 keV electron beams.

Figure 4 shows the potential contours at belly level after ten minutes of irradiation by four 6 keV beams. The surface potentials in this plane range from -5.0 to -2.8 kV, and there is electric field sign reversal in front of the relatively positive surfaces. An object charged in this manner will exhibit strong SGEMP enhancement with a high probability of synergistic surface flashover, as avalanching secondary electrons will be drawn back to the emitting surface. However, it is unlikely that a simple object such as this would charge to such a state in the relatively isotropic environment of space.

Further calculations were performed with an object more nearly representative of the

*This work supported by NASA/Lewis Research Center, Cleveland OH under Contract NAS3-22536 and Defense Nuclear Agency, Washington, D. C. under Contract DNA 001-79-C-0079.

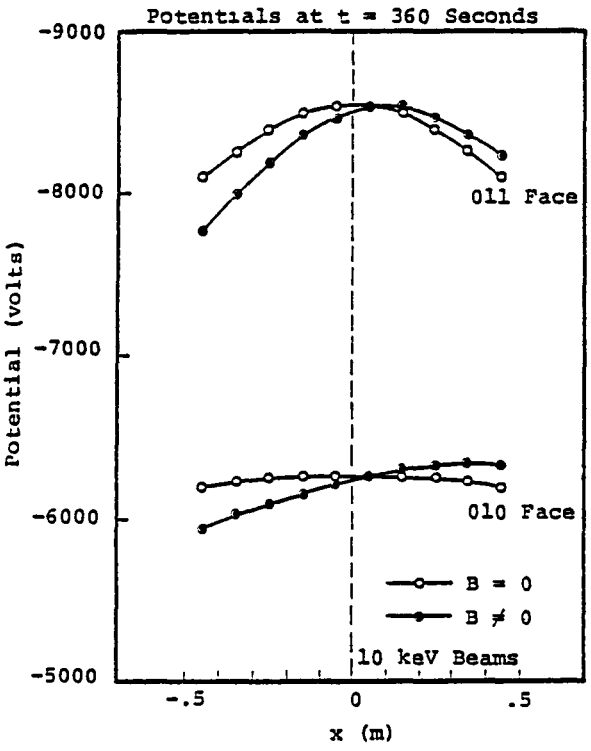

Figure 3. Potential (after six minute exposure) along two lines parallel to the cylinder axis, with and without magnetic field.

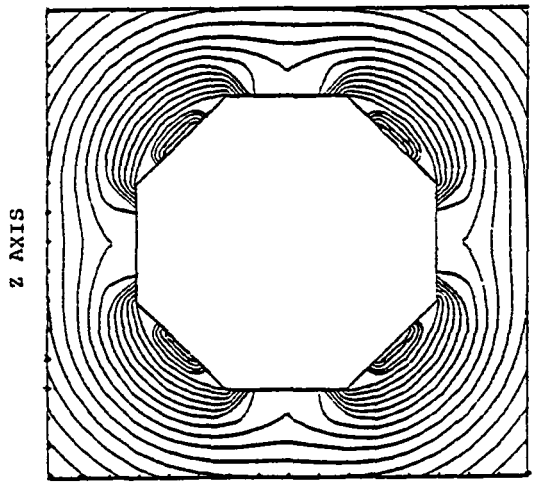

Figure 4. Potential contours at belly level after 10 minute irradiation by four 6 keV electron guns, illustrating achievement of electric field reversal. Minimum potential is -4996 volts; maximum potential is -1149 volts; contour interval is 200 volts.

actual Lewis experiments. The object (Figure 5) was an octagonal cylinder with its axis in the y direction. The circumferential surface was mainly SiO_2 with an aluminum bellyband. Two teflon patches were on the bellyband, and an indium oxide patch was placed near the lower rim. Properties for teflon and SiO_2 were those recommended by Purvis.[7] The gun locations were analogous to those shown in Figure 1, but 0.3 m above the midplane of the object. The gun half-angle was narrowed to 15 degrees, and the incident current at the object surface approximated 10^{-5} A/m^2. The code resolution was 0.114 m, and a zero magnetic field was used.

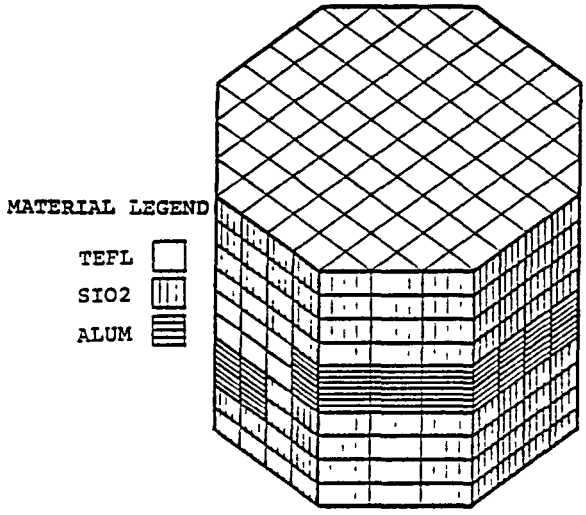

Figure 5. Spacecraft model indicating surface materials.

We first performed a simulation of four 6 keV guns irradiating a grounded, stationary spacecraft. For this case, the experiment indicated periodic potentials on the SiO_2 (similar to the potentials of Figure 4) ranging from -1 kV to -4 kV. The calculation predicted (∿15 cm above the bellyband) similar potentials ranging from -0.8 kV to -3.4 kV. Next, the case of a rotating spacecraft was simulated by using eight uniformly spaced electron guns, such that all eight faces of the octagon were hit by a similar angular mix of electrons. The experiment measured a potential varying rapidly from -1 to -4 kV on the scale of the coverslip dimension. The calculation, which did not resolve the gaps between the coverslips, predicted potentials ranging from -1.8 kV to -2.0 kV. The experiment and theory both indicated no long-period potential variations on the SiO_2. In the stationary case, the calculation predicted substantial areas of field-reversed SiO_2, and discharges were observed in the experiment. For the rotating case, no field reversal was predicted, and no discharges observed.

Finally, we calculated the charging of the model spacecraft under floating conditions exposed to four bi-energy guns. The gun energies were set to 10 keV and 20 keV, each beam having intensity $\sim 10^{-5}$ A/m^2 at the uncharged surface. The potential versus time is shown in Figure 6. For this case, the high secondary emission and backscatter coefficients for obliquely incident electrons stopped the rapid charging process at about -7.6 kV. (With the 10 keV beams alone, the potential reached -6 kV.) (Recall that the kapton cylinder, despite low secondary and backscatter coefficients, charged only to -7.2 kV in four 10 keV beams.) At this potential the incident flux from the low energy beams is about 40 percent of the flux from the high energy beams. For those surfaces which continue to charge negatively, the low energy beam is attenuated further. After nine minutes, surface potentials range from -5.3 to -9.1 kV, and about 20 percent of the surface is in a field-reversal condition. As the metallic substrate continues to charge negatively, the amount of field-reversed surface increases. The "bootstrap effect"[8] eventually causes the entire spacecraft to drop below -10 kV, repelling completely the lower energy beam. After about a half hour, equilibrium is reached at about -17 kV.

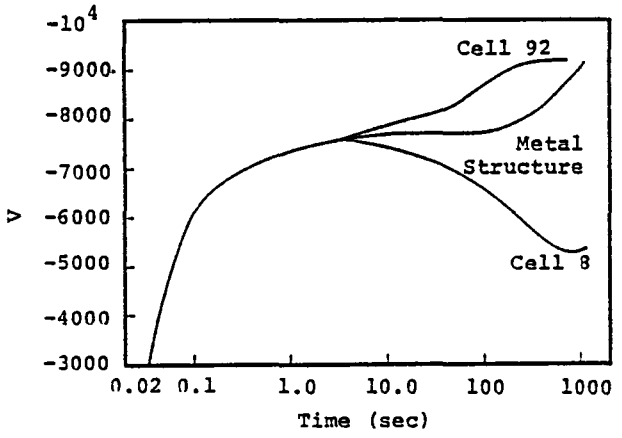

Figure 6. Potential versus time for spacecraft model irradiated by four bi-energy (10 and 20 keV) electron guns. Cell 92 is a teflon cell on the bellyband with $\bar{1}$ 0 1 surface normal. Cell 8 is an SiO_2 cell with $\bar{1}$ 0 0 normal near the aft (bottom) end.

We conclude that great care must be taken in design and interpretation of satellite irradiation experiments. Several electron beams in a vacuum tank need not provide a good three-dimensional simulation of a hot plasma. The calculations presented here agree well with recent laboratory experiments[4] that showed several thousand volts of differential charging due to electron beam placement. Our calculations have also shown that the field reversal conditions necessary for surface flashover may be caused by these asymmetries. This is in contrast to previously observed and calculated results for the irradiation of planar samples. Although this type of asymmetry is not expected in space, similar field reversal conditions can occur due to material differences[8] or associated with artificial charging.[9] Analysis of SCATHA data shows several occurrences of field-reversal effects.[10] Since the recent three-dimensional laboratory experiments exhibited discharges similar to those observed in space, this flashover mechanism may be responsible for arcing observed on spacecraft.

References

1. Staskus, J. V. and J. C. Roche, "Testing of a Spacecraft Model in a Combined Environment Simulator," 1981 IEEE-NSRE Conference, Paper I-3.

2. Flanagan, T. M., M. J. Treadaway and R. Denson, "Strawman Plasma Environment Simulation Requirements for SXTF," JAYCOR Report 200-80-223/2066 (1980).

3. Halverson, W. D., "Engineering Assessment of the SXTF Spacecraft Charging Capability," SPIRE Report (1980).

4. Katz, I., J. J. Cassidy, M. J. Mandell, G. W. Schnuelle and P. G. Steen, "The Capabilities of the NASA Charging Analyzer Program," presented at USAF/NASA Spacecraft Charging Technology Conference (1978).

5. Katz, I., D. E. Parks, M. J. Mandell, J. M. Harvey, D. H. Brownell, Jr., S. S. Wang and M. Rotenberg, "A Three Dimensional Dynamic Study of Electrostatic Charging in Materials," NASA CR-135256, August 1977.

6. Salehi, M. and E. A. Flinn, "Dependence of Secondary-Electron Emission from Amorphous Materials on Primary Angle of Incidence," J. Appl. Phys. 52, 994 (1981).

7. Purvis, C. K. and J. V. Staskus, "SCATHA SSPM Charging Response: NASCAP Predictions Compared to Data," Spacecraft Charging Technology, 1980, NASA CP-2182 (1981).

8. Stannard, P. R. and I. Katz, "Bootstrap" Charging of Surfaces Composed of Multiple Materials," 1981 IEEE-NSRE Conference, Paper I-12.

9. Katz, I. and M. J. Mandell, to be published.

10. Stannard, P. R., to be published.

APPENDIX C

"BOOTSTRAP" CHARGING OF SURFACES COMPOSED OF MULTIPLE MATERIALS

P. R. Stannard, I. Katz and D. E. Parks

IEEE Transactions on Nuclear Science, NS-28, p. 4563, 1981.

"BOOTSTRAP" CHARGING OF SURFACES COMPOSED OF MULTIPLE MATERIALS*

P. R. Stannard, I. Katz and D. E. Parks
Systems, Science and Software
P. O. Box 1620, La Jolla, CA 92038

Abstract

We examine the charging of a checkerboard array of two materials, only one of which tends to acquire a negative potential alone, using the NASA Charging Analyzer Program (NASCAP). The influence of the charging material's field causes the otherwise "non-charging" material to acquire a negative potential due to the suppression of its secondary emission ("bootstrap" charging). The NASCAP predictions for the equilibrium potential difference between the two materials are compared to results based on an analytical model.

Introduction

In the presence of a plasma, exposed surfaces of both insulators and conductors collect a current of incident charged particles and may acquire an electrostatic potential. The tendency to charge in this way is different for different materials since the net current collected depends on the nature of the surface as well as the plasma parameters. While the latter determine the magnitude of the primary incident electron and ion currents, i_e and i_{ion}, processes such as secondary electron emission, backscatter and (in the presence of sunlight) photoemission also make a contribution to the net current:

$$i_{net} = i_{ion} - i_e + i_e(\delta+\eta) - i_{ion}\,\delta_{ion} + i_p.$$

In this equation δ and δ_{ion} are the secondary electron emission yields for electron and ion impact at the material surface respectively, η is the electron backscatter yield and i_p the photocurrent emitted.

The values of the yields for these processes depend strongly on the nature of the surface material.[1] Satellites orbiting at high altitude are bathed in plasmas with temperatures in the kilovolt range and densities on the order of 10^6 m^{-3}. The many different materials that comprise the surface of a satellite may respond differently to this environment, leading to the buildup of substantial (~several kV) differential potentials between neighboring surfaces, and even damaging discharges.

As a result of both experimental observation and numerical modeling of spacecraft charging it has become evident that the charging behavior of an exposed surface depends on the response of its neighbors as well as just its own properties.[2,3] In this study we investigate this phenomenon and examine the charging response of a slab composed of a checkerboard-like arrangement of two materials (Figure 1), and compare it to the response of each material alone.

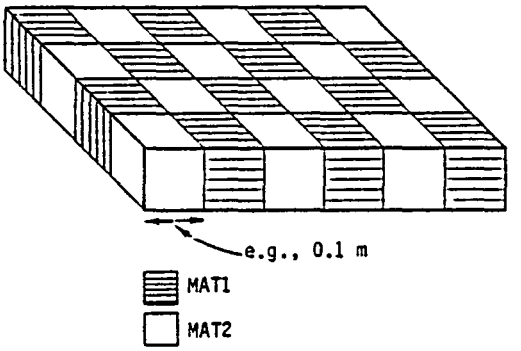

Figure 1. Checkerboard slab of two different materials, MAT1 and MAT2.

"Charging" and "Non-charging" Materials

For a given plasma environment, similar to those encountered at high earth orbit, a pure sample of a material will either acquire a significant potential negative with respect to the plasma, or remain essentially neutral. Large positive potentials can never be achieved by natural charging (i.e., in the absence of electron emitters or other outside biases). To understand this consider how a surface reaches its equilibrium potential. For a neutral plasma the incident electron current is much greater than the ion current due to the mass difference between the two species. Hence there is a net flow of negative charge to the material and the surface begins to acquire a negative potential. The incident current is opposed by the secondary electron current and photocurrent emitted from the surface. The surface will continue to charge negatively until its potential retards the incident current sufficiently to exactly balance the emitted current giving a net flow of zero. This balance point is the equilibrium surface potential ϕ. Values of ϕ may be many kilovolts negative, or just a few volts positive according to the magnitude of the secondary emission yield for the material, and the intensity of illumination. If the emitted current initially exceeds the incident flow of negative charge the material will tend to acquire a positive potential. However, because the energy of the emitted secondary and photoelectrons is only a few electron volts, once the potential reaches a positive value of similar magnitude the emitted current is unable to escape and charging stops. Thus all materials tend to stay within 2 or 3 volts from neutral in the presence of strong sunlight, where photoemission dominates. In eclipse on the other hand, for a given set of plasma parameters, materials either charge rapidly to significant negative potentials or remain close to neutral according to their secondary emission yields. Those materials that do acquire a negative potential are designated as "charging" materials and those that remain neutral are called "non-charging". Obviously this partition depends completely on the choice of plasma environment.

*This work supported by NASA/Lewis Research Center, Cleveland, OH, under Contract NAS3-22536, and U. S. Air Force Geophysics Laboratory, Hanscom Air Force Base, MA.

Simulation of Charging of a Checkerboard Array

To investigate the effect of neighboring materials on charging, the response of the object shown in Figure 1 to a 5 keV, 10^6 m^{-3} electron/proton plasma was simulated using the NASA Charging Analyzer Program (NASCAP). NASCAP is a highly sophisticated three-dimensional spacecraft charging code, capable of detailed representation of both objects and environments. A full description of its capabilities has been given elsewhere.[4] The NASCAP model assumes that both dielectric materials are present as thin films covering the same floating conductor. Bulk conductivity between the exposed surface and the conductor is taken into account by the code, but its magnitude is small compared to current collection from the plasma.

Three materials were chosen for study; kapton, teflon and solar cell coverglass ("solar"). The latter is a silicon dioxide glass with a MgF_2 reflective coating. Of these materials only kapton charged in the environment chosen. The thicknesses and other material properties of these dielectrics covering the underlying conductor were chosen to correspond to the values used on the SCATHA (P78-2) satellite.[2] In all but the last case the material patches were 0.1 m x 0.1 m. The computational grid was 3.5 m x 3.5 m in the plane of the slab and extended 7 m in the remaining (z) direction.

Four cases are discussed.

1. Both materials kapton, i.e., a pure kapton slab.
2. The first material kapton and the second "solar".
3. The first material kapton and the second teflon.
4. An expanded checkerboard model with 0.4 m x 0.4 m patches of kapton and solar.

In the first case the slab quickly (4 secs) charged to an equilibrium potential of -3.67 kV for both the surface and the underlying conductor. In both of the remaining two cases the kapton surfaces began to charge negatively, but on a much longer timescale (100 secs). The "non-charging" surfaces also began to charge, lagging behind the kapton until the equilibrium was reached. At equilibrium kapton again had a potential of -3.67 kV but the underlying conductor and the remaining surfaces reached a smaller potential. This is shown in Figure 2 for kapton and solar. Kapton and teflon behaved very similarly. To understand these results we must examine the local electric fields above the surface.

"Bootstrap" Charging

The charging of the otherwise "non-charging" teflon and solar in the presence of the strongly charging kapton is due to the suppression of secondary emission by the electric field above the surface. The potential contours across the surface as the kapton charges are shown schematically in Figure 3. The negative potential on the kapton patch influences the potential in front of the "non-charging" patch causing a barrier or saddle point to form. Once the height of this barrier exceeds the energy of the secondary electrons (2 or 3 volts) they can no longer escape. The equilibrium potential for the "non-charging" material is hence shifted from approximately zero to a much more negative potential and it too may begin to charge.

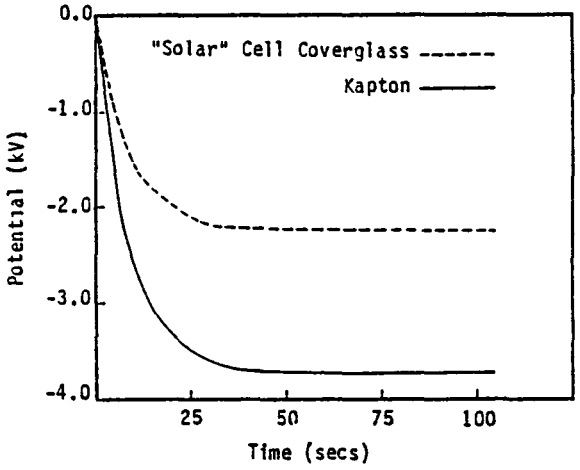

Figure 2. Charging of kapton/solar cell coverglass, checkerboard array.

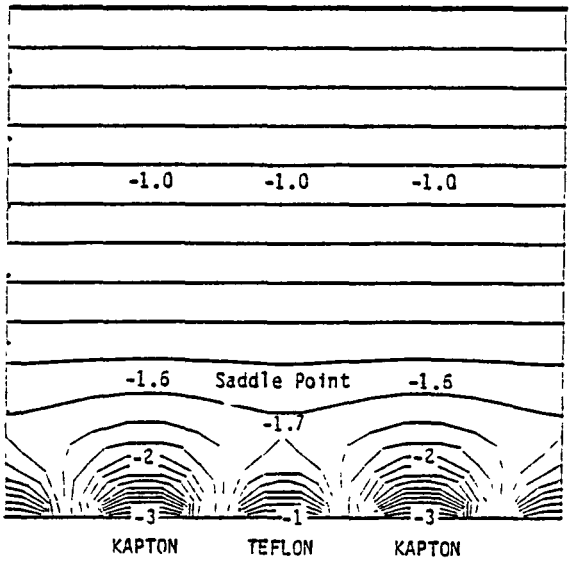

Figure 3. Potential contours above the checkerboard surface with kapton fixed at -3 kV and teflon at -1 kV.

While in the absence of secondary emission both teflon and solar would charge to potentials much more negative than -3.67 kV, their potentials must lag behind that of the kapton for their secondary emission to remain suppressed. The extent to which their potential lags is determined mainly by the geometrical relationship between the kapton surface potential and the potential felt just above the "non-charging" surfaces. The properties of the non-charging surface can, in principle, play a role however. Since backscattered electrons have an energy similar to those incident they are not fully suppressed by the potential barrier and their yield is different for each material. In addition, the proportion of the secondary electrons that escape depends on the overlap of the emission spectrum and the local retarding potential. While this proportion is close to zero, some secondaries do escape and this too may influence the final potential of the "non-charging" surfaces.

The fact that the final potentials of the teflon and solar coverglass are almost identical (Table 1) shows that in this case the geometrical effects dominate and both materials still have a strong tendency to charge as negatively as the kapton will let them; i.e., their potentials are fixed essentially by the potential from the kapton felt immediately above their surfaces. One could imagine a case perhaps where the "non-charging" material could only charge to say -1 kV even with its secondary emission suppressed. Such a material would charge no more than this value regardless of how much the kapton charged. In this case the potential lag would be determined entirely by material properties.

When an otherwise "non-charging" material is made to charge by its proximity to other charging surfaces, these surfaces are said to "bootstrap" the "non-charging" material up towards their potential. This phenomenon is very similar in nature to the charging of sunlit surfaces, under the influence of fields from neighboring surfaces charging in eclipse. As explained by Mandell et al.[5] a potential barrier due to the negatively charged shadowed surfaces prevents the escape of photoelectrons from nearby sunlit surfaces and they too begin to acquire negative potentials.

Table 1. NASCAP Equilibrium Potentials of a Checkerboard Slab Exposed to a 5 keV 10^6 m^{-3} Maxwellian Plasma

"Charging" Material (kV)		"Non-Charging" Material (kV)	
Kapton	-3.7	Solar	-2.2
Kapton	-3.7	Teflon	-2.2
Kapton*	-3.7	Solar*	-2.9

*Expanded model of a checkerboard with 0.4 m x 0.4 m patches. The first two results refer to 0.1 m x 0.1 m patches.

Estimation of Differential Potentials

For a regular checkerboard array the difference in potential between two materials charging free from material property limitations can be estimated analytically. In Figure 4 the shaded patches are charged to a potential V_0 more negative than the blank patches. This difference in potential is periodic across the surface in the x and y directions and we may separate contributions to the overall potential of the slab into a periodic component oscillating between $+V_0/2$, and an underlying mean potential $\bar{V}$. If V_c is the potential of the "charging" patches (kapton) the mean potential $\bar{V}$ is given by:

$$|\bar{V}| = |V_c| - V_0/2$$

The periodic component is separable in the x, y and z directions. Solving Laplace's equation subject to zero-potential boundary conditions gives the following solution for the potential V.

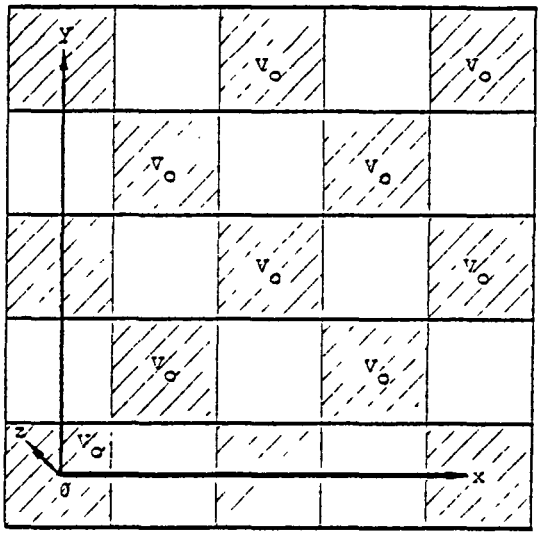

Figure 4. Analytical model for potentials above the checkerboard (x,y) plane.

$$V(x,y,z) = \frac{V_0}{2} + \frac{8V_0}{\pi^2} \sum_{n,m=0}^{\infty} \frac{(-1)^{n+m}}{(2n+1)(2m+1)} \cdot \cos\left(\frac{(2n+1)2\pi x}{L}\right) \cdot \cos\left(\frac{(2m+1)2\pi y}{L}\right) e^{-\frac{2\pi z[(2n+1)^2 + (2m+1)^2]^{1/2}}{L}} \quad (1)$$

where L is the period length on the surface. The field in the z direction at the surface due to this periodic potential is given by $-(dV/dz)_{z=0}$.

$$\frac{dV}{dz} = E_z = \frac{16V_0}{\pi L} \sum_{m,n=0}^{\infty} \frac{(-1)^{n+m}[(2n+1)^2 + (2m+1)^2]^{1/2}}{(2n+1)(2m+1)} \cdot \cos\left(\frac{(2n+1)2\pi x}{L}\right) \cos\left(\frac{(2m+1)2\pi y}{L}\right) e^{-\frac{2\pi z[(2n+1)^2 + (2m+1)^2]^{1/2}}{L}} \quad (2)$$

Equilibrium is achieved in front of the blank patches when the sum of the z field due to $\bar{V}$ and the z field due to the periodic potential is zero. We may estimate the former quantity from the field calculated by NASCAP in front of the slab uniformly charged to -3.7 kV. For the 0.1 m x 0.1 m patch model this is calculated to be -8900 V m^{-1}. This field is proportional to the surface potential thus the field $\bar{E}$ at $\bar{V}$ is given by:

$$\bar{E} = -(3700 - V_o/2)\,\frac{8900}{3700}$$

The field E_z^o due to the periodic potential is given by summing the convergent series in Eq. (2).

$$E_z^o = \frac{16\ V_o}{\pi L} \times 1.29 \quad .$$

L = 0.2 m and so

$$E_z^o = 32.85\ V_o \quad .$$

V_o is the solution to the equation

$$E_z^o + E = 0.$$

$$32.85\ V_o - \left(3700 - \frac{V_o}{2}\right)\frac{8900}{3700} = 0$$

$$\therefore \quad V_o = 260 \text{ volts}$$

and

$$\bar{E} = -8540\ \text{V m}^{-1}.$$

This differs considerably from the value of 1500 V predicted by NASCAP (Table 1). The source of this discrepancy lies in the crude spatial resolution of our slab model. As can be seen from (2) the periodic field E_z decreases exponentially with distance above the slab with a scale length $L/2\pi\sqrt{2}$. NASCAP assumes only a linear decrease across each finite element zone. Thus unless the zone size is much smaller than the scale length NASCAP underestimates the field due to the periodic potential at the surface, compared to that predicted analytically, for the same potential drop across a zone. This is illustrated schematically in Figure 5. In the case of the 0.1 m x 0.1 m slab model the scale length is 0.02 m, five times smaller than the zone size. Hence NASCAP underestimates the field due to its charging neighbors immediately in front of a blank patch and so requires a much larger potential drop across a zone than that predicted by the analytical model, to produce the same field at the surface. The larger potential drop across a zone can only occur by reducing the magnitude of the potential of the blank patches, i.e, by increasing the difference between the two surfaces V_o. So NASCAP predicts a larger potential difference V_o than the analytical model.

This discrepancy in the value of V_o predicted by the two models should decrease as the ratio of zone size to scale length decreases. To test this hypothesis an expanded model of the slab was constructed with 0.4 m x 0.4 m patches. The NASCAP results in Table 1 show a V_o value of 800 volts. The field in front of this expanded model uniformly charged to -3.7 kV is calculated to be -3700 V m^{-1}. With this value the analytical model predicts V_o to be 425 V and agreement between the models is closer as expected.

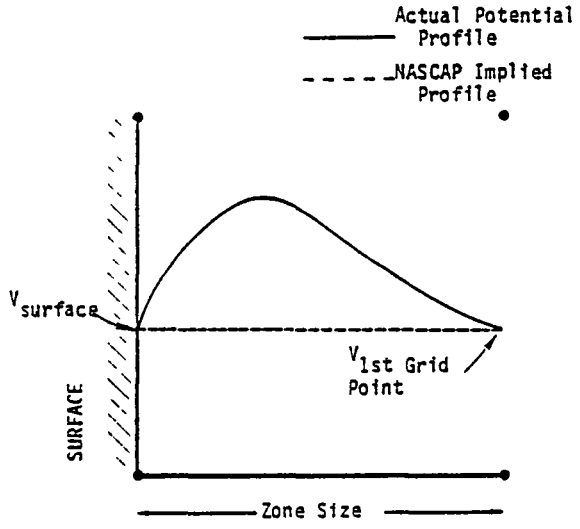

Figure 5. While NASCAP correctly estimates potentials at the grid points, in this case it provides a poor estimate of behavior within the first zone, and underestimates the slope (field) at the surface.

Charging Timescales

The rate at which potential changes depends upon the rate of charge accumulation and the capacitance C of the system being charged.

$$C\phi = \text{charge} = i_{net}\,\Delta t$$

Given the same i_{net} the charging rate depends on the inverse of the capacitance

$$\frac{d\phi}{dt} = \frac{i_{net}}{C}$$

A circuit diagram of two dielectric surfaces covering a conductor is shown in Figure 6. There are two main sources of capacitance.

1. The small capacitances of any surface to infinity. (For a sphere these have the well known form $C = 4\pi\varepsilon_o/r$.)
2. The much larger capacitance between the two surfaces via the underlying conductor. (A small through space capacitance is also present.)

In series the inverse of capacitances are additive,

$$\frac{1}{C} = \frac{1}{C_1} + \frac{1}{C_2}$$

and initially the small capacitances dominate, causing rapid charging of all the surfaces and the underlying conductor together, until current balance for the whole object is achieved. The excess charge

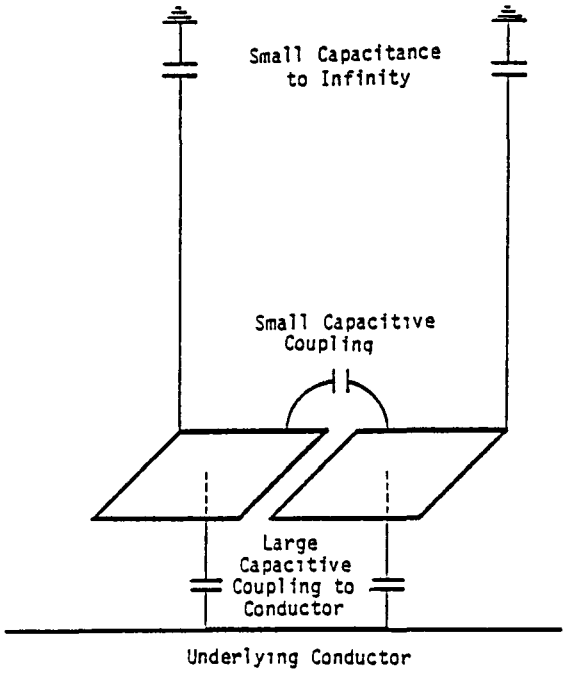

Figure 6. Circuit diagram of two surfaces coupled via an underlying conductor.

on net emitting surfaces is then redistributed to absorbing surfaces and the large capacitances begin to charge. This occurs on a correspondingly slower timescale. Only as differential charging occurs in this way can suppression of secondary emission begin. Thus "bootstrap" charging occurs on a long differential charging timescale (100 secs) dominated by the large capacitances. Charging of pure kapton, however, is determined only by the initial small capacitance response and occurs on a much shorter (4 secs) timescale.

Conclusions

The most important conclusion from this study is that regular arrays of different materials can charge according to their most charging constituent, but on a considerably longer timescale. This may be most significant in modeling the response of solar arrays where the coverglass is typically non-charging and the grouting may be charging. In addition, comparison of NASCAP calculations with an analytical treatment shows the importance of sufficient finite element resolution in determining numerical accuracy.

To summarize we have shown that otherwise non-charging materials can be made to charge by their proximity to charging surfaces on a fairly long timescale. This phenomenon arises from the suppression of secondary emission by the field derived from the adjacent charging surface. The potential to which the "bootstrapped" surfaces charge is determined by geometric effects when their secondary-suppressed equilibrium potential exceeds the potential of the neighboring charging surface. Otherwise only the secondary-suppressed equilibrium potential is reached.

REFERENCES

1. Katz, I., et al., "A Three Dimensional Dynamic Study of Electrostatic Charging in Materials," NASA CR-135256, August 1977.

2. Stannard, P. R., et al., "Analysis of the Charging of the SCATHA (P78-2) Satellite," Systems, Science and Software Final Report, SSS-R-81-4798, December 1980.

3. Purvis, C. K., et al., "Charging Rates of Metal-Dielectric Structures," Spacecraft Charging Technology-1978, NASA Conference Publication 2071, AFGL-TR-79-0082, 1979.

4. Katz, I., et al., "The Capabilities of the NASA Charging Analyzer Program," USAF/NASA Spacecraft Charging Technology Conference, November 1978, AFGL TR-79-0082.

5. Mandell, M. J., et al., "The Decrease in Effective Photocurrents Due to Saddle Points in Electrostatic Potentials Near Differentially Charged Spacecraft," IEEE Trans. on Nuc. Sci., Vol. NS-25, No. 6, December 1978.

APPENDIX D

FLUID MODEL OF PLASMA OUTSIDE A HOLLOW CATHODE NEUTRALIZER

D. E. Parks, M. J. Mandell and I. Katz

To be published in Journal of Spacecraft and Rockets, 1982.

FLUID MODEL OF PLASMA OUTSIDE A HOLLOW CATHODE NEUTRALIZER

D. E. Parks,* M. J. Mandell,** I. Katz†
Systems, Science and Software
La Jolla, California 92038

Abstract

The present study analyzes the capability of a fluid model of electron transport to explain observed properties of the external plasma of a hollow cathode neutralizer used to neutralize beams emerging from ion thrusters. Calculations reported here show that when the effective collision frequency in such a model is near the plasma frequency, the resulting electric potential and electron temperature variations are in qualitative agreement with values measured in the plume mode of the hollow cathode. Both theory and experiment show strong variations of temperature and potential within a few centimeters of the cathode orifice.

Nomenclature

E	kinetic energy of an electron
$\vec{E}$	electric field
$\vec{j}$	net current density
k	Boltzmann's constant
m	electron mass
n	electron density
p	scalar electron pressure
q	magnitude of electron charge
$\vec{q}$	heat flux
$\vec{r}$	position vector
$\vec{R}$	collisional drag force between electrons and ions
T	electron temperature
$u = \vec{V}_- - \vec{V}_+$	
$\vec{V}_-$	drift velocity of electrons
$\vec{V}_+$	drift velocity of ions
λ_c	mean free path for pair collisions between electrons
λ_D	Debye length
$\Theta = kT$	
η	plasma resistivity
κ	thermal conductivity of plasma
ν	effective collision frequency
ν_{ei}	electron-ion collision frequency
$\sigma = \eta^{-1}$	
ϕ	electric potential
ω	frequency of oscillation of fluctuating field
ω_p	electron plasma frequency

1. Introduction

The purpose of the present study is to further examine the capability of a fluid model of electron transport to explain observed properties of spacecraft generated plasmas. Calculations reported here show that when the effective collision frequency in such a model is near the electron plasma frequency, the resulting electric potential variations and electron temperatures are in qualitative agreement with values measured beyond the orifice of a mercury hollow cathode neutralizer used to neutralize thruster ion beams. The same conclusion had been reached in previous applications of the fluid model[1] to the study of neutralized ion beams.

We propose to explain the plasma properties observed in the aforementioned experiments in terms of anomalous resistance of the plasma to the flow of electron current. The calculations are based on fluid equations expressing conservation of charge, momentum, and energy. We adopt the classical (ignoring thermoelectric effects) form of the equations of electron transport,[2] but permit reduced values of the transport coefficients.

While the plasma is not collision dominated, randomization of electron velocities may still occur through enhanced levels of fluctuating fields, such as those initiated by streaming instabilities. The fluctuating fields are probably effective in coupling neutralizer electrons into the bulk plasma and in equalizing the mean drift of electrons with ions in the system. These effects are often approximated by introducing an effective collision frequency, ν.

Within a few centimeters of the orifice the electron densities satisfy

$$n \lesssim 10^{13} \text{ cm}^{-3}$$

and their velocity distribution is characterized by temperatures Θ between about one and five electron volts. The Debye length

$$\lambda_d \approx 700 \sqrt{\frac{\Theta}{n}} \text{ cm}$$

is typically small compared to distances $L \sim 1$ cm over which there is a substantial variation of macroscopic plasma properties such as density, potential, and temperature. On the other hand, the mean free path for pair collisions λ_c

$$\lambda_c \approx 10^{12} E^{1/2} \Theta^{1/2} / n \text{ cm}, \quad E \lesssim \Theta$$

for electrons of energy E (eV) is typically long compared to L, so that as previously asserted the behavior of the plasma is controlled by collective rather than collisional effects. Since $\lambda_D \ll L$, the plasma is quasineutral, departures from neutrality amounting roughly to

$$\delta n/n \sim \left(\frac{\lambda_D}{L}\right)^2 \sim 10^{-4}$$

*Senior Research Scientist, **Research Scientist, †Program Manager

the space around the neutralizer is strongly shielded from surface potentials. This is in contrast to the situation that prevails in charging of spacecraft in geosynchronous orbit where effects of space charge are entirely negligible and potentials are determined as solutions of Laplace's equation.

Although collisionless, neutralizer and thruster-generated plasmas exhibit macroscopic behavior similar in many respects to that of a collisional plasma. Such behavior is perhaps not totally unexpected in view of the fact that in both non-equilibrium and equilibrium plasmas electrons are scattered by fluctuating electric fields. A primary difference between the equilibrium and non-equilibrium cases is in the magnitude of the fluctuating fields.

Several investigators have measured properties of thruster generated plasmas. [3-9] In the experiments of Sellen and Bernstein [5,6] and Ogawa, et al. [7,8] on cesium ion beams neutralized by electrons from a hot wire, measurements were made of the density, potential, and electron temperature in the beam plasma. The potential difference between the neutralizer wire and the plasma could be varied by changing the position of the wire, the large potential differences (electron injection voltages) occurring when the wire was completely withdrawn from the beam plasma. An important result of the Ogawa experiments was that over a wide range of conditions electron density n and plasma potential ϕ were well correlated by the barometric law

$$n(\vec{r}) = \text{const}\, \exp(q\phi(\vec{r})/kT) \qquad (1)$$

The approximate validity of the barometric law was further verified by Kaufman. [9]

Siegfried and Wilbur conducted probe measurements of the plasma temperature and potential outside a hollow cathode operating in both plume and spot modes. [10] In the plume mode, the measurements show strong variations of potential and temperature within a centimeter or so of the orifice. Such results cannot be explained on the basis of a barometric law. We anticipate, however, that the observed behavior should be explained in terms of the anomalous resistivity of the plasma to the flow of electron current. Thus, the primary objective of the following sections of the report is to determine the capability of simple transport models to explain, at least qualitatively, the experimental results.

The next section summarizes the fluid equations for the electrons in terms of conservation of charge, momentum, and energy and discusses the method of solution. Application of the equations to the exterior plasma of a hollow cathode is the subject of Section 3. The results are discussed in Section 4. Section 5 summarizes this study and the conclusions drawn from it.

2. Approximations for Electron Gas

Consider that the plasma is in a steady state and that quasi-neutrality pertains throughout the bulk plasma (that is, away from electrodes and collecting surfaces). The electrons and ions each satisfy the particle continuity equation

$$\nabla\cdot n_i\vec{V}_i = 0 \quad (i = +,-) \qquad (2)$$

with $n_+ = n_- = n$. The momentum equation simplifies considerably if the electron drift velocity $\vec{V}$ is small compared to the random velocity and if the velocity distribution is nearly isotropic. Then, in the absence of magnetic fields,

$$\nabla p + qn\vec{E} = \vec{R} \qquad (3)$$

where $\vec{R}$ represents the collisional drag between ions and electrons. In a classical plasma dominated by collisions, $\vec{R}$ is composed of a part proportional to the relative motion $\vec{u} = \vec{V}_- - \vec{V}_+$ between electrons and ions, leading to plasma resistivity, and to a thermal part proportional to the gradient of electron temperature, which is frequently neglected. In this approximation,

$$\nabla p + qn\vec{E} = \eta nq\vec{j} \qquad (4)$$

where

$$p = nkT = n\theta \qquad (5)$$

is the electron pressure, $\vec{j}$ is the net current density, and the plasma resistivity η is related to the electron-ion collision frequency ν_{ei} by

$$\eta^{-1} = \frac{\omega_p^2}{4\pi}\frac{1}{\nu_{ei}} \qquad (6)$$

If the plasma is non-resistive and isothermal, equation (4) yields the barometric law, equation (1). In this sense, equation (4), or more generally the complete electron momentum equation, may be regarded as the generalization of the barometric law.

If the plasma is not collision dominated, randomization of electron velocities may still occur through the enhanced levels of fluctuating fields in the plasma, such as occur for electron two-stream instabilities, or electron-ion instabilities of the ion-acoustic or Bunemann type. [11,12] These mechanisms are probably effective in coupling neutralizer electrons into the bulk plasma and in equalizing electron and ion mean drift velocities. They are often approximated by introducing an effective collision frequency, ν, in place of ν_{ei}.

The determination of electron temperatures in the plasma requires consideration of the energy balance equation. Making the same approximations in the equation expressing conservation of energy that were made in the momentum equation, yields

$$\nabla\cdot\vec{q} = \eta j^2 \qquad (7)$$

The heat flux, $\vec{q}$, contains new features. Classically, $\vec{q}$ contains two terms; one proportional to the relative drift velocity between electrons and ions, and the other proportional to the gradient of electron temperature. [2]

For the initial calculations, we ignore the drift contributions to the energy flux and the electron-ion heating, and assume that the heat flux is proportional to the temperature gradient. The energy balance equation thus assumes the simple form

$$\nabla\cdot\kappa\nabla\theta + \eta j^2 = 0 \qquad (8)$$

Equations (2-8) have been incorporated into a two-dimensional R-Z computer code. For the present applications, the ion density is a specified function of position and ion velocities are set to zero.

The net current in the plasma is given by

$$\vec{j} = \sigma\left(-\nabla\phi + \frac{q}{n}\nabla p\right) \quad , \qquad (9)$$

[For $\sigma\to\infty$ and $qkT\to\theta$ (constant) we find $\phi = \theta\ell n\ n$.] The code determines electrostatic potentials by solving $\nabla\cdot\vec{j} = 0$. It is necessary to iterate between this equation and the temperature equation (equation 8), since the pressure is a function of temperature. On the various boundary regions, either isothermal or insulating boundary conditions may be specified. Since, in practice, we take κ to have a power law dependence on θ, $\kappa = n\kappa'\theta^{n-1}$, the equation actually solved is

$$-\nabla\cdot\kappa'\nabla(\theta^n) = \frac{j^2}{\sigma} \quad . \qquad (10)$$

For convenience, the transport coefficients σ and κ' are calculated by a single isolated subroutine. The conductivity σ may depend on both density and temperature, and κ' on density only. The present version assumes a relaxation rate proportional to the plasma frequency so that

$$\sigma = n^{1/2}\frac{e^2}{m}\frac{1}{8.98\alpha} \qquad (11)$$

where the parameter α is taken to be 0.51. By the classical Weideman-Franz law,

$$\kappa = \frac{3}{2}\sigma\left(\frac{k}{q}\right)^2 T \quad . \qquad (12)$$

If we measure temperature in eV, $k = q$, so that $\kappa' = 3/4\ \sigma$.

3. Application to Neutralizer Plasma

Siegfried and Wilbur [10] conducted experiments to determine the density, electric potential and electron temperature in the exterior plasma produced by a hollow cathode neutralizer. The experimental results together with essential geometrical features, discharge current I_D, discharge voltage V_D and ampere equivalent neutral mercury flow rate $\dot{m}$ are given in Figures 1 and 2. The plume mode discharge occurred between the hollow cathode and an anode a few centimeters downstream from the 0.75 mm diameter orifice of the hollow cathode. Measurements were also made for spot mode operation, but the corresponding theoretical analysis has not been performed.

For theoretical analysis of the plume mode results, a version of the code was constructed with 0.002 m radial resolution and 0.004 m axial resolution and applied to the region downstream from the keeper. Ion density, falling according to the inverse square law from a point source 1 cm behind the keeper, was normalized to a density of 10^{18} m^{-3} on axis in the keeper plane. A current of 2 amperes, assumed to flow uniformly through a 1 cm radius keeper, was distributed in proportion to the ion density at the downstream boundary of the computational grid. The electron temperature was set to 1 eV at the keeper plane in approximate conformance with the measured value; a null heat flux condition, $\nabla\theta = 0$, was applied at all other boundaries to simulate the effect of an electron repelling sheath.

The theoretical results (Figures 3 and 4) show, in agreement with experiment, a sharp rise in both temperature and potential, followed by a gradual drop as one proceeds downstream from the keeper. The quantitative agreement between theory and experiment is quite good. (Observe expanded scales along axes in Figures 3 and 4.)

4. Discussion

Theory and experiment agree in exhibiting strong structure in temperature and potential profiles downstream from the orifice of the neutralizer. Theoretically, the spatial structure is obtained within the context of a quasi-neutral plasma; that is, the structure a few millimeters downstream from the orifice is not associated with Debye screening effects. Such screening effects should not be present, since owing to the high plasma density $N \sim 10^{12}$ cm^{-3}, the Debye screening length

$$\lambda_D \sim 10^{-3}\ \text{cm}$$

is much shorter than the observed length scale of potential and temperature variations.

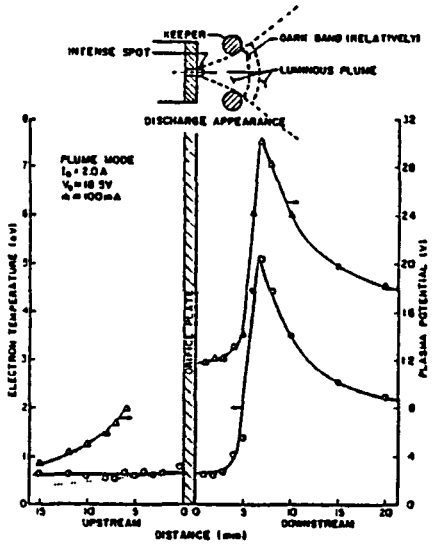

Fig. 1 Cathode plasma potential and electron temperature profiles - plume mode (from reference 10).

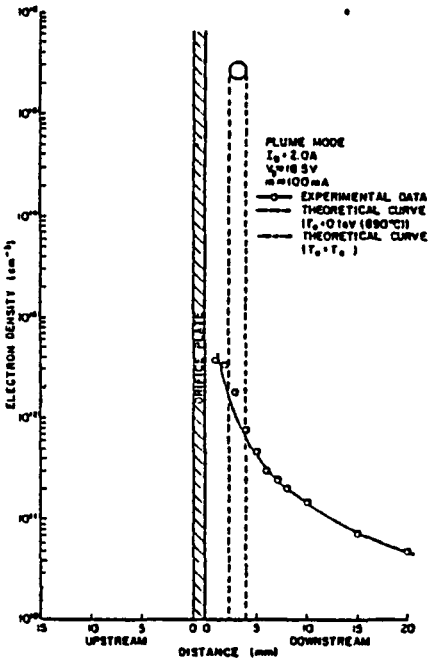

Fig. 2 Cathode electron density profiles - plume mode (from reference 10).

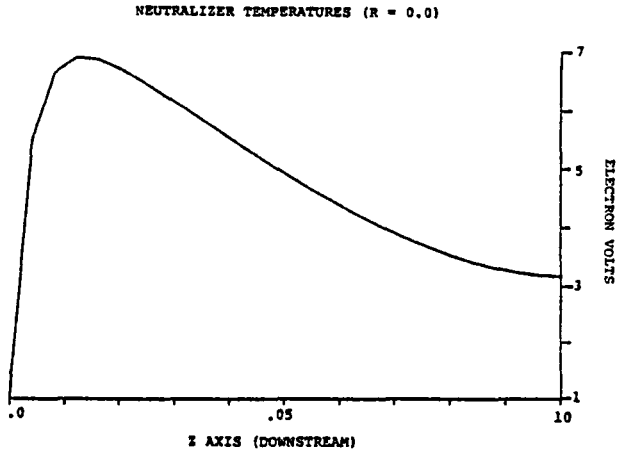

Fig. 3 Computed electron temperature on axis as a function of position downstream from keeper plane.

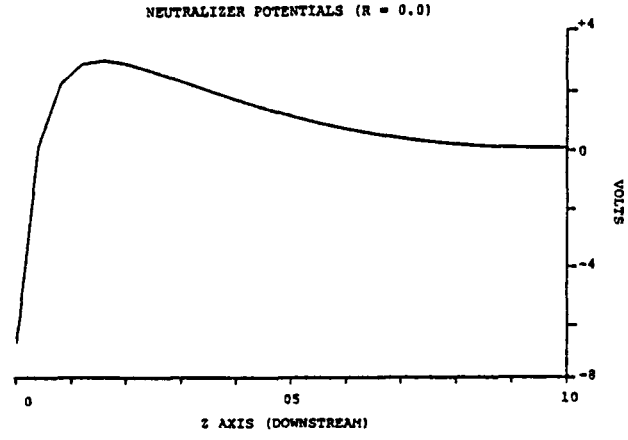

Fig. 4 Computed electron potential on axis as a function of position downstream from keeper plane.

The theoretical basis adopted for our analysis is dependent on the existence of strongly fluctuating electric fields to randomize the velocities of electrons in the vicinity of the neutralizer. If such fields exist and oscillate at a frequency ω, the effective collision frequency seen by electrons would be of order

$$\nu \sim \omega_p \frac{\langle E^2 \rangle}{n\Theta}$$

where $\langle E^2 \rangle$ is the mean square amplitude of the fluctuating field. In a classical collisional plasma

$$\langle E^2 \rangle \sim \frac{n\Theta}{n\lambda_D^3}$$

and ν reduces to the ordinary classical collision frequency. In general for a field oscillating at frequency ω, the

jitter velocity of electrons is

$$\tilde{v} = \frac{qE}{m\omega}$$

so that

$$\frac{3}{2} n\theta \sim \frac{n}{2} m\langle v^2 \rangle = \frac{1}{2} n \frac{q^2 \langle E^2 \rangle}{m\omega^2}$$

$$= \frac{1}{8\pi} \frac{\omega_p^2}{\omega^2} \langle E^2 \rangle$$

Thus, for $\omega \sim \omega_p$, the mean energy density of fluctuating fields and the mean particle energy density are comparable and $\nu \sim \omega_p$. In this circumstance, a condition of strong turbulence would exist near the neutralizer. Reducing ν by an order of magnitude below ω_p would lead to nearly flat temperature and potential profiles, thus destroying the agreement between theory and measurement. The spatial extent of strong turbulence is not known, nor are the conditions for its occurrence. Resolutions of such questions, requiring separate equations for the intensities of waves in the plasma, is beyond the scope of this study.

It would be informative to carry out calculations without the specification of ion density as a prescribed input quantity. Such calculations would involve an independent determination of degree ionization from appropriate rate equations and a knowledge of the flow rate of neutral mercury through the orifice. Whether or not such an augmented model would yield the observed plasma density and the transition from plume to spot mode at larger discharge currents has not been determined.

5. Summary and Conclusions

The consequences of the assumption that the electron gas in the exterior plasma of a hollow cathode neutralizer operating in the plume mode is effectively collisional have been analyzed. We find, in agreement with previous studies,[1] that $\nu \sim \omega_p$ is required to give calculated plasma properties in agreement with measured ones.

Further work should be performed to test the qualitative and quantitative capabilities and limitations of fluid models of thruster generated plasmas, and to better understand the relationship between such models and the underlying plasma physical mechanisms embodied in the collisionless Vlasov equation.

References

1. Parks, D. E., M. J. Mandell and I. Katz, "Fluid Model of Neutralized Ion Beams," AIAA-81-0141, AIAA 19th Aerospace Sciences Meeting, St. Louis, MO, 1981.

2. Braginskii, S. I., Reviews of Plasma Physics, Vol. 1, Ed. M. A. Leontovick, Consultants Bureau, New York, p. 205, 1965.

3. Kerslake, W. R., D. C. Byers and J. F. Staggs, "SERT II: Mission and Experiments," J. Spacecraft 7, 1, p. 4, 1970.

4. Byers, David C. and John F. Staggs, "SERT: Thruster System Ground Testing," J. Spacecraft 7, 1, p. 7, 1970.

5. Sellen, J. M., Jr., W. Bernstein and R. F. Kemp, "Generation and Diagnosis of Synthesized Plasma Streams," Rev. Sci. Instr. 36, p. 316, 1965.

6. Bernstein, W. and J. M. Sellen, Jr., "Oscillations in Synthetic Plasma Beams," Phys. Fluids 6, p. 1032, 1963.

7. Ogawa, H. S., R. K. Cole and J. M. Sellen, Jr., "Factors in the Electrostatic Equilibration Between a Plasma Thrust Beam and the Ambient Space Plasma," AIAA-70-1142, AIAA 8th Electric Propulsion Conference, 1970.

8. Ogawa, H. S., R. K. Cole and J. M. Sellen, Jr., "Measurements of Equilibration Potential Between a Plasma Thrust Beam and a Dilute Space Plasma," AIAA-69-263, AIAA 7th Electric Propulsion Conference, 1969.

9. Kaufman, Harold R., "Interaction of a Solar Array with an Ion Thruster Due to the Charge-Exchange Plasma," NASA Report CR-135099, 1976.

10. Siegfried, D. E. and P. J. Wilbur, "An Investigation of Mercury Hollow Cathode Phenomena," AIAA-78-705, AIAA/DGLR 13th International Electric Propulsion Conference, San Diego, CA, 1978.

11. Krall, Nicholas A. and Alvin W. Trivelpiece, Principles of Plasma Physics, McGraw-Hill, New York, 1973.

12. Bunemann, O., "Dissipation of Currents in Ionized Media," Phys. Rev. 115, p. 503, 1959.

Acknowledgments

This work supported by NASA/Lewis Research Center, Cleveland, OH under Contract NAS3-21762.

REFERENCES

1. Katz, I., D. E. Parks, M. J. Mandell, J. M. Harvey, D. H. Brownell, Jr., S. S. Wang and M. Rotenberg, "A Three Dimensional Dynamic Study of Electrostatic Charging in Materials," NASA CR-135256, August 1977.

2. Hackenberg, O. and W. Bauer, Advances in Electronics and Electron Physics, 16, p. 145, 1962.

3. Feldman, C., Physical Review, 117, p. 455, 1960.

4. Ashley, J. C., C. J. Tung, V. E. Anderson and R. H. Ritchie, (i) AFCRL-TR-75-0583; (ii) RADC-TR-76-220; (iii) RADC-TR-76-125; (iv) IEEE Transactions on Nuclear Science, NS-25/6, p. 1566, 1978.

5. Stevens, N. J., J. V. Staskus, J. C. Roche and P. F. Mizera, "Initial Comparison of SSPM Ground Test Results and Flight Data to NASCAP Simulations," NASA Technical Memorandum 81394, presented at 18th Aerospace Sciences Meeting, AIAA, Pasadena, CA, January 14-16, 1980.

6. Goldstein, H., Classical Mechanics, Addison-Wesley, Reading, MA, p. 83, 1957.

7. ibid, p. 135.

DISTRIBUTION LIST

National Aeronautics and Space Administration
Washington, D. C. 20546
Attn: W. R. Hudson/Code RP — 1 copy
D. P. Williams, III/Code RS-5 — 1 copy

National Aeronautics and Space Administration
Ames Research Center
Moffett Field, CA 94035
Attn: H. Lum, Jr./M.S. 244-7 — 1 copy

National Aeronautics and Space Administration
Goddard Space Flight Center
Greenbelt, MD 20771
Attn: R. O. Bartlett/Code 408.0 — 1 copy
A. Kampinsky/Code 727.0 — 1 copy
E. G. Stassinopoulos/Code 601.0 — 1 copy
R. S. Bever/Code 405.0 — 1 copy

Jet Propulsion Laboratory
4800 Oak Grove Drive
Pasadena, CA 91103
Attn: Ray Goldstein — 1 copy
H. Garrett — 1 copy
E. V. Pawlik — 1 copy
Paul Robinson — 1 copy

National Aeronautics and Space Administration
Lyndon B. Johnson Space Center
Houston, TX 77058
Attn: J. E. McCoy/Code SN3 — 1 copy
A. Konradi/Code SN3 — 1 copy

National Aeronautics and Space Administration
Langley Research Center
Hampton, VA 23665
Attn: J. W. Goslee/M.C. 364 — 2 copies

National Aeronautics and Space Administration
Lewis Research Center
21000 Brookpark Road
Cleveland, OH 44135
Attn: Head, Mechanics, Fuels and Physics Section/
M.S. 501-11 — 1 copy
Technology Utilization Office/M.S. 7-3 — 1 copy
Report Control Office/M.S. 5-5 — 1 copy
Office of Reliability and Quality Assurance/
M.S. 500-211 — 1 copy
AFSC Liaison Office/M.S. 501-3 — 2 copies
Library/M.S. 60-3 — 2 copies
J. C. Roche/M.S. 77-4 — 24 copies
Patent Counsel/M.S. 500-318 — 1 copy

DISTRIBUTION LIST (Continued)

National Aeronautics and Space Administration
George C. Marshall Space Flight Center
Marshall Space Flight Center, AL 35812
Attn: C. R. Chappell/ES 51 — 1 copy
J. H. Harlow/PF 13 — 1 copy
M. R. Carruth/PF 13 — 1 copy
R. N. Seitz/EF 31 — 1 copy

National Aeronautics and Space Administration
Scientific and Technical Information Facility
P. O. Box 8757
Baltimore/Washington International Airport
Maryland 21240
Attn: Accessioning Department — 10 copies

Air Force Geophysics Laboratory
Hanscom Air Force Base, MA 01731
Attn: PH/C. P. Pike — 1 copy
PHG/A. G. Rubin — 1 copy

Air Force Materials Laboratory
Wright-Patterson Air Force Base, OH 45433
Attn: MBE/W. Lehn — 1 copy

Air Force Office of Scientific Research
Bolling Air Force Base
Washington, D. C. 20332
Attn: H. R. Radoski/NP — 1 copy

Air Force Weapons Laboratory
Kirtland Air Force Base, NM 87117
Attn: Capt. W. G. Kuller — 1 copy
Capt. D. Hanifen — 1 copy

Headquarters Space Division (AFSC)
Los Angeles AF Station
P. O. Box 92960
Worldway Postal Center
Los Angeles, CA 90009
Attn: YLVS/Lt. R. Weidenheimer — 1 copy

Defense Nuclear Agency Headquarters
Washington, D. C. 20305
Attn: RAEV/Maj. H. Joonsar — 1 copy

Department of Electrical Engineering
Pennsylvania State University
121 Electrical Engineering
East Building
University Park, PA 16801
Attn: J. Robinson — 1 copy

Department of Physics
University of California at San Diego
P. O. Box 109
La Jolla, CA 92037
Attn: E. C. Whipple — 1 copy

Aerojet Electrosystems Company
1100 West Hollyvale Street
Azusa, CA 91720
Attn: C. Fischer/Dept. 6751 — 1 copy

Aerospace Corporation
P. O. Box 92957
Los Angeles, CA 90009
Attn: J. R. Stevens — 1 copy
R. M. Broussard — 1 copy
J. F. Fennell — 1 copy

Beers Associates, Inc.
P. O. Box 2549
Reston, VA 22090
Attn: Dr. Brian Beers — 1 copy

Boeing Aerospace Company
P. O. Box 3999
Seattle, WA 98124
Attn: H. Liemohn/M.S. 8C-23 — 1 copy
D. Tingey/M.S. 8C-23 — 1 copy

Communications Satellite Corporation
Comsat Laboratories
Clarksburg, MD 20734
Attn: A. Meulenberg, Jr. — 1 copy

European Space Agency
ESTEC
Zwartweg, Noordwijk
Netherlands
Attn: John Reddy, P.B. TTM, 1719 8 2883 — 1 copy

Ford Aerospace and Communications Corporation
Western Development Laboratories Division
3939 Fabian Way
Palo Alto, CA 94303
Attn: D. M. Newell/M.S. G-80 — 1 copy
J. Pherson/M.S. N-01 — 1 copy

General Dynamics Convair
Kearny Mesa Plant
P. O. Box 80847
San Diego, CA 92138
Attn: J. I. Valerio/Mail Zone 42-6210 — 1 copy

General Electric Company
Valley Forge Space Center
P. O. Box 8555
Philadelphia, PA 19101
Attn: V. Belanger/U-2439 — 1 copy
A. Eagles — 1 copy

Grumman Aerospace
Bethpage, NY 11714
Attn: M. Stauber — 1 copy

Hughes Aircraft Company
P. O. Box 92919
Los Angeles, CA 90009
Attn: E. Smith/M.S. A620 — 1 copy
A. H. Narevsky — 1 copy

Hughes Research Laboratories
3011 Malibu Canyon Road
Malibu, CA 90265
Attn: Dr. Jay Hyman — 1 copy

IRT Corporation
P. O. Box 80817
San Diego, CA 92138
Attn: J. Wilkenfeld — 1 copy

JAYCOR
P. O. Box 85154
San Diego, CA 92138
Attn: E. P. Wenaas — 1 copy

Kaman Science
1500 Garden of the Gods Road
Colorado Springs, CO 80907
Attn: F. Rich — 1 copy

Lee W. Parker, Inc.
252 Lexington Road
Concord, MA 01742
Attn: L. Parker — 1 copy

Lockheed Palo Alto Research Laboratory
3251 Hanover Street
Palo Alto, CA 94303
Attn: J. B. Reagan/Bldg. 205, Dept. 52-12 — 1 copy
D. P. Cauffman — 1 copy

Martin Marietta Corporation
P. O. Box 179
Denver, CO 80201
Attn: D. E. Hobbs/M.S. D8350 — 1 copy
K. Killian/M.S. D8350 — 1 copy

Massachusetts Institute of Technology
Lincoln Laboratory
P. O. Box 73
Lexington, MA 02173
Attn: F. G. Walther — 1 copy

McDonnell Douglas Astronautics Company
5301 Bolsa Avenue
Huntington Beach, CA 92647
Attn: W. P. Olson — 1 copy

Mission Research Corporation
5434 Ruffin Road
San Diego, CA 92123
Attn: V. van Lint — 1 copy

RCA Astroelectronics Division
P. O. Box 800
Princeton, NJ 08540
Attn: H. Strickberger/M.S. 91 — 1 copy
W. Franklin — 1 copy

Science Applications, Inc.
101 Continental Building
Suite 310
El Segundo, CA 90245
Attn: D. McPherson — 1 copy

Science Applications, Inc.
2860 South Circle Drive
Colorado Springs, CO 80906
Attn: E. E. O'Donnell — 1 copy

Simulation Physics, Inc.
41 B Street
Burlington, MA 01803
Attn: R. G. Little — 1 copy

SRI International
333 Ravenswood Avenue
Menlo Park, CA 90425
Attn: J. Nanevicz — 1 copy

TRW Systems
One Space Park
Redondo Beach, CA 90278
Attn: G. T. Inouye/Bldg. R-5, Rm. 2011 — 1 copy

Lockheed Missile and Space Company
P. O. Box 504
Sunnyvale, CA 94086
Attn: G. Pack — 1 copy

End of Document